

EXPERIMENTAL INVESTIGATION ON ASSESSMENT AND PREDICTION OF SPECIFIC ENERGY IN ROCK CUTTING

Thesis

Submitted in partial fulfillment of the requirements for the degree of

DOCTOR OF PHILOSOPHY

By

VIJAYA RAGHAVAN

102002MN10P03



**DEPARTMENT OF MINING ENGINEERING
NATIONAL INSTITUTE OF TECHNOLOGY KARNATAKA
SURATHKAL, MANGALORE - 575025
JULY, 2021**

Dedicated to

My Daughters,

DECLARATION

by the Ph.D. Research Scholar

I hereby *declare* that the Research Synopsis entitled “**Experimental Investigations on Assessment and Prediction of Specific Energy in Rock Cutting**” which is being submitted to the **National Institute of Technology Karnataka, Surathkal**, in partial fulfillment of the requirements for the award of the Degree of **Doctor of Philosophy in Mining Engineering** is a bonafide report of the research work carried out by me. The material contained in this Research Thesis has not been submitted to any University or Institution for the award of any degree.



Vijaya Raghavan

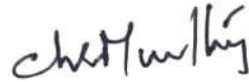
102002MN10P03

Place: NITK, Surathkal

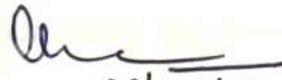
Date: 24.07.2021

CERTIFICATE

This is to certify that the Research Synopsis entitled **“Experimental Investigations on Assessment and Prediction of Specific Energy in Rock Cutting”** submitted by **Mr. Vijaya Raghavan**, (Register Number **102002MN10P03**) as a record of the research work carried out by him, is accepted as the Research Thesis submission in partial fulfillment of the requirements for the award of Degree of **Doctor of Philosophy**.



Dr. Ch. S. N. Murthy
Professor - HAG & Research Guide
Department of Mining Engineering



03/08/2021

Dr. M. Aruna
HOD & Chairman, DRPC
Department of Mining Engineering
(Signature with Date)
Chairman - DRPC

Department of Mining Engineering
National Institute of Technology Karnataka, Surathkal.
P.O. Srinivasnagar-575 025, Mangalore.
Karnataka State, India.

ACKNOWLEDGEMENT

I am indebted to my supervisor **Dr. Ch. S. N. Murthy**, Professor-HAG, Department of Mining Engineering, National Institute of Technology Karnataka (N. I. T. K), Surathkal, for his excellent guidance and support throughout the research work. His constant encouragement, help and review of the entire work during the course of the investigation are invaluable.

I wish to thank all the members of the Research Program Assessment Committee, including **Dr. Shrihari**, Professor, Department of Civil Engineering and **Dr. Ravi Kiran Kadoli**, Professor, Department of Mechanical Engineering, National Institute of Technology Karnataka (N. I. T. K), Surathkal, for their appreciation, support and suggestions all through this research work.

I wish to express my sincere thanks to **Dr. M. Aruna**, Associate Professor and Head of the Department of Mining Engineering, for extending the departmental facilities, which ensured the satisfactory progress of my research work.

I would like to thank **Dr. V. R. Sastry**, Professor- HAG, **Dr. Mandela Govinda Raj**, Professor, **Dr. Harsha Vardhan**, Professor, **Dr. Karra Ramchandrar**, Associate Professor, **Dr. Anup Kumar Tripathi**, Assistant Professor, **Dr. Bijay Mihir Kunar**, Assistant Professor, **Dr. Sandi Kumar Reddy**, Assistant Professor, Department of Mining Engineering, N. I. T. K, Surathkal, for their continuous help and support throughout the research work.

I would like to thank all the **Teaching** and **Non-teaching staff** members of the Department of Mining Engineering, N. I. T. K Surathkal, for their continuous help and support throughout the research work.

I owe my deepest gratitude to **Sri. Chandrahas Rai**, Assistant Executive Engineer, **Dr Sreekant R. Lamani**, Assistant Engineer and technicians **Sri. Mahabala Poojari**,

Department of Mining Engineering, N. I. T. K, for their help in carrying out experimental work in the Rock Mechanics laboratory. I also thank **Dr. Vijay Kumar S, Dr. Harish Kumar N S, Dr. Ch. Vijaya Kumar, Mr. Harish Kumar H, Mr. Tejeswaran** and **Research Scholars**, Department of Mining Engineering, N. I. T. K helping in all aspects to submit the thesis.

Further, I am thankful to **Mr. Balaji Rao K**, Research Scholar, Department of Mining Engineering, N. I. T. K, for his excellent guidance in numerical modelling (ANSYS).

I am very much thankful to **Mr. Shankar, Mr. Venkatesh,** and **Mr. Sai Vivek**, former B. Tech students of Dr. T. T. I. T, K. G. F, for their help to conduct the experiments in the Rock Mechanics laboratory.

I would like to thank Late **Dr. Thimmaiah (President Emeritus), Dr. T. Venkata Vardhan**, President, Dr Thimmaiah Institute of Technology, K. G. F, and **Dr. Syed Ariff**, Principal and **Mr. Ramesh**, Foreman, Department of Mining Engineering, Dr T. Thimmaiah Institute of Technology, K.G. F, Teaching and Non-Teaching of Dr T. Thimmaiah Institute of Technology, K.G.F, for their continuous help and support throughout the research work.

The list goes on, and there are many others I should thank who helped me all the way and supported me when I didn't even realize I needed it, or needed it now, or needed it constantly. Listing all of them would fill a book itself, so I merely will have to limit myself to a few words. I THANK YOU ALL.....!

Finally, I would like to share this moment of happiness with my parents, **Sri. B. Perumal, Smt. P. Parimalam Perumal**, my wife **Smt. Chitra S, Brother, Sister, Sister-in-law, Brother-in-law** and their Family for their constant encouragement and appreciation.



[VIJAYA RAGHAVAN]

ABSTRACT

The rock cutting machine was fabricated to measure the cutting rate and specific energy (SE). The variable parameters include attack angle, pick angle, RPM, cutting force, and torque to determine the cutting parameters. For measuring the cutting force and torque, a cutting tool dynamometer is used. Experimental investigations were also carried out to determine physico-mechanical properties of the rocks, namely density, uniaxial compressive strength (UCS), Brazilian Tensile strength (BTS), abrasivity and brittleness of the rocks were determined as per ISRM standards. During the cutting process, the RPM is varied from 225, 300, 325 and 350 and the cutting force is measured at each RPM. The cutting process was carried using point attack picks of 45°, 50°, 55° and 65° pick angles and 45°, 55° and 65° attack angles. During the cutting process, the cutting force was varied using a hydraulic pressure valve. In this research, for each RPM and thrust combination, cutting is done for 60 seconds and cutting depth is measured using a digital vernier calliper. The rock cuttings are collected and weighed using a digital weighing machine. Then, the SE (J/m^3) is calculated by cutting force multiplied by the depth of cut and divided by volume collected during the cutting process.

The increase in RPM, torque, and cutting force observations reveals that the increase in the parameters increases the cutting rate with a corresponding decrease in SE. With cutting rate, the minimum and maximum variation irrespective of the rock type are found to be 0.3 to 4.8% for pick angles, 0.2 to 32% for attack angles, 0.05 to 4.08% for RPM, 0.05 to 3.2% for torque and 0.05 to 3.2% for cutting force. With specific energy, the minimum and maximum variations irrespective of the rock type are found to be 0.023 to 4.41% for pick angles, 21.91 to 51.26% for attack angles, 0.03 to 4.41% for RPM, 0.03 to 7.8% for torque and 0.18 to 7.36% for cutting force. Hence, attack angle has more influence on cutting rate and specific energy.

The cutting rates and specific energy values were determined for the pick tool subjected to wear of 5mm at an 45° attack angle. a comparison of the same was made. A decrease in cutting rate is observed with a proportional increase in specific energy. The minimum

and maximum variations irrespective of the rock type are 24.5 to 33.36% for pick angles, 24.5 to 30.36% for RPM, 21.56 to 35.16% for torque and 20.05 to 32.61% with cutting force for cutting rate. For specific energy, the minimum and maximum variations irrespective of the rock type are 21.86 to 35.81% for pick angles, 21.80 to 32.66% for RPM, 21.89 to 36.20% for RPM torque and 21.98 to 36.64% for cutting force.

A property correlation with specific energy was also plotted as a line graph. It was observed that, with the increase in density, UCS, BTS, abrasivity, and brittleness of the rock, SE increases linearly. This is because, with the increase in the strength of rock, the cutting resistance increases linearly.

The regression models shown in Equations 6.1, 6.2 and 6.3 were developed and can be used to estimate the SE during rock cutting as they can be used as guidance in practical applications. The developed regression model results showed that the SE's significant operating variables were attack angle, type of pick followed by other cutting parameters, such as the rock's mechanical properties. The results showed that input parameters were significant, and the model possesses an R-Square value of 99.55%. The respective variance account for (VAF), root mean square error RMSE and mean absolute percentage error (MAPE) indices for predicting SE are VAF of 99.17, RMSE of 12.08 and MAPE of 0.032535, respectively, from the multiple regression model (testing). The result of the current study provides opportunities to evaluate the cuttability of rocks before involving complicated experimental procedures. Error graphs also resulted in the goodness of fits of a statistical model.

Artificial Neural Network (ANN), was developed to predict the SE. the input parameters include cutting force, pick angle, attack angle, depth of cut, volume broken and rock properties like density, UCS, BTS, abrasivity and brittleness. The ANN results showed that the model's predictive performance for VAF, RMSE and MAPE indices are VAF of 99.98289, RMSE of 9.47741, MAPE of 0.0000158 for training and VAF, RMSE and MAPE for validation were VAF of 99.97602, RMSE of 11.85352, MAPE of 0.0000666. Error graphs also resulted in the goodness of fits of a statistical model.

A numerical model using Finite Element Method (FEM) analysis was constructed to determine the depth of cut for all pick-rock combinations considered using the cutting force values from experimental rock cutting tests (up to loading cycle only). Then the depth of penetration obtained in FEM analysis of all pick-rock combinations was compared with the respective depth of cut obtained with experimental results. The depth of penetration obtained during experiments is lesser than FEM analysis for all pick-rock combinations considered and ranges from 1 to 8% (except a few). Further, the results indicated that displacement decreases from the loading axes towards the boundary in all directions. The stress analysis was carried using Ansys workbench for all the pick-rocks combinations considered along X, Y and Z - directions. The results showed that the maximum compressive stress generated is at the tip of the cut zone.

In this research, a new concept is proposed: Rock Cutting Resistance (RCR), i.e., the resistance offered by the rock against the cutting force required to achieve a unit depth of cut, and is expressed as N/mm. The results of the RCR (Experimental and FEM) can be used to predict the depth of cut during rock cutting. Hence, RCR can be used for the efficient design of the rock cutting parameters and the machine.

TABLE OF CONTENTS

	CONTENTS	PAGE NO.
	Declaration	i
	Certificate	ii
	Acknowledgement	iii
	Abstract	v
	Contents	vii
	List of Figures	xi
	List of Tables	xxiv
	Nomenclature	xxv
1	INTRODUCTION	1- 6
1.1	Motivation and aims	6
2	LITERATURE REVIEW	7- 38
2.1	Introduction	7
2.1.1	Cutting mechanism	7
2.1.2	The initial stage of cutting	7
2.1.3	Crush zone and dust generation	8
2.1.4	Formation of crush and rock fragments	9
2.2	Research on cutting force and specific energy in rock cutting	11
2.3	Artificial Neural Networks (ANN)	26
2.4	Numerical Modeling of cutter-rock interface	30
2.4.1	Continuum methods	31
2.4.2	Discontinuum methods	31
2.5	Problem statements	35
2.6	Objectives of the Study	36
2.7	Thesis Outline	36

3	EXPERIMENTAL INVESTIGATIONS	39-56
3.0	Introduction	39
3.1	Methodology	39
3.2	Collection of Coal and different types of rocks from different sources for the preparation of core samples	42
3.3	The Mechanical Properties of the rocks under study	38
3.3.1	The Density of rocks.	42
3.3.2	The Uniaxial compressive strength of rocks	43
3.3.3	The Brazilian Tensile strength of rocks	44
3.3.4	The Brittleness of the rocks	45
3.3.5	The Abrasivity of the rocks	45
3.4	Calibration for cutting tool dynamometer	48
3.5	Description of Rock Cutting Machine	51
3.5.1	Main frame	52
3.5.2	Cutting head	52
3.5.3	Coal block holder	53
3.5.4	Cutting picks	53
3.5.5	Hydraulic units	54
3.5.6	Speed controller	54
3.6	Experimental Work	55
4.	ARTIFICIAL NEURAL NETWORK MODELING	57-68
4.1	Introduction	57
4.2	Fundamental concepts in ANN	58
4.3	Multi-layer perception	60
4.4	Back-propagation algorithm	61
4.5	Development of ANN model in this present study	63
5.	NUMERICAL MODELING	69-74
5.1	General	69

5.1.1	Pre-processing phase	70
5.1.2	Solution phase	70
5.1.3	Processing phase	70
5.2	FEM analysis of pick penetration into rock	71
5.2.1	Description of the numerical model	71
5.2.1.1	Defining element type	71
5.2.1.2	Material properties	71
5.2.1.3	Mesh generation	71
5.2.1.4	Method of applying load	74
6	RESULTS AND DISCUSSIONS	75-133
6.1	Experimental Results	75
6.1.2	Influence of Cutting Parameters on cutting rate and Specific energy	75
6.1.2.1	Influence of pick angle and attack angle on the cutting rate	75
6.1.2.2	Influence of RPM on cutting rate	78
6.1.2.3	Influence of torque on cutting rate	82
6.1.2.4	Influence of cutting force on cutting rate	86
6.1.2.5	Influence of pick angles and attack angles on the specific energy	90
6.1.2.6	Influence of RPM on Specific energy	92
6.1.2.7	Influence of torque on Specific energy	96
6.1.2.8	Influence of cutting force on Specific energy	100
6.2	Influence of rock properties on specific energy	104
6.2.1	Introduction	104
6.2.2	Multiple Linear regression analysis	104
6.2.3	Regression analysis of Specific energy	105
6.3	Analysis of Results	107
6.3.1	Influence of UCS on Specific energy	108
6.3.2	Influence of BTS on Specific energy	109

6.3.3	Influence of Abrasivity on Specific energy	110
6.3.4	Influence of Brittleness on Specific energy	111
6.3.5	Influence of Cutting rate on Specific energy	112
6.3.6	Influence of Depth of cut on Specific energy	113
6.3.7	Influence of Attack angle on Specific energy	114
6.4	Analysis of Results for Predicative (Regression) Models	116
6.4.1	Performance prediction of the derived models	116
6.4.2	Error Analysis of the derived regression models	117
6.5	Analysis of Results for Artificial Neural Network Results	118
6.6	Analysis of Numerical Modeling Results	121
6.6.1	Comparison of results obtained from rock cutting Experimental and FEM analysis	121
6.6.2	Results of Von Misses stress field	127
6.7	Determination of Rock Cutting Resistance (RCR)	131
6.7.1	Analysis of RCR Results	133
7	CONCLUSION AND FUTURE WORK	135-138
7.1	Conclusion	135
7.2	Scope for Future work	137
	REFERENCES	139-156
	Appendix-I	157-197
	Appendix-II	198-210
	Appendix-III	211-229
	List of Publications	230
	Bio-data	231

LIST OF FIGURES

Figure No.	Description	Page No.
Figure 1.1	Point attack picks	3
Figure 2.1	Pressure bulb during penetration	8
Figure 2.2	Evolution of crush zone and fragments	9
Figure 2.3	Schematic of Evan's tensile breakage theory	12
Figure 2.4	The general effect of cutter spacing on Specific energy	17
Figure 2.5	The graph for the relation between compressive strength and tensile strength of rock	24
Figure 3.1	Flow chart of the plan of experimental design and analysis	40
Figure 3.2	Uniaxial Compression testing machine with sample	43
Figure 3.3	Brazilian testing apparatus with specimen	44
Figure 3.4	Specimen prepared for Los Angeles abrasion test	45
Figure 3.5	Los Angeles abrasion test apparatus	45
Figure 3.6	Cutting tool dynamometer	48
Figure 3.7	Digital multi-component force and torque indicator	48
Figure 3.8	Method of calibrating the cutting tool dynamometer	49
Figure 3.9	Calibration chart for cutting force	50
Figure 3.10	Calibration chart for torque	50
Figure 3.11	(a) Rock cutting machine (b) Line diagram of Rock cutting machine	51
Figure 3.12	Cutting drum with picks	52
Figure 3.13	Picks used for the experimental investigation	53
Figure 3.14	Hydraulic unit for the rock cutting machine	54
Figure 3.15	Speed controller used for rock cutting machine	54
Figure 3.16	The groove which is formed during cutting of coal	56
Figure 3.17	The groove which is formed during cutting of sandstone	56
Figure 3.18	The groove which is formed during cutting of limestone	56

Figure 3.19	The groove which is formed during cutting of dolomite	56
Figure 4.1	Architecture of simple neuron	58
Figure 4.2	Feed-forward ANN network	59
Figure 4.3	Pictorial representation of training model for training data	65
Figure 4.4	Performance model for training data	65
Figure 4.5	Prediction model of ANN for training data	66
Figure 4.6	Pictorial representation of training model for validation data	66
Figure 4.7	Performance model for validation data	67
Figure 4.7	Prediction model of ANN for training data	67
Figure 5.1	Influence of rpm on cutting rate for 50° Pick angle at 45° Attack angle	72
Figure 5.2	Influence of rpm on cutting rate for 55° Pick angle at 45° Attack angle a & b	73
Figure 5.3	Resolution of forces and their application in Ansys	74
Figure 6.1	Influence of pick angle on cutting rate at 45° attack angle.	77
Figure 6.2	Influence of pick angle on cutting rate at 55° attack angle.	77
Figure 6.3	Influence of pick angle on cutting rate at 65° attack angle.	77
Figure 6.4	Influence of pick angle on cutting rate at 45° attack angle. with 5 mm wear	77
Figure 6.5	Influence of rpm on cutting rate at 45° pick angle at 45° attack angle	79
Figure 6.6	Influence of rpm on cutting rate at 50° pick angle at 45° attack angle	79
Figure 6.7	Influence of rpm on cutting rate at 55° pick angle at 45° attack angle	79
Figure 6.8	Influence of rpm on cutting rate at 65° pick angle at 45° attack angle	79
Figure 6.9	Influence of rpm on cutting rate at 45° pick angle at 55° attack angle	79

Figure 6.10	Influence of rpm on cutting rate at 50° pick angle at 55° attack angle	79
Figure 6.11	Influence of rpm on cutting rate at 55° pick angle at 55° attack angle	80
Figure 6.12	Influence of rpm on cutting rate at 65° pick angle at 55° attack angle	80
Figure 6.13	Influence of rpm on cutting rate at 45° pick angle at 65° attack angle	79
Figure 6.14	Influence of rpm on cutting rate at 50° pick angle at 65° attack angle	79
Figure 6.15	Influence of rpm on cutting rate at 55° pick angle at 65° attack angle	80
Figure 6.16	Influence of rpm on cutting rate at 65° pick angle at 65° attack angle	80
Figure 6.17	Influence of rpm on cutting rate at 45° pick angle at 45° attack angle with 5 mm wear	81
Figure 6.18	Influence of rpm on cutting rate at 50° pick angle at 45° attack angle with 5 mm wear	81
Figure 6.19	Influence of rpm on cutting rate at 55° pick angle at 45° attack angle with 5 mm wear	81
Figure 6.20	Influence of rpm on cutting rate at 65° pick angle at 45° attack angle with 5 mm wear	81
Figure 6.21	Influence of torque on cutting rate for 45° Pick angle at 45° Attack angle	83
Figure 6.22	Influence of torque on cutting rate for 50° Pick angle at 45° Attack angle	83
Figure 6.23	Influence of torque on cutting rate for 55° Pick angle at 45° Attack angle	83
Figure 6.24	Influence of torque on cutting rate for 65° Pick angle	

	at 45° Attack angle	83
Figure 6.25	Influence of torque on cutting rate for 45° Pick angle at 55° Attack angle	83
Figure 6.26	Influence of torque on cutting rate for 50° Pick angle at 55° Attack angle	83
Figure 6.27	Influence of torque on cutting rate for 55° Pick angle at 55° Attack angle	84
Figure 6.28	Influence of torque on cutting rate for 65° Pick angle at 55° Attack angle	84
Figure 6.29	Influence of torque on cutting rate for 45° Pick angle at 65° Attack angle	84
Figure 6.30	Influence of torque on cutting rate for 50° Pick angle at 65° Attack angle	84
Figure 6.31	Influence of torque on cutting rate for 55° Pick angle at 65° Attack angle	84
Figure 6.32	Influence of torque on cutting rate for 65° Pick angle at 65° Attack angle	84
Figure 6.33	Influence of torque on cutting rate for 45° Pick angle at 45° Attack angle with 5 mm wear	85
Figure 6.34	Influence of torque on cutting rate for 50° Pick angle at 45° Attack angle with 5 mm wear	85
Figure 6.35	Influence of torque on cutting rate for 55° Pick angle at 45° Attack angle with 5 mm wear	85
Figure 6.36	Influence of torque on cutting rate for 65° Pick angle at 45° Attack angle with 5 mm wear	85
Figure 6.37	Influence of Cutting force on Cutting rate with 45° Pick angle at 65° Attack angle	87
Figure 6.38	Influence of Cutting force on Cutting rate with 45° Pick angle at 45° Attack angle	87

Figure 6.39	Influence of Cutting force on Cutting rate with 50° Pick angle at 45° Attack angle	87
Figure 6.40	Influence of Cutting force on Cutting rate with 65° Pick angle at 45° Attack angle	87
Figure 6.41	Influence of Cutting force on Cutting rate with 45° Pick angle at 55° Attack angle	87
Figure 6.42	Influence of Cutting force on Cutting rate with 50° Pick angle at 55° Attack angle	87
Figure 6.43	Influence of Cutting force on Cutting rate with 55° Pick angle at 5° Attack angle	88
Figure 6.44	Influence of Cutting force on Cutting rate with 65° Pick angle at 55° Attack angle	88
Figure 6.45	Influence of Cutting force on Cutting rate with 45° Pick angle at 65° Attack angle	88
Figure 6.45	Influence of Cutting force on Cutting rate with 45° Pick angle at 65° Attack angle	88
Figure 6.46	Influence of Cutting force on Cutting rate with 50° Pick angle at 65° Attack angle	88
Figure 6.47	Influence of Cutting force on Cutting rate with 55° Pick angle at 65° Attack angle	88
Figure 6.48	Influence of Cutting force on Cutting rate with 55° Pick angle at 65° Attack angle	88
Figure 6.49	Influence of Cutting force on Cutting rate with 45° Pick angle at 45° Attack angle with 5mm wear	89
Figure 6.50	Influence of Cutting force on Cutting rate with 50° Pick angle at 45° Attack angle with 5mm wear	89
Figure 6.51	Influence of Cutting force on Cutting rate with 65° Pick angle at 45° Attack angle with 5mm wear	89
Figure 6.52	Influence of Cutting force on Cutting rate with 45°	

	Pick angle at 45° Attack angle with 5mm wear	89
Figure 6.53	Influence of pick angles on the specific energy at 45° attack angle.	91
Figure 6.54	Influence of pick angles on the specific energy at 55° attack angle.	91
Figure 6.55	Influence of pick angles on the specific energy at 55° attack angle.	91
Figure 6.56	Influence of pick angles on Cutting rate with 5 mm wear at 45° attack angle for all rocks	91
Figure 6.57	Influence of rpm on Specific energy for 45° Pick angle at 45° attack angle.	93
Figure 6.58	Influence of rpm on Specific energy for 50° Pick angle at 45° attack angle.	93
Figure 6.59	Influence of rpm on Specific energy for 55° Pick angle at 45° attack angle	93
Figure 6.60	Influence of rpm on Specific energy for 65° Pick angle at 45° attack angle.	93
Figure 6.61	Influence of rpm on Specific energy for 45° Pick angle at 55° attack angle.	93
Figure 6.62	Influence of rpm on Specific energy for 50° Pick angle at 55° attack angle.	93
Figure 6.63	Influence of rpm on Specific energy for 55° Pick angle at 55° attack angle.	94
Figure 6.64	Influence of rpm on Specific energy for 65° Pick angle at 55° attack angle.	94
Figure 6.65	Influence of rpm on Specific energy for 45° Pick angle at 65° attack angle.	94
Figure 6.66	Influence of rpm on Specific energy for 50° Pick angle at 65° attack angle.	94
Figure 6.67	Influence of rpm on Specific energy for 55° Pick angle at 65° attack angle.	94

Figure 6.68	Influence of rpm on Specific energy for 65° Pick angle at 65° attack angle	94
Figure 6.69	Influence of rpm on Specific energy for 45° Pick angle at 45° attack angle with 5mm wear.	95
Figure 6.70	Influence of rpm on Specific energy for 50° Pick angle at 45° attack angle with 5mm wear.	95
Figure 6.71	Influence of rpm on Specific energy for 55° Pick angle at 45° attack angle with 5mm wear.	95
Figure 6.72	Influence of rpm on Specific energy for 65° Pick angle at 45° attack angle with 5mm wear.	95
Figure 6.73	Influence of torque on Specific energy for 45° Pick angle at 45° attack angle.	97
Figure 6.74	Influence of torque on Specific energy for 50° Pick angle at 45° attack angle.	97
Figure 6.75	Influence of torque on Specific energy for 55° Pick angle at 45° attack angle	97
Figure 6.76	Influence of torque on Specific energy for 65° Pick angle at 45° attack angle.	97
Figure 6.77	Influence of torque on Specific energy for 45° Pick angle at 55° attack angle.	97
Figure 6.78	Influence of torque on Specific energy for 50° Pick angle at 55° attack angle.	97
Figure 6.79	Influence of torque on Specific energy for 55° Pick angle at 55° attack angle.	98
Figure 6.80	Influence of torque on Specific energy for 65° Pick angle at 55° attack angle.	98
Figure 6.81	Influence of torque on Specific energy for 45° Pick angle at 65° attack angle.	98
Figure 6.82	Influence of torque on Specific energy for 50°	

	Pick angle at 65° attack angle.	98
Figure 6.83	Influence of torque on Specific energy for 55° Pick angle at 65° attack angle.	98
Figure 6.84	Influence of torque on Specific energy for 65° Pick angle at 65° attack angle	98
Figure 6.85	Influence of torque on Specific energy for 45° Pick angle at 45° attack angle with 5mm wear.	99
Figure 6.86	Influence of torque on Specific energy for 50° Pick angle at 45° attack angle with 5mm wear.	99
Figure 6.87	Influence of torque on Specific energy for 55° Pick angle at 45° attack angle with 5mm wear.	99
Figure 6.88	Influence of torque on Specific energy for 65° Pick angle at 45° attack angle with 5mm wear.	99
Figure 6.89	Influence of cutting force on Specific energy for 45° Pick angle at 45° attack angle.	101
Figure 6.90	Influence of cutting force on Specific energy for 50° Pick angle at 45° attack angle.	101
Figure 6.91	Influence of cutting force on Specific energy for 55° Pick angle at 45° attack angle	101
Figure 6.92	Influence of cutting force on Specific energy for 65° Pick angle at 45° attack angle.	101
Figure 6.93	Influence of t cutting force on Specific energy for 45° Pick angle at 55° attack angle.	101
Figure 6.94	Influence of cutting force on Specific energy for 50° Pick angle at 55° attack angle.	101
Figure 6.95	Influence of cutting force on Specific energy for 55° Pick angle at 55° attack angle.	102
Figure 6.96	Influence of cutting force on Specific energy for 65° Pick angle at 55° attack angle.	102

Figure 6.97	Influence of cutting force on Specific energy for 45° Pick angle at 65° attack angle.	102
Figure 6.98	Influence of cutting force on Specific energy for 50° Pick angle at 65° attack angle.	102
Figure 6.99	Influence of cutting force on Specific energy for 55° Pick angle at 65° attack angle.	102
Figure 6.100	Influence of cutting force on Specific energy for 65° Pick angle at 65° attack angle	102
Figure 6.101	Influence of cutting force on Specific energy for 45° Pick angle at 45° attack angle with 5mm wear.	103
Figure 6.102	Influence of cutting force on Specific energy for 50° Pick angle at 45° attack angle with 5mm wear.	103
Figure 6.103	Influence of cutting force on Specific energy for 55° Pick angle at 45° attack angle with 5mm wear.	103
Figure 6.104	Influence of cutting force on Specific energy for 65° Pick angle at 45° attack angle with 5mm wear.	103
Figure 6.105	Influence of UCS on Specific energy at 45° attack angle for all rocks.	108
Figure 6.106	Influence of UCS on Specific energy at 45° attack angle for all rocks.	108
Figure 6.107	Influence of UCS on Specific energy at 45° attack angle for all rocks.	109
Figure 6.108	Influence of UCS on Specific energy at 45° attack angle with 5mm wear for all rocks.	109
Figure 6.109	Influence of BTS on Specific energy at 45° attack angle for all rocks.	109
Figure 6.110	Influence of BTS on Specific energy at 55° attack angle for all rocks.	109
Figure 6.111	Influence of BTS on Specific energy at 65° attack	

	angle for all rocks.	110
Figure 6.112	Influence of BTS on Specific energy at 45° attack angle with 5mm wear for allpicks for all rocks.	110
Figure 6.113	Influence of Abrasivity of rock on Specific energy at 45° attack angle for all rocks	110
Figure 6.114	Influence of Abrasivity of rock on Specific energy at 55° attack angle for all rocks.	110
Figure 6.115	Influence of Abrasivity of rock on Specific energy at 65° attack angle for all rocks	111
Figure 6.116	Influence of Abrasivity of rock on Specific energy at 45° attack angle with 5mm wear for all picks for all rocks	111
Figure 6.117	Influence of Brittleness on Specific energy at 45° attack angle	111
Figure 6.118	Influence of Brittleness on Specific energy at 55° attack angle	111
Figure 6.119	Influence of Brittleness on Specific energy at 65° attack angle	112
Figure 6.120	Influence of Brittleness on Specific energy at 45° attack angle with 5mm wear for all picks	112
Figure 6.121	Influence of Cutting rate on Specific energy at 45° attack angle	112
Figure 6.122	Influence of Cutting rate on Specific energy at 65° attack angle	112
Figure 6.123	Influence of Cutting rate on Specific energy at 55° attack angle	112
Figure 6.124	Influence of Cutting rate on Specific energy at 45° attack angle with 5mm wear for all picks	113
Figure 6.125	Influence of Depth of cut on Specific energy at 45° attack angle	113

Figure 6.126	Influence of Depth of cut on Specific energy at 55° attack angle.	113
Figure 6.127	Influence of Depth of cut on Specific energy at 65° attack angle.	114
Figure 6.128	Influence of Depth of cut on Specific energy at 45° attack angle with 5mm wear for all picks.	114
Figure 6.129	Influence of UCS on Specific energy at different angles	115
Figure 6.130	Influence of BTS on Specific energy at different Attack angles	115
Figure 6.131	Influence of Brittleness on Specific energy at different Attack angles	115
Figure 6.132	Influence of Abrasivity on Specific energy at different Attack angles	115
Figure 6.133	Plot for comparison between experimental and regression prediction specific energy	117
Figure 6.134	Error plot for specific energy with regression modeling	118
Figure 6.135	Comparisons of Calculated SE and Predicted SE with ANN	119
Figure 6.136	Training Error plot for specific energy with ANN modeling	119
Figure 6.137	Validation Error plot for specific energy with ANN modeling	120
Figure 6.158	Influence of Cutting force on displacement with FEM at 45° attack angle	122
Figure 6.159	Influence of Cutting force on displacement with FEM at 55° attack angle	122
Figure 6.160	Influence of Cutting force on displacement with FEM at 65° attack angle	122
Figure 6.161	Influence of Cutting force on displacement with FEM at 45° attack angle with different picks.	122
Figure 6.162	Influence of density on displacement with FEM at 45° attack angle	122

Figure 6.163	Influence of density on displacement with FEM at 55° attack angle	122
Figure 6.164	Influence of density on displacement with FEM at 65° attack angle	123
Figure 6.165	Influence of density on displacement with FEM at 45° attack angle with 5 mm wears for all picks.	123
Figure 6.166	Influence of UCS on displacement with FEM at 45° attack angle	123
Figure 6.167	Influence of UCS on displacement with FEM at 55° attack angle	123
Figure 6.168	Influence of UCS on displacement with FEM at 65° attack angle	123
Figure 6.169	Influence of UCS on displacement with FEM at 45° attack angle with 5 mm wear for all picks.	123
Figure 6.170	Influence of BTS on displacement with FEM at 45° attack angle	124
Figure 6.171	Influence of BTS on displacement with FEM at 55° attack angle	124
Figure 6.172	Influence of BTS on displacement with FEM at 65° attack angle	124
Figure 6.173	Influence of BTS on displacement with FEM at 45° attack angle with 5 mm wear for all picks.	124
Figure 6.174	Influence of Abrasivity on displacement with FEM at 45° attack angle	124
Figure 6.175	Influence of Abrasivity on displacement with FEM at 55° attack angle	124
Figure 6 176	Influence of Abrasivity on displacement with FEM at 65° attack angle	125
Figure 6.177	Influence of Abrasivity on displacement with FEM at	

	45° attack angle with 5 mm wear for all picks.	125
Figure 6.178	Influence of Brittleness on displacement with FEM at 45° attack angle	125
Figure 6.179	Influence of Brittleness on displacement with FEM at 55° attack angle	125
Figure 6.180	Influence of Brittleness on displacement with FEM at 65° attack angle	125
Figure 6.181	Influence of Brittleness on displacement with FEM at 45° attack angle with 5 mm wear for all picks	125
Figure 6.182	Influence of Cutting force on Von Misses Stress with FEM at 45° attack angle	127
Figure 6.183	Influence of Cutting force on Von Misses Stress with FEM at 55° attack angle	127
Figure 6.184	Influence of Cutting force on Von Misses Stress with FEM at 65° attack angle	127
Figure 6.185	Influence of Cutting force on Von Misses Stress with FEM at 45° attack angle with 5 mm wears for all picks.	127
Figure 6.186	Influence of density on Von Misses Stress with FEM at 45° attack angle	128
Figure 6.187	Influence of density on Von Misses Stress with FEM at 55° attack angle	128
Figure 6.188	Influence of density on Von Misses Stress with FEM at 65° attack angle	128
Figure 6.189	Influence of density on Von Misses Stress with FEM at 45° attack angle with 5 mm wear for all picks.	128
Figure 6 190	Influence of UCS on Von Misses Stress with FEM at 45° attack angle	128
Figure 6.191	Influence of UCS on Von Misses Stress with FEM at	

	55° attack angle	128
Figure 6.192	Influence of UCS on Von Misses Stress with FEM at 65° attack angle	129
Figure 6.193	Influence of UCS on Von Misses Stress with FEM at 45° attack angle with 5 mm wear for all picks.	129
Figure 6.194	Influence of BTS on Von Misses Stress with FEM at 45° attack angle	129
Figure 6.195	Influence of BTS on Von Misses Stress with FEM at 55° attack angle	129
Figure 6.196	Influence of BTS on Von Misses Stress with FEM at 65° attack angle	129
Figure 6.197	Influence of BTS on Von Misses Stress with FEM at 45° attack angle with 5 mm wear for all picks.	129
Figure 6.198	Influence of Brittleness on Von Misses Stress with FEM at 45° attack angle	130
Figure 6.199	Influence of Brittleness on Von Misses Stress with FEM at 55° attack angle	130
Figure 6.200	Influence of Brittleness on Von Misses Stress with FEM at 65° attack angle	130
Figure 6.201	Influence of Brittleness on Von Misses Stress with FEM at 45° attack angle with 5 mm wear for all picks.	130
Figure 6.202	Influence of Abrasivity on Von Misses Stress with FEM at 45° attack angle	130
Figure 6.203	Influence of Abrasivity on Von Misses Stress with FEM at 55° attack angle	130
Figure 6.204	Influence of Abrasivity on Von Misses Stress with FEM at 65° attack angle	131
Figure 6.205	Influence of Abrasivity on Von Misses Stress with FEM at 45° attack angle	131

Figure 6.206	Influence of density on RCR with Experimental values and FEM values	132
Figure 6.207	Influence of UCS on RCR with Experimental values and FEM values	132
Figure 6.208	Influence of BTS on RCR with Experimental values and FEM values	132
Figure 6.209	Influence of Abrasivity on RCR with Experimental values and FEM values	132
Figure 6.210	Influence of Brittleness on RCR with Experimental values and FEM values	132

List of Tables

Table No.	Description	Page No.
Table 3.1	Details of parametric variations investigated	41
Table 3.2	Mechanical properties of rock samples tested	46
Table.3.3	Calibrations chart of cutting tool dynamometer	49
Table.4.1	Performance of Neural Network with different hidden neurons	68
Table 6.1	ANOVA results (F tests)	106
Table.6.2	Regression model summaries	107
Table.6.3	Significance of model components with student's t-test	107
Table 6.4	Performance indices of regression models of all pick	117
Table 6.5	Performance indices of ANN models of all attack angles	120
Table 6.6	Comparison of Regression and ANN models of all attack angles	120

NOMENCLATURE

SE	Specific energy
UCS	Uniaxial Compressive Strength
BTS	Brazilian Tensile Strength
ISRM	International Society for Rock Mechanics
ANN	Artificial Neural Network
VAF	Variation Account For
RMSE	Root Mean Square Error
MAPE	Mean Absolute Percentage Error
FEM	Finite Element Method
RPM	Revolution per Minute
ICR	Instantaneous Cutting rate
MRDE	Mining Research and Development Establishment
NCB	National Coal Board
RCR	Rock cutting Resistance
RMCI	Rock Mass Cuttability Index
TBM	Tunnel Boring Machine
USBM	United States Bureau of Mines

CHAPTER 1

INTRODUCTION

A coal drill or a cutting machine depends on the penetrative action of a wedge of some shape or form into the surface of coal and rock face. In the case of a hand pick, a single wedge is repeatedly struck on the face. The force and position of the blow are left to the mine worker's experience and judgment. The intelligence of the miner and his inherent physical flexibility provides him with additional variables in the use of the wedge. No mining machine is certainly as efficient as a man in terms of the coal produced per unit of work done. However, mining machines can concentrate more power vastly in the confines of a coal face than that obtained from the workforce. A large number of high-powered, fast-moving wedges can be used in a machine to cut coal seamlessly, but doing so in a non-thinking repetitive fashion, unresponsive to the type of opportunity for ease of extraction could result in the unexploitation of the knowledge of coal extraction. (Roxborough et al. 1981).

Fundamentally, coal breakage refers to forcing the cutting tool into the rock under the thrusting action of the cutting machine. When the stresses induced in the rock due to the penetrating action of the tool exceed its compressive strength or tensile strength, the rock fails by forming fragments. Cutting tools provide the energy required to break the rock from the machine. Therefore the efficiency of the tool depends on the operational parameters like RPM, cutting force, torque, the weight of the cutting machine and rock properties like uniaxial compressive strength, tensile strength bear a significant effect on the efficiency of the mechanical excavating machine (Colorado School of Mines, 1999).

Rock excavation by point attack pick is crucial to the productivity of the rock cutting machine. Accurate prediction of the cutting force and Specific energy help improve cutting efficiency and estimate the cutter head torque and the machine's power for different rock types. Therefore, prediction of the cutting force and Specific energy has become salient and has attracted many mining researchers and experts to work on these parameters (Bilgin et al. 1996, Mishnaevsky, 1998, Hood, 2000; Inyang, 2002;

Bilgin et al. 2006). Evans (1982) developed a cutting force model assuming that frictionless penetration of a point attack pick will give rise to radial compressive stress and hoop tensile stress in the rock. However, when the tensile stress in the rock exceeds more than its tensile strength, breakage occurs, inducing asymmetric, V-shaped fragments in the end. Besides, it is also assumed that the normal contact pressure between the pick and the rock distributes uniformly and circumferentially along an imaginary hole. The predicted force could be considered a reference to select the suitable power of the cutting machine. However, Goktan (1995) found that the estimated force deviated considerably from measurements in rock cutting.

Several researchers have come forward to improve Evan's cutting theory (1958) (Evan's theory states that the failure of homogeneous material under stress when there is an appreciable departure from the linearity between stress and strain that is observed during elastic behavior) based on the cutting action of a symmetrical chisel pick on coal. Roxborough et al. (1995) and Goktan et al. (1995) are not agreed with Evan's theory because friction angle was not considered in the model. Goktan et al. (2005) found that in spite of considering the friction angle, the predicted peak cutting force was still much lower than the actual measurements in full-scale laboratory experiments. They demonstrated that the effect of attack angle (defined as an angle between the tool axis and the tangent of the cutting path) in these two models led to inconsistency. Later, they added the rake angle (the angle between the front or cutting face of the tool and a line perpendicular to the rock) to Evan's formula based on their full-scale experimental data. However, a fundamental understanding of the chip's mechanism is lacking. Many similar studies were carried by Goktan et al. (2005) on the rock cutting process and validated the importance of the attack angle, which is now considered as an essential geometrical parameter in optimizing cutting efficiency. However, the incorporation of the attack angle effect in estimating the cutting force remains empirical.

Selection of pick for soft or hard rock conditions can drastically increase the cost of the cutting operation. Therefore, predicting the suitable pick and machine type emerges to be very important in cutting operation (Fowell and McFeat-Smith, 1987).

The selection of cutting tools for rock and coal excavation has a substantial influence on machine performance. Drag tools with an extended life span are crucial for a successful excavation operation. Worn and damaged tools generate high cutting forces that are often higher than those recorded for sharp tools (Altinoluk, 1981). The machines on which drag tools are employed are slewing force limited (the angle of rotation of the road header boom (upper/lower or right/left)) and haulage force limited (Horizontal movement of coalface shearers). The worn tools reduce the cutter's advance per revolution. Abrasion results in heat generation of the tool, resulting in the rapid development of the tool wear, causing a further drop in performance.

Point attack picks are categorized among tangential picks that generally consist of a conical tungsten carbide tip inserted symmetrically into a cylindrical body; therefore, the pick axis is in line with the conical tip (Figure 1.1). Earlier, point attack picks had considerable application in coal cutting; however, they are no longer preferred in this field. They are increasingly employed in medium and hard rock cutting and have become an inevitable tool on medium and heavy-duty road headers (Fowell and McFeat-Smith, 1987).

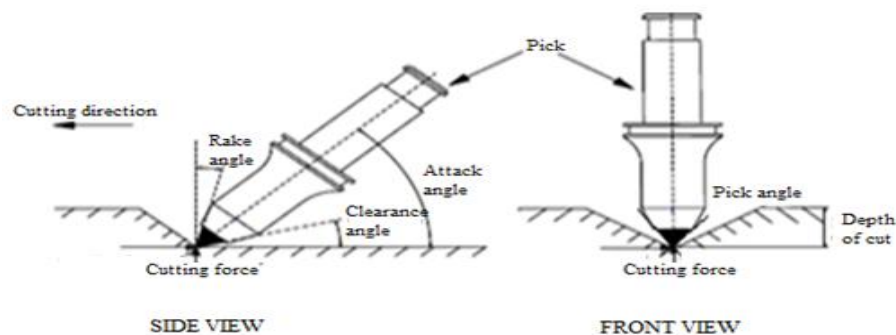


Figure 1.1 Point attack picks

In contrast to the radial pick, the point attack tool is distinguished by its self-sharpening character resulting from the action of rotation of the pick in the holder. Therefore, these picks practically last longer than other picks. Laboratory investigations carried by (Hurt and Evans, 1981) on three different picks have shown that point attack picks generate the highest tool forces in sharp conditions. However, tools had the lowest forces when they become blunt after 600m of cutting. The longer service life of the point attack tools provides an uninterrupted, efficient excavation operation, provided they rotate during the cutting operation. The pick rotation is

practically due to operational and design reasons. It is claimed that introducing an offset angle (the angle between a plane perpendicular to the cutter axis and a plane tangent to the surface of the revolution of the cutting edges) may assist pick rotation. An optimum value for this angle is presently unavailable and is reported to vary according to the cutting head type (Kleinert, 1982).

The attack angle provides good contact between the pick and the rock, while failure to position the pick at its correct position will significantly alter the practical tool geometry. The kinematic requirements are also considered 50° since the lowest cutting forces are generated with picks of 75° cone angle (Evans, 1982). When cutting hard rock, the cone angle was increased; consequently, the rake angle emerges to be smaller. In order to offset the value of clearance angle (the angle between the flank surface and the cutting velocity), the attack angle has to be larger (e.g., at 90° cone angle, the attack angle should be at least 55°). It is also reported that, this angle should not exceed 48° at a high rotational speed (Kleinert, 1982).

The coal cutting was characterized by a rapid linear increase in the force acting on the pick during penetration. Eventually, this force exceeds the strength of the coal, and a coal chip is produced and a rapid reduction of pick force. The coal chips extend ahead of the pick, latter then advancing under zero or negligible force until it re-engages a fresh coal surface, after which the formation process of chips is repeated (Roxborough et al. 1981). Although coal was known to possess time-dependent stress-strain properties, these properties are of no practical significance during cutting, even at the slowest speeds. From this standpoint, coal can be regarded as a brittle rock. Evan's model provides a valuable analytical insight into the mechanics of coal chip formation by a wedge.

Evan's cutting theory, which is entirely consistent with the laboratory experiment, shows that the cutting force acting on a pick is linearly proportional to the depth of the cut. Low Specific energy (i.e., the work done or energy consumed to produce unit volume or mass of coal) implies a high efficiency. The capability of excavation machines to drive in and effectively cut the firm rock and cutting tools to resist high forces. Mean and peak cutter forces acquired with high reliability from the linear cutting tests are essential for a given rock condition. The force acting on a cutting tool

constantly changes in magnitude during a cutting process due to the chips and the brittle nature of the rock. Averages of all forces change during the cutting action course, giving that mean cutter forces and mean peak forces are the averages of peak forces for a given cutting condition. High forces may result in serious fracture damage to the tungsten carbide cutting tip and the machine components, in addition to an exceedance of the machine's torque and thrust capacities. Therefore, it is essential to understand the basic aspects of rock cutting mechanisms both theoretically and practically to reduce the cost incurred during testing with the excavation machine in the field.

The efficiency of a given rock cutting process is measured by the parameter Specific energy, which is defined as the amount of work done in excavating a unit volume of rock. Specific energy is the most widely used parameter to measure the efficiency of a rock cutting system within a given rock, with lower values indicating higher efficiencies.

Specific energy is an essential parameter in rock cutting using a particular breakage method. It can also be considered as an essential aspect of the mechanical efficiency of a rock cutting process to specify drill/cutter conditions and rock quality, such as strength, hardness, abrasivity and texture. However, it is highly reliant on the mode of rock breaking and the form and dimension of the equipment used. There are many methods of evaluating specific energy, but results are only comparable if the cutting or the apparatus is the same. Specific energy was also used concerning different excavation methods to evaluate efficiency (McFeat and Fowell, 1977; Aleman, 1982; Rogers et al. 1991). Specific energy is a quick means of assessing rock drillability (Fowell and McFeat-Smith, 1987). Teale (1965) defined specific energy as the energy required to remove a unit volume of rock.

The concept of specific energy by Hughes (1972) and Mellor (1972) has been used for many decades in evaluating the efficiency of the cutting processes and excavation of rock masses. It is a factor that can be resolved in real-time from the data on the efficiency of a rock cutting machine.

Rock fracture analyses using numerical methods have gained popularity with the advent of higher computing power. Several methods, such as finite element method (FEM), discrete element method (DEM), boundary element method (BEM) and hybrid FEM/DEM, have been successfully used in the study of fracture mechanics of rock. FEM is used in this research to quickly model both the continuum and the discontinued state of a material.

The present investigation is carried out to assess (estimate) and predict (value obtained from the statistical model) the specific energy in rock cutting for different pick-angles and different attack angles for each pick-rock experimentally. In this study, the trends in the specific energy of point attack pick on different rocks are obtained experimentally and predicted specific energy with regression and ANN.

1.1 Motivation and Aim of the Thesis

This thesis aims to improve the understanding of the rock cutting process and mechanisms, mainly to gain a better insight into the interaction between tools and rocks at different attack angles and pick angles and operational parameters on specific energy through experimental and numerical studies. An extensive, theoretical and experimental analysis of rock cutting with point attack picks was specifically conducted and numerical modelling was performed to determine the depth of cut and the new concept of rock cutting resistance is predicted; regression and Artificial neural networks were developed to predict specific energy.

CHAPTER 2

LITERATURE REVIEW

2.1 Introduction

Mechanical rock cutting is a technique that has been changing gradually for many years. Primary enhancements are centred on metallurgical improvements and advancements in the engagement of tools with the face. Mechanised rock cutting traditionally makes use of tools that are dragged across the face, typically driven by a rotary drum for removing the coal. These tools are commonly named either point attack, or radial drag picks because these terms best describe the generic method of engaging the coal.

2.1.1 Cutting mechanism

The rock cutting mechanism was initially investigated in the early 1950s to obtain a deep understanding of the mechanical behaviour of the rock. As reported in the studies of Lindqvist (1982) and Mishnaevsky (1993, 1998), rock fracture under point attack pick in rock cutting typically undergoes three stages, building up of the stress field, forming of the crush zone, and cracking and chipping of the subsurface rocks. The details of the processes are described in detail in the subsequent sections.

2.1.2 The initial stage of cutting

Lindqvist (1982) and Mishnaevsky (1993, 1998) observed a consolidation and deflection process in the rock with a further surface deformation before the failure happened. Successively, Moscalev (1972) reported that the surface destruction induced the formation of the destroyed layers and then the crushed rock. Evans (1981) and Australian Tunnel Society (2007) reported that in sharp penetrations with a point attack pick, a three-dimensional stress region is formed, as shown in Figure 2.1. Increased force induces the gradual densification of the porous rock in this region, followed by a series of radial cracks, which radiate away from the axis of the pick.

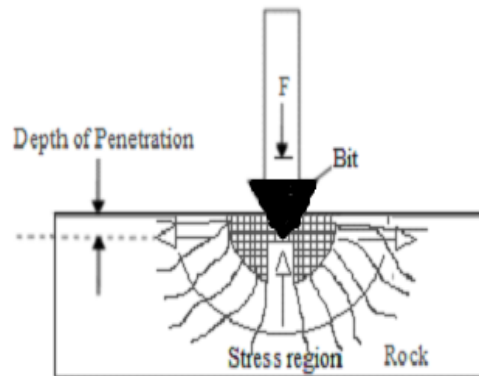


Figure 2.1 Pressure bulb during penetration

The radial cracks produced were not sufficiently dominant to develop bigger chips and led to the production of fine dust, which had a high potential for coal dust ignition. Respirable dust may be produced by microstructures of cut rock, in which the rock is more easily pulverised into micro or nanoparticles (Zeuch et al. 1985).

2.1.3 Crush zone and dust generation

The stress region is enlarged and then transited into a crush zone after the densification process of the rock (Australian Tunnel Society, 2007). Research was carried out to clarify the formation of the crush zone. Zeuch (1985) described that the fractures are nucleated in the rock of the pick tip to form an crushed and powdered region at the trailing edge of the chip. Zeuch (1985) also suggested that the formation of the crush zone might reflect the dominance of the intense tri-axial compression, which is relevant to the shear behaviour. Lindqvist (1983) pointed out that the crushed zone in sandstone and granite is formed with inelastic deformation by the shear action and brittle fracture. Blokhin (1982) and Nikiforovsky (1979) further demonstrated that shear failure over the slip lines results in the crush zone.

During crushing, dust and fine grains are generated. Evan's (1958) conducted rock cutting experiments to explore the internal mechanism of the crush zone and found that the radial cracks lead to fine chips. Howarth et al. (1988) further pointed out that dust or fine chips are induced explicitly by two major processes, the crushing near the pick tip and the shear fracturing on the macro crack surfaces, as shown in Figure 2.2. Zipf (1989) also suggested that rubbing contact between the pick and macro crack surfaces is a major source of fine-grain creation.

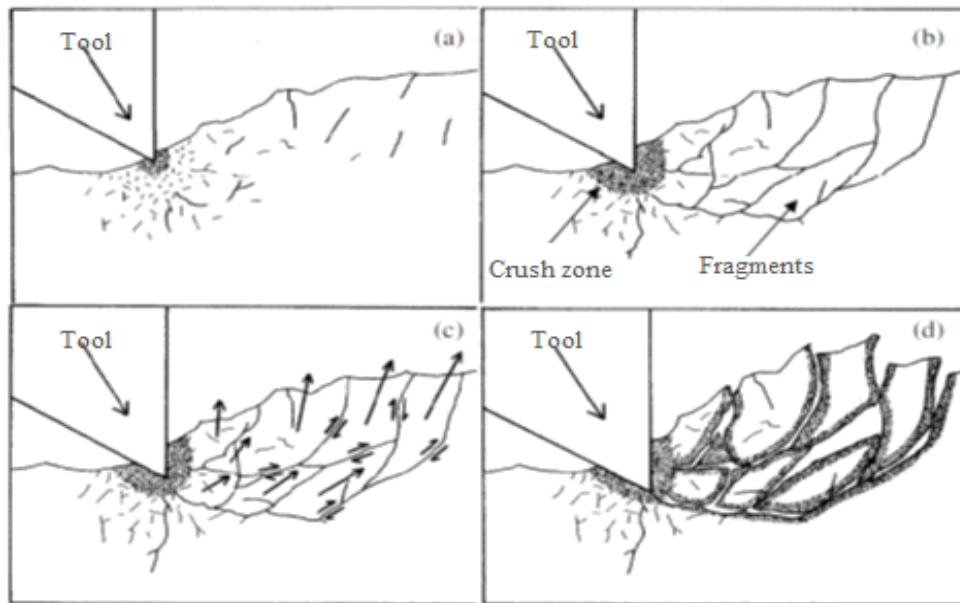


Figure 2.2 Evolution of crush zone and chips (Zipf, 1989)

Zipf (1989) further pointed out that fine-grain generation is also affected by the size of the crush zone which is dominated by pick geometry and attack angle. Therefore, it is of interest that observation and comparison of fine grains can be used to evaluate the efficiency of the pick.

2.1.4 Formation of crush and rock chips

It is noteworthy that crushing is hard to be avoided as the cutting pick creates a major crack until the crush zone expands to a certain level. Research work has been carried out relating to the formation of the crush zone, crack propagation and chips failure in the past 50-60 years. Evan's (1958) proposed that a rock chip is induced by the action of tensile stress. Hood (2000) indicated that the drag pick induces tensile cracks to form chips. Grey (1962) considered that the chip's trajectory takes a logarithmic contour and the initial cracks are formed by shear stress. Later, Mishnaevsky (1995) demonstrated that the cracks (a line on the surface along which it has split without breaking apart) and failure (stressed beyond its ultimate strength and breaks apart) produced are tensile and shear stress modes.

Therefore, further understanding of the crack mechanism became crucial due to its relevance in forming chips. Experimental and numerical investigations were undertaken by (Hoek et al. 1965; Wang et al. 1976; Zeuch et al. 1983; Saouma et al.

1984; Guo et al. 1992; Korinets et al. 1996; Tang, 1997; Kou et al. 1999; Liu, 2002) to explore the crack mechanism using the drag pick. Lindqvist (1984) found that the prediction of crack propagations can be realised by stress analysis during fragmentation by simulated tests. Besides, numerical modelling was also used to explore the fundamental mechanism of crack propagations. Wang et al.(1976) and Saouma et al.(1984) found that the finite element method can be well applied to simulate the crushing, cracking and fragmentation processes. Korinets et al. (1996) successfully used LS-DYNA software to simulate the crack propagation of rock cutting. Tang (1997). Kou et al.(1999) and Liu (2002) set up 2D models to plot the crack path with consideration of Mode I (applied to the crack opening) and Mode II (applies to the crack sliding) stress intensity factors for the mixed mode of fracture. Kou et al.(1999) and Liu (2002) confirmed that fracture mechanics could be a good tool to investigate rock fracture.

Integrating all features from previous researchers on simulation of rock fragmentation, Guo (1992) successfully predicted the crack path at different rake angles with a good match to the stress calculations. Guo's predictions were based on the set-up of a linear rock cutting model by using a displacement discontinuity method and linear elastic mechanics. As a whole, experimental and simulated results demonstrate that theoretical stress calculations can be used to analyse the crack path during rock fragmentation. The crack becomes unstable when it propagates to a certain length (Wei et al. 2003), and the chips are formed. In order to examine the relationship between chip's dimensions and other variables, such as cutting force and Specific energy, Evans (1962), Nishimutsu (1972), Roxborough (1973) and Finnie et al. (1977) approximated the chips geometry to model the peak cutting force with two basic assumptions, all broken chips had the same geometry, and the top rock surface was smooth without preceding cuts. Thus, by focusing on chips formation, the cutting force can be formulated by pick and chip's geometry and rock properties with validation of experimental results on some rock specimens. However, their assumptions are no longer valid in continuous cutting. To a large extent, the rock surface is affected by previous cuts, and it is hard to quantify its influence. Even in a homogeneous rock, chip's are present in many different shapes and sizes. Instead of using a deterministic description of the rock chips, Evan's (1962) statistically analysed

the chip's dimensions, in which a mathematical function describes the surface area of the chip. Poisson's distribution is found to be suitable for describing the distribution of the chip's size. The chips may be regarded as a group of similar size, and therefore, the total surface area of fracture can be calculated by using the mathematical function and size of the group. It demonstrates that statistical analysis could link the chip's size and total surface area of the fracture, which is closely related to the fracture energy based on Griffith's theorem. Hence, cutting efficiency can be investigated by the total fracture surface energy concerning the total cutting energy.

In summary, a deep understanding of the formation of cracks in relation to chips paves the way for further investigations on the cutting process of brittle and porous rocks related to cutting force and Specific energy prediction.

2.2 Research on cutting force and Specific energy in rock cutting

From the past 50 years, an acceptable amount of work was carried out by different investigators on theoretical aspects of the rock and coal cutting process. Among all theories, the most commonly accepted theory was formulated by Evan's (1958) cutting model for point attack picks and conical pick of the cutting tools, as shown in Eq 2.1, 2.2. Also, many of the investigators have modified Evan's (1958) theory for point attack and conical picks of the cutting tool (Nishimatsu's 1972, Hurt 1981, Ranman 1985 and Roxborough 1985). The theories related to coal and rock cutting processes are insignificant to understand the overall effect of the cutting process. Due to geological formation, mineralogical, petrographic, anisotropic of rock and coal varies from one source to another (Bilgin, 1977). Hence, along with the theoretical background, suitable laboratory experiments must be carried out to understand the effect of cutting forces.

A number of investigators have formulated mathematical models to advance the excavation machines design and find the best configuration of cutting tools for the efficient cutting process (Evenden et al. 1985). The original effort on rock cutting mechanism was carried out by Evan's and Pomeroy, (1966). Evan's established theoretically that tensile strength and compressive strength are important rock properties with point attack picks and point attack tools in rock cutting, as formulated

below in Equations. 2.1 and 2.2 and Figure 2.3 Schematic of Evan's tensile breakage theory.

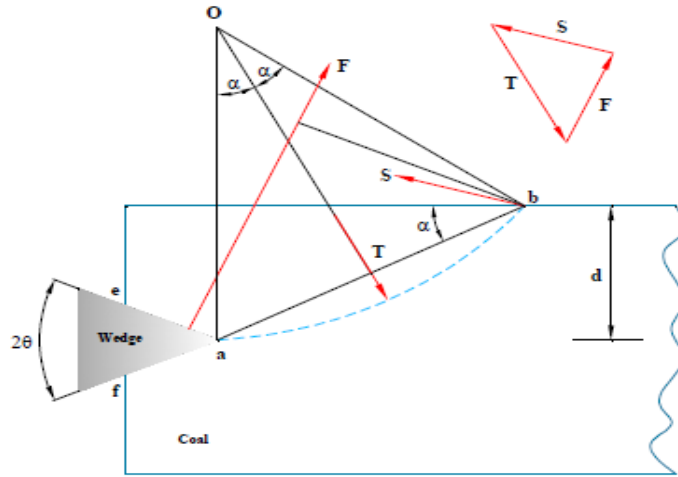


Figure 2.3 Schematic of Evan's tensile breakage theory

$$F_c = \frac{2\sigma_t d w \sin \frac{1}{2} \left(\frac{\pi}{2} - \alpha \right)}{1 - \sin \frac{1}{2} \left(\frac{\pi}{2} - \alpha \right)} \quad (\text{kN}) \quad (2.1)$$

where

F_c = Cutting force (kN)

σ_t = Tensile strength of rock (MPa)

d = Depth of cut (mm)

w = Tool width (mm)

α = Rake angle (degrees)

$$F_c = \frac{16\pi d^2 \sigma_t^2}{\cos^2 \left(\frac{\theta}{2} \right) \sigma_c} \quad (\text{kN}) \quad (2.2)$$

where

F_c = Cutting force (kN)

σ_t = Tensile strength of rock (MPa)

d = Depth of cut (mm)

σ_c = Compressive strength of rock (MPa)

θ = Tip angle (degrees)

Evan's (1966) also formulated optimum spacing for point attack picks as three to four times the pick width.

Roxborough (1973) established that calculating the cutting force experimentally for point attack picks and calculating theoretically using Equation 2.1 are one and the same. Guo et al.(1992) showed that compared to conventional rock mechanics methods (such as the well-known Mohr-Coulomb failure criterion), linear elastic fracture mechanics could provide greater insight into the rock cutting mechanisms. Guo et al.(1992) elaborate the fracture mechanics advancement presents detailed information on progressive crack failure, crack propagation path, corresponding load requirement and stability of the crack propagation.

Goktan (1997) recommended a revision on Evan's cutting theory for point attack tools as indicated in Equation 2.3 and proved that the obtained values of force both with equation and previously published experimental values are close to each other.

$$F_c = \frac{4\pi\sigma_t d^2 \sin^2\left(\frac{\alpha}{2} + \psi\right)}{\cos\left(\frac{\alpha}{2} + \psi\right)} \quad (\text{kN}) \quad (2.3)$$

where

F_c = Cutting force (kN)

σ_t = Tensile strength of rock (MPa)

d = Depth of cut (mm)

α = Rake angle (degrees)

ψ = Friction coefficient between the cutting tool and rock

Roxborough et al. (1995) recommended revising the cutting theory of Evan's for point attack tools as indicated in Equation 2.4. They suggested that, with Grindleford sandstone, the mean peak cutting force predicted were in good agreement with modified cutting theory.

This result was obtained at a 16° friction angle using a steel block and a natural flat rock surface.

$$F_c = \frac{16\pi\sigma_c d^2 \sigma_t^2}{\left[2\sigma_t + (\sigma_c \cos\left(\frac{\theta}{2}\right) \left(\frac{1 + \tan\psi}{\tan(\psi/2)}\right))\right]^2} \quad (\text{kN}) \quad (2.4)$$

F_c =Cutting force (kN)

σ_c =Compressive strength of rock (MPa)

d =Depth of cut (mm)

σ_t = Tensile strength of rock (MPa)

θ = Tip angle (degrees)

ψ = Friction coefficient between the cutting tool and rock

Nishimatsu (1972) found that shear strength failure is essential in cutting high strength rocks as formulated below in Equation.2.5.

$$F_c = \frac{2\sigma_s d w \cos(\psi - \alpha) \cos(i)^2}{(n+1) [1 - \sin(i + \psi - \alpha)]} \quad (\text{kN}) \quad (2.5)$$

Where F_c = Cutting force (kN)

σ_s = Shear strength of rock (MPa)

d = Depth of cut (mm)

w = Tool width (mm)

ψ = Friction coefficient between the cutting tool and rock

α = Rake angle (degrees)

i = Internal friction angle (degrees)

$$n = 12 - (\alpha/5)$$

An important factor to be considered for excavation efficiency was to design of cutting drum and head for shearers, roadheaders and continuous miners. In the past, significant laboratory and in situ investigation works were carried out in this respect on rock and coal excavation. Hekimoglu and Fowell (1990) state that by a proper design of its cutting head, dangerous vibration of the cutting head can be rectified. At 65°–70° tilt angles (the angle between the axis of the pick and the normal direction of the rock surface being cut by the pick) offered lower Specific energy and the relative freedom from vibration problems.

Hurt et al.(1982) in previous National Coal Board (NCB) and Mining Research Development Establishment (MRDE) studies investigated in detail to increase production and efficient design of cutting head and to reduce cutting head vibration, and to reduce wear of components (Hurt et al.1981,1982,1985,1988). They recommended that, by efficient cutting head design, cutter force can be estimated. MRDE mainly concentrated on rock cutting mechanism of point attack cutter tools

performance (Hurt 1979, 1980; Hurt et al. 1980; Hurt et al. 1981). The results obtained are summarised as follows,

1. Sharp point attack tools generate higher forces than wedge tools.
2. Point attack tools might resist higher forces and last longer than wedges in abrasive rocks.
3. At an attack angle of 50° corresponding to 12° back clearance angle, point attack tool exhibited minimum cutting forces.
4. During cutting, at 30° tilt angle had no greater effect on the tool forces. However, the tilt angle reduces pick damage and helps rotate the cutters, resulting in uniform blunting (not self-sharpening) and extended tool life.

United States Bureau of Mines (USBM) carried out experimental studies and accepted the results obtained by MRDE on rock cutting mechanisms. Radial picks appeared to assist coal cutting in the tensile mode, while point attack picks show to chip the coal with a more complex mode of failure (Sundae et al. 1987). The depth of cut is found to be the main significant factor affecting Specific energy, cutter forces and airborne respirable dust (Roepke et al.1984). These are well-summarised works published in "Comprehensive Rock Engineering" (Fowell, 1993).

Roxborough et al. (1981) carried out experimental studies to prove that some of the theories of coal cutting are applicable to the continuous miner and found that the normal and cutting forces acting on a cutter increased linearly with the depth of cut. Pick spacing has to be considered relative to the depth of cut, the point attack-shaped picks are more efficient than the pointed shape tools only at relatively shallow depths of cut. The pointed pick is proved to be consistent of a more efficient shape at comparatively large depths. There was no evidence to suggest that pick speed affected cutting forces and Specific energy (Roxborough et al. 1981; Roxborough et al. 1982). Specific energy is one of the most vital factors in determining the efficiency of cutting systems and is defined as the work to excavate a unit volume of rock. Hughes (1972) and Mellor (1972) demonstrated that Specific energy might be formulated as expressed in Equation 2.6 and 2.7.

$$SE = \frac{\sigma_c^2}{2E} \quad (\text{J/m}^3) \quad (2.6)$$

where SE=Specific energy (J/m^3)

E = Secant elasticity modulus from zero to failure load (GPa)

σ_c =Compressive strength of the rock (MPa)

Detailed rock cutting tests, however, showed that Specific energy is not only a function of rock properties but also closely related to operational parameters, such as rotational speed, cutting power of excavation machines and tool geometry. Roxborough reported that Specific energy decreased dramatically to a certain level with an increasing depth of cut and decreasing tool angle (Roxborough et al.1973, 1975, 1985).

The cutting efficiency basically depends on the depth of cut and the interval between the cuts is shown in Figure 2.3. If the interval is too small (a), this leads to over crushing and high tool wear resulting from friction during the interaction of tool and rocks, which is well illustrated in Johnson and Fowell's work (Johnson and Fowell.,1986). The investigators found a decrease in tool consumption with arching force (force of the boom to rock penetration). In unrelieved cutting, the rubbing and shallow penetration resulting significant consumption of tools increased. In a drilling operation, it is also illustrated that the insufficient thrust resulting in tool consumption increased Referring to Figure 2.4 (Ergin et al. 2000).

If the interval is too large (c), efficient cutting cannot be performed as failure to generate relieved cutting (adjacent cuts failure to interact with tensile cracks in forming a chip), the groove is created. For the appropriate interval to cut depth ratio, the Specific energy is minimum (b). Generally, between 1 and 5 are the optimum cutter interval ratio to cut depth for pick cutters.

Roadheader cutting modes also affect the in situ Specific energy values. McFeat-Smith defined four distinct cutting modes for roadheaders, over-cutting (coal cutting are used to cut just below the roof), undercutting (coal cutting are used in watery mines to cut just above the floor level), sumping (the preliminary undercut in the face of coal made by a roadheader), and traverse cutting (a lateral move or going mainly sideways rather than up or down) (McFeat., 1978). Fowell and McFeat-Smith observed that higher Specific energy required for sumping resulted in an inefficient method of excavation compared to traversing (Fowell and McFeat-Smith., 1976). These modes of cutting are related linearly by the following Equation2.7.

$$SE_{\text{sumping}} = 3SE_{\text{traversing}} \quad (\text{J/m}^3) \quad (2.7)$$

where,

SE_{sumping} and $SE_{\text{traversing}}$ are in-situ Specific energy requirements during sumping and traversing, respectively.

Farmer and Garrity(1987) and Pool (1987) showed that instantaneous cutting rate m^3/h and specified cutting power could be predicted from specific energy values as illustrated in Equation.2.7. Krupa et al. (1994) and Sekula et al. (1991) observed that the tunnel boring machine advance rate could be predicted from Specific energy as formulated in

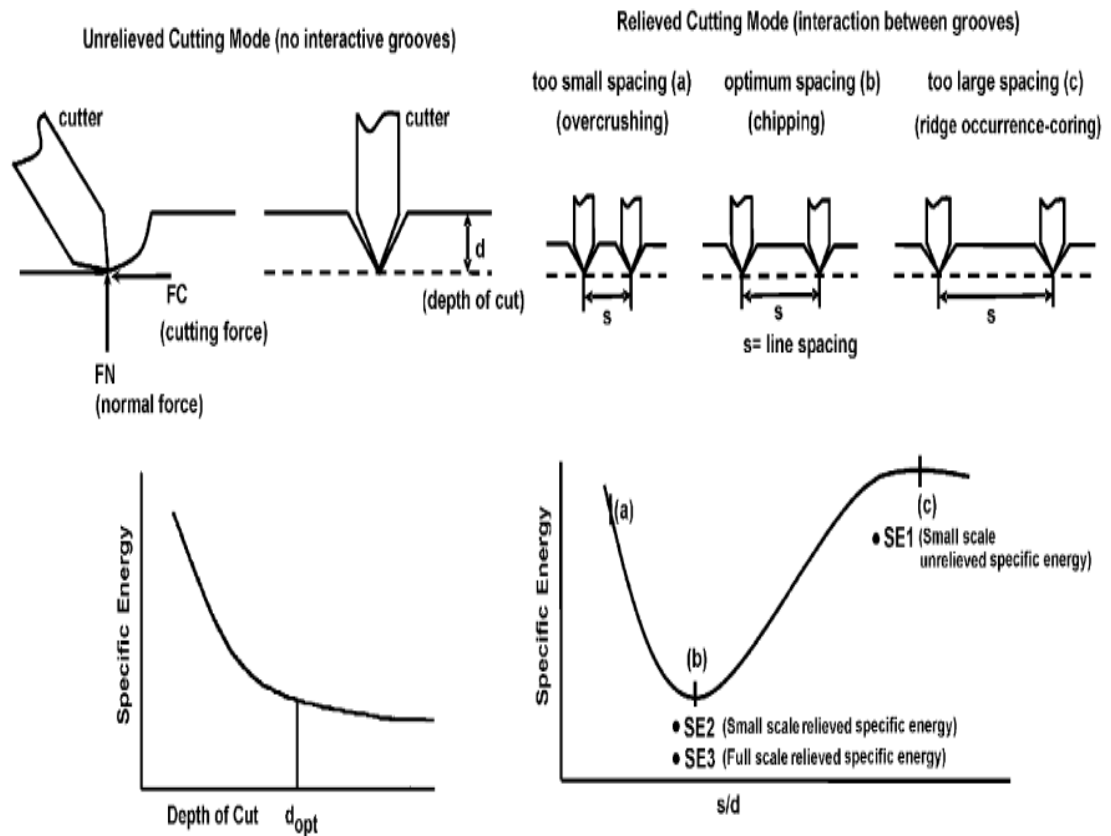


Figure 2.4 The general effect of cutter spacing on Specific energy

Equation 2.6. Kahraman et al. (2003) proved that the penetration rates of percussive drills can be estimated from Specific energy values calculated from Equation 2.6.

McFeat-Smith et al.(1976) illustrated that the performance of roadheader can be estimated from Specific energy. The in-situ Specific energy was measured with Bretby power transducer. They observed that roadheader cutting rate increased with a

reduction in values of in-situ Specific energy. However, they found that cutting rates has a major effect on geological weakness planes, such as joints, bedding planes and fissures. They found that Specific energy reduces with an increase in breaking index, and it is defined as a number of weaknesses intersecting vertical and horizontal scan line per meter. Fowell and Johnson (1982) correlated roadheaders cutting rate and rock mass rating of geological formation (Fowell and Johnson, 1982, 1991, Fowell et al. 1984).

Widely recognised rock classification and the inference of roadheader performance is based on the Specific energy found from the core cutting test (Fowell and Johnson, 1982, Fowell et al.1984, 1994). The test involved instrumented cutting tests on 76mm diameter cores at a 5mm depth of cut, cutting speed of 150 mm/s with a point attack-shaped tungsten carbide tool having 10% cobalt by weight, 3.5-mm nominal grain size, rake angle of (-5°), back clearance angle of 5°, and tool width of 12.7 mm. Detailed laboratory and in-situ investigations carried out by Fowell and McFeat-Smith showed that there is a close relationship between Specific energy values obtained from core cutting tests and cutting rates of medium and heavy-weight roadheaders (Fowell and Johnson, 1982, 1991, Fowell et al.1984, 1994). They formulated core cutting Specific energy as in Equation 2.8.

$$SE = -0.65 + 0.41CI^2 + 1.81k^{1/3}2.6 \quad (J/m^3) \quad (2.8)$$

where

SE= laboratory Specific energy (J/m³)

CI = cone indenter value

k = plasticity index.

The researchers also reported that tool consumption might be predicted from weight loss of cutter used in core cutting test and Cerchar abrasivity tests (McFeat et al. 1979; Fowell et al. 1982; Johnson et al.1984, 1986).

A paper published by Fowell et al.(1994) described large instrumented cutter tests conducted on full-scale boom tunnelling research rig that led to the development of performance prediction models.

Rock cuttability classification based on the core cutting test was usually criticised because the effect of rock discontinuities was not well reflected in performance prediction. Bilgin and co-workers developed a performance predictor equation based

on rock compressive strength and rock quality designation as given in Equations. 2.9 and 2.10 (Bilgin et al.1996, 1997).

$$ICR=0.28 P (0.974)^{RMCI} \quad (m^3/hr) \quad (2.9)$$

Where ICR = the instantaneous cutting rate of roadheaders in m³/h,

P = power of cutting head (HP),

RMCI= rock mass cuttability index,

$$RMCI=\sigma_c (RQD/100)^{2/3} \quad (2.10)$$

RMCI= rock mass cuttability index,

σ_c = uniaxial compressive strength in (MPa)

RQD = rock quality designation in percentage.

Bilgin et al. (1996, 1997) and Fowell et al. (1994) compared the models described in a research work at Kambalda Mine where Voest Alpine AM75 roadheader was used. Two distinct groups of data were evident. The data was grouped around Bilgin's line and strongly influenced by the jointing and weakness zones in the rock mass. The other group of data on the line was produced by Fowell and McFeat-Smith (1976) and corresponded to areas where fewer jointing and weakness zones were present.

The area under the stress-strain curve as destruction work had the unit of Specific energy, and it was proved that there was an excellent statistical relationship between destruction work and drilling rate of drill rigs and cutting rates of different excavation machines, such as roadheaders and TBMs (Thuro and Plinninger, 1998, 1999, 2003). One of the most widely established methods to predict the cutting rate of any excavation machine is to use cutting power and Specific energy obtained in full-scale laboratory linear cutting test and to use the energy transfer ratio from cutting head to rock formation as in Equation 2.11 (Rostami et al. 1994),

$$ICR=k(P/SE_{opt}) \quad (m^3/hr) \quad (2.11)$$

Where ICR = the instantaneous cutting rate (m³/h),

k = energy transfer ratio,

P = cutting power of cutting head (kW)

SE_{opt}= optimum Specific energy in (kWh/m³)

Neil et al. (1994) strongly emphasised that the predicted value of the cutting rate is more realistic, if Specific energy value in Equation 2.11 was obtained from full-scale linear cutting tests using production cutters. Rostami and Ozdemir (1994) pointed out that k changed between 0.45 and 0.55 for roadheaders and from 0.85 to 0.90 for TBMs. They also highlighted that, the prediction of optimum Specific energy from rock properties would greatly help predict advance rates of any excavation machine. Schneider (1988) also reported that the net cutting rate of roadheader might be found by dividing the cutting power of the machine by Specific energy, which is closely related to the compressive strength of the rock (Neil et al. 1994). In-situ observations of the other practising engineers demonstrated that the cutting rate of roadheaders is inversely proportional to rock compressive strength (Uehigashi, 1987; Schneider, 1988; Gehrin, 1989, 1997).

The power consumption of mechanical excavators depends on the Specific energy (SE) and of cutter forces. SE is the amount of energy consumed to excavate a unit volume (or mass) of rock using a particular cutter. The lower the SE, the lesser the power required to be installed on the machine employing that cutter. In other words, lower SE means that a given machine will produce more cut rock for given power consumption or that a smaller/less expensive machine may be used to produce the required amount of cut rock. Generally, a mechanical excavator equipped with a cutter that can produce a lower SE value is preferred for a given production rate, as it provides a high cutting efficiency.

Estimating optimum Specific energy is important in predicting the cutting rates of excavation machines, as explained in Equation 2.11. Specific energy is best predicted from uniaxial compressive strength and tensile strength, verifying some of the previously published results (Copur et al. 1997). Copur and co-workers state that if the power and weight of the roadheaders are considered together, the relationship between cutting rate and compressive strength is more realistic (Copur et al. 2001).

Copur et al. (2003) reported that optimum Specific energy values obtained from full-scale cutting tests might be predicted from the product of compressive and tensile strength of the rock. They also defined indices based on macro-scale rock cutting tests

for assessing the rock cutting performance. They concluded that the force and brittleness indices were moderately correlated with cutter performance, including Specific energy and mechanical properties of rocks.

Teale (1965) defined Specific energy as the energy required to remove a unit volume of rock. However, Paithankar and Misra (1976) defined Specific energy as the energy required to create a new surface area. Rabia (1982, 1985) concluded that Specific energy in terms of either unit volume or new surface area is not a fundamental inherent property of a rock and that the breakage parameters or operational parameters (rotational speed, cutting power of excavation machines and tool geometry) control the numerical value of Specific energy. Wayment and Grantmare (1976) and Mahyera et al. (1982) studied high energy hydraulic impactors and concluded that Specific energy is proportional to the inverse root of the blow energy for a given rock type. Destruction of rocks by drilling, cutting, breaking or sawing is one of the mechanical similarities. Specific energy is a common concept of rock destruction that governs the efficiency of any rock excavation process.

The quantity of rock broken is logically and geometrically measured by volume rather than by mass since it is determined by a stress pattern that is geometrical by itself. It is self-evident that to excavate a given volume of rock, a certain theoretically attainable minimum quantity of energy will be required. The amount of energy will depend entirely on the nature of the rock. Actual mechanical processes may or may not approach this theoretical minimum; the difference between actual and theoretical requirements would be a measure of work dissipated in, for example, breaking the excavated rock into more minor chips than necessary, in friction between tools and rock (which perhaps amounts to the same thing on a microscopic scale), or in mechanical losses quite outside the rock system.

Farmer et al. (1987) and Pool (1987) used the same concept as explained earlier and showed that for a given power of roadheader, the excavation rate in m^3/h might be significantly predicted using Specific energy values as given in Equation 2.11. Further, Krupa et.al. (1993, 1994) noticed that for a given power, the advance rate of a

full face TBM is directly related to the Specific energy values as formulated in equation 2.11.

There are some models in percussive drilling or rotary cutting in which it was assumed that thrust force is a product of rock compressive strength and tool projectile area, given with a good agreement between predicted and actual advance rate values (Roxborough and Phillips, 1975; Bernola and Oyanguran, 1987). This fact emphasises that rock compressive strength should be considered as one of the major properties in a model for estimating drilling rates (Akun and Karpuz, 2005; Altindag, 2004, 2006). However, tensile strength, compressive strength and shear strength are the important rock properties in rotary drilling or in rock cutting in which drag tools are used, as explained by Evans and Pomeroy (1966) and Nishimatsu (1972).

Detournay and Defourny (1992) developed a model that related the unconfined strength of a rock to the Specific energy required to cut the rock. Richard et al. (1998) proposed a scratch test (hardness test) to measure the unconfined compressive strength of sedimentary rocks. The proposed Specific energy model by Richard et al. (1998) implies that the Specific energy and the internal friction angle of the rock can be calculated from two measurements made at different confining pressures of the Specific energy used for cutting. Further, a Mohr-Columb failure model for rock allows the determination of strength as a function of confining pressure if the unconfined strength and the internal friction angle of the rock are known. Therefore, it is hypothesised that the Mohr-Columb strength parameters for rock can be determined on the basis of specific energies required for cutting the rock measured at two different confining pressures.

Detournay and Tan. (2000) used a scratch test to measure the cutting load required to break the rocks under confining stress and used the measured load to calculate the Specific energy required to break the rock. They proposed a model for predicting Specific energy at failure for dilatant shear rocks as a function of the unconfined Specific energy at failure, cutter rake angle (θ), internal friction angle of the rock (ϕ), an assumed interface friction angle (ψ) between the rock and the cutter and the confining pressure. Based on the proposed models, they concluded that the Specific

energy (ϵ) required to cut a unit volume of the rock varies linearly with the bottom hole pressure (pm) and that the interfacial friction angle on the cutting face (ψ) can be assumed to be equal to the internal friction angle of the rock.

Ersoy and Atici (2007) computed specific cutting energy (SE_{cut}) at different feed rates and depths of cut at a constant peripheral speed on 11 varieties of rocks. They measured velocities of P (V_p) and S (V_s) waves for the rocks according to ISRM (1981) standards. They found relationships between P waves, S waves and dominant rock properties like hardness, abrasiveness, density, porosity and silica contents. They also found relationships between P and S waves and SE_{cut} . Excellent linear relation between V_p and SE_{cut} (0.94) and a good linear relationship between V_s and SE_{cut} (0.80) were found to be existing. The clear trend was that an increase in the SE_{cut} increased the velocities of P and S waves.

Altindag (2003) studied the mechanics and effects of rock and coal brittleness on the efficiency of cutting picks and found no universally accepted concept of brittleness being used as a measure of cutting efficiency. The researcher states that the effect of brittleness on rock cutting has not been completely explained, and the aim of his study was to correlate the relationships between SE and brittleness concepts. The applicability of various brittleness measurement methods for rock cutting efficiency was investigated.

The determination of brittleness is mainly empirical. Usually, brittleness measures the relative susceptibility to two competing mechanical responses, deformation and fracture and ductile-brittle transition. The used brittleness concepts in Altindag's (2003) study are given in Equations 2.12, 2.13 and 2.14 below.

a—The determination of brittleness from the ratio of uniaxial compressive strength to the tensile strength of the rock (Figure 2.5 a & b),

$$B1 = \frac{\sigma_c}{\sigma_t} \quad (2.12)$$

b—The determination of brittleness from tensile strength and UCS,

$$B2 = \frac{\sigma_c - \sigma_t}{\sigma_c + \sigma_t} \quad (2.13)$$

c—The determination of brittleness from the area under the line of $\sigma_c - \sigma_T$ graph (Figure 1b),

$$B_3 = \frac{\sigma_c \times \sigma_t}{2} \quad (2.14)$$

where B_1 , B_2 and B_3 are brittleness, σ_c is the UCS of rock (MPa), σ_t is the tensile strength of rock (MPa).

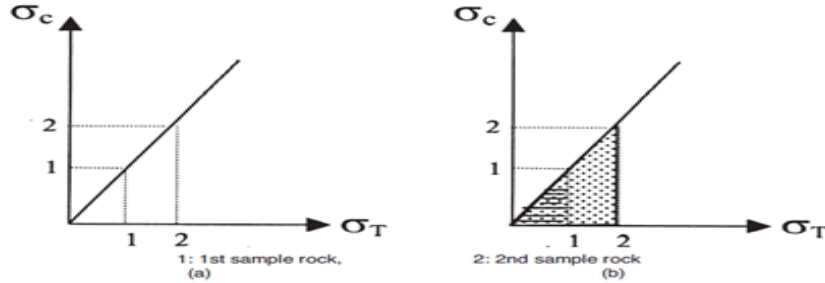


Figure 2.5 The graph for the relation between compressive strength and tensile strength of the rock

Raw data derived from previous empirical studies were used and the relationships between SE and brittleness concepts were investigated in Altindag's (2003) study. The two previously used brittleness concepts were named B_1 (the ratio of compressive strength to tensile strength) and B_2 (the ratio of compressive strength minus tensile strength to compressive strength plus tensile strength), and a newly introduced brittleness concept named B_3 (the area under the line concerning compressive strength and tensile strength) were evaluated in Altindag's (2003) study. The relations among these brittleness concepts for rock cutting efficiency were established by using regression analysis. No correlation was found between the SE values and the brittleness of B_1 and B_2 values. The SE was strongly correlated with the brittleness of B_3 and suggested that the B_3 concept could be used as an indicator in analysing the efficiency of rock cutting as its correlation coefficients are $r= 0.97$, $r= 0.99$, $r= 0.96$, respectively.

Atici and Ersoy (2009) carried rock cutting tests and fully instrumented laboratory drilling tests on five types of rocks. They determined SE_{cut} and SE_{drill} . They carried out regression analysis to find the relationship between SE_{cut} and SE_{drill} with rock brittleness B_1 (σ_c / σ_t), B_2 ($(\sigma_c - \sigma_t) / (\sigma_c + \sigma_t)$), B_3 ($(\sigma_c \times \sigma_t) / 2$). The regression analyses indicated linear, exponential and logarithmic relationships between SE_{cut} of circular diamond saw blades and the brittleness of B_1 , B_2 and B_3 , with high correlation coefficients of 0.98, 0.93 and 0.85, respectively. No good correlation was found

between SE_{drill} of poly diamond crystalline (PDC) and impregnated diamond core picks and non-core picks.

Yurdakul et al. (2012) developed models to predict Specific energy based on the operational parameters of block cutters and properties of rock for large circular saws during natural stone cutting. They used UCS, bending strength, Brazilian tensile strength, point load strength, Shore hardness test, Schmidt hammer hardness test, seismic velocity, water absorption at atmospheric pressure, apparent density, open porosity, saw blade diameter and depth of cut values as input parameters in the statistical analysis for predicting SE_{cut} . The developed model can predict the SE_{cut} values successfully for carbonate rocks in the stone-cutting process for large diameter circular saws in natural stone processing.

Aydin et al. (2013) developed a predictive model for the Specific energy of circular diamond saw blades in the sawing of granite rocks. They investigated the influence of operating variables and rock properties on specific energy. They employed statistical analysis to predict the most significant operating parameters and rock properties influencing the specific cutting energy (SE_{cut}). They developed models to predict the SE_{cut} from operating variables and predict the SE_{cut} from rock properties.

Engin et al. (2013) carried rock cutting experiments on 12 different types of rock samples using a circular sawing (CS) machine and an abrasive water jet cutting (AWJC) machine. Specific energy values were determined and compared to evaluate the efficiency of rock cutting methods in their study. The experimental results showed that the Specific energy values in AWJC were higher than those in CS. A relationship was found between Specific energy values and rock properties. Multiple regression equations for Specific energy for AWJC system ($R^2 = 0.95$) and CS system ($R^2 = 0.98$) were generated. The developed equations were statistically significant.

Joel Langham and Paul Hagan (2014) carried out the rock cutting test to correlate the results between the strength and cuttability of rocks. A reasonable correlation of 0.85

for Specific energy and 0.78 for cutting force was found between the UCS and cuttability performance of the rock samples.

Sarwary E. and Hagan P. C. (2015), in their studies, explored the effect of the initial onset of pick wear on changes in the cutting performance as reflected by an increase in pick tip angle at varying depths of cut using two different rock types. Rock cutting tests were performed in Gambier limestone and Gosford sandstone at depths ranging from 5 mm to 20 mm using a pointed pick having tip angles of 70°, 90° 100° and 110°. The results reveal that an increase in tool angle has a more pronounced effect on normal force with a three to four-fold increase compared to less than a two-fold increase in cutting force. Forces and specific energy were also found to increase with the depth of cut over the range of tip angles.

Lin Fu et al. (2015) have studied the influence of pick working angles on cutting performance of auger miner's aiguille, aiguilles with different pick working angles were developed, and their performance were tested on coal cutting test-bed. Cutting performance evaluation system of the aiguille was established first, and then evaluation indexes such as average load, load fluctuation coefficient, and specific energy were analysed by statistical method. The research indicates that the torque and specific energy of the aiguille decrease first and then increase with increased pick working angles. The feed resistance decreases with the increase in two working angles. The energy consumed by the feed resistance is very small relative to the total energy and can be ignored. When the cutting angle is between 45° and 50° and the tilt angle is about 20°, the torque and specific energy of the aiguille will be at a minimum and the load stability of the aiguille will also be ideal.

Jin young park et al., (2018) conducted a laboratory scale linear cutting machine was manufactured to investigate the rock cutting mechanism and a range of design factors of point attack pick cutters. Tests were performed on three samples with different strengths and measured cutting forces which were used to calculate the specific energy, an indicator of cutting efficiency. In their study proposed design conditions such as cut spacing, depth, skew angle and attack angle for the cutting head to achieve

efficient rock cutting while minimising specific energy. In addition, the structural stability of the pick cutter and holder concerning skew angle was analysed. The relation between structural stability and durability is discussed in terms of the resultant force and skew angle. A series of finite element analyses explored the structural stability of the assembly. The results indicated two sites of concentrated stress that depend on the skew angle and can accelerate undesired abrasion of the pick and a positive skew angle appears beneficial in terms of both cutting efficiency and structural stability.

Shahabedin H et al., (2018) in their studies, suggest the prediction model to estimate the specific energy of a pick cutter using gene expression programming (GEP) and particle swarm optimisation (PSO). Estimating the performance of mechanical excavators was of crucial importance in the early design stage of tunneling projects, and the specific energy (SE) based approach serves as a standard performance prediction procedure applicable to all excavation machines. This research aims to investigate the relationship between *UCS*, *BTS*, penetration depth, cut spacing, and *SE*. A total of 46 full-scale linear cutting test results using pick cutters and different depth of cut and cut spacing on various rock types was collected from the previous study for the analysis. The Mean Squared Error (*MSE*) associated with the conventional Multiple Linear Regression (*MLR*) method is more than two times larger than the *MSE* generated by the GEP-PSO algorithm. The R^2 value associated with the *GEP-PSO* algorithm is about 0.13 higher than the R^2 associated with *MLR*.

Kang K.X et al., (2020) studied the effects of cutting angle of conical picks affecting rock breaking capacity and was researched to calculate the low construction efficiency of the conical picks at hard rock cutting. Firstly, according to the construction situation of the conical picks, the rotary milling test bench of rock was built. Secondly, the physical and mechanical properties of four kinds of rocks (blue sandstone, red sandstone, limestone, granite.) were measured and the brittleness index of the four kinds of rocks was calculated. Finally, four kinds of rocks were tested at six cutting angles, respectively. The results of the experiments indicate that the radial force is the largest, the tangential force is the second and the lateral force is the smallest in the three-axis of the pick against the four rocks over 50MPa. With the

increase of the rock compressive strength, the ratio of radial force to tangential force increases gradually. Therefore, more down-force of the machine is needed to improve the impact penetration ability of the pick. While considering milling resistance and specific energy consumption as an index, the cutting angle of 63 for the green sandstone and red sandstone and the cutting angle of 58 for the limestone and granite are helpful to improve the efficiency of the whole machine.

2.3 Artificial Neural Networks (ANN)

Artificial Neural Networks (ANN) can be successfully used to develop models to predict the rock properties accurately and precisely (Haykin, 1999). Neural networks can be used as an alternative for statistical methods, such as correlation, multivariable regression, linear regression and other statistical analysis and techniques (Singh et al., 2003). Neural networks, with their outstanding capability to obtain useful output from complicated or imprecise data, can be used to find the extract patterns and detect too complex trends to be noticed by either humans or other computer techniques. Rumelhart and McClelland., (1986) reported that a trained neural network might be thought of as an "expert" in the category of information. It has been assigned to analyse and provide information for a given new situation of interest (Simpson, 1990).

Other advantages of ANN include adaptive learning, self-organisation, real-time operation and fault tolerance via redundant information coding. However, some network capabilities may be retained even with major network damage (Yilmaz et al., 2008).

ANN technology, the ability to learn and generalise interactions among many variables, has been reported to be very useful in modelling the rock material behaviour by many researchers (Ghabousi et al. 1991; Ellis et al. 1992). Meulenkamp et al. (1999) investigated the possibility of predicting unconfined compressive strength by ANN from the hardness of rocks using Equotip hardness tester and other rock properties like hardness, porosity, density and grain size. Singh et al. (2001) developed predictive models for uniaxial tensile strength (UTS), Uniaxial Compressive Strength (UCS), and axial point load strength from the rock properties.

Similarly, many investigators have developed ANN models to predict the UCS and shear strength from physical properties (Sarkar et al., 2010). The ANN methods could be applied for the prediction of the UCS and modulus of elasticity of intact rock properties (Dehghan, 2010). Zorlu et al.(2008) developed ANN models to predict the UCS from petrographic properties.

ANN models were developed by Sonmez et al. (2006) and Ibrahim et al.(2012) to predict the modulus of elasticity of intact rock from UCS and unit weight. Similarly, ANN models were developed for predicting UCS and static modulus of elasticity (E) of intact rocks from their other properties, such as NCB cone indenter hardness, dry density and Shore scleroscope hardness (Tiryaki, 2008). ANN models were developed by Yilmaz et al.(2008) to predict rock properties like modulus of elasticity, unconfined compressive strength from slake durability index, Schmidt hammer rebound number, effective porosity and point load index. ANN models of radial basis function (RBF) and multi-layer perceptron (MLP) exhibit were developed by Yilmaz et al. (2011) for predicting the swell percentage of soils.

The conclusion from all the above ANN modelling methods is that the prediction performance of the neural network model is higher than those of multiple regression equations. The use of the neural network may provide new approaches and methodologies and minimise the potential inconsistency of correlations.

ANN modelling concepts are used to find the drillability, optimum pick selection and cuttability of rocks (Yilmaz, 2002). The neural network system has also been used in predicting the advance rates of Tunnel Boring Machines (Benardos and Kaliampakos, 2004) and saw ability prediction of carbonate rocks (Kahraman et al. 2006).

Similar modelling methods offer a profound understanding of the physical problem (like finding cutting depth in rocks caused by a hemispherical indenter) and help to identify the most important governing parameters or factors that reflect the essence of the rock cutting events. The target problem is thus simplified, and the artificial neural network provides an advanced computing model, which allows more factors to be involved, and the predictions obtained by using this combined approach (similarity

methods and artificial neural network) are in better agreement with the experimental results than the predictions obtained by using other methods (Kou et al.1999).

Furthermore, fuzzy logic and ANN have been used for the construction of predictive models in mining and tunnelling applications in the last few years. However, ANN has not yet been used to predict SE and a rock cutting index from intact rock properties in rock drillability applications where tungsten carbide cutter picks are employed. In the present study, ANN models are developed to predict SE from rock properties.

2.4 Numerical Modeling of cutter-rock interface

Various procedures, processes, and phenomena treated in science and engineering are often described in terms of differential equations formulated using their continuum mechanics models. Solving differential equations under various conditions, such as boundary or initial conditions, leads to understanding the phenomena and predicting the future of the phenomena. However, precise solutions for differential equations are generally difficult to obtain. Hence, numerical methods are adopted to obtain approximate solutions for differential equations. The numerical methods of cutting those approximate continua with an infinite degree of freedom by a discrete body with a finite degree of freedom are called discrete analytical methods (Stolarski et al. 2006).

Modelling has been a useful tool for engineering design and analysis. The definition of modelling may vary depending on the application, but the basic concept remains the same, that is, the process of solving physical problems by appropriate simplification of reality. In engineering, modelling is divided into two major parts, physical/empirical modelling and theoretical/analytical modelling. Laboratory and in situ model tests are examples of physical modelling, from which engineers and scientists obtain useful information to develop empirical or semi-empirical algorithms for tangible application. The increases in computational technology have led to many numerical models and software programs for various engineering practices.

The most commonly applied numerical methods for rock mechanics problems are,

2.4.1 Continuum methods

- Finite Difference Method (FDM),
- Finite Element Method (FEM), and
- Boundary Element Method (BEM).

2.4.2 Discontinuum methods

- Discrete Element Method (DEM),
- Discrete Fracture Network (DFN) method,
- Hybrid continuum/discontinuum models,
- Hybrid FEM/BEM,
- Hybrid DEM,
- Hybrid FEM/DEM
- Other hybrid models.

The FEM requires dividing the problem domain into a collection of elements of smaller sizes and standard shapes (triangle, quadrilateral, tetrahedral, etc.) with a fixed number of nodes at the vertices and/or on the sides. The trial functions, usually polynomial, are used to approximate the behavior of partial differential equations at the element level and generate the local algebraic equations representing the behavior of the elements. The local elemental equations are then assembled according to the topologic relations between the nodes and elements into a global system of algebraic equations, whose solution then produces the required information in the solution domain after imposing the properly defined initial and boundary conditions. The FEM is perhaps the most widely applied numerical method in engineering because of its flexibility in handling material heterogeneity, non-linearity, and boundary conditions with many wells developed and verified commercial codes with large capacities in terms of computing power, material complexity and user-friendliness. Due to the interior discretisation, the FDM and FEM cannot simulate infinitely large domains (as sometimes presented in rock engineering problems, such as half-plane or half-space problems), and the efficiency of the FDM and FEM will decrease with too high a number of degrees of freedom, which are generally proportional to the number of nodes(Jing, 2003).

The FEM method has been used by Wang (1976), Tang (1997), Kou et al. (1999) and Liu et al. (2002) to simulate fracture propagation during rock cutting. Generally, these models used a stress-based criterion to form cracks that are normal to the maximum principal stress (tensile stresses taken as positive) at the element-integration points. Failure occurs if the maximum tensile stress exceeds the specified fracture strength. The models utilised a Mohr-Coulomb failure criterion in compression to form shear cracks at the element-integration points. After the cracks were formed, the strains normal to both the tensile and shear cracks were monitored in subsequent time/load steps to determine if the cracks were open or closed. If a crack is open, the normal and shear stresses on the crack face are set to zero for a tensile crack.

Wang (1976) developed a general mathematical rock failure model and applied the available finite element technique to an established computer code, which allowed simulation of the sequence of penetration mechanisms and provided a better description of the failure phases, such as initial cracking crushing and chipping. Wang (1976) also used the 'stress transfer' method suggested by Zienkiewicz (1968) to convert excessive stresses that an element cannot bear to nodal loads. These nodal loads are reapplied to the element nodes and thereby to the system. Compressive normal stress can be carried if a crack is closed, but the shear stress is limited to a value described by the Coulomb friction model. The analytical results presented in the studies conducted by Wang (1976) show reasonable agreement with experimental observations.

Numerical analysis of the wedge rock cutting problem was conducted by Huang et al. (1997) by using the code FLAC software. The numerical analysis indicated that maximum tensile stress (interpreted as the point of crack initiation) moves away from the rock cutting axis as the lateral confinement increases. They found that a slight increase in the confining stress from zero induces a significant increase in the inclination of this point on the rock cutting axis. However, the confinement does not significantly reduce the maximum tensile stress and hardly influences the rock cutting pressure.

Carpinteri et al. (2004) conducted tests of rock cutting of brittle and quasi-brittle materials. Fracture patterns in homogeneous brittle solids were obtained by the finite element method in the framework of linear elastic fracture mechanics. Micro-structural heterogeneities were taken into account by the lattice model simulation. Although the reality was often much more complex than the theoretical models applied, the study provides interesting indications for improving the performance of cutting tools. The FRANC2D software, developed at Cornell University, has been used to simulate fracture in the homogeneous case. This software can simulate plane stress, plane strain, and asymmetric crack propagation in the framework of linear elastic fracture mechanics (LEFM). The researchers concluded that the cutting performances could be significantly improved by reducing the crushing component and enhancing the chipping ability of the indenters (e.g. by increasing their sizes or depth of penetration).

Liu et al. (2002) simulated the rock fragmentation processes induced by single and double truncated indenters by the rock and tools interaction code, R-T2D, based on the Rock Failure Process Analysis (RFPA) model. The simulated crack patterns were in good agreement with rock cutting experiments and a better understanding was gained. According to the simulated results, a simple descriptive and qualitative model of the rock fragmentation process induced by truncated indenters had been developed. The simulated results for the rock fragmentation process induced by double indenters reproduced the propagation, interaction and coalescence process of side cracks induced by the two indenters and the formation of large rock chips. The researchers pointed out that the simultaneous loading of the rock surface by multiple indenters seemed to provide a possibility of forming larger rock chips, controlling the direction of subsurface cracks and consuming minimum Specific energy.

Wang et al. (2011) examined the rock fragmentation processes induced by double drill picks subjected to dynamic and static loading by a numerical method. Micro-heterogeneities of the rock was considered in this numerical model. The simulated results reproduced the progressive process of brittle rock fragmentation during rock

cutting for the static case. Numerical simulations represented radial cracks, incipient chips, pulverised zones, and shell cracks for the dynamic case. Comparing the static and dynamic cases, the dynamic loading can lead to rock fragmentation more efficiently.

Additionally, the numerical results indicated that the dynamic pressure (P_{\max}) plays an essential role in the failure process of specimens with two indenters. Furthermore, the heterogeneity of the rock can also affect the failure modes of the rock when two indenters are used. Finally, the numerical results demonstrated the effect of the spacing between the indenters on the rock. The numerical code RFPA2D (Rock Failure Process Analysis, 2D) (Zhu and Tang., 2006) is used to consider the heterogeneity of rock and simulate the evolution of dynamic fracture initiation and propagation due to the impact loading from double indenters.

Saksala et al. (2013) simulated a numerical method for dynamic rock cutting. The method was validated via dynamic rock cutting experiments with single and triple indenters on Kuru granite. The simulation method included a constitutive model for rock and a model implemented in FEM to simulate the dynamic pick-rock interaction. Being a combined visco-plastic-damage model, the constitutive model accommodated the strong strain-rate dependency of rock via visco-plastic hardening/softening laws, both in tension and compression. The researchers carried out rock cutting experiments with single- and triple-button indenters using a set-up similar to percussive drilling. Despite the current continuum approach, the model can capture the salient features of the dynamic pick-rock interaction involved in dynamic rock cutting and applications alike. They concluded that a reasonably good agreement existed between the simulated and experimental results on dynamic rock cutting on kuru granite, and the model can be a useful tool (e.g. in a percussive drill design).

Sulem et al. (2002) carried out a numerical analysis of the rock cutting test. They modelled rock as an elastoplastic medium with Cosserat microstructure and consequently possessing an internal length. The response of the rock cutting curve was studied for various values of the indenter's size compared to the internal length of the rock to assess the scale effect. Using finite element numerical simulations, they

concluded that for material with Cosserat microstructure, the apparent strength and rigidity increase as the size of the indenter decreases. This scale effect for the strength can reach 15% for a statistical model and 50% for a kinematical Cosserat model when the size of the indenter tool is comparable to the grain size of the rock. They concluded that this scale effect was not significantly affected by the interface condition at the rock tool interface, and such a scale effect was experimentally observed for metals. They expressed a lack of relevant quantitative experimental data for the scale effect in the case of rocks. Further, they expressed that the analysis suggested that this effect may be important and has to be investigated further. The rock cutting tests appeared as an experimental tool for the testing and validating continuum theories with microstructure and calibration of internal lengths' parameters.

2.5 Problem Statements

A comprehensive literature survey on rock cutting was carried out to understand the interaction of cutting tool-rock with point attack picks. Earlier researchers have highlighted the parameters influencing rock cutting performance but have not discussed the influence of attack angle and its influence on rock cutting performance. Improper positioning of attack angle will significantly alter the effective rock breaking/mechanism, and it results in high consumption of energy, the minimum amount of material removed and high cost. This causes an increase in specific energy, which governs the assessment of rock cutting efficiency. So, the best means of assessing the performance of rock cutting is by varying the attack angle (45° , 55° , 65°) and pick angle (45° , 50° , 55° , 65°), to study the influence of rock properties like density, UCS, BTS, abrasivity and brittleness on the efficiency of the rock cutting process.

2.6 Objectives of the Study

The main objectives of this study are enumerated as follows,

1. To carry out laboratory experiments using fabricated set up of rock cutting machine to determine the cutting rate on different rocks, namely coal, sandstone, limestone and dolomite by varying the parameters like RPM, thrust and torque and to study their influence on cutting rate.
2. To determine the mechanical properties of rocks like density, Uniaxial Compressive Strength (UCS), Brazilian Tensile strength (BTS), abrasivity and brittleness of the rocks.
3. To measure energy in rock cutting using cutting tool dynamometer and then to determine Specific energy.
4. To study the influence of operational parameters, such as RPM, cutting force, torque on cutting rate and Specific energy.
5. To predict Specific energy in rock cutting using regression, ANN and compare with laboratory experimental result.
6. To carry out Finite Element Modeling (FEM) analysis to determine the depth of penetration and stresses generated for all pick-rock combinations considered taking the force values from rock cutting test and to compare depth of cut obtained in FEM analysis of all pick-rock combinations considered with experimental results and to predict rock cutting resistance of the rocks by considering the experimental and Numerical modelling values.

2.7 Thesis Outline

To address the various issues discussed in the literature survey the thesis consists of five chapters.

Chapter 1 The introduction includes the types of picks mainly used for rock cutting, the principle of rock cutting and its operating parameters, the influence of Specific energy on rock cutting, influence of pick angle and attack angle on Specific energy and influence of rock properties on Specific energy.

Chapter 2 provides a comprehensive review of the literature available on rock cutting technology. Various cutting models are introduced, along with failure modes and mechanisms. Cutting tools and their geometries are discussed, and their influence on the cutting process is reviewed. Specific energy is introduced, and its correlation with rock properties is discussed.

Chapter 3 Experimental methodologies are presented in which discusses the rock cutting tests; sample preparation for testing mechanical properties, including density, compressive strength, tensile strength, abrasivity and brittleness of rocks, and the calibration of cutting tool dynamometer, experimental set-up presents rock cutting machine picks used for the experiments.

Chapter 4 Artificial neural network techniques are adopted to predict specific energy

Chapter 5 Numerical modelling techniques are adopted to predict the depth of cut by applying the experimental cutting force as input parameters.

Chapter 6 Presents the results of experimental tests and the analysis of the data obtained. Specific energy, cutting rate, the cutting forces are plotted, and their relationship explored. Comparative studies and analysis of ANN models to predict Specific energy from operational and rock properties. Numerical modelling (FEM analysis to find the depth of cut in various rocks and Von Misses Stress distribution in all the axes (X, Y and Z directions). The rock cutting resistance concepts are introduced to predict the resistance offered by the rock considering the cutting force and depth of cut achieved with the experiment and the displacement achieved by FEM

Chapter 7 The conclusions are drawn from experimental and numerical work. The section on future work proposes research that can be carried to further the knowledge of rock cutting resistance at the rock-tool interaction.

CHAPTER 3

EXPERIMENTAL INVESTIGATION

3.0 Introduction

This chapter explicates on experimental design, the procedure of conducting experiments in the laboratories, It illustrates the experimental setup used in the laboratory to determine the cutting rate and Specific energy during rock cutting tests. It elucidates the procedure to determine the Specific energy in rock cutting tests and procedures to find the mechanical properties of various rocks considered for the study. It explicates the mathematical modelling, i.e. development of predictive models using multiple regression analysis and the development of Artificial Neural Network models to estimate the Specific energy from the operational parameters and some selected properties of rocks. Finally, it explicates the numerical modelling (Finite Element Analysis) analysis to determine the depth of cut and compare these results with experiment results.

3.1 Methodology

The following methodology is adopted in the present research work.

1. To fabricate the experimental setup of the rock cutting machine with necessary arrangements like holding the rock specimen, varying RPM and thrust were applied and torque is measured at each rpm.
2. Collection of rocks from various mines and cutting and polishing those to suitable sizes of 0.3 m width \times 0.3 m height \times 0.45 m length) to carry out rock cutting experiments.
3. Determination of mechanical properties of rocks like density, Uniaxial compressive strength, Brazilian tensile strength, abrasivity and brittleness of the rock.
4. Determination of depth of cut in rock cutting tests and measuring specific energy at different attack angles for different pick-rock combinations by varying the RPM and measuring cutting force and keeping cutting force

constant and measuring the torque and measuring cutting rate and Specific energy.

5. Development of regression models to correlate properties of rock and specific energy for different pick-rock combinations.
6. Development of Artificial Neural Network model to estimate the specific energy in the rock cutting process for different pick-rock combinations.
7. Finite Element Modeling for stress distribution in rock cutting and determination of the depth of cut for different pick-rock combinations and their comparison with experimental data and Figure 3.1 show the methodology adopted in this project. Table 3.1 shows the details of parametric variations investigated.

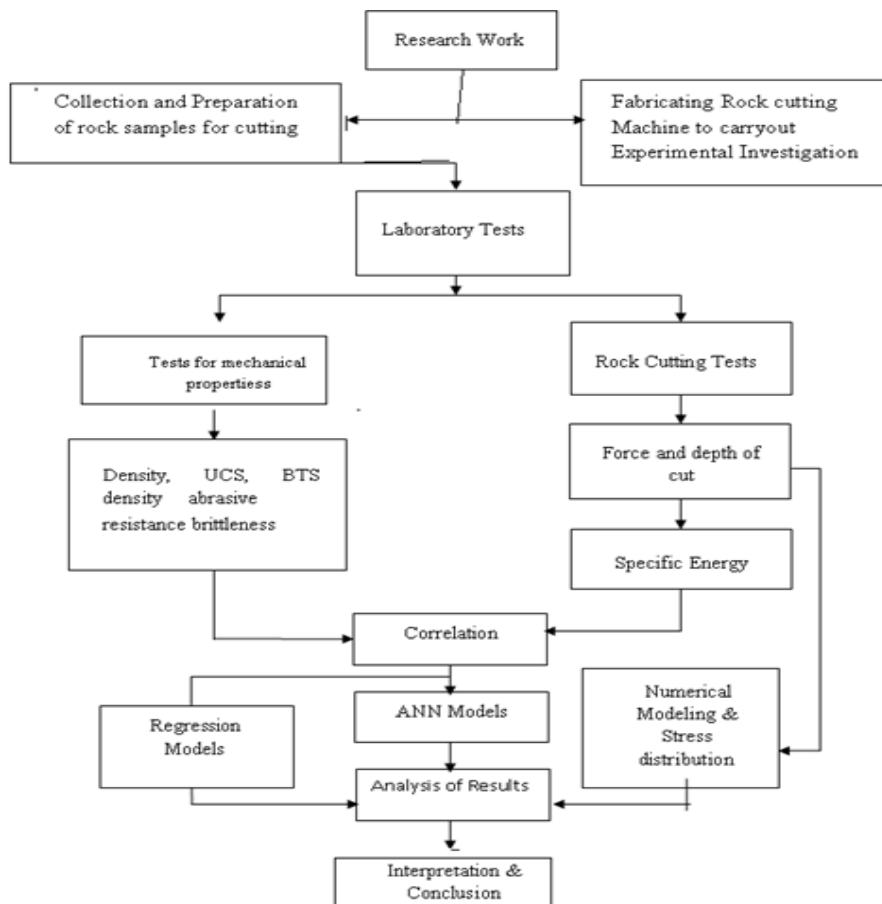


Figure 3.1 Flow chart of the plan experimental design and analysis

Table 3.1 Details of parameter variations investigated

Parameters	Variables
LABORATORY INVESTIGATIONS	
1. ROCK CUTTING TESTS	
a) Picks used	
i. Pick type	Conical Point attack picks
ii. Pick geometry	Conical picks with 45°, 50°, 55° and 65°
iii. attack angle	45°, 55° and 65°
b) Rock Parameters	
i. Type of rocks	Coal, sandstone (3 types), limestone (4 types) and dolomite (2 types)
c) Measured Parameters	RPM, Cutting force, Torque, Displacement, Volume and Specific energy
2. Determination of mechanical properties	Density, Uniaxial Compressive Strength, Brazilian tensile strength, abrasivity and brittleness of the rock.
PARAMETERS	VARIABLES
RPM, cutting force, torque,	Depth of the cut, Volume and specific energy
LABORATORY INVESTIGATIONS	
1. ROCK CUTTING TESTS	
a) Picks used	
i. Pick type	Conical Point attack picks
ii. Pick geometry	Conical picks with 45°, 50°, 55° and 65°
iii. Attack angle	45°, 55° and 65°
b) Rock Parameters	
i. Type of rocks	Coal, sandstone (3 types), limestone (4 types) and dolomite (2 types)
c) Measured Parameters	Displacement and Von Misses stress developed under conical picks and at different attack angles.

3.2 Collection of Coal and different types of rocks from different sources for preparation of core samples

The coal and sandstone blocks were collected from mines of M/S The Singareni Collieries Company Limited (SCCL), Ramagundam Area-I, Telangana state. The limestone and dolomite blocks were collected from Chaitanya Industries, JK cement, Muddapur, Bagalkot, Karnataka, and Ananthapur and Cuddapah districts Andhra Pradesh. Core samples were prepared, and the physico-mechanical properties were determined as per the International Society of Rock Mechanics (ISRM) standards.

The specimen prepared from the core drilling machine is cylindrical, which was used to determine the mechanical properties of the collected samples. Core samples and test specimens were prepared according to ISRM standards. Both the ends of the specimen were polished such that the surface of the core is not irregular. Each sample's length to diameter ratio is considered and varies as per ISRM standards and same details given below.

Compressive strength tests $L = 2$ to $3D$

Brazilian tests $L = 0.5$ to $1D$

Where, L: length of the specimen in mm, D: diameter of the specimen in mm,

3.3 The Mechanical Properties of the rock under study.

The core samples prepared in the laboratory were preserved adequately for laboratory testing without altering the true nature of the rocks. The mechanical properties of the rock tested are given in Table 3.2.

3.3.1 The Density of rocks.

The density of rock is determined by taking a graduated cylinder filled with half full of water. Then determine the exact water volume using the cylinder scale. Then dip the rock into the graduated cylinder completely immersed into the water, then note down the level of the water. Again measure the volume of the cylinder. Further, subtract the initial volume from the final volume in the cylinder to calculate the volume of rock and divide the mass of the rock by its volume as shown in Equation 3.1, and the calculated values are shown in Table 3.2.

$$\text{Density} = \frac{\text{Mass of the rock (grams)}}{\text{Volume of the rock (cubiccm)}} \quad (\text{gm/cm}^3) \quad (3.1)$$

3.3.2 The Uniaxial Compressive Strength of rocks

The test specimens were circular cylinders having a height to diameter ratio of 2.5 and a diameter of not less than 54 mm, as shown in Figure 3.2. The number of specimens used for the test was 3. The end faces of the specimen were flat to 0.02 mm and perpendicular



Figure 3.2 Uniaxial Compression testing machine with sample to the specimen axis within 0.250 (0.25mm in 50mm). The sides of the cylinder were smooth, free of abrupt irregularities and straight to within 0.5 mm over the full length of the specimen. The diameter of the specimen was recorded to the nearest 0.1mm by taking two perpendicular measurements at three different heights of the cylinder. The height of the cylinder was determined to be the nearest 0.1mm. Specimens should preferably be tested at their natural water content. Precautions must be taken to ensure that the water content is preserved during storage and specimen preparation. The rate of loading applied in the test was 0.5 MPa/sec. The load at failure was recorded, and the unconfined compressive strength (UCS) was calculated by using the following formula shown in Equation 3.2 and the calculated values are shown in Table 3.2.

$$\text{UCS} = \frac{\text{Load at Failure (kN)}}{\text{cross sectional area of the specimen (mm}^2\text{)}} \quad (\text{MPa}) \quad (3.2)$$

3.3.3 The Brazilian Tensile strength of rocks

The test specimen was cylindrical, with end faces perpendicular to the axis, as shown in Figure 3.3. The cylindrical surface was free from obvious tool marks and any irregularities, and the thickness of the specimen did not exceed 0.025 mm. The end faces were flat to within 0.25 mm and square and parallel to within 0.25. At least three specimens were taken from one sample to obtain a meaningful average. The sample rock was anisotropic due to the presence of weakness planes or preferred orientation of minerals, and the specimens were prepared in such a way that both directions were

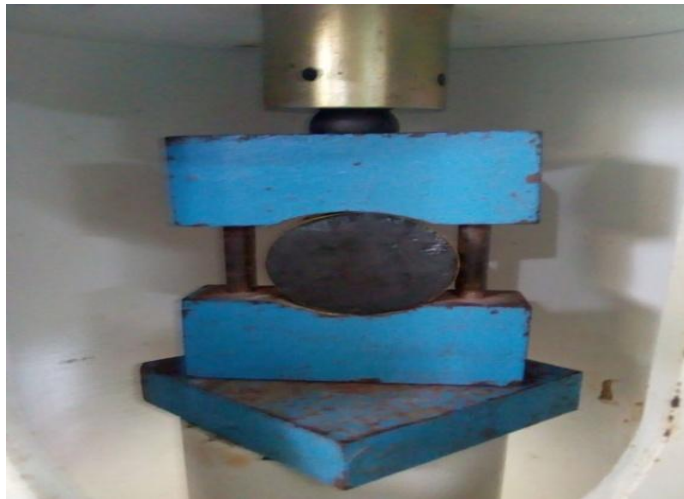


Figure 3.3 Brazilian testing apparatus with specimen parallel as well as perpendicular to such planes and were tested (axis of the cylinder parallel to the plane). The specimen diameter was NX core size (54 mm), and the thickness/diameter ratio was 0.5 to 0.6. The loading rate was 10 to 50 kN/minute, the load at failure (KN) was recorded, and the tensile strength was calculated using the following formula shown in Equation 3.3 and the calculated values shown in Table 3.2.

$$BTS = \frac{\text{Load at Failure (kN)}}{\text{cross sectional area of the specimen (mm}^2\text{)}} \quad (\text{MPa}) \quad (3.3)$$

3.3.4 The Brittleness of the rocks

Based on the previous study by Altindag's (2003), the formula is shown in Equation.3.4. This equation is used to determine the brittleness in rock cutting considering UCS and BTS of the rock, and the values are determined as shown in table 3.2.

$$\text{Brittleness} = \frac{\sigma_c \times \sigma_t}{\sigma_c + \sigma_t} \quad (3.4)$$

Where σ_c =UCS of rock (MPa)

σ_t = Brazilian Tensile strength of rock (MPa)

3.3.5 The Abrasivity of the rocks

The test sample consists of clean aggregates dried in an oven at 105°C – 110°C. The sample conformed to any of the gradings, as shown in Figure 3.4. The test specimen and abrasive charge were placed in the Los Angeles abrasive testing machine, as shown in Figure 3.5. The opening was closed with a dust-tight cover. The testing machine was started and allowed to rotate for 500 revolutions.



Figure 3.4 Specimen prepared for Los Angeles abrasion test



Figure 3.5 Los Angeles abrasion test apparatus.

When the testing machine completed rotating the required number of revolutions, the cover was removed, and the entire contents were carefully emptied into a pan. The abrasive charge was removed from the pan. The test specimen on the 4.75-mm sieve was separated, and then the passing 4.75-mm rock was sieved on the 1.70-mm sieve. The rocks retained on the 4.75 and 1.70-mm sieves were combined, weighed, and recorded to the nearest 1 g. If the mass of rock retained on the 1.70-mm sieve was determined after 100 revolutions, the entire test specimen, including the rock passing the 1.70-mm sieve, was returned to the testing machine. The opening in the testing machine was closed and operated for the required number of additional revolutions and calculated using Equation.3.5, and values are shown in Table 3.2.

$$\% \text{ Wear} = \frac{A-B}{A} \times 100 \quad (3.5)$$

where, A = Mass of the original test specimen, to the nearest 1 g,

B = Mass retained on the 1.70-mm sieve after the specified number of revolutions, to the nearest 1 g

Table 3.2 Mechanical properties of rock samples tested (3 samples)

Density (gm/cm ³)										
SL No	coal	Sand stone 1	Sand stone 2	Sand stone 3	Lime stone 1	Lime stone 2	Lime stone 3	Lime stone 4	Dolomite 1	Dolomite 2
1	1.41	1.98	2.1	2.1	2.1	2.4	2.74	2.8	2.4	2.5
%	7.8	2.1	10.47	9.5	10	23	0.72	7.14	8.3	8
2	1.52	1.94	1.88	1.9	1.89	1.84	2.72	2.6	2.6	2.3
%	13	4.1	3.19	1.05	5	20.6	4.4	4.6	3.8	17.39
3	1.32	1.86	1.82	1.88	2	2.22	2.6	2.72	2.5	2.7
%	6.8	6.1	13.3	10.4	4.76	7.5	5.1	2.8	4.1	8
Avg	1.41	1.92	1.94	1.95	1.99	2.2	2.69	2.7	2.5	2.5
SD	0.100	0.061	0.147	0.121	0.105	0.285	0.075	0.101	0.1	0.2

Unconfined compressive strength (MPa)										
SL No	coal	Sand stone 1	Sand stone 2	Sand stone 3	Lime stone 1	Lime stone 2	Lime stone 3	Lime stone 4	Dolomite 1	Dolomite 2
1	16.6	14.8	18.8	24.6	47.6	58.8	70.1	71.8	44.2	71.4
%	10.8	8	5.3	3.2	2.5	0.34	1.7	3.6	0.45	0.84
2	14.8	13.6	17.8	23.8	46.4	58.6	68.9	69.2	44.4	70.8
%	9.4	4.4	2.8	1.6	0.4	0.34	1.4	1.3	0.9	0.56
3	13.4	14.2	18.3	24.2	46.2	58.8	69.9	70.1	44.8	71.2
%	15.6	4.05	2.6	1.6	2.9	0.2	0.28	2.36	1.3	0.28
Avg	14.9	14.2	18.3	24.2	46.8	58.6	69.7	70.3	44.4	71.2
SD	0.86	0.6	0.5	0.4	0.75	0.11	0.64	1.32	0.30	0.30

Brazilian Tensile strength (MPa)										
SL No	coal	Sand stone 1	Sand stone 2	Sand stone 3	Lime stone 1	Lime stone 2	Lime stone 3	Lime stone 4	Dolomite 1	Dolomite 2
1	1.5	1.42	1.8	2.5	4.3	5.8	6.8	7.3	4.1	7.5
%	0	0	5.5	0	4.6	5.17	0	2.7	2.4	8
2	1.5	1.42	1.7	2.5	4.5	5.5	6.8	7.1	4.2	6.9
%	6.67	2.8	5.5	4.1	2.2	0	1.4	2.8	4.7	7.2
3	1.4	1.46	1.8	2.4	4.6	5.5	6.9	6.9	4.4	7.4
%	6.67	2.8	0	4.1	6.9	5.17	1.4	5.4	7.3	1.3
Avg	1.4	1.4	1.8	2.5	4.4	5.6	6.8	7.1	4.2	7.2
SD	0.057	0.023	0.057	0.057	0.152	0.173	0.057	0.2	0.152	0.321

Brittleness of the rocks										
SL No	coal	Sand stone 1	Sand stone 2	Sand stone 3	Lime stone 1	Lime stone 2	Lime stone 3	Lime stone 4	Dolomite 1	Dolomite 2
1	1.27	1.29	1.64	2.26	3.94	5.27	6.19	6.62	3.75	6.78
%	7.09	0.78	5.49	0.00	4.06	4.74	0.16	2.87	2.13	7.37
2	1.36	1.28	1.55	2.26	4.10	5.02	6.18	6.43	3.83	6.28
%	7.35	3.13	5.16	3.54	1.95	0.00	1.62	2.33	4.44	6.69
3	1.26	1.32	1.63	2.18	4.18	5.02	6.28	6.28	4.00	6.70
%	0.79	2.33	0.61	3.54	6.09	4.74	1.45	5.14	6.67	1.18
Avg	1.3	1.3	1.63	2.26	4.02	5.11	6.19	6.44	3.83	6.53
SD	0.05	0.02	0.05	0.05	0.12	0.14	0.05	0.17	0.13	0.27

Abrasive of Rock (%)										
SL No	coal	Sand stone 1	Sand stone 2	Sand stone 3	Lime stone 1	Lime stone 2	Lime stone 3	Lime stone 4	Dolomite 1	Dolomite 2
1	17	21	22	25	28	23	26	38	47	54

3.4 Calibration for cutting tool dynamometer

The knowledge of cutting force was one of the basic objectives of rock cutting. Rational design and dimensioning of the cutting tool parts and optimum choice of cutting tool was then necessary.

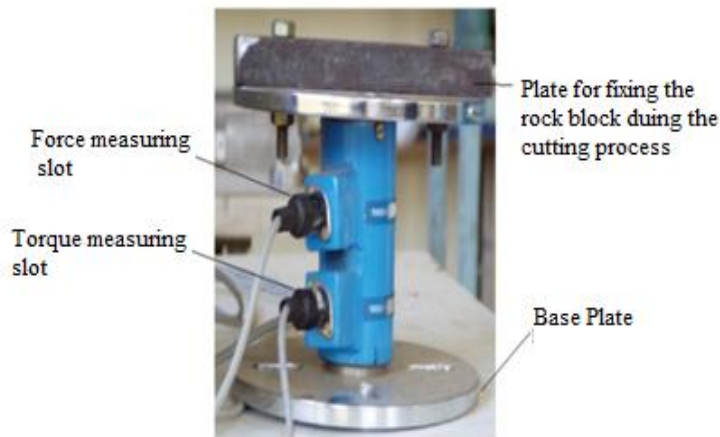


Figure 3.6 Cutting tool dynamometer

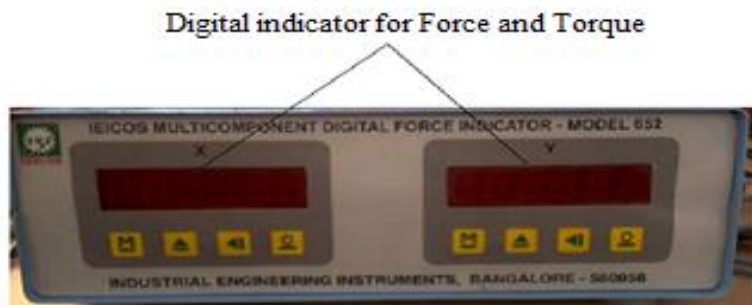


Figure 3.7 Digital multi-component force and torque indicator

Cutting tool dynamometer is a modified drilling tool dynamometer which measures the thrust and torque generated during cutting coal/rock. Cutting tool dynamometer shown in Figure 3.6 consists of a sensing block with strain gauge mounted for torque/thrust sensing and a digital multi-component force and torque indicator shown in Figure 3.7 was used to independently measure the cutting force and torque acting in X and Y directions.

Cutting tool dynamometer was calibrated prior to its use. The main purpose of the calibration process was to establish the transfer functions between the applied load and the thrust and torque generated during the cutting process. The strain gauge

calibration process is shown in Figure 3.8. Two channels A_{th} and A_{tq} were recorded when either the thrust or the torque was applied such that the cross-talk terms can be estimated. The relationship between the applied thrust (or torque) and the applied load on the dynamometer is shown in Table 3.3 and plotted in Figure 3.9 and Figure 3.10.



(a) Force

(b) Torque

Figure 3.8 Method of calibrating the cutting tool dynamometer

Table.3.3 Calibrations chart of cutting tool dynamometer

Applied Load (Kgs)	Cutting force (N)	Applied load (Kgs)	Torque(N-m)
0	0	0	0
50	494	0.5	5
100	1052	1	10
150	1534	1.5	15
200	2040	2	20
250	2515	2.5	25
300	2990	3	30
350	3480	3.5	35
400	3996	4	40
450	4426	4.5	45
500	4996	5	50

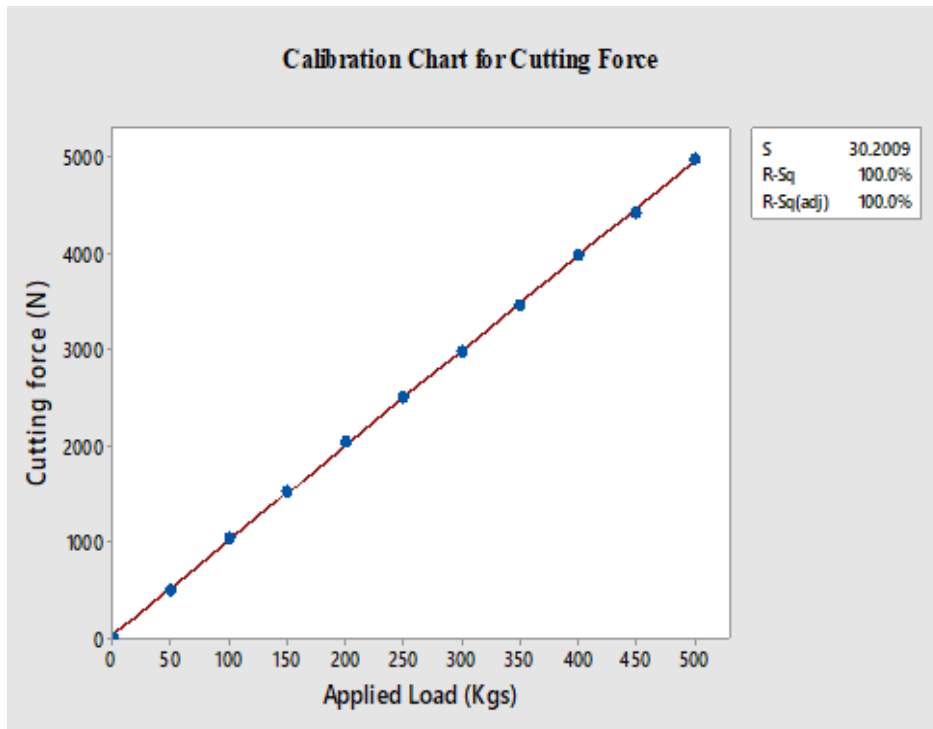


Figure 3.9 Calibration chart for cutting force

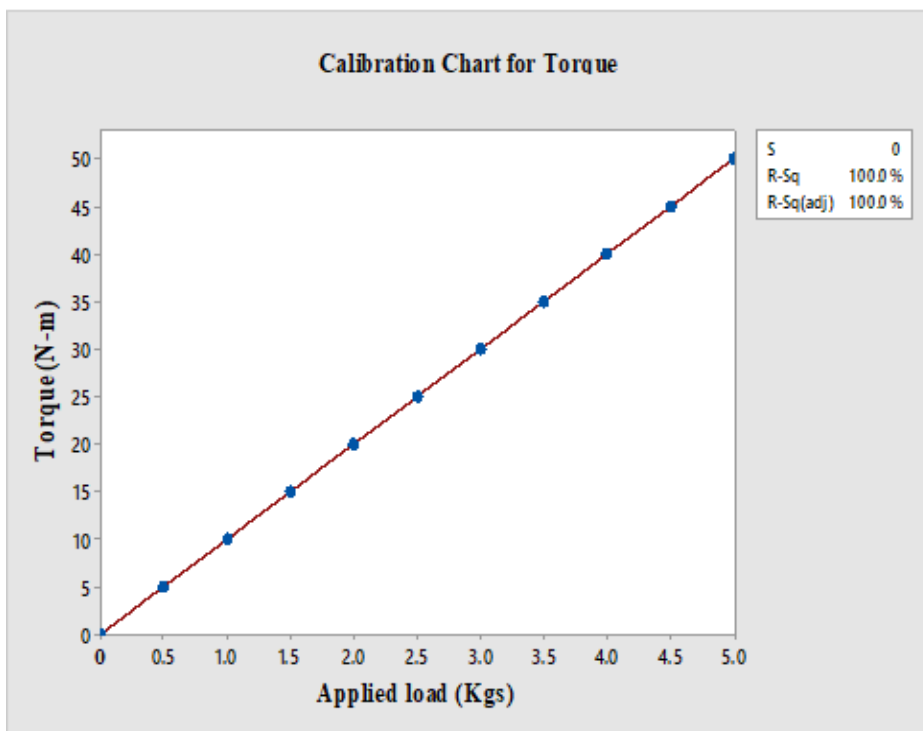


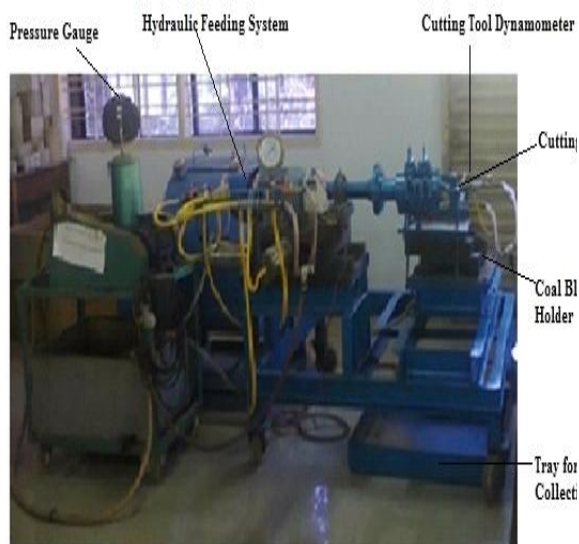
Figure 3.10 Calibration chart for torque

3.5 Description of Rock Cutting Machine

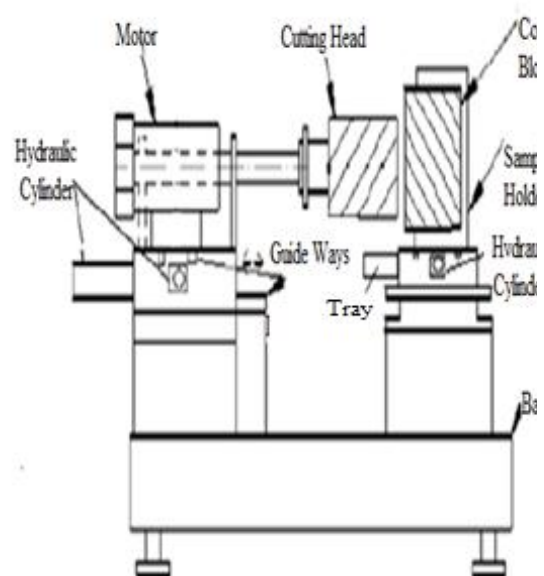
The rock cutting machine was fabricated to study the influence of cutting parameters like thrust, torque, RPM, attack angle and pick angle and their influence on cutting rate and specific energy.

Rock cutting machine, as shown in Figure 3.11 consists of a firm base with two protruding parts out of which one part is a prime mover (motor) mounted on it. Guide ways is a base plate attached to the motor, which helps in the to and fro and sideway movements. A motor is attached to a shaft pulley by a belt drive. The cutter head is attached to the shaft by a flange. The cutter head consists of a drum head with picks mounted on it.

The other part of a rock cutting machine is a firm sample holder connected to a hydraulic cylinder and can provide sideways movement during the cutting operation and a tray for collecting cut material. The machine can be subdivided into pressure gauge, hydraulic feeding system, cutting tool dynamometer, cutting drum, coal block holder and tray for material collection.



(a)



(b)

Figure 3.11 (a) Rock cutting machine (b) Line diagram of Rock cutting machine

The rock cutting machine consists of five main parts, namely, are

3.5.1 Mainframe,

3.5.2 Cutting head,

3.5.3 Pick block,

3.5.4 Cutting picks

3.5.5 Hydraulic units and

3.5.6 Speed controller.

3.5.1 Mainframe

The machine is mounted on a rectangular frame of 1.524 m x 1.066 m side dimensions with four legs that are mounted on wheels for easy manoeuvring capability. The legs are 0.9738 m in height and are made of a hollow pipe rock into which a 0.0508 m pipe is attached to support the frames. Figure 3.10 shows a rock cutting machine.

3.5.2 Cutting head

The cutting drum is six inches in diameter and four inches in width. The hydraulic flow controls help in controlling the speed of the cutting drum. The picks are placed 8 cms apart in spiral positions. The picks are placed inside a ball, wherein the attack angle can be adjusted to any angle from 45° to 65°. Figure 3.12 shows the cutting drum with picks.



Figure 3.12 Cutting drum with picks

3.5.3 Coal block holder

The block holder is a stand that holds the block of coal/rock firmly with two bolts, and a thick plate is placed above the block, which grips and holds the block tightly during the cutting process.

3.5.4 Cutting picks

The picks (Figure 3.13) themselves consist of a steel body containing a recess into which a cemented carbide tip is brazed. The cemented carbide tip is the cutting portion of the pick.






Serial Number	Cutting angle	Picks
1.	Point attack picks with 45° (PA45°) pick angle.	
2.	Point attack picks with 50° (PA50°) pick angle.	
3.	Point attack picks with 55° (PA55°) pick angle.	
4.	Point attack picks with 65° (PA65°) pick angle.	
5.	Point attack picks with 5 mm wear on the tip for all picks used in this research.	

Figure 3.13 Picks used for the experimental investigation

3.5.5 Hydraulic units

The hydraulic unit (shown in Figure 3.14) is the main part of the rock cutting machine that supplies hydraulic fluids to the cylinders, with the cutting force is the main parameter for the machine in achieving the desired depth of cut and material yield.



Figure 3.14 Hydraulic unit for the rock cutting machine

3.5.6 Speed controller

The rock cutting machine is provided with a speed controller (shown in Figure 3.15). During the cutting process, the speed was varied from 225 RPM to 325 RPM for both coal and rock in this experiment.



Figure 3.15 Speed controller used for rock cutting machine

3.6 Experimental Work

Rock cutting tests were conducted on the rock types, namely coal, sandstone (3 types), limestone (4 types) and dolomite (2 types). These tests were carried out with four attack angles viz 45°, 55°, 65° and 45° attack angle with 5mm wear picks, and for each attack angle, the experiment was conducted on each pick angles viz 45°, 50°, 55° and 65°.

To carry out rock cutting tests, rectangular blocks (0.3 m width × 0.3 m height × 0.45 m length) were prepared with the help of a hand drilling and saw cutting machine from the rock blocks collected from various mines in India. They were polished to produce perfectly parallel and mutually perpendicular faces.

The rock samples which were prepared were kept in the sample holder and fixed firmly by tightening the screw plates, and it is ensured that during the cutting process, the sample should not get disturbed and at the rear end of the sample, the cutting tool dynamometer is placed to measure cutting force and torque during the cutting process. Before starting the cutting process, the cutting tool dynamometer was calibrated, and the calibration chart was prepared, and the values measured are calibrated values.

In this laboratory experiment, the attack angles of 45°, 55° and 65° were considered, and for each attack angle, four pick angles of 45°, 50°, 55° and 65° were considered for all pick-rock combinations and operational parameters, i.e. RPM and thrust considered during the present laboratory investigation.

The cutting process was started with 45° attack angle with all picks like 45°, 50°, 55° and 65° and material broke by individual picks are collected, volume was calculated of the rock and cutting force multiplied with depth of cut and divided by volume collected and the Specific energy (J/m³) of that operation shown in Equation.3.6.

$$\text{Specific energy} = \frac{\text{Cutting force (N)} \times \text{depth of cut (m)}}{\text{Volume broken (m}^3\text{)}} \quad (\text{J/m}^3) \quad (3.6)$$

Once the cutting process was completed with 45° attack angle with all picks considered in this experiment. Further, the cutting process was started by re-adjusting the attack angle to 55°, 65° and with 45° attack angle with all picks considered. The experimental procedure was repeated, and the Specific energy was calculated.

In laboratory rock cutting, the RPM and thrust were varied from 225 RPM to 350 RPM, and thrust was measured from 1300 N to 2100 N, respectively. For each RPM-thrust combination, cutting was done for 60 seconds at different attack angles, and for each pick angle and the depth of cut is measured with a digital vernier caliper, and the rock chips were collected in the tray and weighted to calculate the Specific energy. During the cutting process, the drum and material have been kept in an enclosure so that the maximum rock chips remain in tray itself and the volume is measured to calculate the SE. Individually the material cut from different attack angles and picks were collected from the tray and weighed, and the specific energy is calculated. In this investigation, wear of 5 mm was fabricated and used for all pick-rock combinations considered, and experiments were carried out for all RPM, and thrust combinations used and figure 3.16 to 3.19 shows the grooves formed during the cutting process. The details of parametric variations investigated are shown in Tables 3.4 to 3.7 (Appendix-I).



Figure 3.16 The groove which is formed during the cutting of coal



Figure 3.17 The groove which is formed during the cutting of sandstone.



Figure 3.18 The groove which is formed during the cutting of limestone.



Figure 3.19 The groove which is formed during the cutting of dolomite.

CHAPTER 4

ARTIFICIAL NEURAL NETWORK MODELING

4.1 Introduction

The primary objective of the statistical methods is to develop a methodology under stringent statistical rules than to predict accurately. Moreover, statistical methods constrain the data along a particular geometry that may not always be favorable to capture nonlinear relationships between various parameters. In general, the problems encountered in real engineering applications are more complex. The algebraic and differential equations are used to describe the behaviour and functionality of properties or processes of real systems, and mathematical models are used to represent them. The complexity in the problem itself may introduce uncertainties that make the modelling non-realistic or inaccurate. In mining and geotechnical engineering, the study of rocks is important as the excavation and construction of the structures are made in or on the rocks and rock mass which are anisotropic and unpredictable. The behavior of rock under stress conditions and the geo-engineering characteristic of the rock is complex and not properly defined.

Artificial Neural Networks (ANN) has been reported to be very efficient in handling such nonlinear and complex relationships, and accurate prediction of the required parameters is possible. ANN implement various algorithms to achieve neurology related performances, such as learning from experience, generalising from similar situations and judging the states in which poor results were achieved in the past. When data is analysed using a neural network, it is possible to detect important patterns that were not previously apparent to a non-expert (Yilmaz et al. 2008).

Various prediction models have been utilised to select and optimise drilling/cutting machines for a long time (Tiryaki, 2008). Prediction of certain measures like the rate of penetration, cutting rate, SE, etc., of drilling and cutting performance for mining machines helps to reduce the capital cost (Rostami et al. 1994). The assessment and prediction of SE during rock cutting are so complicated that accurate modelling will be difficult because of the complexity of the rock cutting process and the nonlinear

relationship existing between SE and other dependent parameters like properties of rocks. Therefore, ANN is used in the present study to predict SE in the rock cutting test.

4.2 Fundamental concepts in ANN

ANN is an efficient information processing system that resembles in characteristics of a biological brain. In the biological brain, natural neurons receive signals through *synapses* located on the dendrites or membrane of the neuron. If the signals received are strong (*threshold*), the neuron is *activated* and emits a signal through the *axon*. This signal may be sent to another synapse and may activate other neurons as well. The axon of each neuron transmits information to a number of neurons. The neuron receives the information at the synapses from a large number of other neurons. Groups of these neurons are organised into subsystems, and the integration of these subsystems form the brain.

ANN is a group of interconnected artificial neurons interacting with one another in a concerted manner. Figure 4.1 shows how information is processed in a single neuron in ANN. Each node in a layer (except the input layer) provides the threshold value. Initially, the scalar input ' p ' is multiplied by the scalar weight ' w ' to form the product wp . Later, the weighted input wp is added to the scalar bias ' b ' to form the net input n . (In this case, we can view the bias as shifting the function f to the left by an amount b . The bias is just like weight, except that it has a constant input of 1). Finally, the net input is passed through the transfer function f , which produces the scalar output a . The names given to these three processes are the weight function, the net input function and the transfer function.

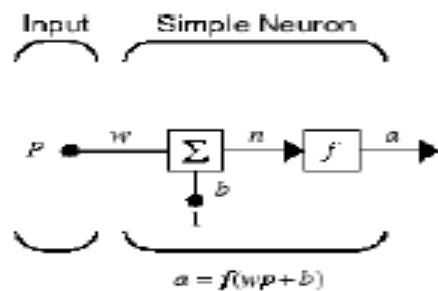


Figure 4.1 Architecture of simple neuron

The transfer function ‘f’ that transforms the weighted inputs into the output ‘a’ is usually a nonlinear function, either sigmoid or logistic, which restricts the output of the node between 0 and 1.

ANN consists of a large number of highly interconnected processing elements called nodes or neurons and a huge number of connection links between them. According to the architecture of the connections, ANNs have been identified as feedforward and recurrent networks. Feedforward networks have one-way connections from the input to the output layer. They are most commonly used for prediction and nonlinear function fitting. Here, the neurons are arranged in the form of layers. A neuron in one layer gets input from the previous layer and feeds the outputs to the next layer. The last layer is called the output layer. Layers between input and output layers are called hidden layers, and the architecture of this type is termed a multi-layered network. Figure 4.2 shows the schematic representation of a multi-layered feedforward network that is used in the present study. The input layer consists of operational parameters and rock properties. The number of nodes in the input and the output layers is dictated by the nature of the problem to be solved, and the number of input and output variables needed to define the problem. The number of hidden layers and neurons in the hidden layer is usually defined by the trial and error method.

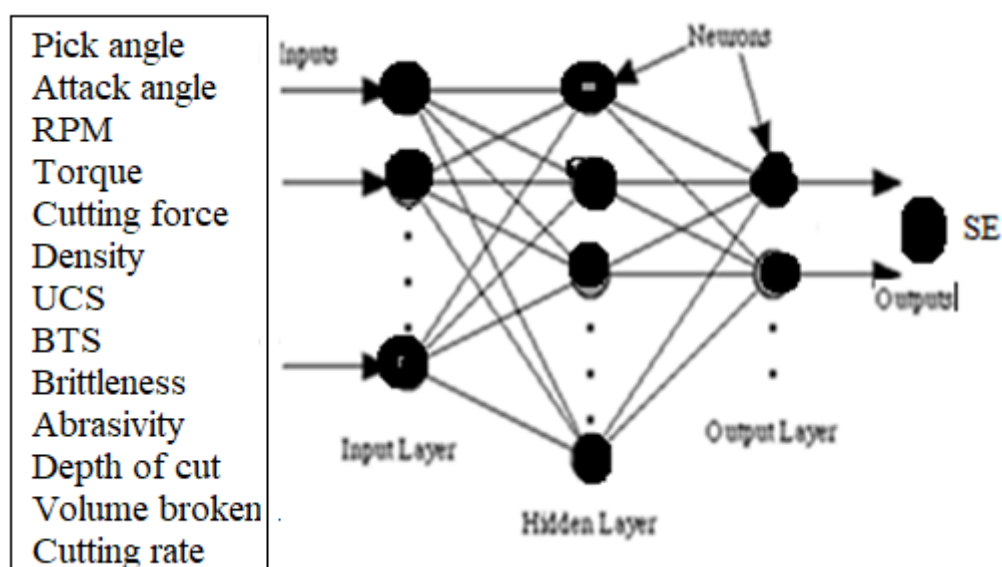


Figure 4.2 Feed-forward ANN network.

ANN studies the input-output relationships by suitably adjusting the synaptic weights in a process known as training. The weights of the given interconnection are adjusted using some learning algorithms.

The methods of learning in neural networks are classified into three types. They are,

- a) Supervised learning
- b) Unsupervised learning
- c) Reinforcement learning

In supervised learning, the target values obtained from experimental results are given to ANN during training so that ANN can adjust its weights to try to match its output to the target values. All the weights are randomly initialised before the learning algorithms are applied to update the weights (Haykin, 1998). The network then produces its own output. These outputs are compared with the target outputs. The difference between them is called the error and is used for adjusting the weights.

In the unsupervised learning method (also known as self-organised learning), the inputs of a similar type are grouped without using training data to specify how a member of each group looks or to which group a number belongs. The training process and the network receives the input patterns and organises these patterns to form clusters. When a new input signal pattern is applied, the neural network gives an output response indicating the class to which the input belongs (Sivanandhan et al. 2011).

In the reinforcement learning method, the learning is similar to supervised learning. In the case of supervised learning, the correct target values are known for each input pattern. However, less information may be available in some cases. Thus, in this method, the learning is based on half of the available information called critical information (Sivanandhan et al. 2011).

4.3 Multilayer perceptron

Multilayer perceptron (MLP) is one of the widely used network architectures for function approximation, classification and prediction problems (Haykin, 1999). It is an efficient neural network type capable of modelling complex relationships between variables. The architecture of MLP is a multi-layered feedforward neural network, in which nonlinear elements (neurons) are arranged in successive layers, and the

information flow is unidirectional, i.e. from the input layer to the output layer through hidden layers. Figure 3.20 shows a typical MLP architecture with the following characteristics.

- The perceptron network consists of three units, namely, input, hidden and output layer
- The network contains one or more layers of hidden neurons between the input and output of the network. These hidden neurons enable the network to learn and solve complex tasks by progressively extracting more meaningful features from the input patterns
- The network exhibits a high degree of connectivity.
- The binary activation function is used in the input and the hidden layer.
- The output of perceptron is given by $y=f(y_{in})$.
- The perception learning rule is used in the weights between the hidden and the output layer.
- The error calculation is based on the comparison of the values of targets and output values.
- The weights will be adjusted based on the learning rule if an error occurs.
- MLP is trained by using one of the supervised algorithms, of which the best Known is the back-propagation algorithm. The basic idea of back-propagation was first described by Werbos (1974) and was later rediscovered by Rumelhart and McClelland (1986), Hinton and Williams (1986). This algorithm's development is considered a landmark in neural networks, as it provides a computationally efficient method for training MLPs (Anderson 1995).

4.4 Back-propagation algorithm

The back-propagation (BP) algorithm is one of the most popular learning algorithms used in ANN. It is applied to multi-layered feedforward networks. There are basically two passes through the different layers of the network, a feedforward pass and a backward pass. All synaptic weights are fixed in the forward pass; whereas, all synaptic weights are adjusted in the backward pass, depending upon the error between

the actual output and the target output. The process is continued until all the input patterns from the training set are learnt. The error is cumulative and computed over the entire training set. This computation is called a training epoch. During the testing phase, the trained network operates in a feedforward manner (Haykin, 1999). The BP algorithm is presented below.

- 1) Initialise the weights and biases to small random values.
- 2) Choose an input pattern from the training set and present to the input layer.
- 3) Compute the activation of neurons in the hidden layer.
- 4) Compute the output of each neuron in the output layer.
- 5) Compute the mean squared error (MSE).
- 6) If MSE is minimum, go to step 8.
- 7) Update the weights between the output and the hidden layers.
 - a. Update the weights between the hidden and the input layer.
 - b. Go to step 2.
- 8) Save all the weights and exit.

The performance of the BP algorithm depends upon the initialisation of weights, learning, output functions of the units, presentation of the training data and the specific pattern recognition tasks like classification, prediction or mapping.

- 1) Initial weights- The network weights are initialised to small random values. The initialisation strongly affects the final solution.
- 2) The transfer function of the nodes- For calculating the value of δ in the backward pass, the activation function should be differentiable. One of the most widely used functions, which is continuously differentiable and also nonlinear, is the sigmoidal nonlinearity. A particular form defined for the sigmoidal nonlinearity is given by $f(x)=1/(1+e^{-x})$ where x is the net internal activity of the neuron and $0 \leq f(x) \leq 1$. This has been used for nodes in the hidden layer and output layer.
- 3) Learning rate- The effectiveness and convergence of the BP algorithm significantly depends on the value of the learning rate η . The value for the learning rate has to be selected by trial and error, which provides an optimum solution. The value is generally less than 1.

- 4) Momentum coefficient- The term ‘momentum is generally used to accelerate the convergence of the error BP algorithm. This involves the use of momentum coefficient α .
- 5) This is a simple method of increasing the rate of learning and yet avoids the danger of instability. The value chosen is generally less than 1.
- 6) The number of hidden neurons, The number of hidden layers and the number of neurons in a hidden layer are the most important considerations while solving the actual problems by using the MLP neural network. The optimal number of hidden layers and hidden neurons in any network for solving any given problem is determined by trial and error. The hidden units play a critical role in the operation of the multilayer perceptron with BP algorithm learning as they act as feature detectors.

Various prediction models have been utilised to select and optimise drilling/cutting machines for many years (Tiryaki, 2008). Prediction of specific measures like penetration, cutting rate, SE, etc., of drilling and cutting performance for mining machines, helps reduce the capital cost (Rostami et al. 1994). The assessment and prediction of SE during rock cutting are so complicated that accurate modelling is complex because of the complexity of the cutting process and the nonlinear relationship existing between the SE and other dependent parameters like properties of rocks. Thus, ANN is used in the present study to predict the SE in rock cutting tests.

4.5 Development of ANN model in this present study

The neural network toolbox in MATLAB 2013 software is used for the development of models. The ANN developed in this study is a Back Propagation layered feedforward network to build the prediction models for SE that consist of three layers, namely, input, hidden and output layers. The learning algorithm comprises two subsequent steps; feedforward and error BP. For feedforward calculations, tangent sigmoid transfers function neurons in the hidden layer and pure linear transfers function neurons corresponding to SE in the output layer.

Designing network architecture requires more than selecting a certain number of neurons in the input, output and hidden layers followed by training only.

Therefore, twelve (12) neurons were used in the input layer corresponding to four independent variables. One neuron corresponding to SE was used in the output layer. According to Seibi and Al-Alawi (1997), determining the number of hidden layers to be used and the number of neurons to be included in each hidden layer is of crucial importance in designing neural network structures.

Research in this area has proved that one or two hidden layers with an adequate number of neurons are sufficient to model any solution for the surface of practical interest. The number of trials was initially conducted to fix the number of neurons in the hidden layer. The number of neurons for which Mean Square Error is minimum was selected as the number of neurons in the hidden layer, as there is no standard procedure to find the optimum number.

The supervised learning algorithm Trainlm, a network training function that updates weight and bias values according to Levenberg-Marquardt optimisation, was used for the training of data in this study. Trainlm is often the fastest Back Propagation algorithm in the neural network toolbox, is highly recommended as a first-choice supervised algorithm, and does not require more memory than other algorithms. The following data sets were used to process the data in the network.

- I. The training set used for computation of the gradient and updating the weights and biases of the neural network;
- II. The validation set used for monitoring the error during the training process because it tends to increase when data is overfitted; and
- III. The test set error can be used to assess the quality of the division of the data set.

In this study, data is randomly divided such that 70% of the sample data is assigned to train the network and 30% for test and validation. The input layer consists of thirteen (13) variables, so initially, the hidden layer had thirteen (13) parameters and one (1) output parameter that is SE. The model was trained with LM algorithm using a Feedforward back propagation network. The estimations of weights to predict the model are derived using a transgmoidal function. An iterative process is carried with 12, 13, 14, 15, 16, 17, 18, 19 and 20 neurons. The performance was optimum (base on

RMSE values) for a model with 16- neurons. The study was categorised into a training model and a validation model. Figure 4.3, 4.4 and 4.5 Shows the Performance of Neural Network at sixteen (16) hidden neurons for training data set. Figures 4.6, 4.7 and 4.8 shows the performance models for the validation data set. The performance report of Neural Network with different hidden neurons is shown in Table 4.1. The model R-Squared value was found to be 99.9% for both training and validation.

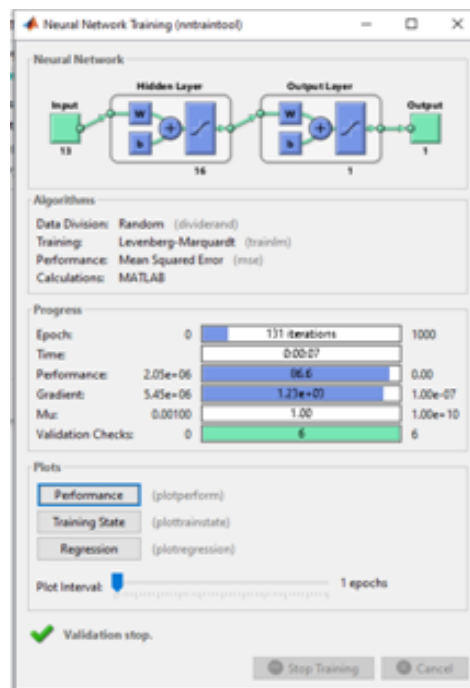


Figure 4.3: Pictorial representation of the training model for training data

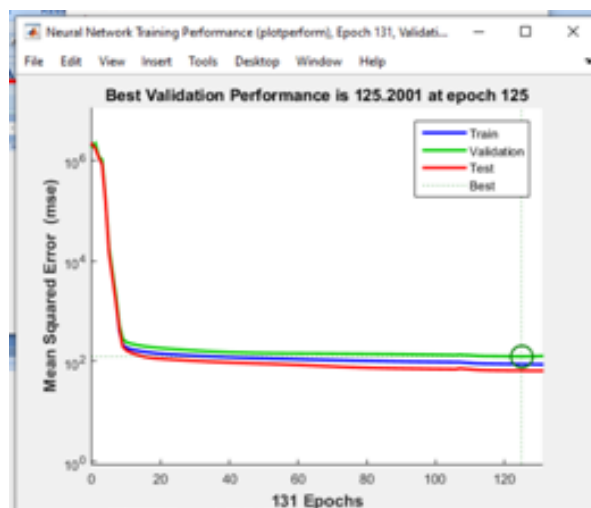


Figure 4.4: Performance model for training data

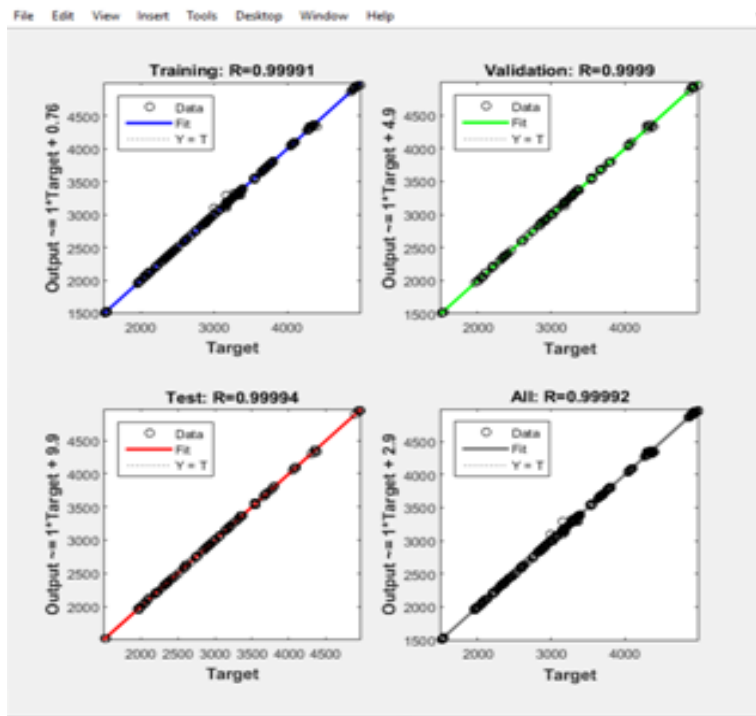


Figure 4.5: Prediction model of ANN for training data

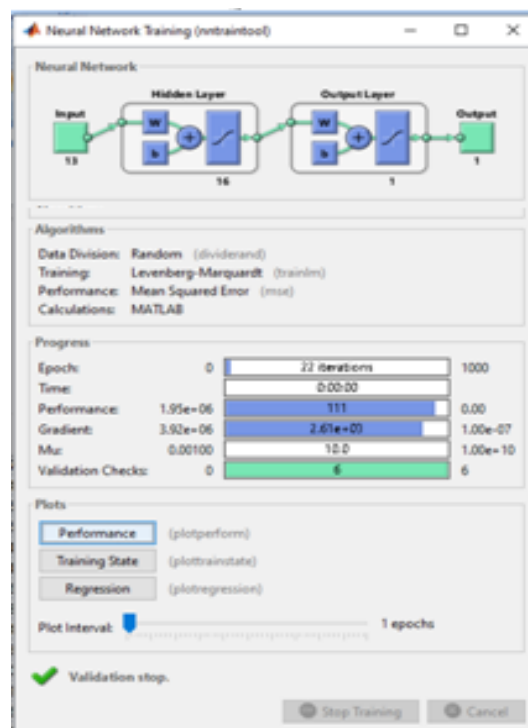


Figure 4.6: Pictorial representation of the training model for validation data

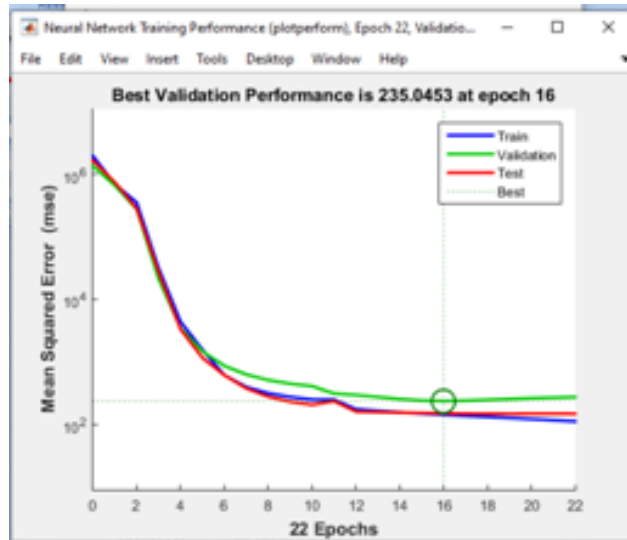


Figure 4.7: Performance model for validation data

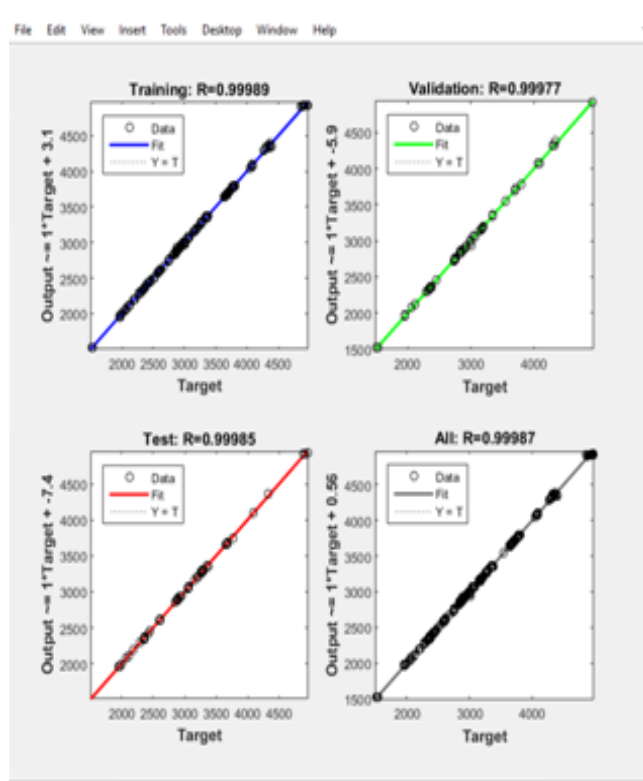


Figure 4.8: Prediction model of ANN for validation data

Table.4.1 Performance of Neural Network with different hidden neurons

Sl. No	Neurons	SE Training RMSE	R ²	SE Validation RMSE	R ²
1	12	10.04679	0.99987	12.10706	0.99987
2	13	11.70058	0.99989	12.88229	0.99986
3	14	11.82621	0.99893	12.98863	0.99986
4	15	11.15395	0.99988	12.52457	0.99974
5	16	9.477841	0.99992	11.85352	0.99987
6	17	11.60578	0.99987	13.64511	0.99779
7	18	12.1123	0.99986	14.10802	0.99992
8	19	10.86117	0.99983	12.16267	0.99953
9	20	10.69871	0.99989	11.94653	0.99955

CHAPTER 5

NUMERICAL MODELING

5.1 General

In general, various phenomena and engineering problems are mathematical models of physical situations. Mathematical models are differential equations with a set of boundaries and initial conditions. Solving differential equations under various conditions, such as boundary and initial conditions, leads to understanding the phenomena and predicting its future. However, the exact solution for differential equations is generally difficult to obtain for many engineering problems. This inability to obtain exact solutions may be due to either the complex nature of governing differential equations or the difficulty in dealing with boundary and initial conditions. In order to deal with such problems, numerical methods are adopted to obtain approximate solutions for differential equations. The advent of high-speed computers has revolutionised the scope of analysis by numerical methods, such as the finite element method (FEM), for complex problems in all branches of engineering. The FEM has become a powerful tool for solving numerous rock mechanics problems. This is one of the most popular, flexible, and valuable analytical computations available to engineers. The basic principle of this method is that the behaviour of parts defines the behaviour of the whole.

The random geometric norms, unusual loading conditions and varying material properties make rigorous mathematical analysis almost impossible in most rock mechanics problems. The need for the FEM analysis has been felt by mining engineers in solving all such complex problems, considering the nonlinearity, non-homogeneity and anisotropy of rock properties. The method has been extensively used for problems related to stress analysis in mining, especially in the location and design of mine structures. However, it has not been extensively used to pick penetration into rock, except the two-dimensional plane strain representation of the problem.

The two basic approaches of FEM analysis are,

- 1) Force approach, in which forces at the nodal points are the unknown aspects of the problem and
- 2) Displacement approach, in which displacement at the nodal points is the unknown aspect of the problem. The governing equations are established in terms of nodal forces or nodal displacements for each node, as the case may be, using the appropriate equilibrium condition for the problem investigated. The general procedure for solving a problem by FEM involves the following steps,

5.1.1 Pre-processing phase

- 1) Create and discretise the solution into finite elements- divide the problem into a number of nodes and elements.
- 2) Selection of the approach, either displacement or force.
- 3) Development of equations for an element and generation of element stiffness matrices.
- 4) Computation of the global stiffness matrix from the element stiffness matrices.
- 5) Incorporating/Applying the boundary conditions like force, displacement or mixed, as applicable for the specific problem.
- 6) Formulation of the system of governing equations for the specific problem.

5.1.2 Solution phase

- I. Solving linear or nonlinear algebraic equations, determines the unknown nodal displacements or forces at nodes.

5.1.3 Post-processing phase

- I. Computation of other quantities of interest, such as nodal stresses and displacements, by averaging the values of the adjacent elements.
- II. Presentation and analysis of results.

The accuracy and the effectiveness of FEM depend on discretisation, which is the type and the number of elements used in the mesh depending upon the geometry (pick and attack angle). The type of element chosen should be compatible with the problem. The compatibilities at the boundaries of the adjoining elements must be taken into account.

5.2 FEM analysis of pick penetration into rock

Several commercial finite element software (e.g. NASTRAN, ANSYS, SAPSO, SOSMOS and EMRC) are available to solve various engineering problems. Some of the programs have been developed in such a flexible manner that the same program is used to solve problems relating to different branches of engineering with little or no modification (e.g. NASTRAN, ANSYS). The present investigation was carried out by using the finite element program, ANSYS, which is available in the CAD-CAM centre of the National Institute of Technology Karnataka (NITK).

5.2.1 Description of the numerical model

The numerical simulations were developed with the commercial finite element software ANSYS version 15. In order to reduce the processing time, a quarter of both of the rock blocks was considered in the model.

5.2.1.1 Defining element type

- I. Composite brick elements with eight nodes were considered in this investigation for all attack angles and four types of picks. A mapped volume mesh that contains only triangular elements was used for meshing. In all the cases, only continuity of displacements across interfaces was ensured. All other interface variables were not taken into consideration.

5.2.1.2 Material properties

In finite element analysis, respective rocks' geo-mechanical properties were considered input parameters, as mentioned in Table 3.2.

5.2.1.3 Mesh generation

The analysis of pick-rock was carried out by adopting a 3-D (3-dimensional) analysis with a displacement approach. Due to the restriction in size (2 GB RAM) and working on a single user basis, the total number of elements for the 3-D model was imposed, forcing the mesh to be relatively fine. However, 2758 elements and 665 nodes for the dimension of 0.3x0.3x0.45M rectangular block were considered a reasonably fine mesh formation; the aspect ratio (ratio of two adjacent sides) of the elements were

maintained at three since it was a structural analysis. Therefore, similar element divisions are maintained in all sizes of the picks.

The problem of memory space requirement was overcome for the above-mentioned large number of elements by generating the element stiffness matrices for one-fourth of the rectangular block because of the symmetry of the problem. Thus, the accuracy of the analysis is not compromised in any way. The detailed theory and the formulation of the ANSYS program are not discussed in the present study, as it is well-known FEM software and figure 5.1 shows the model and mesh generated with triangular elements.

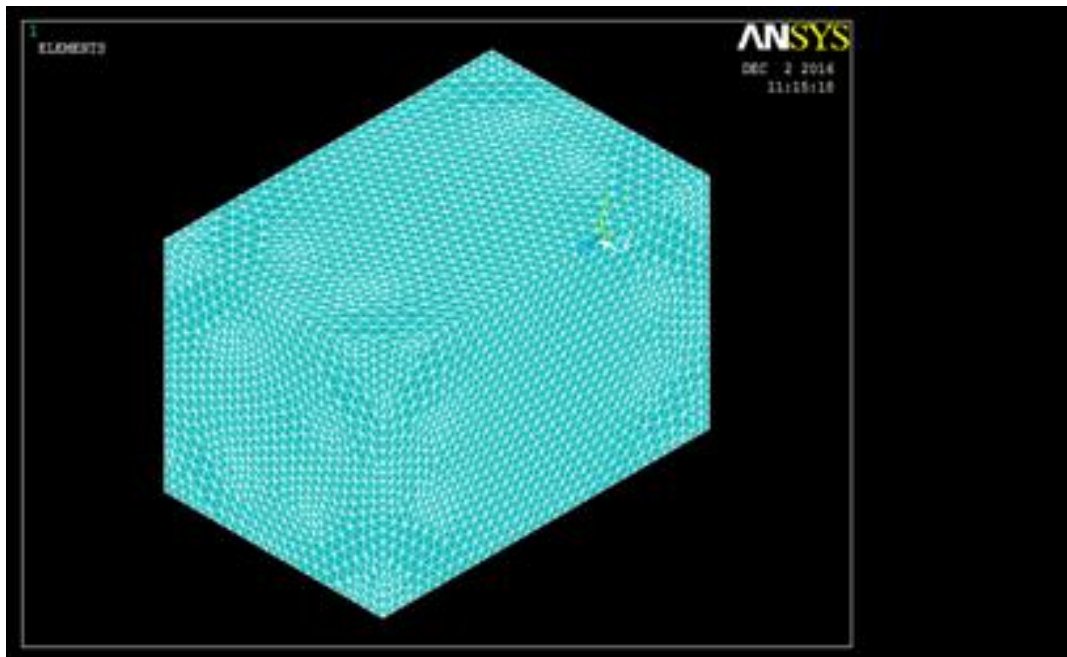
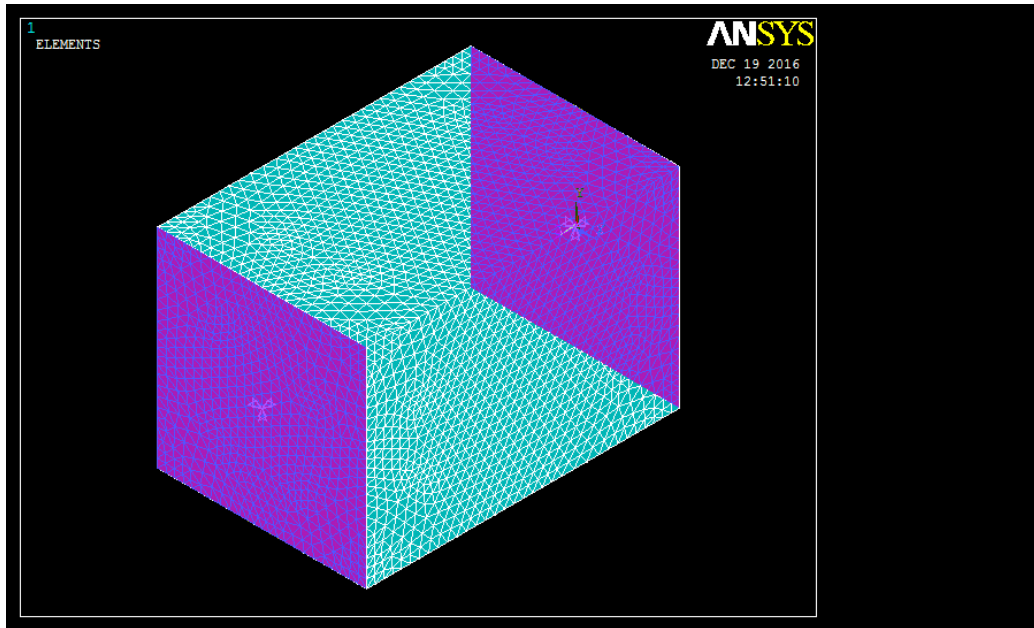
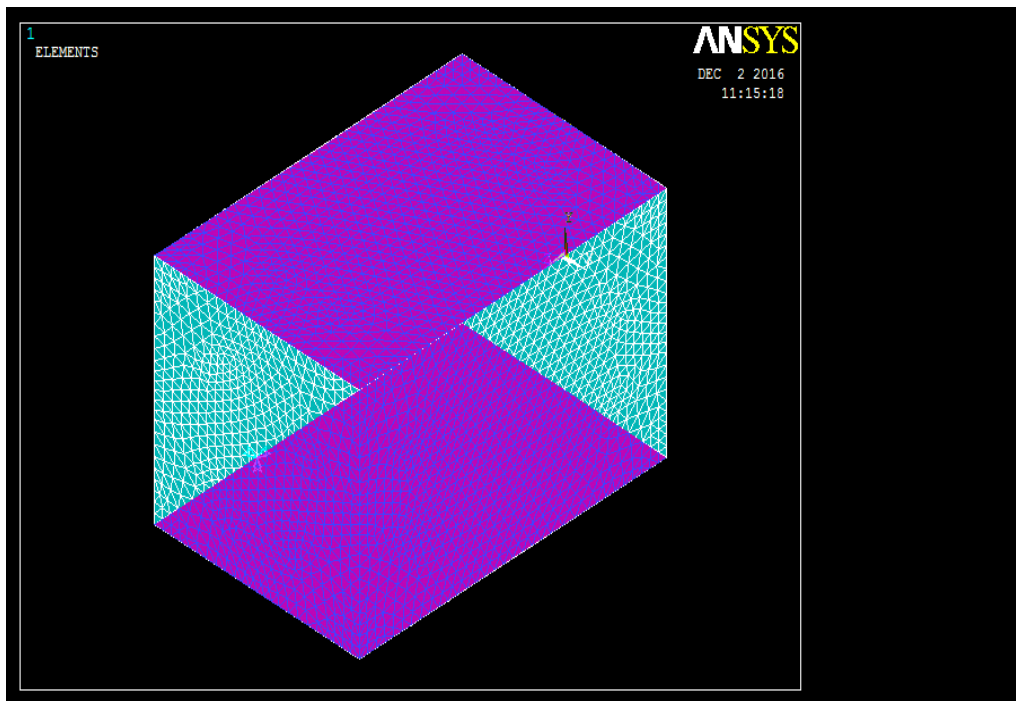


Figure 5.1 Boundary conditions adopted

In the present work, the symmetric boundary condition was adopted for the analysis. Owing to the limitation of obtaining a sufficient number of large size blocks of each rock type for the laboratory experiment test, 0.3M x 0.3M x 0.45M is considered to reasonably represent the semi-infinite condition and Figure 5.2 (a) & (b) shows the boundary conditions adopted for FEM analysis.



(a)



(b)

Figure 5.2 (a) & (b) shows the boundary conditions adopted for FEM analysis.

5.2.1.4 Method of applying load

1. The model geometry is, however simple rectangular block hence. Though Ansys's can import complex geometry too wide various formats.
2. Meshing the structure has 2758 elements and 665 nodes for the dimension of 0.3x0.3x0.45M rectangular block considered a reasonably fine mesh formation.
3. To apply the cutting force (at different pick angles and at different attack angles); the cutting force measured initially with the experiment is applied to determine the deformation and determine stress produced during the cutting process. To apply the same loads in Ansys's there are two viable options. We need to rotate the node at the point of application of load to the concerned attack angle (α), or the forces can also be resolved in two directions as the third direction is fixed (Z-direction). Resolving the force (F) along the X direction is $-F \cos \alpha$, and along Y direction is $F \sin \alpha$. Figure 5.3 shows the resolution of forces and their application in Ansys.
4. Further results after post-processing were obtained and shown in Appendix -II

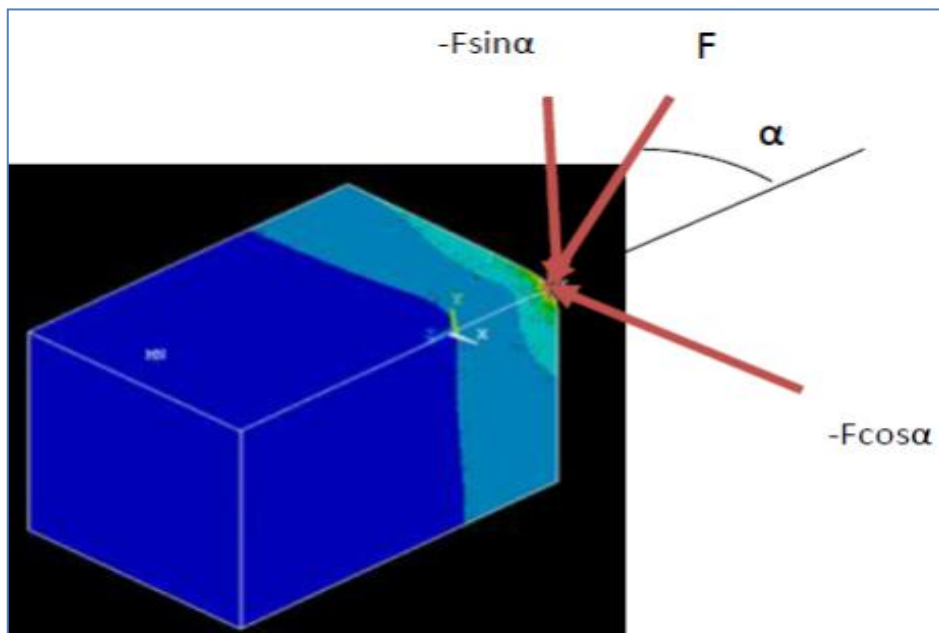


Figure 5.3 Resolution of forces and their application in Ansys

CHAPTER 6

RESULTS AND DISCUSSIONS

6.1 Experimental Results

The rock cutting tests were carried on ten types of rocks, namely coal, Sandstone (3 types), Limestone (4 types) and Dolomite (2 types) at 45°, 50°, 55°, 65° pick angle with each attack angle, the experiments were carried to study the influence of pick angle and attack angle on Specific energy for various pick-rock combination considered. The Specific energy values obtained at each combination of pick angle and attack angle were determined and are listed in Table 3.4 to 3.7 (Appendix-I)

6.1.2 Influence of Cutting Parameters on cutting rate and Specific energy

The results have been analysed to identify the important parameters affecting the cutting performance of the rock cutting process in terms of cutting rate and Specific energy consumed in the breaking process. The cutting parameters, namely pick angle (45°, 50°, 55°, 65°) and the attack angle (45°, 55°, 65°) and 45° attack angle with 5mm wear picks are used in the laboratory to study the influence of individual cutting parameters on rock cutting performance.

An extension to work is estimating the cutting rate and specific energy for an attack angle of 45° attack angle with 5 mm wear. A comparison is evaluated between the 45° attack angle and attack angle with 5 mm wear for testing the significance of pick angle, attack angle, torque, rpm and cutting force.

6.1.2.1 Influence of pick angle and attack angle on the cutting rate

Figures 6.1 to 6.4 Shows the influence of various pick angles on the cutting rate at 45°, 55° and 65° attack angles, respectively. The cutting rate is the measure of the yield/volume broken. When the depth of cut increases, the volume broken increases which indicates the increase in cutting rate. The cutting rate is found to form an

increasing trend. i.e., the cutting rate is found to increase linearly with the increase in pick angle. The highest cutting rate was found at the highest pick angle (65°) at all attack angles. The study intended to measure the variation of cutting rate with different attack angles. It is observed that with a 55° attack angle, coal and sandstones possess higher cutting rates at the highest pick angle. The maximum percentage variations in the cutting rates measured for coal compared to 45° and 65° attack angles are 18% and 25% at the highest pick angle, respectively. For sandstones 1, 2 and 3, the maximum percentage variation of 45° and 65° attack angles compared to 55° attack angles are 6% and 21%, 10.2% and 23%, 10.3% and 28% at the highest pick angle, respectively.

The limestones and dolomites, attack angle of 45° possess higher cutting rates than 55° and 65° attack angles. The maximum percentage variations in the cutting rates measured for Limestone 1, 2, 3 and 4 as compared to 55° and 65° are 3% and 28%, 0.2% and 24%, 2.2% and 23%, 2.1% and 32% respectively. For dolomite 1 and 2, the maximum percentage variation of 55° and 65° attack angles with 45° attack angles are 2.4 and 26%, 1.4 and 30%, respectively.

The influence of pick angle is compared between attack angle of 45° attack angle, and 45° attack angle with 5mm wear. The observation revealed that the cutting rate decreases with 5mm wear condition. The maximum increased percentage variation observed is 26.65% for coal, 27.72% for sandstone 1, 33.36% for sandstone 2, 31.61% for sandstone 3, 28.49% for limestone 1, 24.50% for limestone 2, 28.7% for limestone 3, 31.19% for limestone 4, 26.56% for dolomite 1 and 25.54% for dolomite 2.

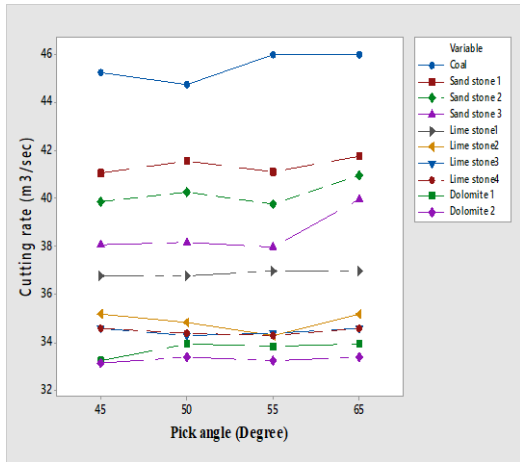


Figure 6.1 Influence of pick angle on cutting rate at 45° attack angle.

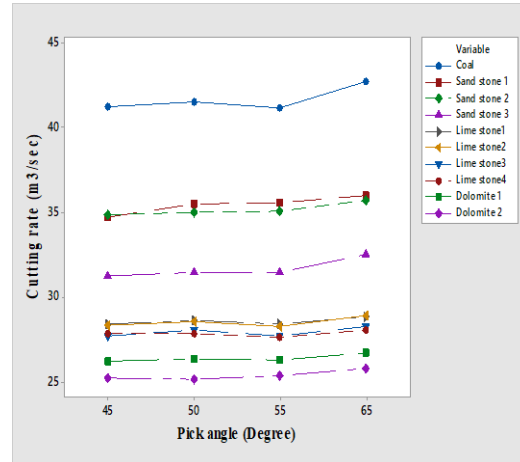


Figure 6.3 Influence of pick angle on cutting rate at 65° attack angle.

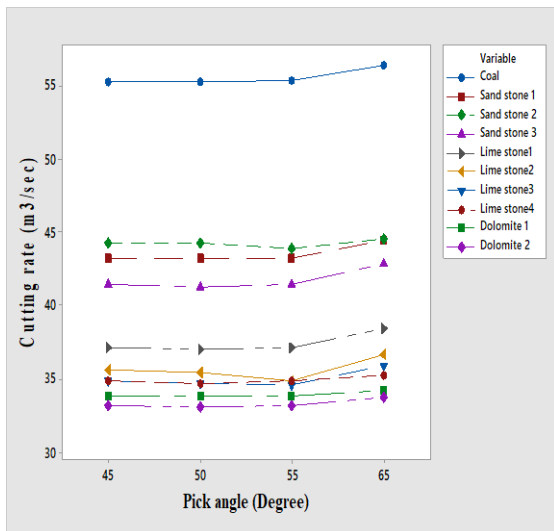


Figure 6.2 Influence of pick angle on cutting rate at 55° attack angle.

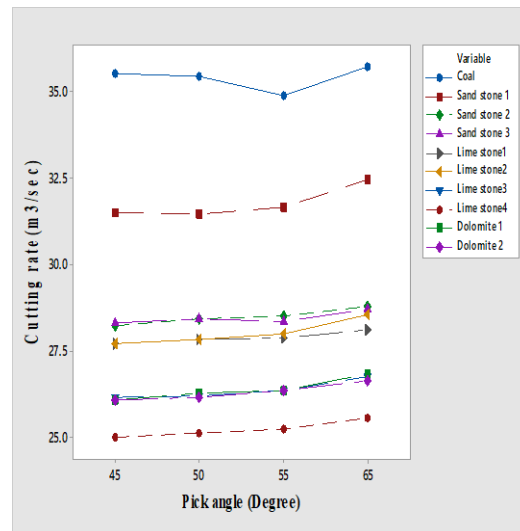


Figure 6.4 Influence of pick angle on cutting rate at 45° attack angle with 5mm wear.

6.1.2.2. Influence of rpm on cutting rate.

The study intends to signify the influence of rpm on the cutting rate. Figure 6.7 to 6.20 illustrates the variations of rpm on the cutting rate at different attack angles. It is observed that with the increase in rpm, the cutting rate also increased linearly. Higher observations correspond to the highest pick angle. The previous observations revealed that the cutting rate is higher for the highest pick angle. Hence a percentage difference in cutting rates is evaluated between the 45° and 65° pick angles corresponding to the highest rpm.

- The difference measured between the maximum rpm (350) at the highest pick angle (65°) and the maximum rpm of the lowest pick angles (45°) at attack angles of 45°, 55° and 65° are found to be 1.34%, 0.23% and 0.21% for coal.
- Similarly, for sandstone 1, it is found to be 1.46%, 2.22% and 1.75%. For sandstone 2 it is 3.49%, 0.8%, and 1.68%. for sandstone 3, it is 4.08%, 1.35% and 0.57% respectively.
- For limestone 1 it is 0.1%, 0.83% and 0.73% respectively. For lime stone 0.1%, 0.83% and 0.73%. For lime stone 3; it is 0.1%, 0.15% and 0.64%. For lime stone 4; it is 0.1%, 0.05% and 0.65% respectively.
- For dolomite 1; it is 1.06%, 0.61% and 1.66%. for dolomite 2; 0.31%, 1.15% and 0.3% respectively.

As far as rpm is concerned, rpm's effect is less significant compared to a specific energy of attack angles.

- The influence of pick angle is compared between attack angle of 45° attack angle, and 45° attack angle with 5mm wear. The observation revealed that the cutting rate decreases with 5mm wear condition. The maximum increased percentage variation observed is 25.65% for coal, 26.72% for sandstone 1, 30.36% for sandstone 2, 27.61% for sandstone 3, 28.49% for limestone 1 , 24.50% for limestone 2 , 28.7% for limestone 3, 30.19% for limestone 4, 26.16% for dolomite 1 and 25.54% for dolomite 2.

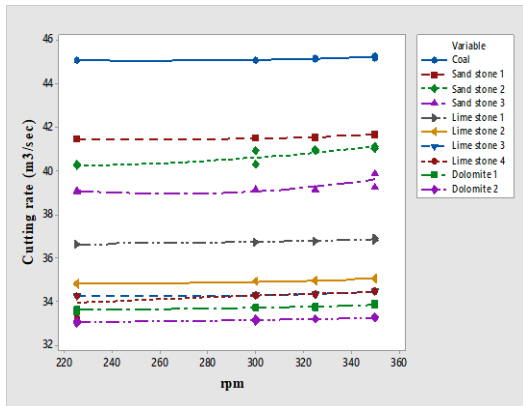


Figure 6.5 Influence of rpm on cutting rate at 45° pick angle with 45° attack angle

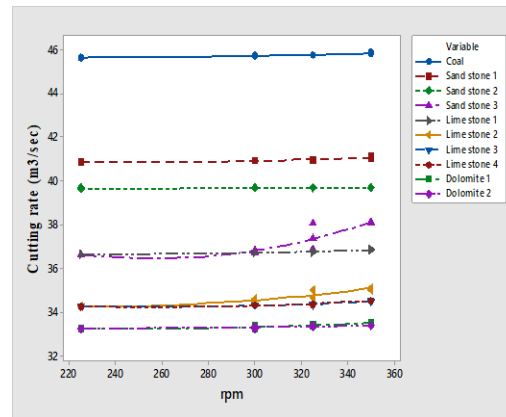


Figure 6.8 Influence of rpm on cutting rate at 65° pick angle with 45° attack angle

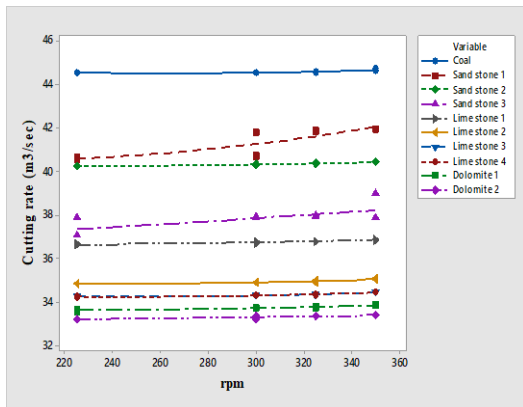


Figure 6.6 Influence of rpm on cutting rate at 50° pick angle with 45° attack angle

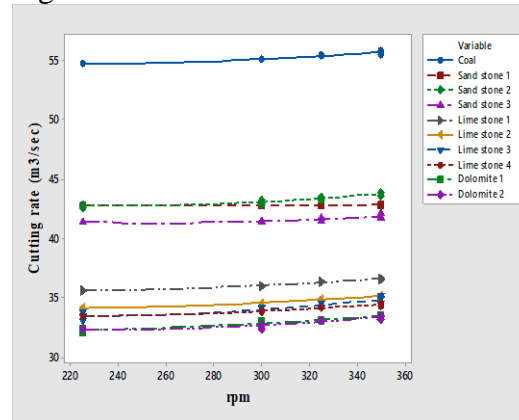


Figure 6.9 Influence of rpm on cutting rate at 45° pick angle with 55° attack angle

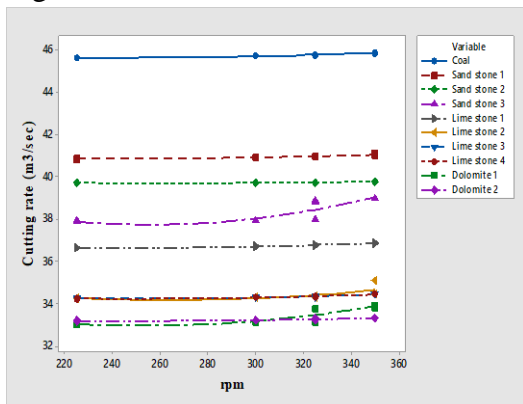


Figure 6.7 Influence of rpm on cutting rate at 55° pick angle with 45° attack angle

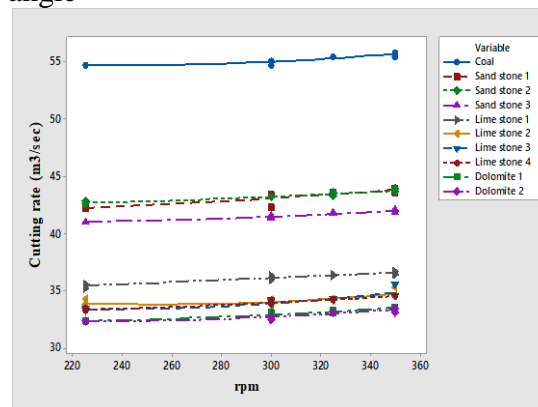


Figure 6.10 Influence of rpm on cutting rate at 50° pick angle with 55° attack angle

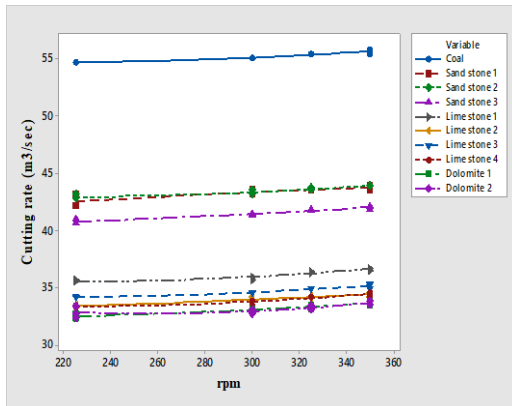


Figure 6.11 Influence of rpm on cutting rate at 55° pick angle with 55° attack angle

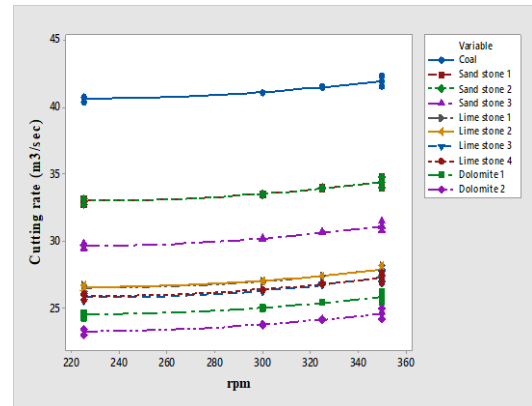


Figure 6.14 Influence of rpm on cutting rate at 50° pick angle with 65° attack angle

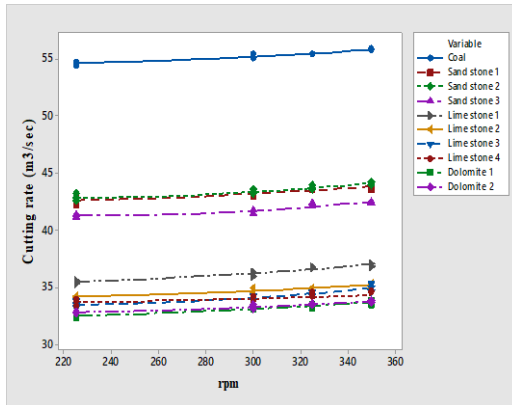


Figure 6.12 Influence of rpm on cutting rate at 65° pick angle with 55° attack angle

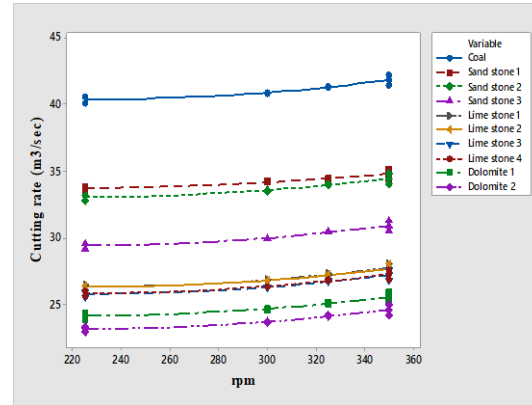


Figure 6.15 Influence of rpm on cutting rate at 55° pick angle with 65° attack angle

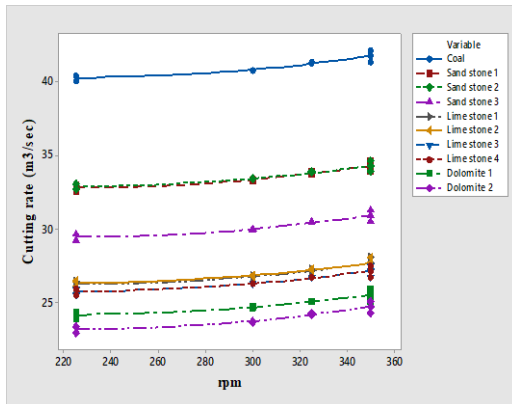


Figure 6.13 Influence of rpm on cutting rate at 45° pick angle with 65° attack angle

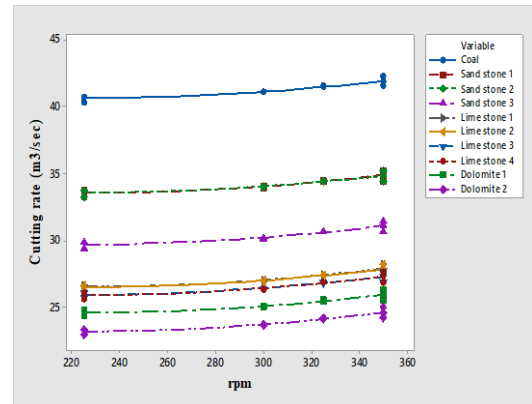


Figure 6.16 Influence of rpm on cutting rate at 65° pick angle with 65° attack angle

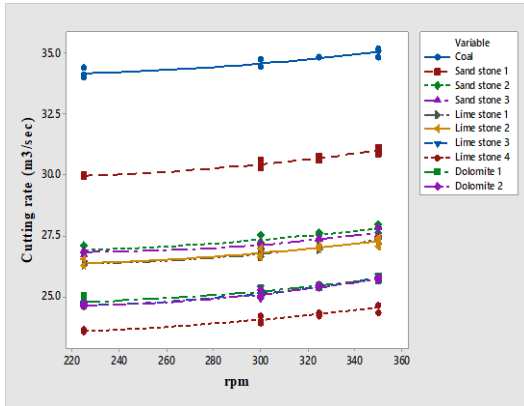


Figure 6.17 Influence of rpm on cutting rate at 45° pick angle with 45° attack angle with 5mm wear

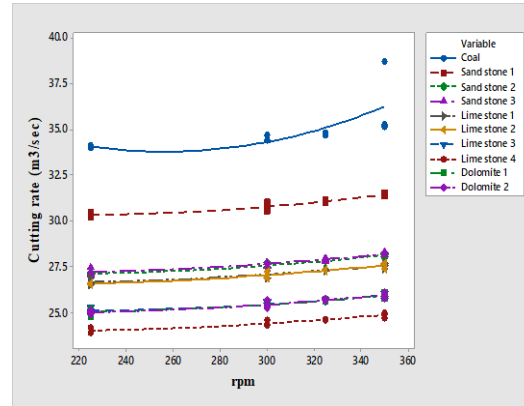


Figure 6.20 Influence of rpm on cutting rate at 65° pick angle with 45° attack angle with 5mm wear

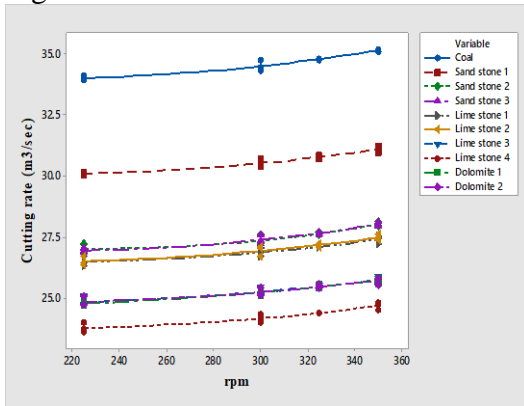


Figure 6.18 Influence of rpm on cutting rate at 50° pick angle with 45° attack angle with 5mm wear

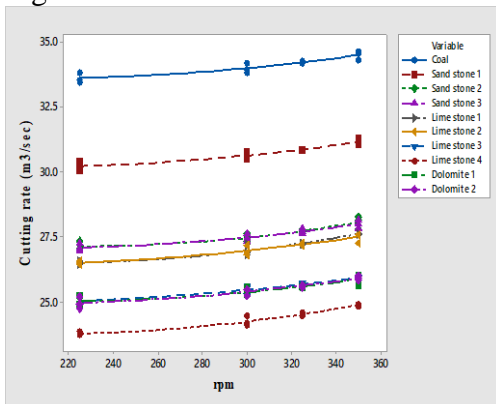


Figure 6.19 Influence of rpm on cutting rate at 55° pick angle with 45° attack angle with 5mm wear

6.1.2.3. Influence of torque on cutting rate.

The study intends to signify the influence of torque on cutting rate. Figure 6.21 to 6.36 illustrates the variations of torque on the cutting rate at different attack angles. It is observed that with the increase in torque, the cutting rate also increased linearly. The previous observations revealed that the cutting rate is higher for the highest pick angle. Hence, a percentage difference in cutting rates is evaluated between the highest (19 N-m) and least (14 N-m) torque values corresponding to the highest rpm.

- The difference measured between the maximum torque and the lowest torque values at attack angles of 45° , 55° and 65° is found to be 1.34%, 0.23% and 0.21% for coal.
- Similarly, for sand stone 1, it is found to be 1.46%, 2.22% and 1.75%. For sand stone 2 it is 3.2%, 0.3%, 0.55%. for sand stone 3, it is 1.6%, 0.36% and 0.05% respectively.
- For limestone 1 it is 0.05%, 0.05% and 0.25% respectively. For lime stone 2 it is 1.10%, 2.09% and 0.05%. For lime stone 3; it is 0.05%, 0.74% and 0.264%. For lime stone 4; it is 0.05%, 0.05% and 0.439% respectively.
- For dolomite 1; it is 0.05%, 0.61% and 0.28%. for dolomite 2; 0.20%, 0.86% and 0.38% respectively.

As far as rpm is concerned, rpm's effect is less significant compared to a specific energy of attack angles.

- The influence of pick angle is compared between attack angle of 45° attack angle, and 45° attack angle with 5mm wear. The observation revealed that the cutting rate decreases with 5mm wear condition. The maximum increased percentage variation observed is 29.65% for coal, 29.72% for sandstone 1, 35.16% for sandstone 2, 31.61% for sandstone 3, 26.49% for limestone 1 , 23.50% for limestone 2 , 28.7% for limestone 3, 30.19% for limestone 4, 21.56% for dolomite 1 and 23.54% for dolomite 2.

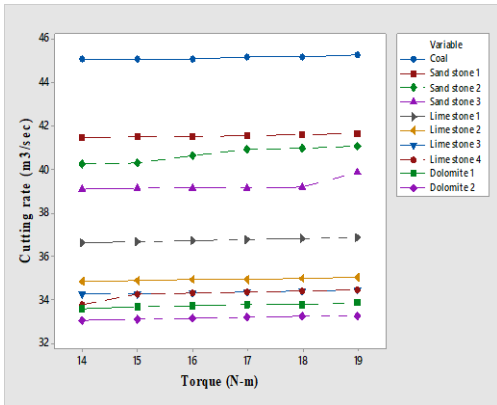


Figure 6.21 Influence of torque on cutting rate for 45° pick angle at 45° attack angles for all rocks.

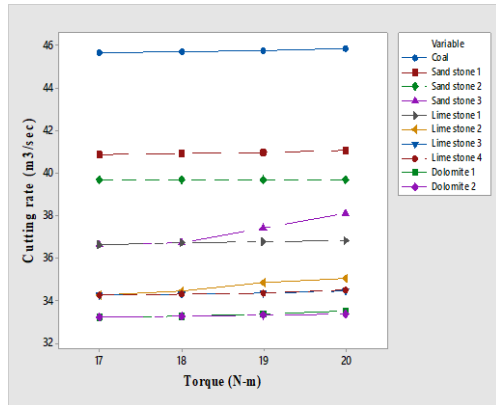


Figure 6.24 Influence of torque on cutting rate for 65° pick angle at 45° attack angle for all rocks.

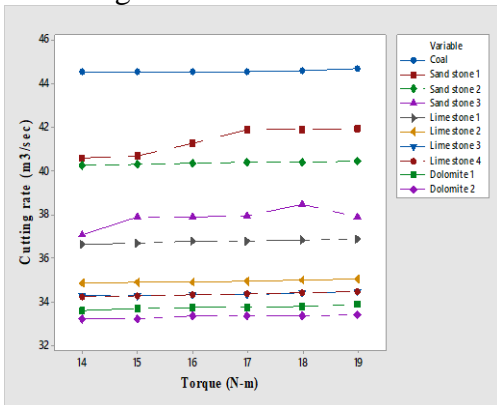


Figure 6.22 Influence of torque on cutting rate for 50° pick angle at 45° attack angle for all rocks.

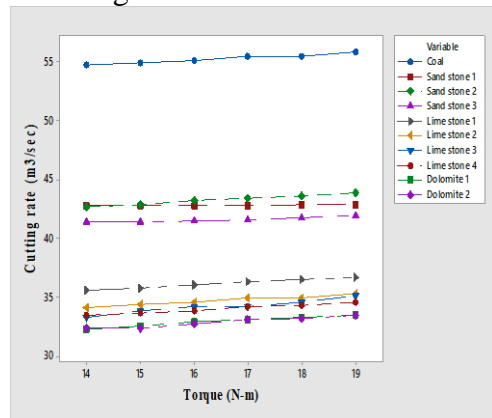


Figure 6.25 Influence of torque on cutting rate for 45° pick angle at 55° attack angle for all rocks.

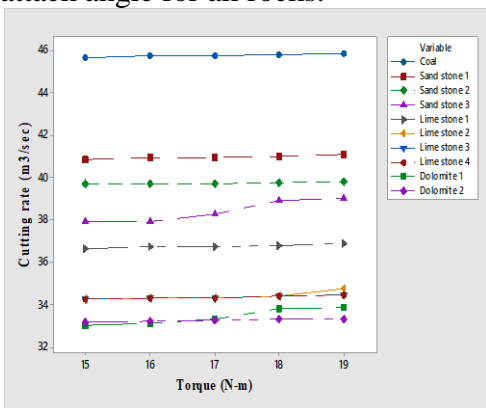


Figure 6.23 Influence of torque on cutting rate for 55° pick angle at 45° attack angle for all rocks.

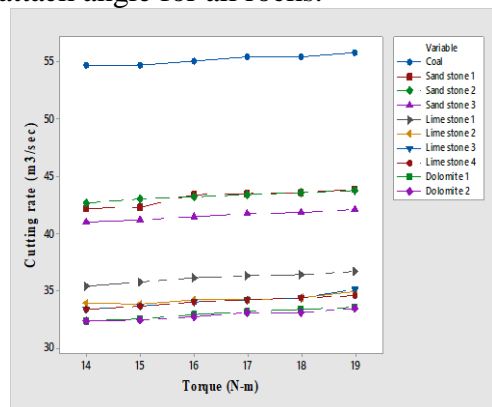


Figure 6.26 Influence of torque on cutting rate for 50° pick angle 55° attack angle.

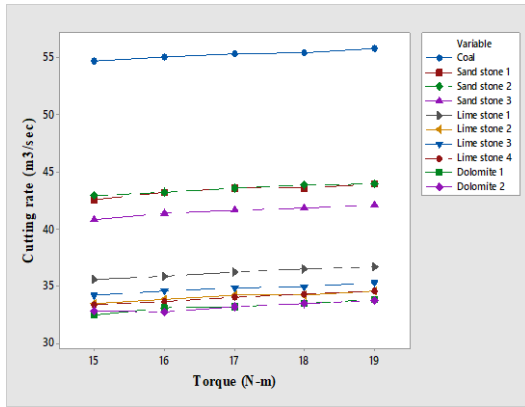


Figure 6.27 Influence of torque on cutting rate for 55° pick angle at 55° attack angle for all rocks.

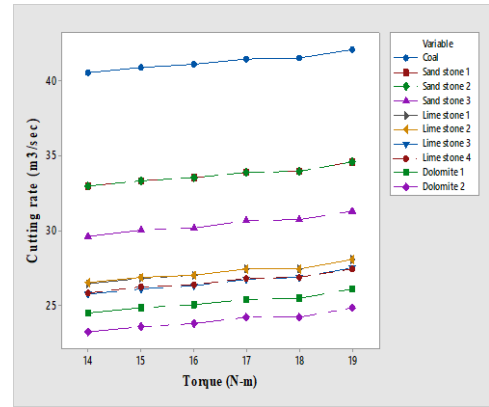


Figure 6.30 Influence of torque on cutting rate for 50° pick angle at 65° attack angle for all rocks.

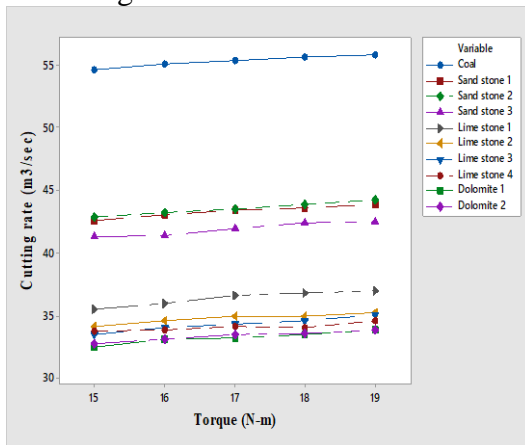


Figure 6.28 Influence of torque on cutting rate for 65° pick angle at 55° attack angle for all rocks.

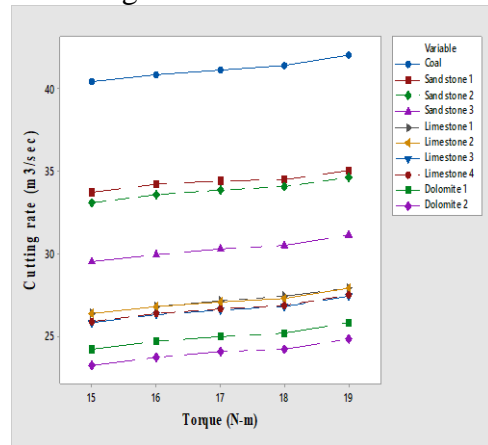


Figure 6.31 Influence of torque on cutting rate for 55° pick angle at 65° attack angle for all rocks.

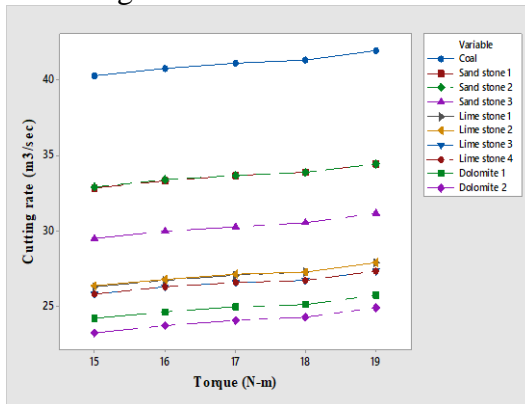


Figure 6.29 Influence of torque on cutting rate for 45° pick angle at 65° attack angle for all rocks.

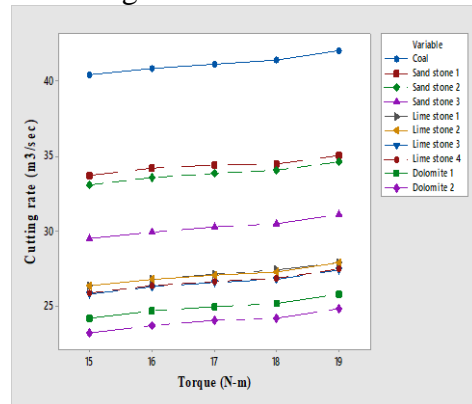


Figure 6.32 Influence of torque on cutting rate for 65° pick angle at 65° attack angle for all rocks.

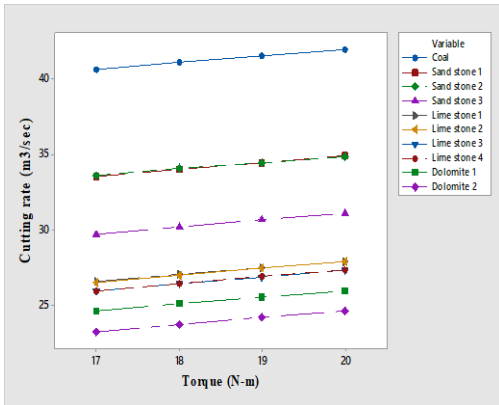


Figure 6.33 Influence of torque on cutting rate for 45° pick angle at 45° attack angle with 5mm wear.

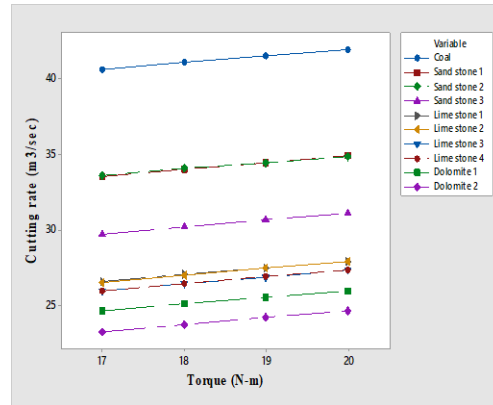


Figure 6.36 Influence of torque on cutting rate for 65° pick angle at 45° attack angle with 5mm wear.

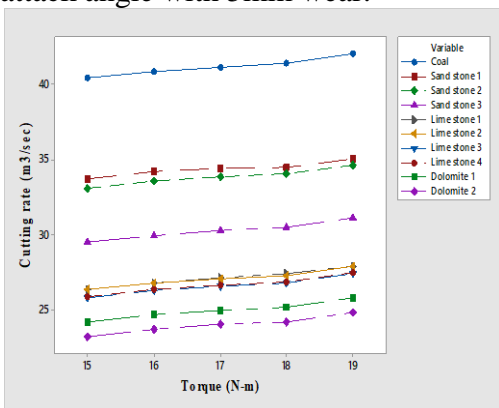


Figure 6.34 Influence of torque on cutting rate for 50° pick angle at 45° attack angle with 5mm wear.

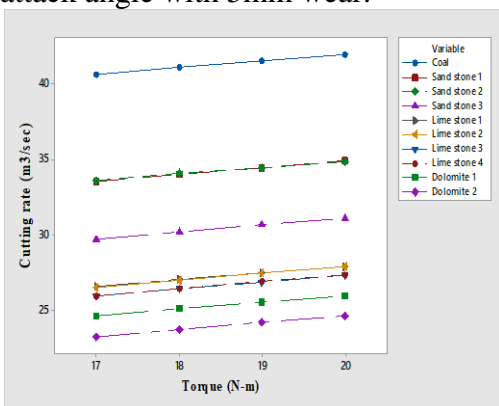


Figure 6.35 Influence of torque on cutting rate for 55° pick angle at 45° attack angle with 5mm wear.

6.1.2.4. Influence of cutting force on cutting rate.

The study intends to signify the influence of cutting force on the cutting rate. Figure 6. 37 to 6.52 illustrates the variations of cutting force on the cutting rate at different attack angles. It is observed that with the increase in cutting force, the cutting rate also increased linearly. The previous observations revealed that the cutting rate is higher for the highest pick angle. Hence, a percentage difference in cutting rates is evaluated between the highest (19 N-m) and least (1.5 N-m) cutting forces corresponding to the highest rpm.

- The difference measured between the maximum cutting force and the lowest cutting force values at attack angles of 45°, 55° and 65° is 1.34%, 0.012% and 0.2867% for coal.
- Similarly, for sand stone 1, it is found to be 1.471%, 2.2065% and 1.61846%. For sand stone 2 it is 3.2%, 0.3%, 0.55%. for sand stone 3, it is 1.6%, 0.36% and 0.05% respectively.
- For limestone 1 it is 0.05, 0.05457 and 0.25929, respectively. For lime stone 2 it is 1.10%, 2.09% and 0.05%. For lime stone 3; it is 0.05%, 0.74% and 0.264%. For lime stone 4; it is 0.05%, 0.05% and 0.439% respectively.
- For dolomite 1; it is 1.2357, 0.61289, and 0.28116, for dolomite 2; 0.20%, 0.86% and 0.38% respectively.

As far as cutting force is concerned, the effect of cutting force is less significant compare to the specific energy of attack angles.

- The influence of rpm is compared between the attack angle of 45° attack angle, and 45° attack angle with 5mm wear. The observation revealed that the cutting rate increases with 5mm wear condition. The maximum increased percentage variation observed is 20.05% for coal, 25.12% for sandstone 1, 30.26% for sandstone 2, 32.61% for sandstone 3, 26.49% for limestone 1, 23.05% for limestone 2 , 24.71% for limestone 3, 26.19% for limestone 4, 25.66% for dolomite 1 and 27.54% for dolomite 2.

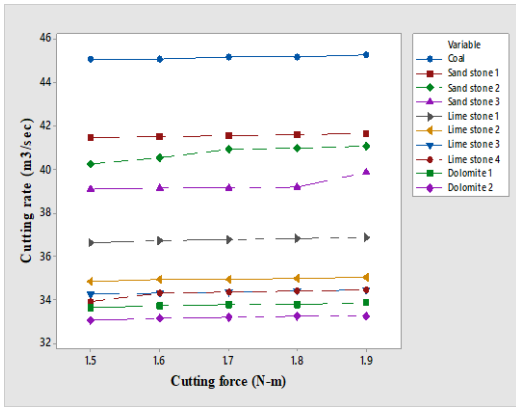


Figure 6.37 Influence of cutting force on Cutting rate with 45° pick angle at 45° attack angle for all rocks

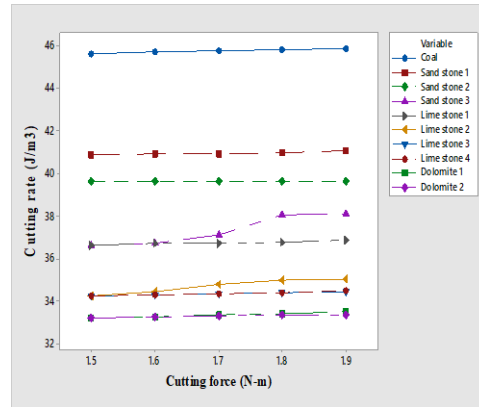


Figure 6.40 Influence of cutting force on Cutting rate with 65° pick angle at 45° attack angle for all rocks

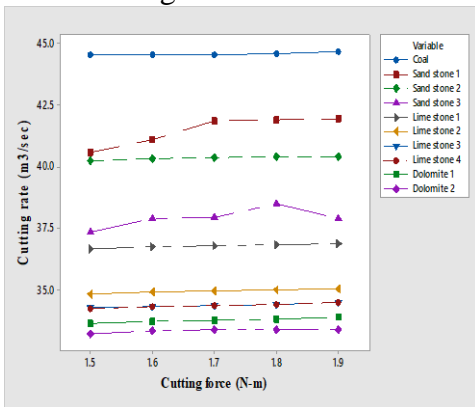


Figure 6.38 Influence of cutting force on Cutting rate with 50° pick angle at 45° attack angle for all rocks

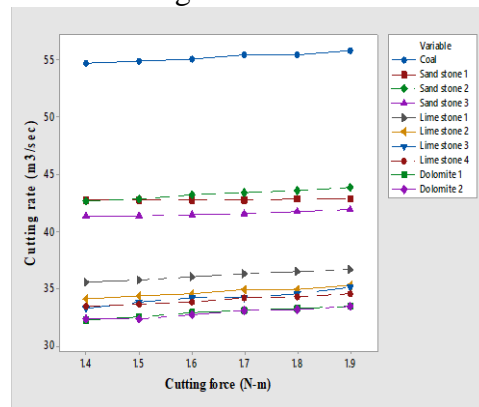


Figure 6.41 Influence of cutting force on Cutting rate with 45° pick angle at 55° attack angle for all rocks

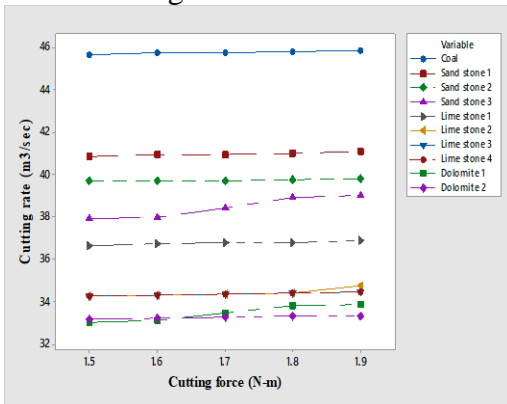


Figure 6.39 Influence of cutting force on Cutting rate with 55° pick angle at 45° attack angle for all rocks

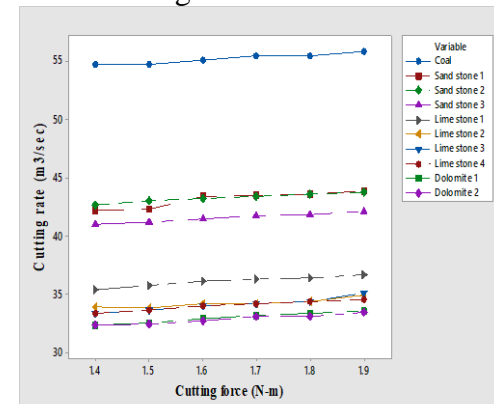


Figure 6.42 Influence of cutting force on Cutting rate with 50° pick angle at 55° attack angle for all rocks

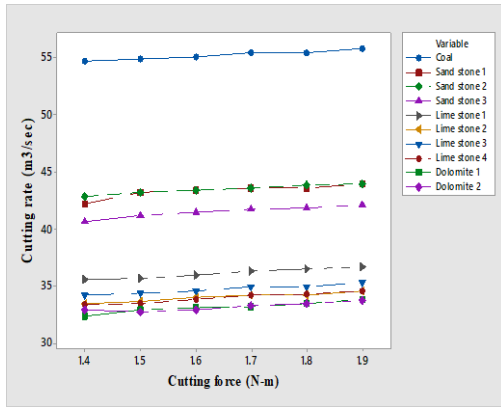


Figure 6.43 Influence of cutting force on Cutting rate with 55° pick angle at 55° attack angle for all rocks

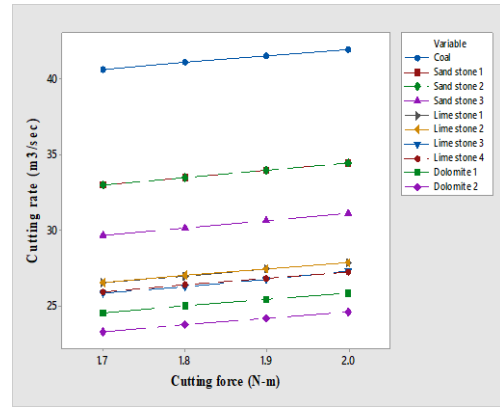


Figure 6.46 Influence of cutting force on Cutting rate with 50° pick angle at 65° attack angle for all rocks

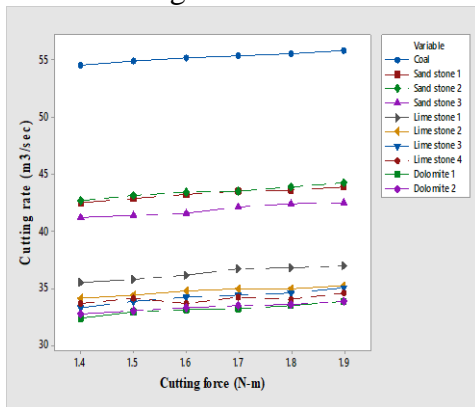


Figure 6.44 Influence of cutting force on Cutting rate with 65° pick angle at 55° attack angle for all rocks

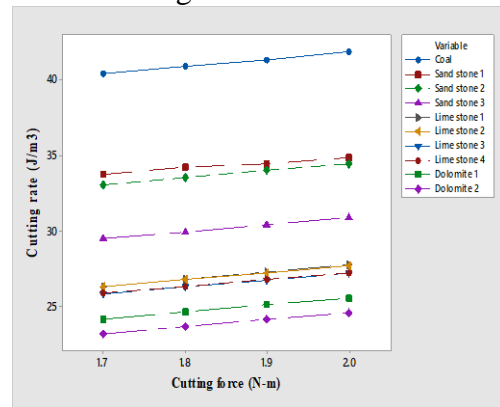


Figure 6.47 Influence of cutting force on Cutting rate with 55° pick angle at 65° attack angle for all rocks

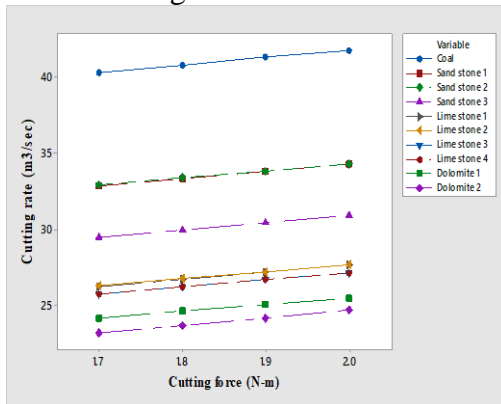


Figure 6.45 Influence of cutting force on Cutting rate with 45° pick angle at 65° attack angle for all rocks

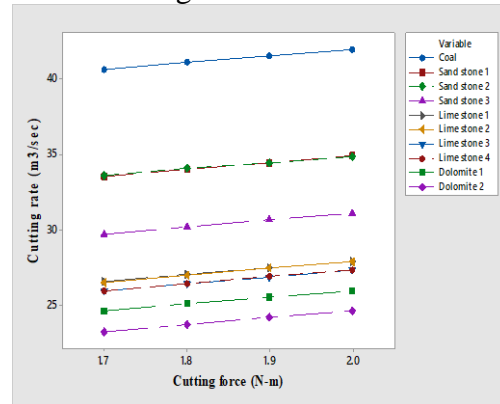


Figure 6.48 Influence of cutting force on Cutting rate with 65° pick angle at 65° attack angle for all rocks

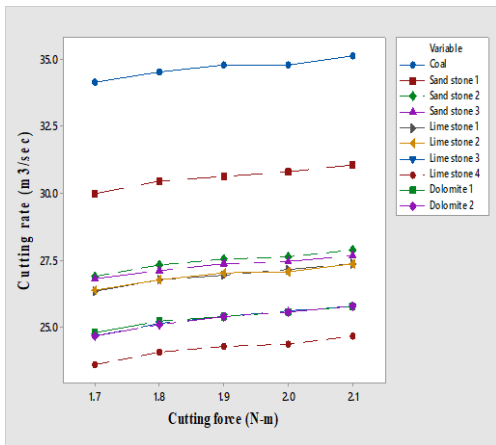


Figure 6.49 Influence of cutting force on Cutting rate with 45° pick angle with 5 mm wear at 45° attack angle for all rocks

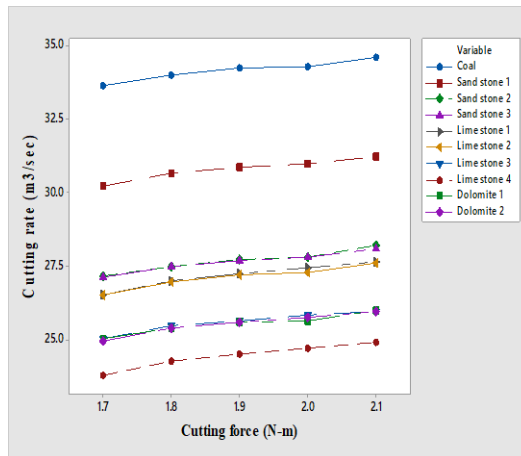


Figure 6.51 Influence of cutting force on Cutting rate with 55° pick angle with 5 mm wear at 45° attack angle for all rocks

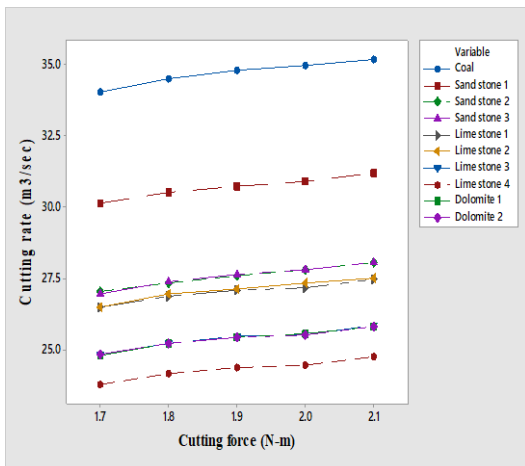


Figure 6.50 Influence of cutting force on Cutting rate with 50° pick angle with 5 mm wear at 45° attack angle for all rocks

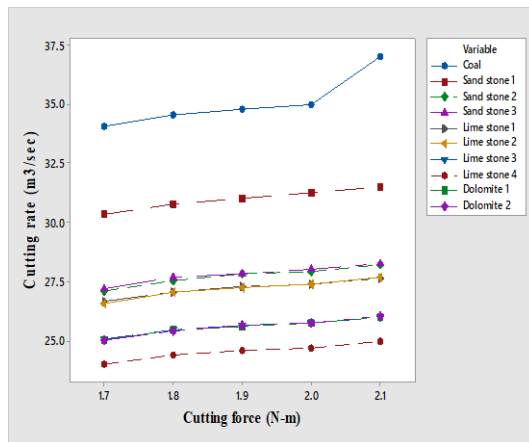


Figure 6.52 Influence of cutting force on Cutting rate with 65° pick angle with 5 mm wear at 45° attack angle for all rocks

6.1.2.5 Influence of pick angles and attack angles on the specific energy

Specific energy is defined as the energy consumption involved in excavating unit volume of rock. Specific energy mainly relies on the depth of cut of the rock samples. Figures 6.53 to 6.56 shows the plot of pick angles influence on specific energy for various attack angles. It is found that the specific energy decreases non-linearly with an increase in pick angles, a small optimisation after 55° pick angle. However, the difference in the variance was much less as compared. A further comparison of specific energies with attack angles is similar to that of cutting rate. With cutting rate, it was found that at 55° attack angle showed the maximum cutting rate. Similarly, with specific energy, An indirectly correlating observation was found as compared to cutting rate. The maximum saving in the specific energy for coal at 55° attack angle is 39.5% and 56.48% compared to

For sandstones 1, 2, and the maximum savings were found to be 21.91% and 42.53%, 26.22 and 40.8%, 34.53% and 51.26% in comparison with 45° and 65° attack angles.

For lime stone 1 , 23.50% and 32.16% for lime stone 2 , 28.7% and 21.98% for lime stone 3, 30.19% and 27.72% for lime stone 4, 21.56% and 30.56% for dolomite 1 and 23.54% and 23.63% , for dolomite 2 25.02% and 29.95%.

The influence of pick angle is compared between attack angle of 45° and 45° attack angle with 5mm wear. The observation revealed that specific energy increases with 5mm wear condition. The maximum increased percentage variation observed is 32.14% for coal, 34.66% for sandstone 1, 30.20% for sandstone 2, 35.81% for sandstone 3, 21.86% for limestone 1, 26.58% for limestone 2, 30.58% for limestone 3, 26% for limestone 4, 25.80% for dolomite 1 and 25.34% for dolomite 2.

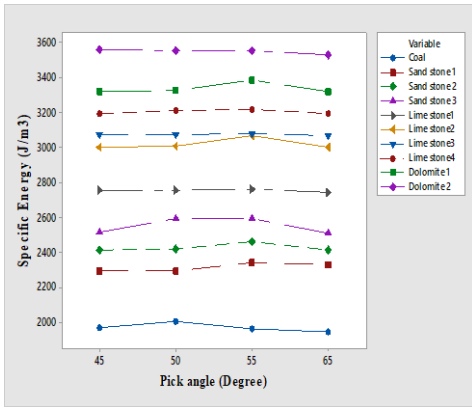


Figure 6.53 Influence of pick angles on the specific energy at 45° attack angle.

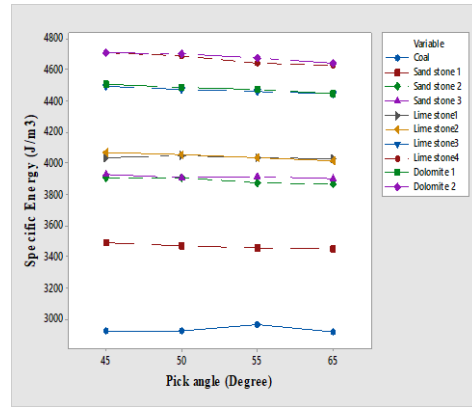


Figure 6.56 Influence of pick angles on Cutting rate with 5 mm wear at 45° attack angle for all rocks

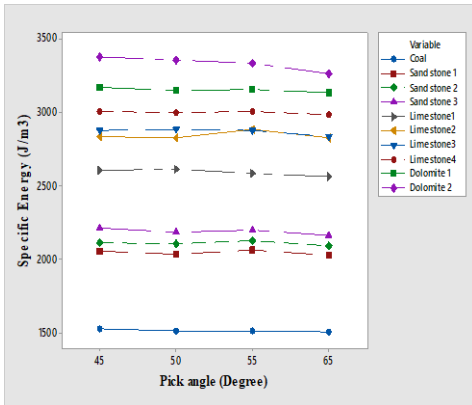


Figure 6.54 Influence of pick angles on the specific energy at 55° attack angle.

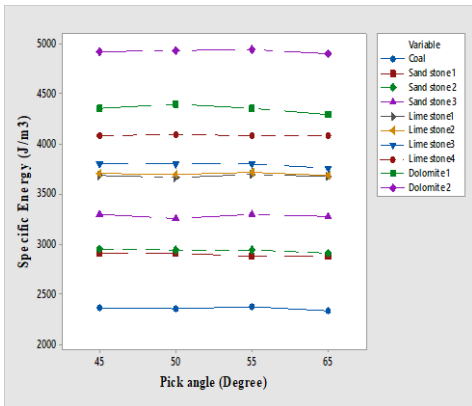


Figure 6.55 Influence of pick angles on the specific energy at 65° attack angle.

6.1.2.6. Influence of rpm on Specific energy

The study intends to signify the influence of rpm on specific energy. Figure 6.57 to 6.72 illustrates the variations of rpm on the specific energy at different angles. It is observed that with the increase in rpm, the specific energy also decreased non-linearly. The previous observations revealed that the specific energy is lesser for the highest pick angle. Hence a percentage difference in cutting rates is evaluated between the 45° and 65° pick angles corresponding to the highest rpm for evaluating specific energy.

- The difference measured between the maximum rpm (350) at the highest pick angle(65°) and the maximum rpm of the lowest pick angles (45°) at attack angles of 45°, 55° and 65° are found to be 0.03%, 0.616% and 1.2% for coal.
- Similarly, for sand stone 1, it is found to be 1.00%, 1.44% and 1.94%. For sand stone 2 it is 2.97%, 1.43%, 1.5%. for sand stone 3, it is 3.81%, 0.18% and 0.41% respectively
- For limestone 1 it is 0.88%, 0.02% and 0.2% respectively. For lime stone 2 2.62%, 0.047% and 1.18%. For lime stone 3; it is 1.08%, 2.07% and 1.5%. For lime stone 4; it is 0.04%, 0.023% and 0.18 %respectively.
- For dolomite 1; it is 2.17%, 1.06% and 3.4%. for dolomite 2; 4.41%, 3.75% and 1.88% respectively.

As far as rpm is concerned, the effect of rpm is less significant compared to specific energy variations of attack angles.

- The influence of pick angleis compared between attack angle of 45° attack angle and 45° attack angle with 5mm wear. The observation revealed that specific energy increases with 5mm wear condition. The maximum increased percentage variation observed is 32.14% for coal, 32.66% for sandstone 1, 28.10% for sandstone 2, 32.11% for sandstone 3, 25.58% for limestone 1, 25.60% for limestone 2, 29.48% for limestone 3, 27% for limestone 4, 21.80% for dolomite 1 and 23.34% for dolomite 2.

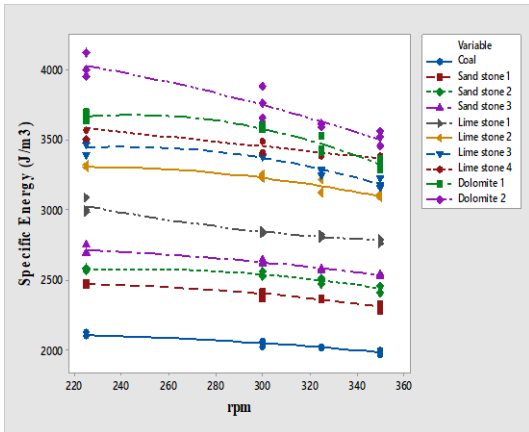


Figure 6.57 Influence of rpm on Specific energy for 45° Pick angle at 45° attack angle.

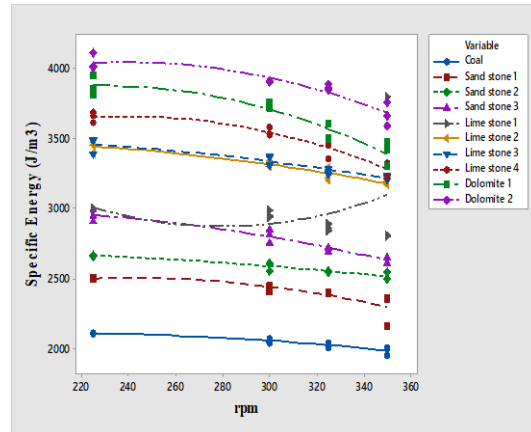


Figure 6.60 Influence of rpm on Specific energy for 65° Pick angle at 45° attack angle.

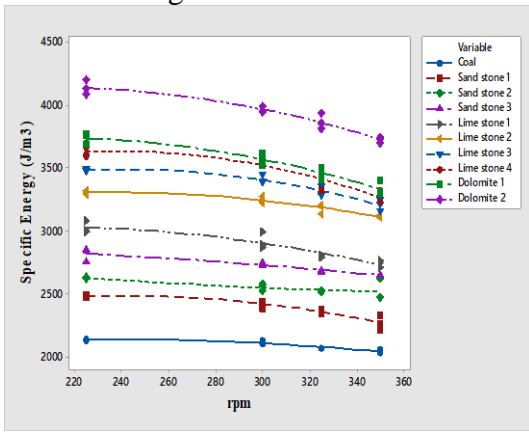


Figure 6.58 Influence of rpm on Specific energy for 50° Pick angle at 45° attack angle.

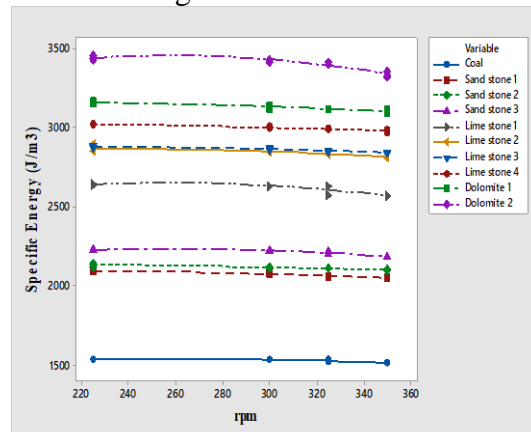


Figure 6.61 Influence of rpm on Specific energy for 45° Pick angle at 55° attack angle.

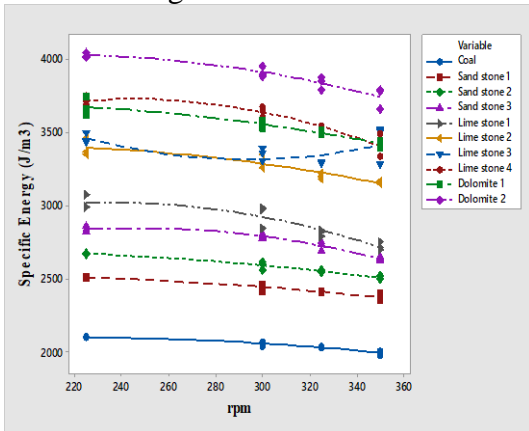


Figure 6.59 Influence of rpm on Specific energy for 55° Pick angle at 45° attack angle.

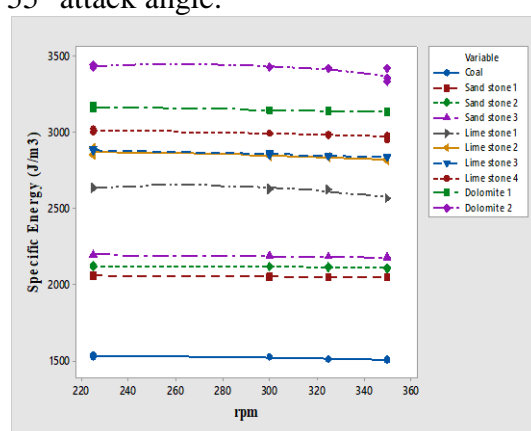


Figure 6.62 Influence of rpm on Specific energy for 50° Pick angle at 55° attack angle.

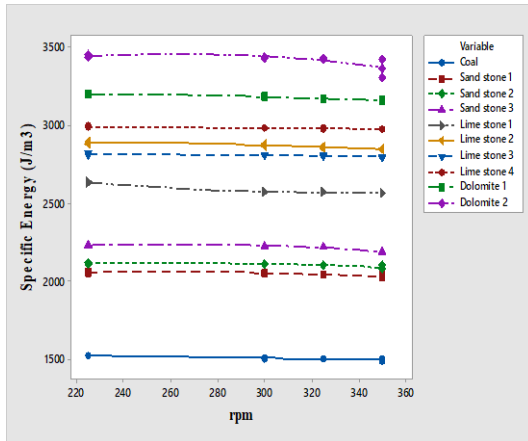


Figure 6.63 Influence of rpm on Specific energy for 55° Pick angle at 55° attack angle.

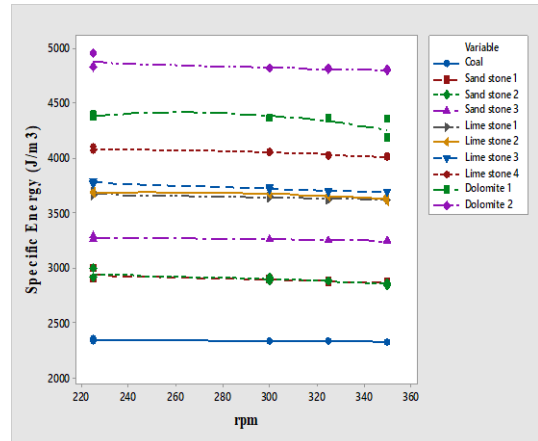


Figure 6.66 Influence of rpm on Specific energy for 50° Pick angle at 65° attack angle.

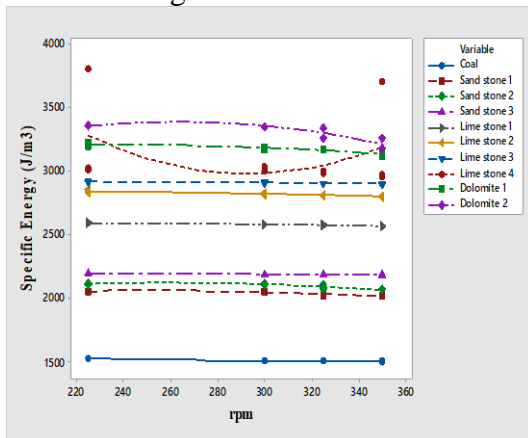


Figure 6.64 Influence of rpm on Specific energy for 65° Pick angle at 55° attack angle.

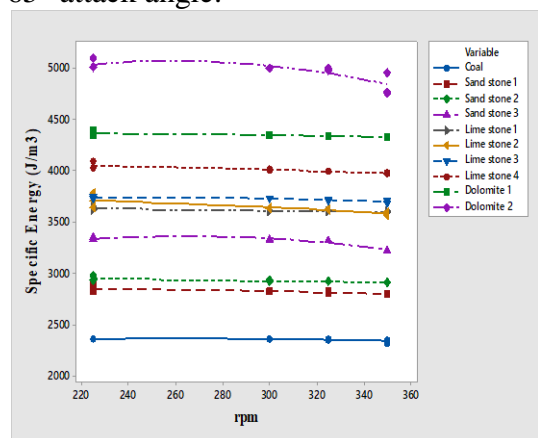


Figure 6.67 Influence of rpm on Specific energy for 55° Pick angle at 65° attack angle.

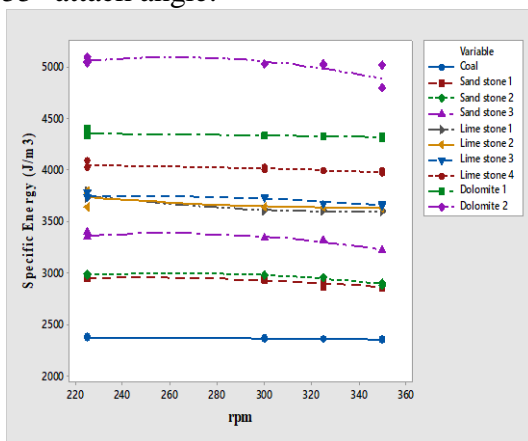


Figure 6.65 Influence of rpm on Specific energy for 45° Pick angle at 65° attack angle.

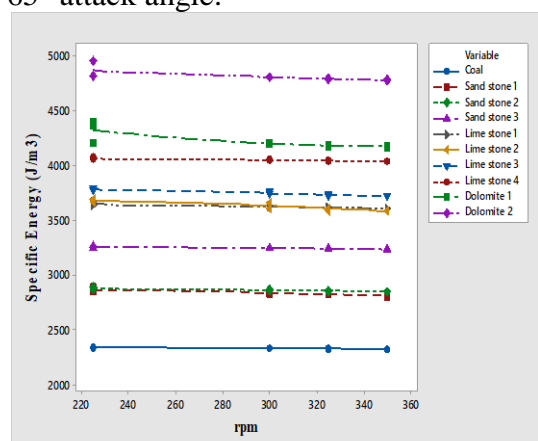


Figure 6.68 Influence of rpm on Specific energy for 65° Pick angle at 65° attack angle.

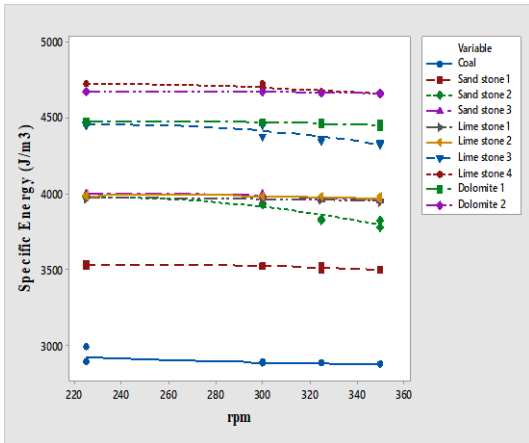


Figure 6.69 Influence of rpm on Specific energy for 45° Pick angle at 45°attack angle with 5mm wear.

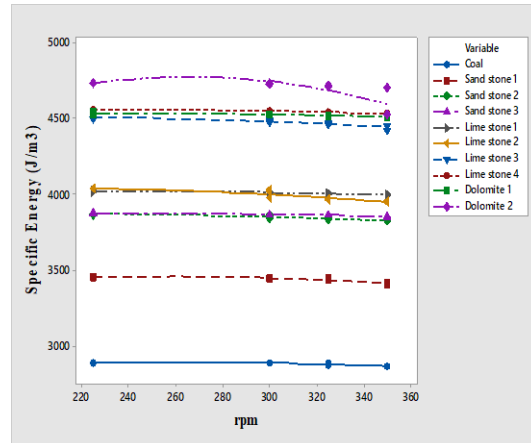


Figure 6.72 Influence of rpm on Specific energy for 65° Pick angle at 45°attack angle with 5mm wear.

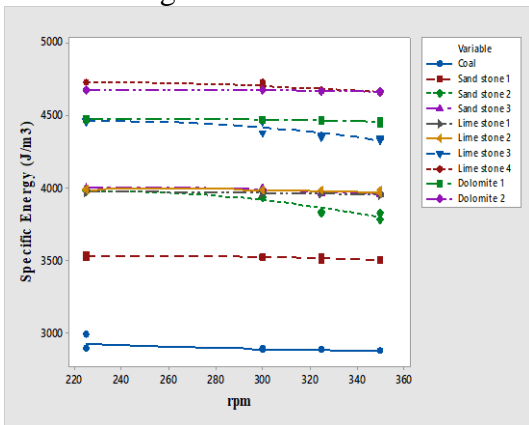


Figure 6.70 Influence of rpm on Specific energy for 50° Pick angle at 45°attack angle with 5mm wear.

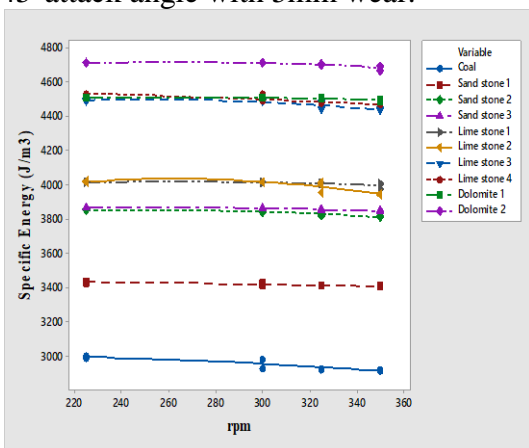


Figure 6.71 Influence of rpm on Specific energy for 55° Pick angle at 45°Attack angle with 5mm wear.

6.1.2.7. Influence of torque on Specific energy.

The study intends to signify the influence of torque on specific energy. Figure 6.73 to 6.88 illustrates the variations of rpm on the cutting rate, at different angles. It is observed that with the increase in torque, the specific energy decreases non-linearly. A percentage difference in specific energy is evaluated between the least and highest torque is evaluated to identify the variation of specific energy in terms of torque.

- The difference measured between the maximum torque and the minimum torque at attack angles of 45° , 55° and 65° is found to be 0.03%, 0.616% and 1.20% for coal.
- Similarly, sandstone 1, it is found to be 1.01%, 1.44% and 1.94%. For sandstone 2 it is 2.97%, 1.42% and 1.50%. for sandstone 3, it is 3.81%, 0.18% and 0.47% respectively
- For limestone 1 it is 0.886%, 0.02% and 0.24% respectively. For lime stone 2 2.62%, 0.47% and 1.18%. For lime stone 3; it is 1.02%, 2.077% and 1.5%. For lime stone 4; it is 2.55%, 7.8% and 1.3% respectively.
- For dolomite 1; it is 2.17%, 1.06% and 3.41%. for dolomite 2; 4.47%, 3.75% and 1.88% respectively.

As far as torque is concerned, the effect of torque is less significant compared to specific energy variations of attack angles.

- The influence of torque is compared between the attack angle of 45° attack angle and 45° attack angle with 5mm wear. The observation revealed that specific energy increases with 5mm wear condition. The maximum increased percentage variation observed is 32.14% for coal, 34.66% for sandstone 1, 36.20% for sandstone 2, 36.07% for sandstone 3, 31.6% for limestone 1, 21.89% for limestone 2, 27.48% for limestone 3, 30.54% for limestone 4, 26.63% for dolomite 1 and 25.80% for dolomite 2.

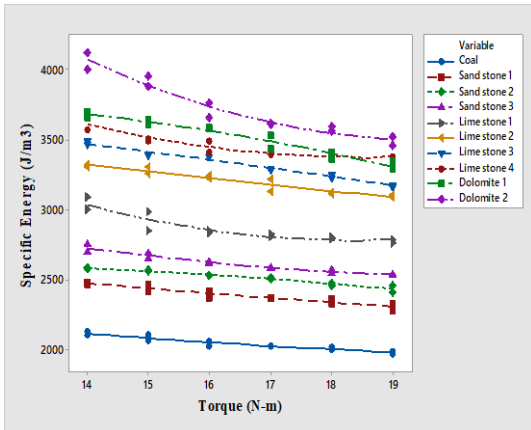


Figure 6.73 Influence of torque on Specific energy with 45° Pick angle at 45° attack angle for all rocks.

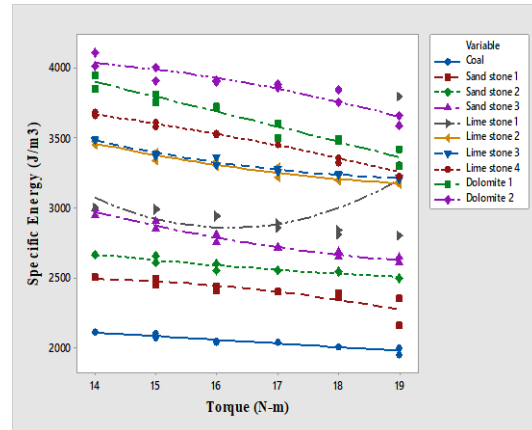


Figure 6.76 Influence of torque on Specific energy with 65° Pick angle at 45° attack angle for all rocks.

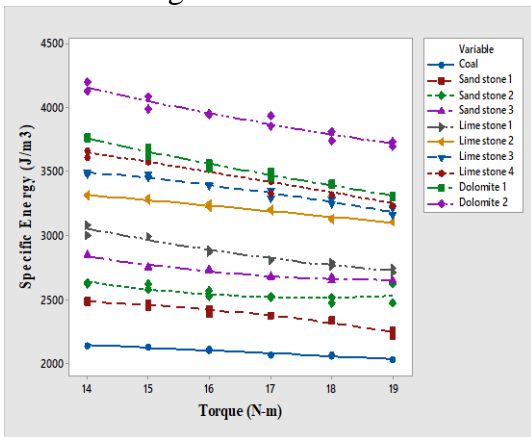


Figure 6.74 Influence of torque on Specific energy with 50° Pick angle at 45° attack angle for all rocks.

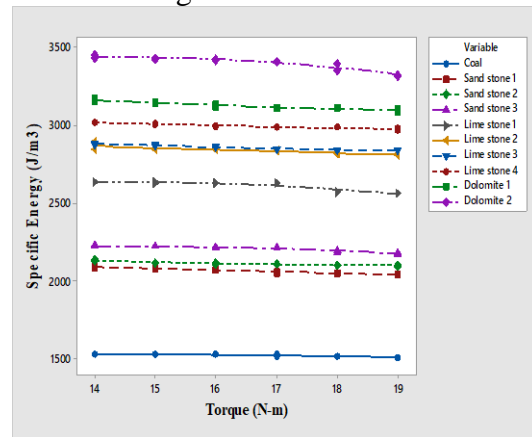


Figure 6.77 Influence of torque on Specific energy with 45° Pick angle at 55° attack angle for all rocks.

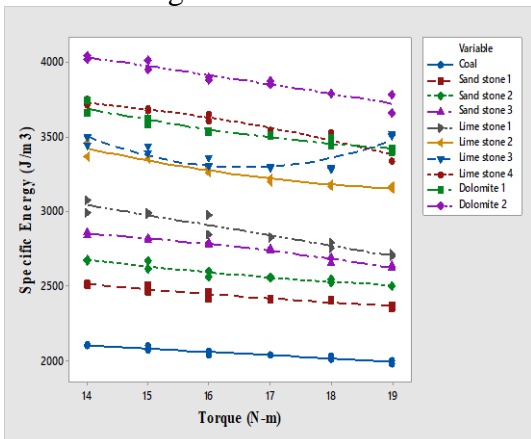


Figure 6.75 Influence of torque on Specific energy with 55° Pick angle at 45° attack angle for all rocks.

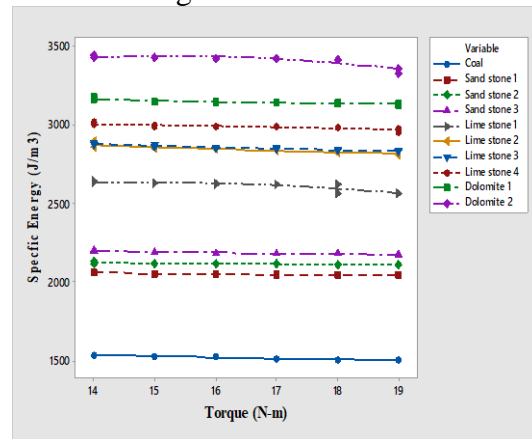


Figure 6.78 Influence of torque on Specific energy with 50° Pick angle at 55° attack angle for all rocks.

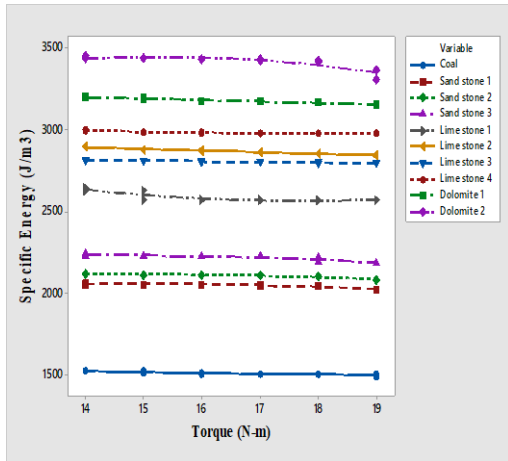


Figure 6.79 Influence of torque on Specific energy with 55° Pick angle at 55° attack angle for all rocks.

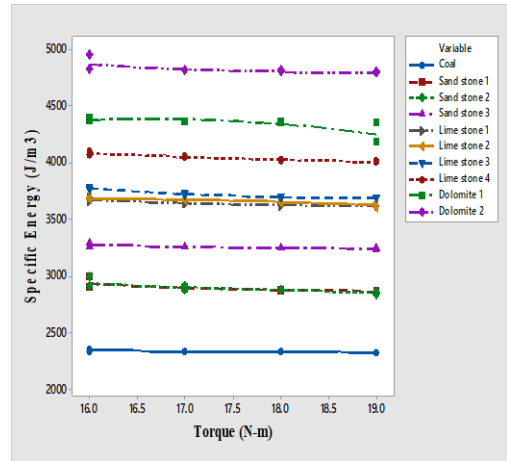


Figure 6.82 Influence of torque on Specific energy with 50° Pick angle at 65° attack angle for all rocks.

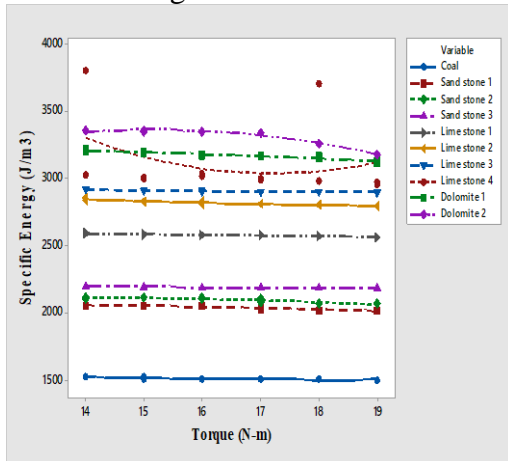


Figure 6.80 Influence of torque on Specific energy with 65° Pick angle at 55° attack angle for all rocks.

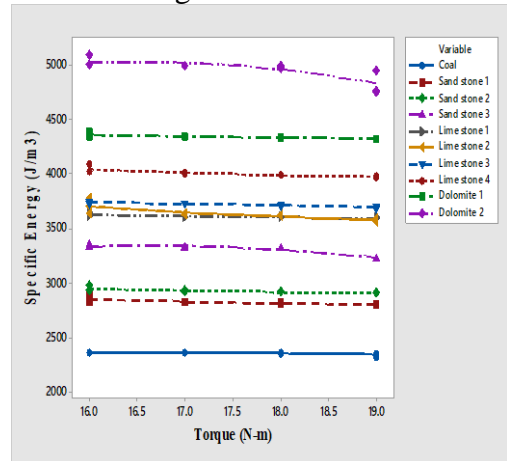


Figure 6.83 Influence of torque on Specific energy with 55° Pick angle at 65° attack angle for all rocks.

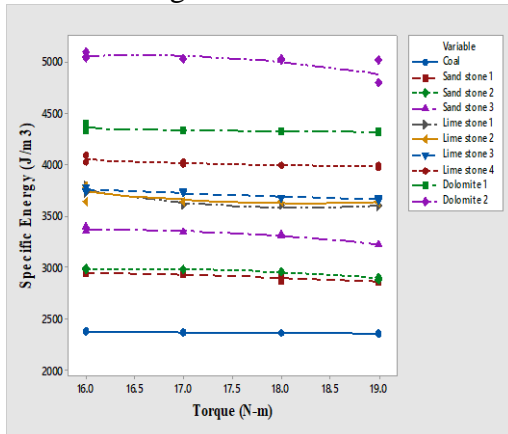


Figure 6.81 Influence of torque on Specific energy with 45° Pick angle at 65° attack angle for all rocks.

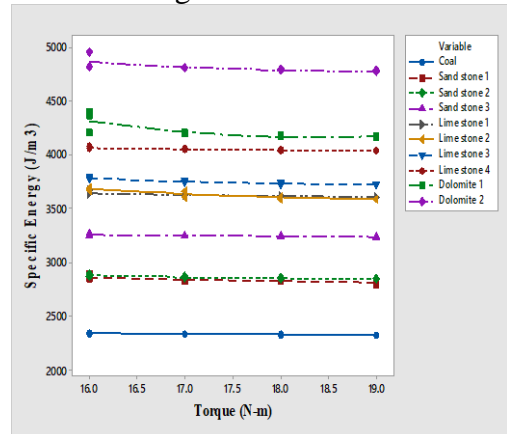


Figure 6.84 Influence of torque on Specific energy with 65° Pick angle at 65° attack angle for all rocks.

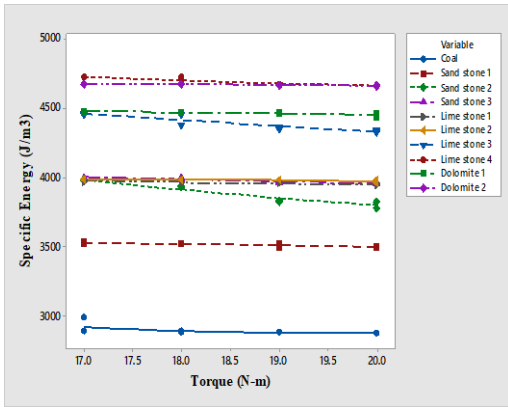


Figure 6.85 Influence of torque on Specific energy with 45° Pick angle 45° attack angle with 5mm wear for all rocks.

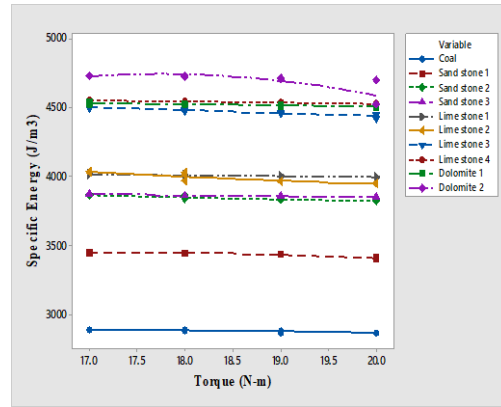


Figure 6.88 Influence of torque on Specific energy with 65° Pick angle at 45° attack angle with 5mm wear for all rocks.

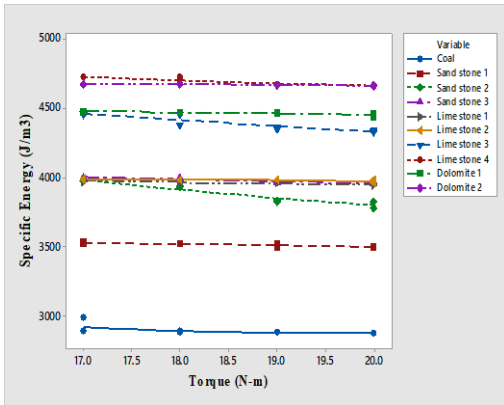


Figure 6.86 Influence of torque on Specific energy with 50° Pick angle at 45° attack angle with 5mm wear for all rocks.

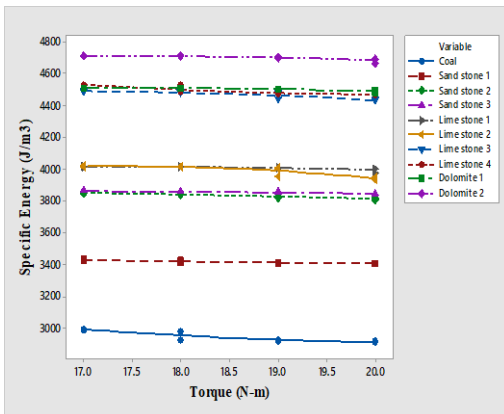


Figure 6.87 Influence of torque on Specific energy with 55° Pick angle at 45° attack angle with 5mm wear for all rocks

6.1.2.8. Influence of cutting force on Specific energy

The study intends to signify the influence of cutting force on specific energy. Figure 6.89 to 6.104 illustrates the variations of rpm on the cutting rate, at different angles. It is observed that with the increase in cutting force, the specific energy decreases non-linearly. A percentage difference in specific energy is evaluated between the least and highest cutting force is evaluated to identify the variation of specific energy in terms of cutting force.

- The difference measured between the maximum cutting force and the minimum cutting force at attack angles of 45° , 55° and 65° is found to be 5.87214%, 1.91263%, and 2.0474% for coal.
- Similarly, sandstone 1, is found to be 7.36047%, 3.46203%, and 4.71133%. For sandstone 2, it is 2.97%, 1.42% and 1.50%. for sandstone 3, it is 3.81%, 0.18% and 0.47% respectively
- For limestone 1 it is 7.28%, 2.69% and 3.91%, respectively. For lime stone 2 2.62%, 0.47% and 1.18%. For lime stone 3; it is 1.02%, 2.077% and 1.5%. For lime stone 4; it is 2.55%, 7.8% and 1.3% respectively.
- For dolomite 1; it is 7.16494%, 0.78084, and 4.27632. for dolomite 2; 4.47%, 3.75% and 1.88% respectively.
- The influence of Cutting force is compared between the attack angle of 45° attack angle and 45° attack angle with 5mm wear. The observation revealed that Specific energy increases with 5mm wear condition. The maximum increased percentage variation observed is 32.14% for coal, 36.64% for sandstone 1, 36.20% for sandstone 2, 36.07% for sandstone 3, 32.16% for limestone 1, 21.98% for limestone 2, 27.72% for limestone 3, 30.54% for limestone 4, 26.63% for dolomite 1 and 26.63% for dolomite 2.

As far as cutting force is concerned, the effect of cutting force is less significant compared to specific energy variations of attack angles.

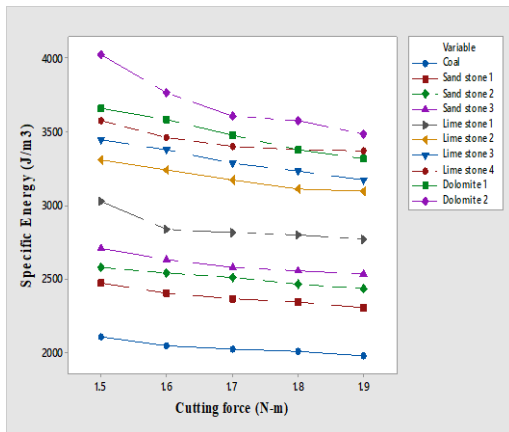


Figure 6.89 Influence of Cutting force on Specific energy with 45° Pick angle at 45° attack angle for all rocks.

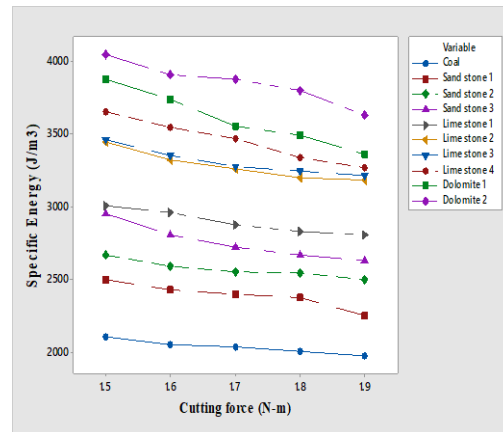


Figure 6.92 Influence of Cutting force on Specific energy with 65° Pick angle at 45° attack angle for all rocks.

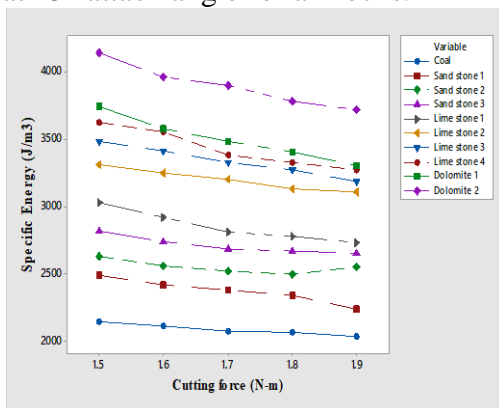


Figure 6.90 Influence of Cutting force on Specific energy with 50° Pick angle at 45° attack angle for all rocks.

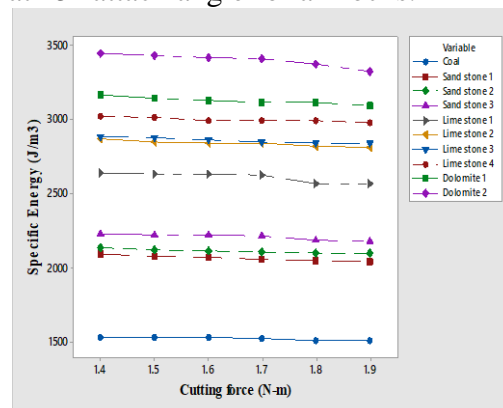


Figure 6.93 Influence of Cutting force on Specific energy with 45° Pick angle at 55° attack angle for all rocks.

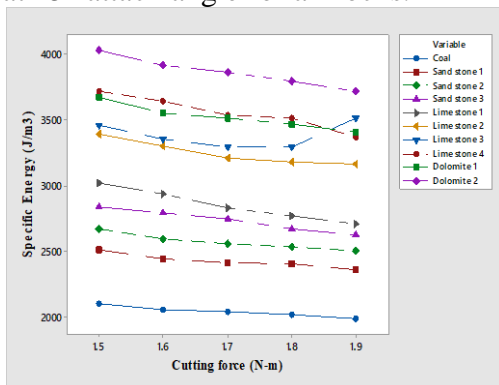


Figure 6.91 Influence of Cutting force on Specific energy with 55° Pick angle at 45° attack angle for all rocks.

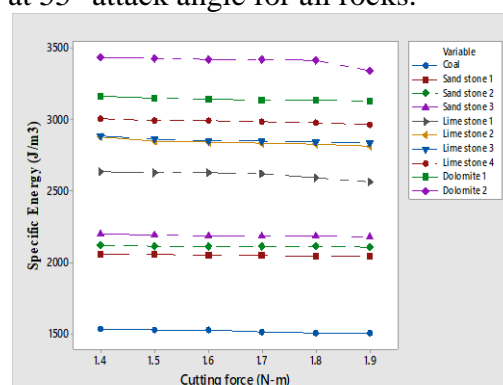


Figure 6.94 Influence of Cutting force on Specific energy with 50° Pick angle at 55° attack angle for all rocks.

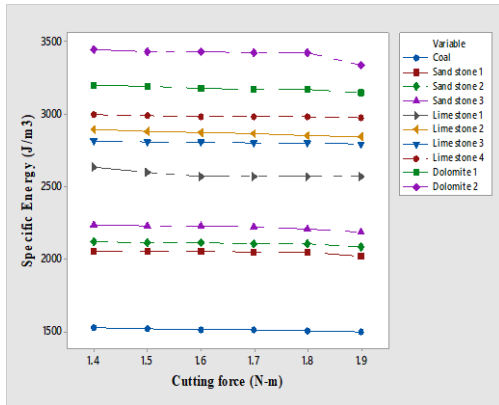


Figure 6.95 Influence of Cutting force on Specific energy with 55° Pick angle at 55° attack angle for all rocks.

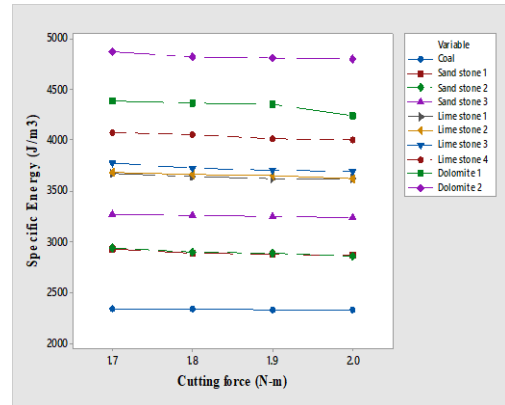


Figure 6.98 Influence of Cutting force on Specific energy with 50° Pick angle at 65° attack angle for all rocks.

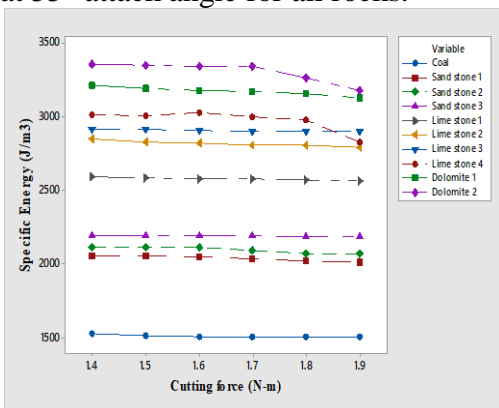


Figure 6.96 Influence of Cutting force on Specific energy with 65° Pick angle at 55° attack angle for all rocks.

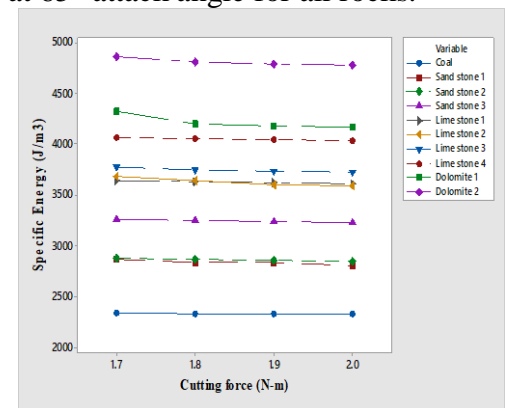


Figure 6.99 Influence of Cutting force on Specific energy with 55° Pick angle at 65° attack angle for all rocks.

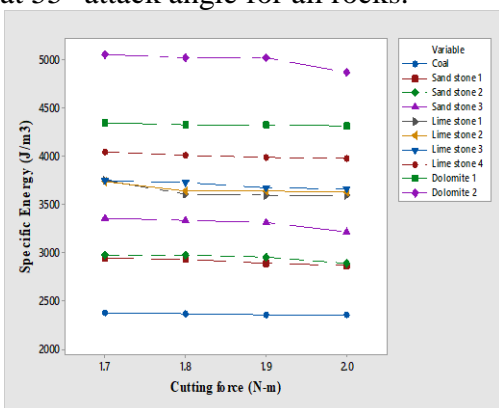


Figure 6.97 Influence of Cutting force on Specific energy with 45° Pick angle at 65° attack angle for all rocks.

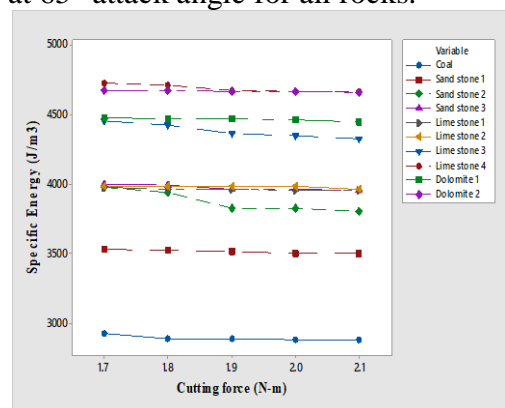


Figure 6.100 Influence of Cutting force on Specific energy with 65° Pick angle at 65° attack angle for all rocks.

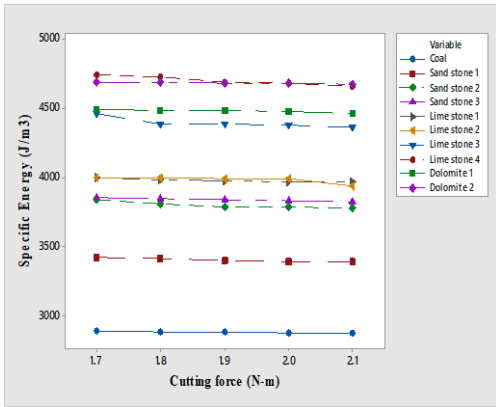


Figure 6.101 Influence of Cutting force on Specific energy with 45° Pick angle at 45° attack angle with 5 mm wear for all rocks.

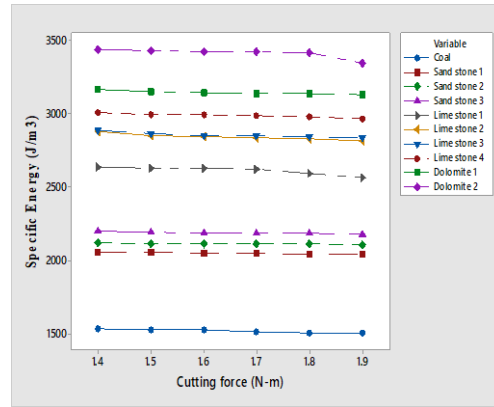


Figure 6.104 Influence of Cutting force on Specific energy with 65° Pick angle at 45° attack angle with 5 mm wear for all rocks.

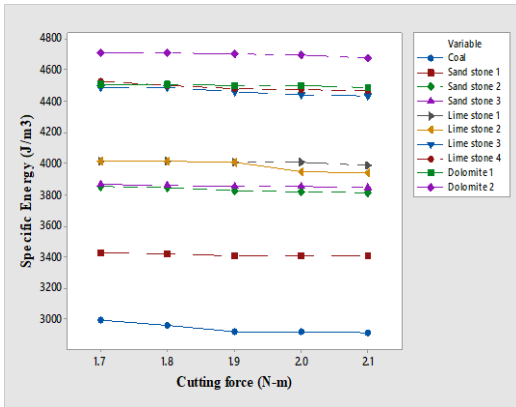


Figure 6.102 Influence of Cutting force on Specific energy with 50° Pick angle at 45° attack angle with 5 mm wear for all rocks.

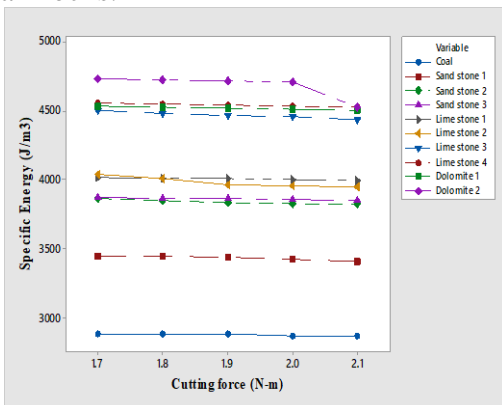


Figure 6.103 Influence of Cutting force on Specific energy with 55° Pick angle at 45° attack angle with 5 mm wear for all rocks.

6.2 Influence of Rock Properties on Specific energy (SE)

6.2.1 Introduction

Statistical analysis was carried out using data obtained from the experiments for all pick-rock combinations considered to study the influence of rock properties on SE. Univariate correlations and linear regression analyses were used to determine the relationship between rocks properties and SE (Tiryaki et al. 2006).

6.2.2 Multiple linear regression analysis

Linear regression analysis is used to fit a straight line belong to two variables. The value of the dependent variable can be predicted for any value of the independent variables. A linear regression analysis based on the least square method was used. The relationship between SE and rock properties was established through linear regression analysis in Tables 6.1 to 6.3 for all pick-rock combinations.

Regression analysis and an analysis of variance (ANOVA) are used to determine the significance of the deviation from linearity for the regression lines. It helps to decide whether the regression line is the best fit curve, representing the relationship between the sample data sets of two correlated variables. The null hypothesis, which states that there is no linearity between two variables, is tested through ANOVA. ANOVA produced two values for each model, where the F-value showed how the regression equation fitted the data, and the t-value revealed the significance of the F-value (p-value). The null hypothesis was rejected when the p-value was less than 0.05 meant that the relationship between SE and the particular independent variable could be expressed as a linear equation at a 95% confidence level. Otherwise, it is assumed that there was no significant statistical relationship represented as a linear regression model (Tiryaki et al. 2006). However, this does not mean that there is no relationship between any two variables under investigation. In the case of the non-linear regression equation, it may be suitable to represent the relationship between such variables. Results of ANOVA for all attack angles are given in Table 6.1. Depending

on these results, the models including the density, UCS, BTS, abrasively and brittleness of the rock were the predictors and were found statistically significant using linear models. These regression models were verified through ANOVA to determine whether they could reliably predict SE from the population, followed by student t-tests. In other words, the significances of the model components (equation constant and the regression coefficient in each regression model) were tested at a 95% confidence level. The significance of the model mentioned above components was considered depending on the probability values (P-values) obtained. If P-value was less than or equal to 0.05, then the relevant model component was considered statistically significant. All the regression models for all the pick-rock combinations that were verified through ANOVA were understood to have components that were statistically significant, too (Table 6.3). This reveals the practicability of these models in predicting SE values from the population (Tiryaki et al. 2006).

Further, the determination (R^2) coefficients were determined and used to measure the goodness of fit for the proposed regression models. R^2 is equal to the square of the correlation coefficient between the observed and the predicted values of the dependent variable. R^2 equals one (plus or minus) if all the predicted values are precisely over the regression line. The values of these two statistical measures that were calculated for the model are given in Table 6.2. According to these values, most of the changes in SE values were successfully and individually expressed by the density, UCS, BTS, abrasiveness and brittleness, in line with the ANOVA shown in Table 6.1 and student's t-test shown in Table 6.3.

6.2.3 Regression analysis of Specific energy

To develop the linear regression equation, the input parameters (independent variables) are rpm, attack angle, pick angle, cutting force, torque, and dependent variables were the depth of cut, volume is broken, and rock properties include density, BTS, UCS, brittleness, abrasive. The cutting rate was not considered because the value is too small to include in regression and will not influence the results as shown in regression Equation 6.1. The regression analysis was carried using Minitab 17 statistical software.

Regression Equation

Specific energy= 6198 + 1.562 Attack angle + 0.047 Pick angle + 0.3861 rpm + 4100 Cutting force - 281.6 Torque - 1013.9 Depth of cut + 752646 Volume - 614.7 Cutting rate in + 61.2 Density + 15.11 UCS + 1696 BTS + 4.186 Abrasivity.

(6.1)

Model Summary

S	R-sq	R-sq(adj)	PRESS	R-Sq(Pred)
50.3992	99.55%	99.54%	3633483	99.53%

Table 6.1 ANOVA results (F tests)

Source	DF	Seq ss	Adj SS	Adj MS	F-Value	P-Value
Regression	13	768829763	768829763	59140751	23283.07	0.000
Attack angle	1	142509518	98375	98375	38.73	0.000
Pick angle	1	64168	191	191	0.08	0.051
rpm	1	558823452	299119	299119	117.76	0.000
Cutting force	1	558823452	2873473	2873473	1131.25	0.000
Torque	1	42992	1352884	1352884	532.62	0.000
Depth of cut	1	44955643	1104674	1104674	434.90	0.000
Volume	1	20863274	20428715	20428715	8042.56	0.000
Cutting rate	1	51196	118686	118686	46.73	0.000
Density	1	613025	94482	94482	37.20	0.000
UCS	1	113686	6404	6404	2.52	0.013
BTS	1	3346	9658	9658	3.80	0.051
Abrasivity	1	709114	601990	601990	237.00	0.000
Brittleness	1	9386	9386	9386	3.70	0.055
Error	1378	3500224	3500224	2540	-----	
Lack-of-Fit	1257	3478153	3478153	2767	15.17	
Pure Error	121	22071	22071	182	-----	
Total	1391	772329987	-----	-----	-----	

The p-values for all the parameters were less than 0.05. Therefore, all the parameters were statistically significant at 95% confidence intervals.

Table 6.2 Significance of model components with student's T-test

Term	Coef.	SE Coef.	T-Value	P-Value
Constant	6198	101	61.29	0.000
Attack angle	1.562	0.251	6.22	0.000
Pick angle	0.047	0.173	0.27	0.051
rpm	0.3861	0.0356	10.85	0.000
Cutting force	4100	122	33.63	0.000
Torque	-281.6	12.2	-23.08	0.000
Depth of cut	-1013.9	48.6	-20.85	0.000
Volume	752646	8393	89.68	0.000
Cutting rate	-614.7	89.9	-6.84	0.000
Density	61.2	10.0	6.10	0.000
UCS	15.11	9.52	1.59	0.013
BTS	1696	870	1.95	0.051
Abrasivity	4.186	0.272	15.39	0.000
Brittleness	-2037	1060	-1.92	0.055

Table 6.3 Regression model summaries

Predictors	R	R²	Adjusted R²	Std. error of estimation
Density	0.862	0.743	0.384	12.744
UCS	0.902	0.836	0.764	14.211
BTS	0.942	0.846	0.798	12.899
Abrasivity	0.968	0.946	0.518	14.166
Brittleness	0.748	0.795	0.442	13.877
Rpm	0.884	0.916	0.844	14.864
Cutting rate	0.912	0.965	0.902	14.876
Depth of cut	0.914	0.965	0.911	14.881
Cutting force	0.893	0.936	0.481	12.831

P-values for all the parameters were less than 0.05. Therefore, all the parameters were statistically significant at 95% confidence intervals.

6.3 Analysis of Results

Correlation coefficients were significant between rock properties and cutting parameters considered at the 0.01 level. Similarly, the univariate correlation was done using Minitab 17 software, and it was found that the values of 'P' for all the independent variables were 0.00. According to the SPSS survival manual by Cohen

(1988), there is a significant correlation if 'r' value is between 0.5 to 1. The 'R' values obtained in the present study were more than 0.5. Therefore, all the independent parameters used in the analysis were statistically significant.

6.3.1 Influence of UCS on Specific energy

UCS is an important rock property that affects rock cuttability because a considerable amount of the cutting energy is consumed in overcoming the UCS of rock for producing a crushed zone under the pick tip at the beginning of the rock cutting process.

In the present study, SE correlates positively with UCS with an $R^2=89.2$ (as shown in Table 6.2 and Figures 6.105 to 6.108). Accordingly, a linear increase in SE is witnessed as UCS increased, complying with most of the previous studies in this area (Roxborough et al. 1986; Roxborough, 1987; Copur et al. 2001; Ersoy et al. 2003; Balci et al. 2004; Bilgin et al. 2005, Tiryaki et al. 2005; Balci, 2006; Irfan Celal Engin et al. 2013; Joel Langham and Hagan, 2014).

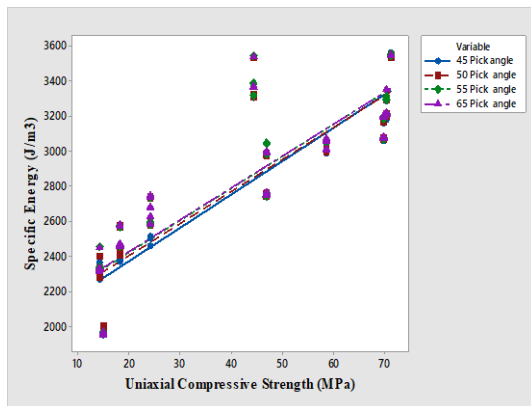


Figure 6.105 Influence of UCS on Specific energy at 45° attack angle for all rocks.

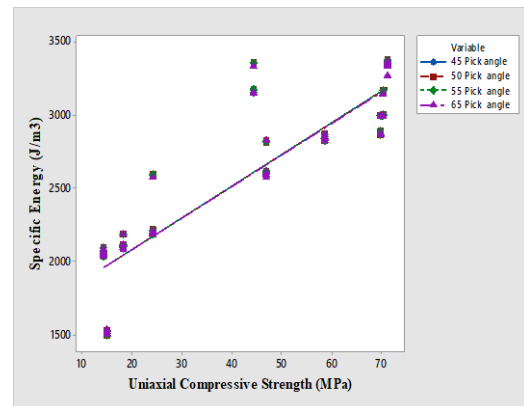


Figure 6.106 Influence of UCS on Specific energy at 55° attack angle for all rocks.

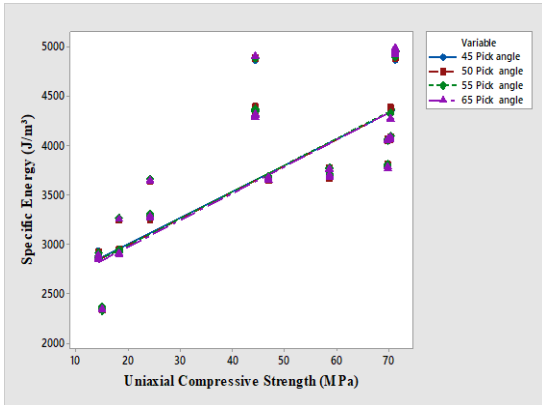


Figure 6.107 Influence of UCS on Specific energy at 65° attack angle for all rocks

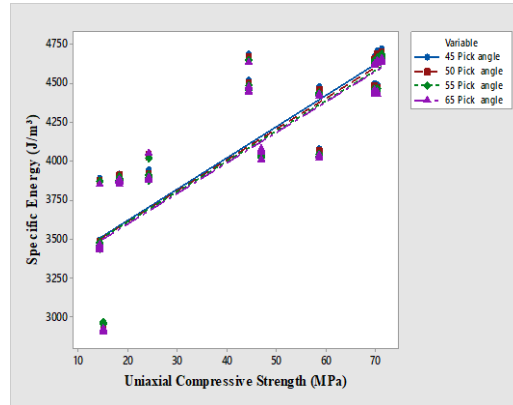


Figure 6.108 Influence of UCS on Specific energy at 45° attack angle with 5mm wear for all rocks.

6.3.2 Influence of BTS on Specific energy

BTS correlates well with the SE with a correlation coefficient of $R^2=84.6$ at a 95% confidence level, which shows the positive relationship between these two parameters (as shown in Table 6.2), and Figures 6.109 to 6.112 show the influence of BTS on SE. This result agrees with most previous studies in this area (Copur et al. 2001; Balci et al.2004; Tiryaki et al. 2005; Bilgin et al. 2006; Balliet al. 2007; Irfan Celal Engin et al. 2013). It is observed that as BTS increased, a corresponding linear increase of SE was witnessed for most of the rocks under this present study.

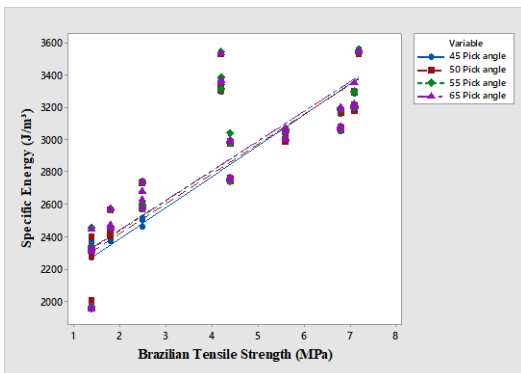


Figure 6.109 Influence of BTS on Specific energy at 45° attack angle for all rocks.

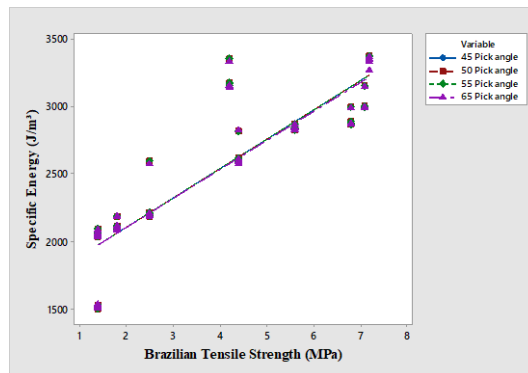


Figure 6.110 Influence of BTS on Specific energy at 55° attack angle for all rocks.

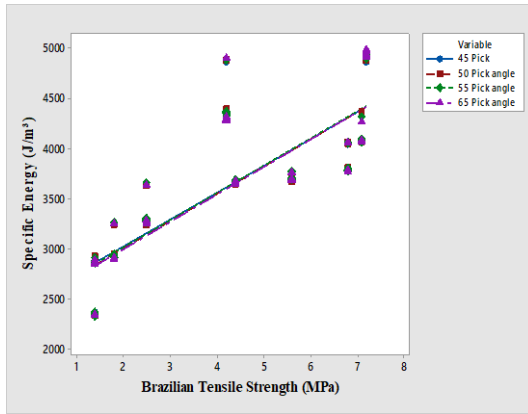


Figure 6.111 Influence of BTS on Specific energy at 65° attack angle for all rocks.

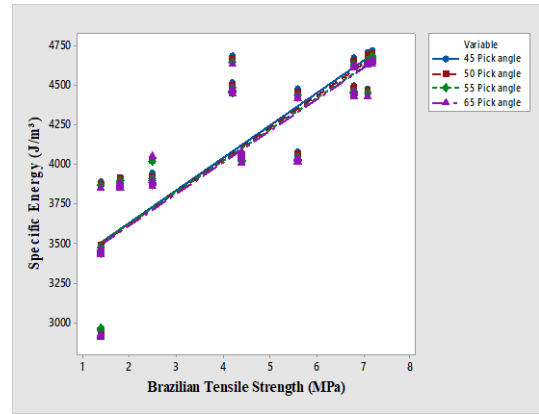


Figure 6.112 Influence of BTS on Specific energy at 45° attack angle with 5mm wear for all picks for all rocks.

6.3.3 Influence of abrasive on specific energy

Abrasivity of rock had a good correlation coefficient with SE at $R^2=94.6$, which is statistically significant at 95% confidence level as shown in Table 6.2 and Figures 6.113 to 6.116 show the influence of abrasiveness on SE. SE increases logarithmically with an increase in the abrasiveness of rock. It is found that abrasive of rock tends to increase with rock strength (Jacobs and Hagan. 2009). As the percentage of abrasive materials in the rocks like quartz and feldspar increases as shown in Table 3.2, it is observed that breaking the rock was difficult, and the cutting force increases logarithmically. When cutting force increases, the Specific energy also increases (Ersoy et al. 2003).

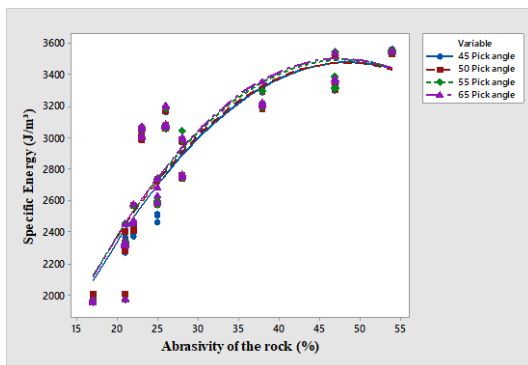


Figure 6.113 Influence of Abrasivity of rock on Specific energy at 45° attack angle for all rocks

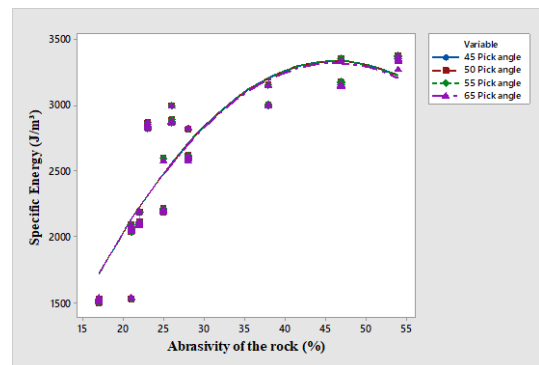


Figure 6.114 Influence of Abrasivity of rock on Specific energy at 55° attack angle for all rocks.

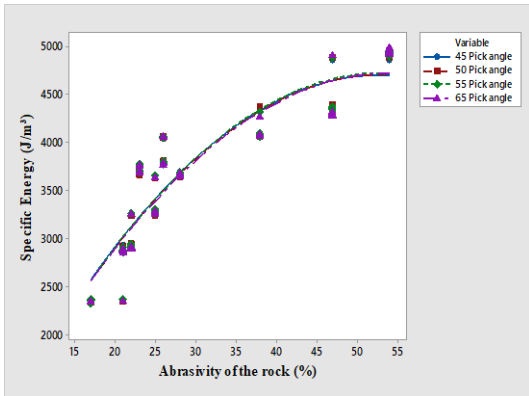


Figure 6.115 Influence of Abrasivity of rock on Specific energy at 65° attack angle for all rocks

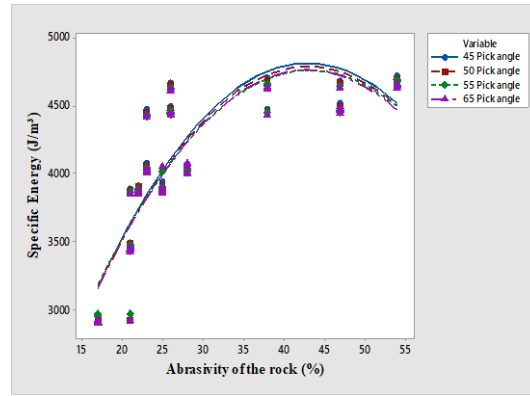


Figure 6.116 Influence of Abrasivity of rock on Specific energy at 45° attack angle with 5mm wear for all picks for all rocks

6.3.4 Influence of Brittleness on Specific energy

Brittleness has a good correlation coefficient with SE at $R^2=79.5$, which is statistically significant at 95% confidence level (Table 6.2), and Figures 6.117 to 6.120 show the influence of brittleness on SE. SE increases linearly with an increase in rock brittleness, which is complying with previous studies in this area (Altindag., 2003, Goktan and Yilmaz., 2005, Engin et al. 2013).

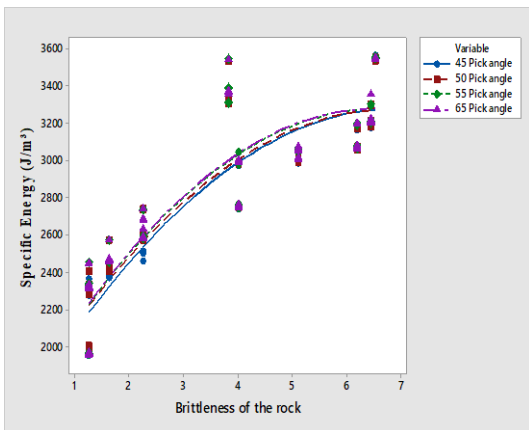


Figure 6.117 Influence of Brittleness on Specific energy at 45° attack angle for all rocks.

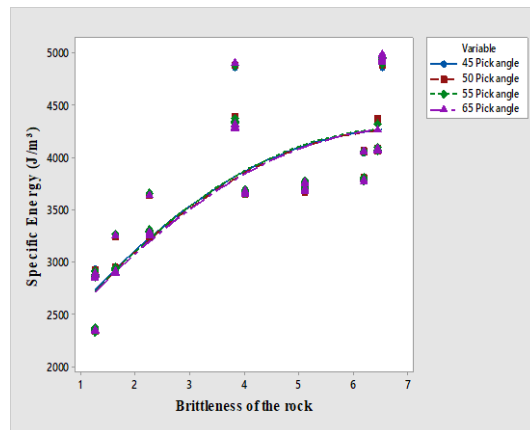


Figure 6.118 Influence of Brittleness on Specific energy at 55° attack angle for all rocks

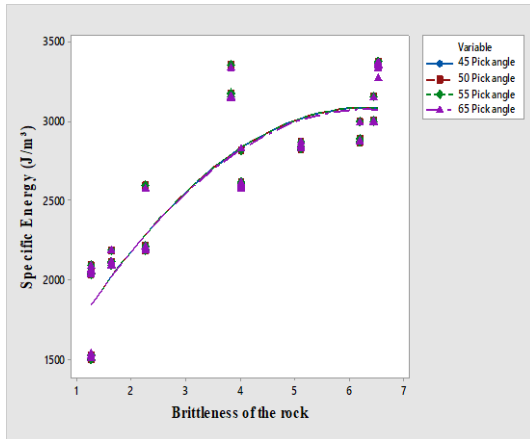


Figure 6.119 Influence of Brittleness on Specific energy at 65° attack angle for all rocks

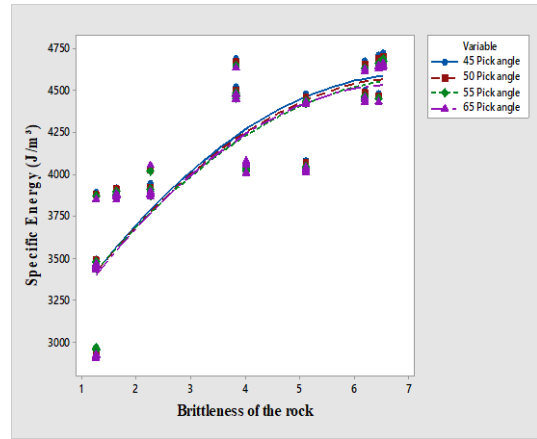


Figure 6.120 Influence of Brittleness on Specific energy at 45° attack angle with 5mm wears for all picks for all rocks.

6.3.5 Influence of Cutting rate on Specific energy

The cutting rate has a good correlation coefficient with SE at $R^2=96.5$, which is statistically significant at 95% confidence level (Table 6.2), and Figures 6.121 to 6.124 shows the influence of the cutting rate on SE. SE decreased exponentially with the increase in cutting rate of the rock. Cutting rate is maximum with 55° attack angle with minimum SE when compared with other attack angles like 45°, 65° and 45° with 5mm wear for all picks.

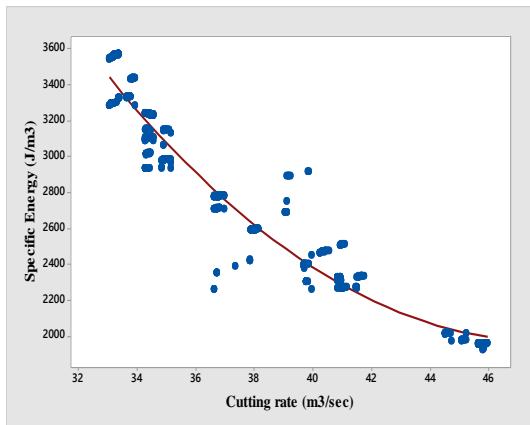


Figure 6.121 Influence of Cutting rate on Specific energy at 45° attack angle for all rocks

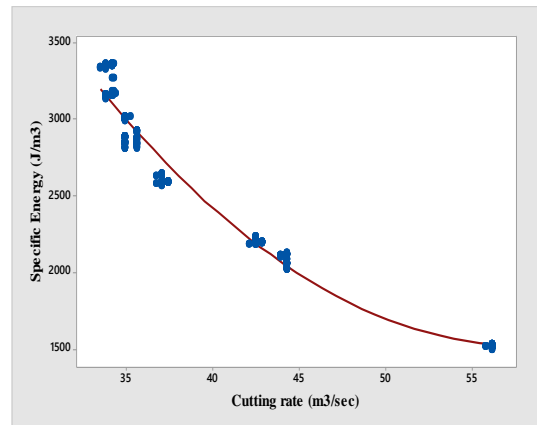


Figure 6.122 Influence of Cutting rate on Specific energy at 65° attack for all rocks

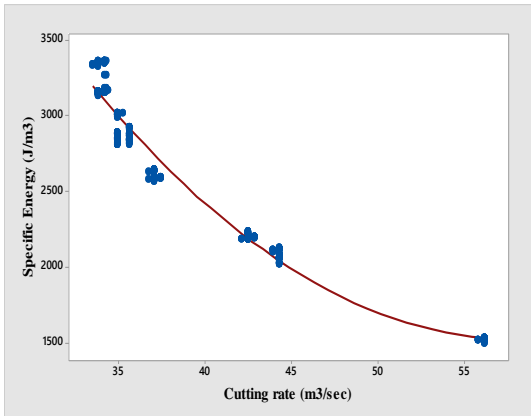


Figure 6.123 Influence of Cutting rate on Specific energy at 55° attack angle for all rocks

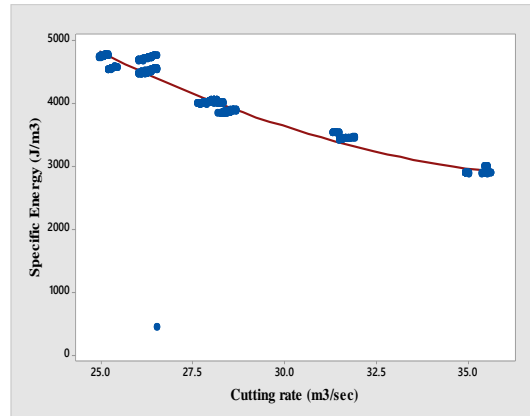


Figure 6.124 Influence of Cutting rate on Specific energy at 45° attack angle 5mm wear for all picks

6.3.6 Influence of Depth of cut on Specific energy

The depth of cut has a good correlation coefficient with SE at $R^2=96.5$ which is statistically significant at 95% confidence level (Table 6.2), and Figure 6.125 to 6.128 shows the influence of depth of cut on Specific energy. SE decreases exponentially with an increase in the depth of cut of the rock. The depth of cut is maximum with 55° attack angle with minimum Specific energy compared with other like 45° attack angle, 65° attack angle and 45° attack angle with 5mm wear for all picks has the higher Specific energy.

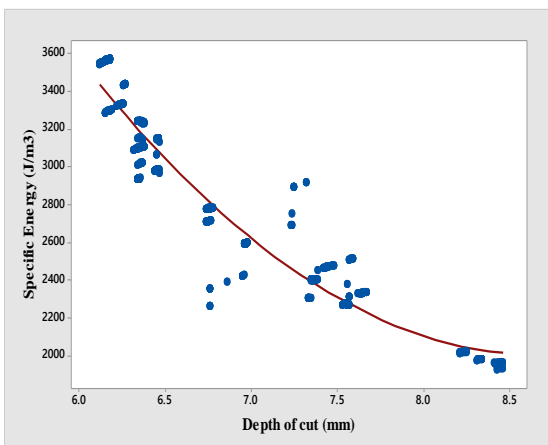


Figure 6.125 Influence of depth of cut on Specific energy at 45° attack angle for all rocks.

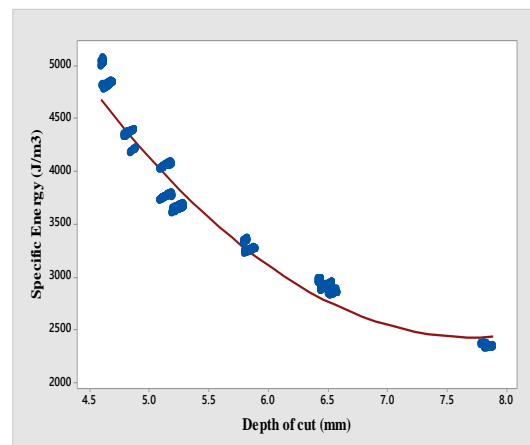


Figure 6.126 Influence of depth of cut on Specific energy at 55° attack angle for all rocks.

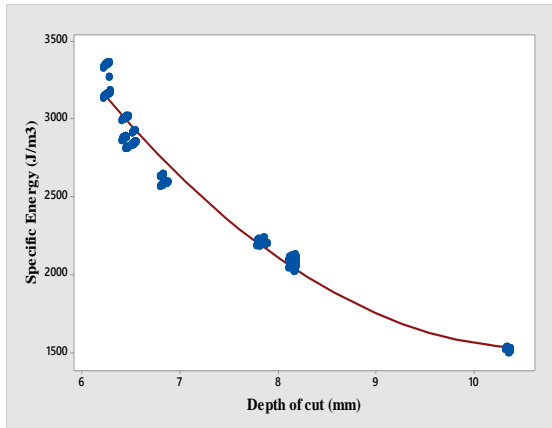


Figure 6.127 Influence of depth of cut on Specific energy at 65° attack angle for all rocks.

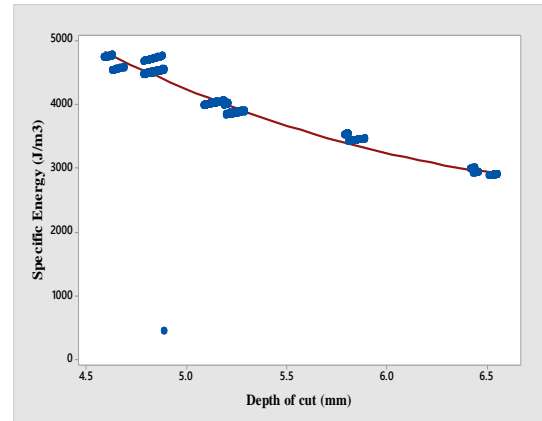


Figure 6.128 Influence of depth of cut on Specific energy at 45° attack angle with 5 mm wear for all rocks.

6.3.7 Influence of attack angle on Specific energy

The performance of the rock cutting process fundamentally depends on the combination of pick angle, attack angle and the mechanical properties of the rock. Figure 6.129 to 6.132 shows the influence of the attack angle on the UCS, BTS, abrasivity and brittleness of the rocks. The pick which was attached to the pick holder, the interaction between the pick-rock results in breaking the rock. The energy which is required to break the rock for the pick is transmitted through the attack angle at which the pick interacts with the rock. In this regard, the energy is directly transmitted to the rock through the pick via the attack angle. As per Table 3.4 to 3.7 (Appendix-I), Table 3.5, which belongs to 55° attack angle, there is the cutting force of 1.381N to 1.879 N and Specific energy 1500 J/m³ to 3360 J/m³, which was less compared to the other attack angles, the reason behind that the energy transfer to the pick and in turn the energy is transferred to the rock in the form of the contact surface, as the pick angle becomes wider (like 45°, 50°, 55°), the pick requires more energy to break the rock which results in requiring more cutting force.

So, in this study, it was found that the combination of 65° pick angle at 55° attack angle was optimum in terms of depth of cut and cutting rate. It was observed that the

Specific energy increases logarithmically with an increase in mechanical properties of the rock under this study.

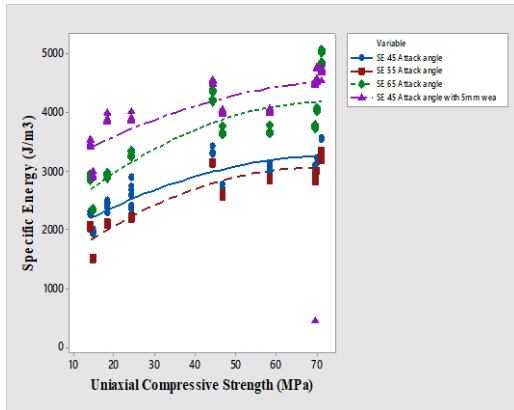


Figure 6.129 Influence UCS on Specific energy at different attack angles for all rocks.

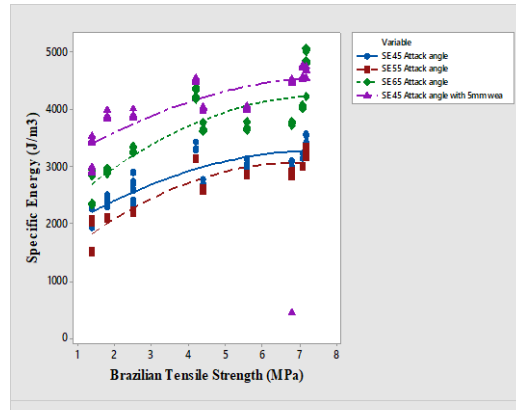


Figure 6.130 Influence BTS on Specific energy at different attack angles for all rocks.

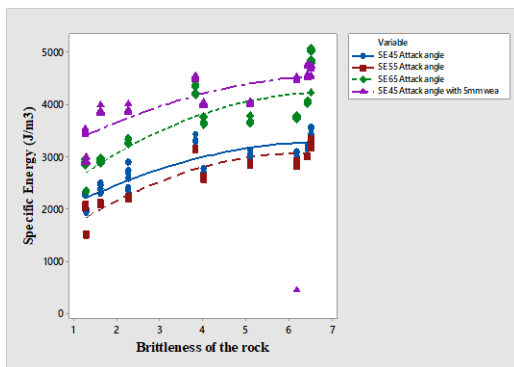


Figure 6.131 Influence of Brittleness on Specific energy at different attack angles for all rocks.

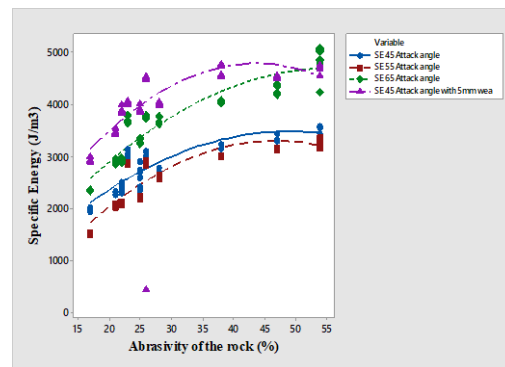


Figure 6.132 Influence of Abrasivity on Specific energy at different attack angles for all rocks.

The minimum Specific energy of 1500 to 3370 J/m³ was obtained with a 55° attack angle followed by a 45° attack angle with Specific energy of 1954 to 3554 J/m³ and the rest of the attack angles. The attack angle with Specific energy has a positive correlation with UCS at R²=83.4, BTS has a positive correlation with Specific energy at R²=83.1, brittleness has a positive correlation with specific energy at R²=83.1, abrasivity has a positive correlation with Specific energy at R²=88.0.

Thus, operational parameters like pick angle, rpm, torque and cutting force increasing linearly with increasing cutting rates. The rpm, torque, cutting force, pick angle exhibit decreasing non-linear correlations with SE. The rock properties like UCS, BTS, abrasiveness and brittleness exhibit increasing linearly and were in positive correlations, and all were statistically significant with SE at 95% confidence interval.

Therefore, operational parameters and rock properties were statistically significant in estimating SE individually, depending on the results obtained from linear regression analysis, ANOVA, student's t-tests and R^2 values.

6.4 Analysis of Results for Predictive (Regression) Models

6.4.1 Performance prediction of the derived models

The correlation coefficient between the measured and predicted values is a good indicator to check the model's prediction performance. Figure 6.133 shows the comparison between experiments and regression prediction specific energy and Figure 6.134 shows the Error plot for specific energy with regression modelling. However, in this study, Variation Account for (VAF) and Root Mean Square Error (RMSE) indices were calculated to compare the performance of the prediction capacity of predictive models developed (Alvarez and Babuska 1999, Finol et al. 2001, Gokceoglu 2002, Yilmaz and Yuksek 2008, Yilmaz and Yuksek 2009, Yilmaz and Kaynar 2011). The prediction performances of the models are shown in Equations 6.2 and 6.3. MAPE usually expresses accuracy as a percentage, as shown in Equation 6.4.

$$VAF = 1 - \frac{var(y-y')}{var(y)} * 100 \quad (6.2)$$

$$RMSE = \sqrt{\sum_{t=1}^n (y - y')^2} \quad (6.3)$$

$$MAPE = \frac{1}{N} \sum_{t=1}^N \left(\frac{A-P_i}{A_i} \right) x 100 \quad (6.4)$$

where the actual value and P_i is the predicted value. Lower values of MAPE indicate that there will be a better correlation between predicted values and experimental results. Using the developed regression models for pick-rock combination, the performance prediction indices for training and test data were calculated and are given in Table 6.4. It is evident from the table that the developed models for predicting SE were good and statistically significant.

Table 6.4 Performance indices of regression models for all picks

Performance Indices with regression analysis	
MAPE	0.032535
VAF	99.97194
RMSE	12.08

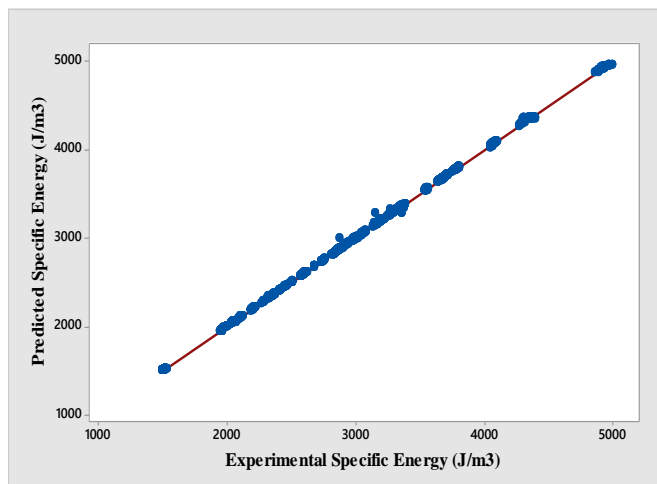


Figure 6.133 plot for comparison between experimental and regression prediction specific energy

6.4.2 Error Analysis of the derived regression models:

Error analysis is used to determine the variations that occur between the experimental values and predicted values. In the present study, error analysis is carried out for the experimental and predicted specific energy values. Fig 6.134 depicts the representation of errors that occurred in the prediction of specific energy. One can signify the application of statistical models based on error analysis. A random distribution of the data on either side of the mean line (0-line) indicates the goodness

of fit for application. A similar observation can be visualised in figure 6.134. a justification is obtained as such and describes that the model holds good for predicting specific energy.

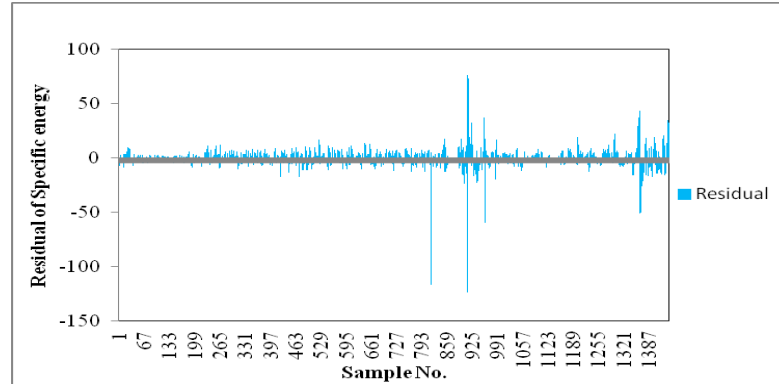


Figure 6.134 Error plot for specific energy with regression modeling

6.5 Analysis of Results of Artificial Neural Network

Figure 6.135 shows the comparison of calculated SE and predicted SE with regression and ANN, and Figure 6.136 and 6.137 show the Error plot for specific energy with ANN modelling with training and validation. It is found that all the predicted SE using ANN models were close to the measured ones (within 1% error) and is shown in Table 6.5. This indicates that all ANN models have quite similar performances and are good choices to predict SE values. The coefficient of determination between the measured and predicted values is a good indicator to check the model's prediction performance.

The VAF and RMSE indices were also calculated to control the performance of the prediction capacity of predictive models developed by Alvarez Grima and Babuska (1999), Finol et al. (2001) and Gokceoglu (2002), as shown in Equations 6.1 and 6.2, where y and y' are measured and predicted values, respectively. If the VAF is 100 and RMSE is 0, then the model will be excellent. MAPE, which is a measure of accuracy in a fitted series value, was also used to check the prediction performances of the models. MAPE usually expresses accuracy as a percentage, as shown in Equation 6.3, where A_i is the actual value and P_i is the predicted value. Lower values of MAPE

indicate that there will be a better correlation between predicted values and experimental results. Using the developed regression models for picks-rock combination, the Table 6.5 shows the Performance Indices with ANN analysis and Table 6.6 shows the performance prediction indices for training and validation data were calculated. Error analysis is used to determine the variations that occur between the experimental values and predicted values. In the present study, error analysis is carried out for the experimental and predicted specific energy values. Fig 6.136 and fig 6.137 depict the representation of errors for training and validation ANN models that occurred in predicting specific energy. One can signify the application of statistical models based on error analysis. A random distribution of the data on either side of the mean line (0-line) indicates the goodness of fit for application. A similar observation can be visualised in figure 6.135. a justification is obtained as such and describes that the model holds good for predicting specific energy.

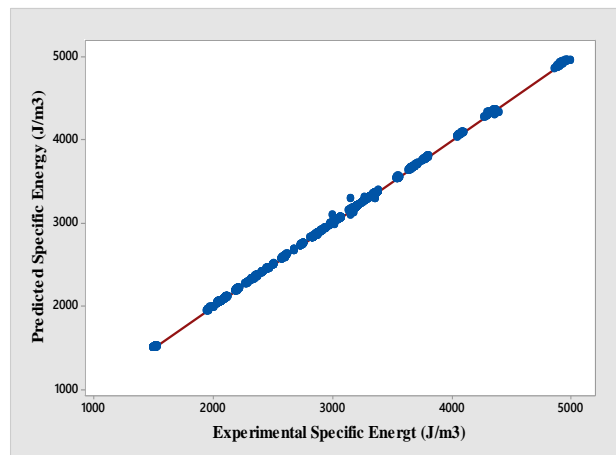


Figure 6.135 Comparisons of Calculated SE and Predicted SE with ANN

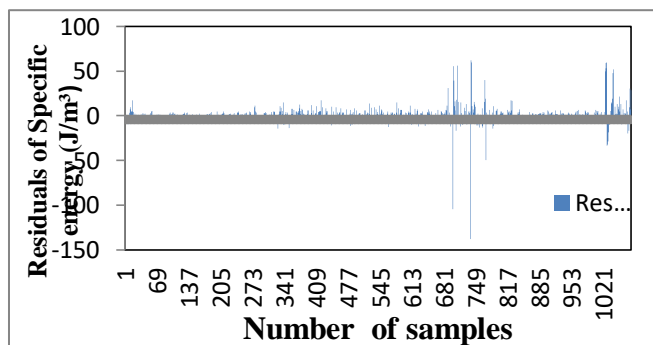


Figure 6.136 Training Error plot for specific energy with ANN modeling

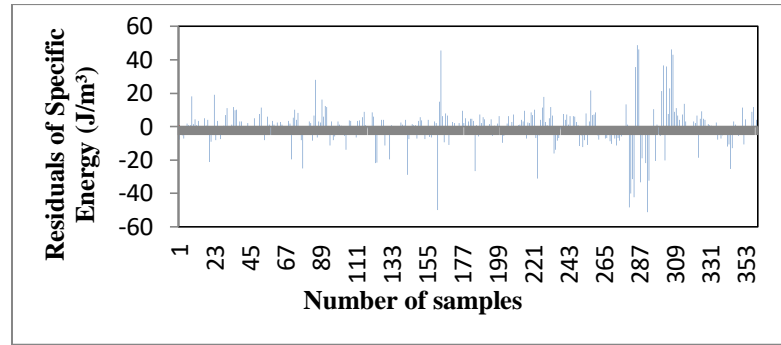


Figure 6.137 Validation Error plot for specific energy with ANN modeling

Table 6.5 Performance Indices with ANN analysis

Sl. No	Neurons	SE Training RMSE	R ²	SE Validation RMSE	R ²
1	12	10.04679	0.99987	12.10706	0.99987
2	13	11.70058	0.99989	12.88229	0.99986
3	14	11.82621	0.99893	12.98863	0.99986
4	15	11.15395	0.99988	12.52457	0.99974
5	16	9.477841	0.99992	11.85352	0.99987
6	17	11.60578	0.99987	13.64511	0.99779
7	18	12.1123	0.99986	14.10802	0.99992
8	19	10.86117	0.99983	12.16267	0.99953
9	20	10.69871	0.99989	11.94653	0.99955

Table 6.6 Values of performance indices of ANN models for all attack angles

Performance Indices with ANN analysis for 16 Neuron		
Training	RMSE	9.477841
	MAPE	1.58E-05
	VAF	99.98289
Validation	RMSE	11.85352
	MAPE	6.66E-05
	VAN	99.97602

The respective VAF, RMSE and MAPE indices for predicting SE were obtained are 99.97194, 12.08 and 0.032535, respectively, from multiple regression model (testing); but, the values for VAF, RMSE and MAPE indices were obtained in a neural network model (testing) were 99.98289, 9.477841 and 1.58E-05 respectively.

It can be concluded from the above ANN modelling that the prediction performances of the neural network model were higher than those of multiple regression equations. This finding confirms that the results were comparably the same as the researchers' earlier findings (Meulenkamp and Alvarez Grima, 1999; Singh et al. 2001, Zorlu et al. 2008; Tiryaki, 2008; Sarkar et al. 2010; Isik Yilmaz et al. 2011; Ibrahim et al. 2012).

6.6 Analysis of Numerical Modelling Results

6.6.1 Comparison of results obtained from rock cutting experimental and FEM analysis

A total of 2758 elements and 665 nodes for the dimension of 0.3x0.3x0.45M rectangular block considered a reasonably fine mesh formation, the aspect ratio (ratio of two adjacent sides) of the elements was maintained at three since it was a structural analysis. Therefore, similar element divisions are maintained in all sizes of the picks.

The results of rock cutting of FEM 3-D analysis for each pick-rock combination considered in the present theoretical investigation following the variables considered in the rock cutting tests are shown in Tables 6.7 to 6.10 (Appendix-II). Figures 6.138 to 6.148 (Appendix-II) represent the nodal displacement contours along X, Y, and Z directions. These correspond to the cutting force values from the rock cutting tests.

The magnitude of rock cutting and details of the crater formed, as obtained from the FEM analysis, under all rocks considered are given in Tables 6.7 to 6.10. Figures 6.148 to 6.157 (Appendix-II) shows stress distribution during loading conditions, and Figure 6.182 to 6.205 shows a graphical representation of stress distribution with rocks properties like Density, UCS, BTS, Abrasivity and Brittleness under this study.

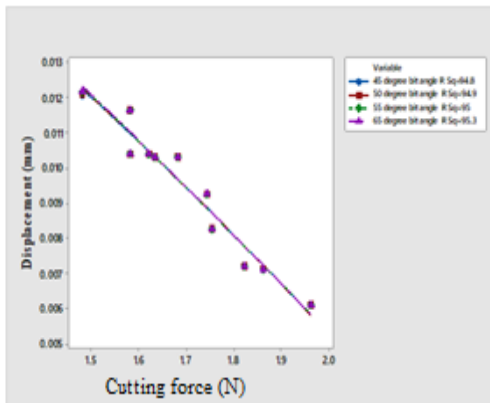


Figure 6.158 Influence of Cutting force on displacement with FEM at 45° attack angle

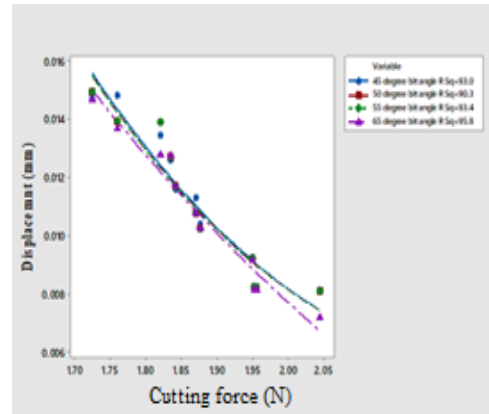


Figure 6.161 Influence of Cutting force on displacement with FEM at 45° attack angle with 5mm wear for different picks.

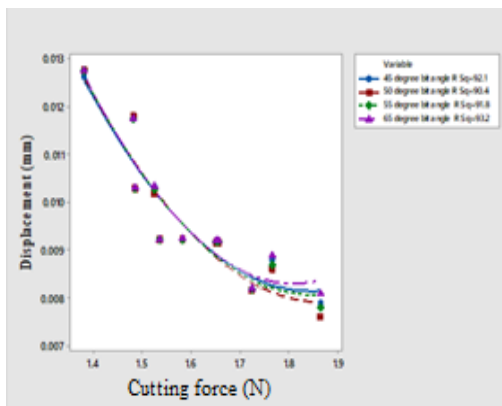


Figure 6.159 Influence of Cutting force on displacement with FEM at 55° attack angle

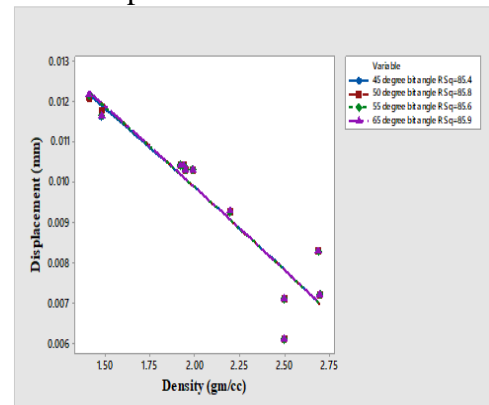


Figure 6.162 Influence of density on displacement with FEM at 45° attack angle

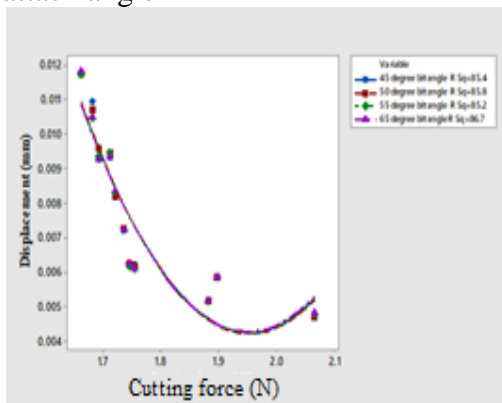


Figure 6.160 Influence of Cutting force on displacement with FEM at 65° attack angle

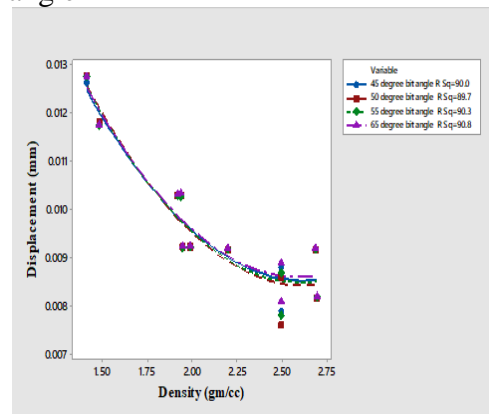


Figure 6.163 Influence of density on displacement with FEM at 55° attack angle

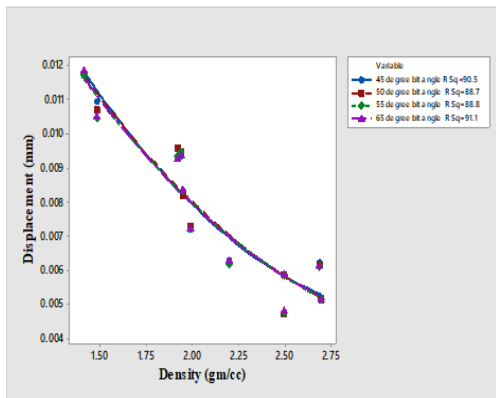


Figure 6.164 Influence of density on displacement with FEM at 65° attack angle

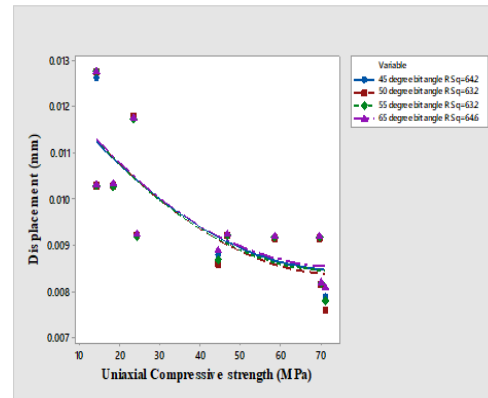


Figure 6.167 Influence of UCS on displacement with FEM at 55° attack angle

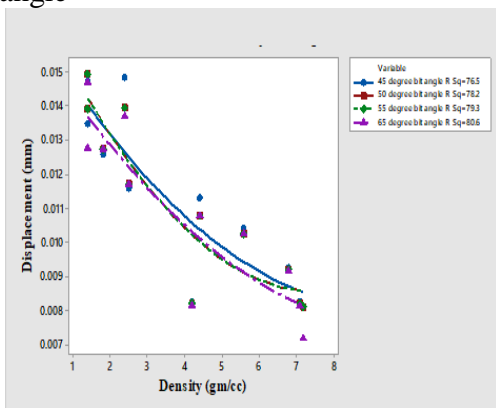


Figure 6.165 Influence of Cutting force on displacement with FEM at 45° attack angle with 5 mm wears for all picks.

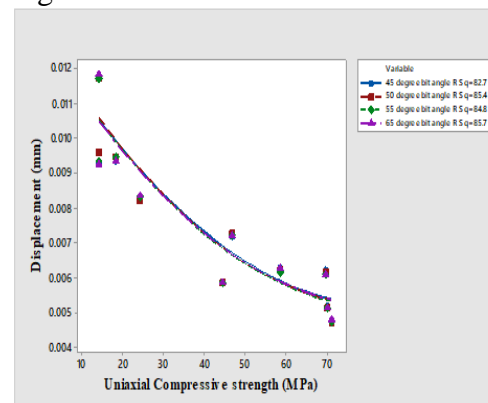


Figure 6.168 Influence of UCS on displacement with FEM at 65° attack angle

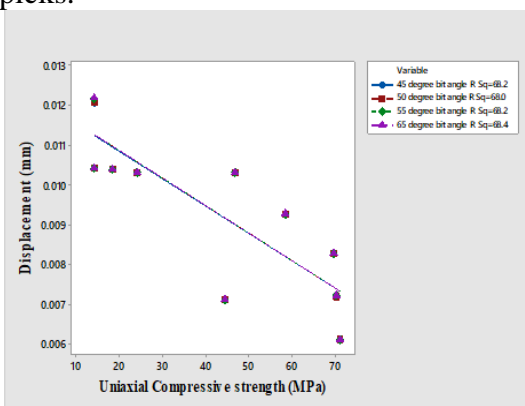


Figure 6.166 Influence of UCS on displacement with FEM at 45° attack angle

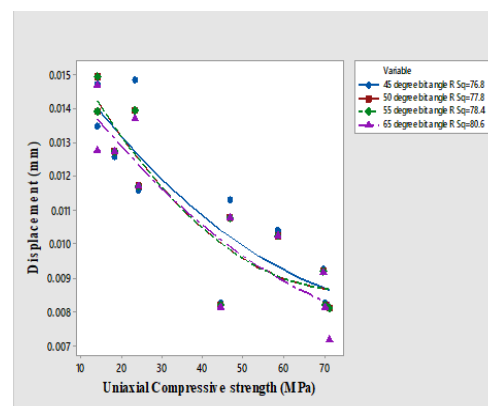


Figure 6.169 Influence of UCS on displacement with FEM at 45° attack angle with 5 mm wear for all picks.

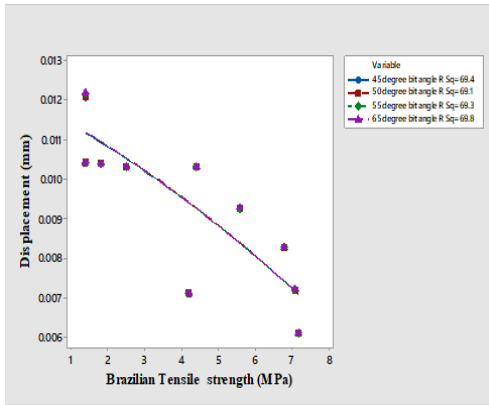


Figure 6.170 Influence of BTS on displacement with FEM at 45° attack angle

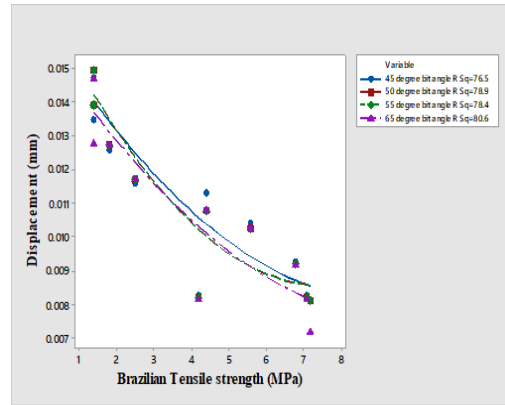


Figure 6.173 Influence of BTS on displacement with FEM at 45° attack angle with 5 mm wear for all picks.

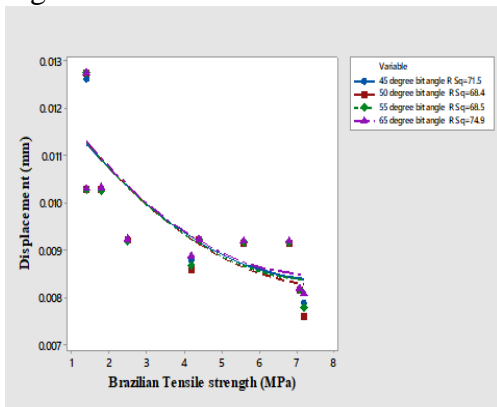


Figure 6.171 Influence of BTS on displacement with FEM at 55° attack angle

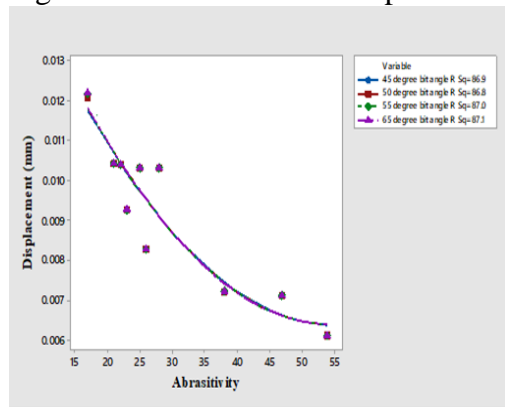


Figure 6.174 Influence of Abrasivity on displacement with FEM at 45° attack angle

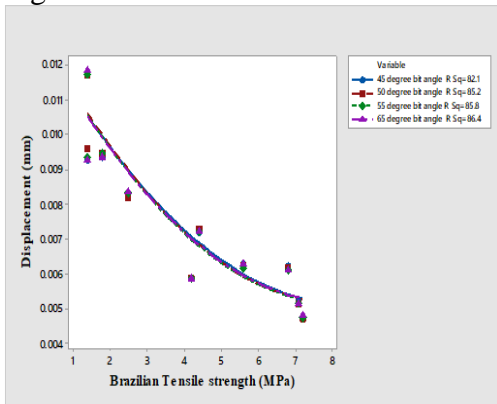


Figure 6.172 Influence of BTS on displacement with FEM at 65° attack angle

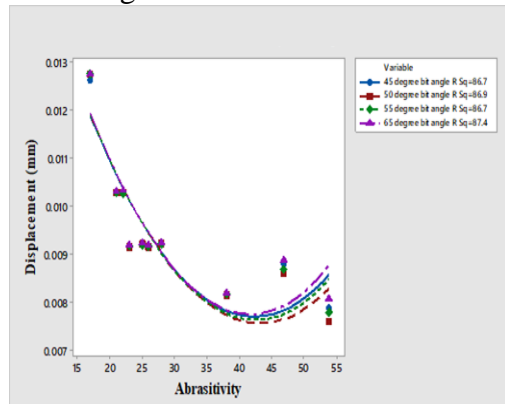


Figure 6.175 Influence of Abrasivity on displacement with FEM at 55° attack angle

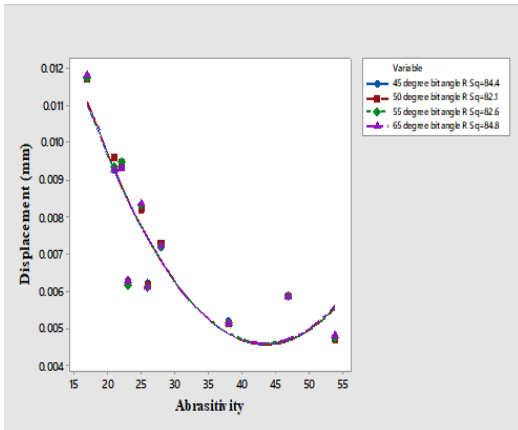


Figure 6.176 Influence of Abrasivity on displacement with FEM at 65° attack angle

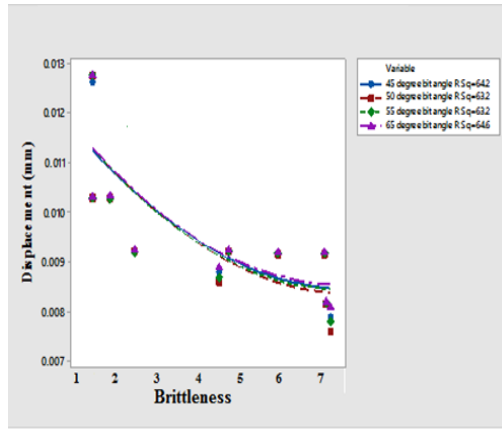


Figure 6.179 Influence of Brittleness on displacement with FEM at 55° attack angle

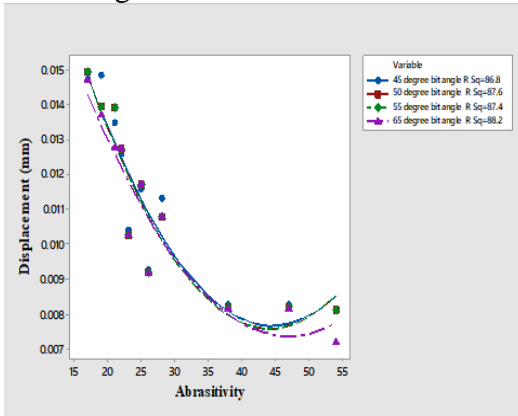


Figure 6.177 Influence of Abrasivity on displacement with FEM at 45° attack angle with 5 mm wear for all picks.

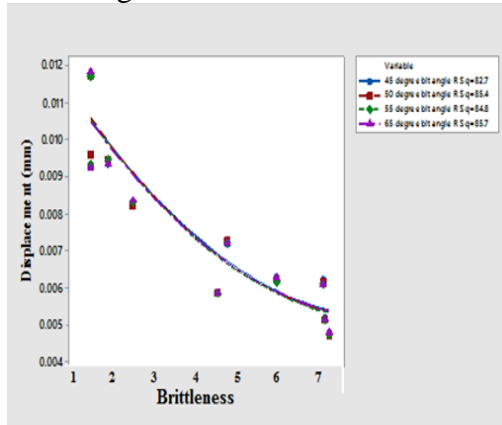


Figure 6.180 Influence of Brittleness on displacement with FEM at 65° attack angle

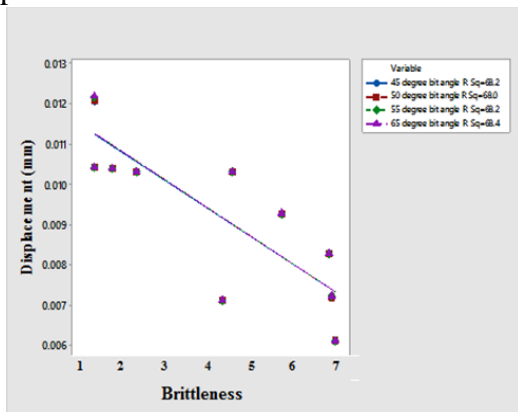


Figure 6.178 Influence of Brittleness on displacement with FEM at 45° attack angle

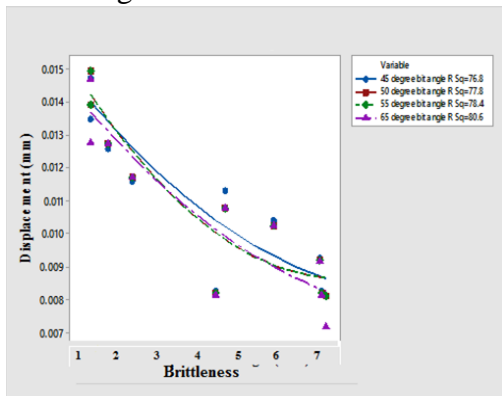


Figure 6.181 Influence of Brittleness on displacement with FEM at 45° attack angle with 5 mm wear for all picks.

The comparative values of cutting force and displacement obtained from FEM analysis are graphically presented from Figures 6.158 to 6.181 for all rocks. Comparison of the results at the peak load, as obtained from FEM analysis and rock cutting tests for all the pick-rock combinations considered, are given in Tables 6.7 to 6.10 (Appendix-II). The comparative values of displacements for all the rocks under study, under the four types of cutting picks and for all the ten stages of loading (as obtained from the FEM analysis and rock cutting tests) are given in Tables 6.7 to 6.10 (Appendix-II). It is observed from both the analysis that in all the rock types investigated, displacement is optimum under the combination of 65° pick angle with 55° attack angle. It may be inferred from these studies that the rock penetration and the volume of the crater formed under a pick do not depend on the applied force alone but also depend on the pick's cutting geometry. Therefore, it is implied that the force needed to cause breakage depends on the cutting geometry (pick angle) of the pick also.

The relationship between the mechanical properties of rocks and displacement for the four pick angles geometries (as obtained from the rock cutting tests and FEM (ANSYS) analysis) were presented together for comparison. It is observed that the FEM analysis results follow a similar trend as same as experimental laboratory results that (displacement decreasing linearly for 45° attack angle, decreasing exponentially for 55° and 65° attack angles) displacement decreases with the increase in the respective rock properties, shown in Figures 6.158 to 6.181, as evident from the rock cutting test.

The comparison mentioned above indicates that even with the fine meshing adopted in the FEM analysis, the theoretical nature of variation agrees with that obtained from rock cutting test results. The presented numerical values indicate that the experimental depth of cut values was lesser than those of FEM analysis and vary from 1% to 8% (Appendix II). This can be attributed to the type of meshing, the homogeneity and the ideal conditions considered in the FEM analysis. It also needs to be observed that even though the geometry (pick and attack angle) of cutting picks is somewhat curved, the line loading along one axis for point attack and two-line loads along two

mutually perpendicular axes were considered FEM analysis. Additionally, friction was not considered at the contact points between the pick and the rock. A more refined mesh with the non-homogenous, non-linear and an-isotropic formulation of the FEM analysis will better agree with the experimental values.

6.6.2 Results of Von Misses stress field

The von miss stress field results obtained from FEM analysis for each pick-rock combination (Ten rock types, four-point attack picks and three attack angles) considered in the present theoretical investigation are given in Figures 6.148 to 6.157 (Appendix-II).

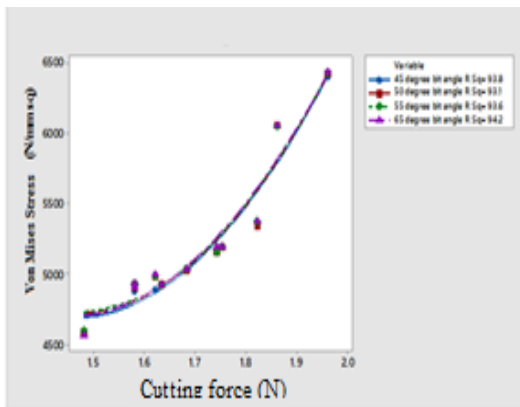


Figure 6.182 Influence of Cutting force on Von Misses Stress with FEM at 45° attack angle.

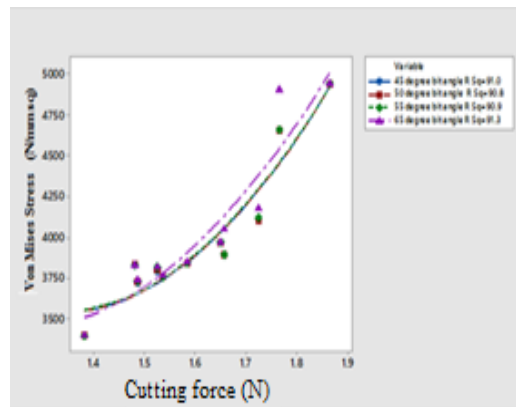


Figure 6.183 Influence of Cutting force on Von Misses Stress with FEM at 55° attack angle.

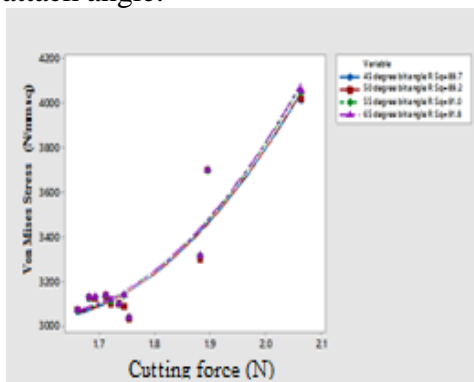


Figure 6.184 Influence of Cutting force on Von Misses Stress with FEM at 65° attack angle.

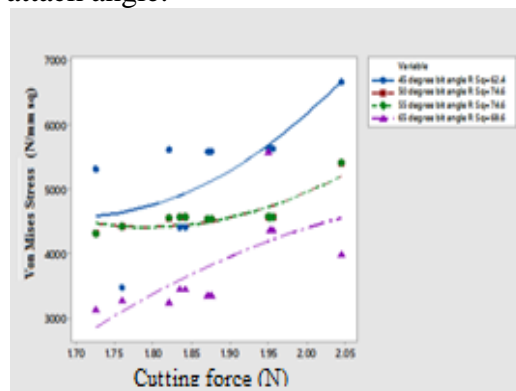


Figure 6.185 Influence of Cutting force on Von Misses Stress with FEM at 45° attack angle with 5mm wear.

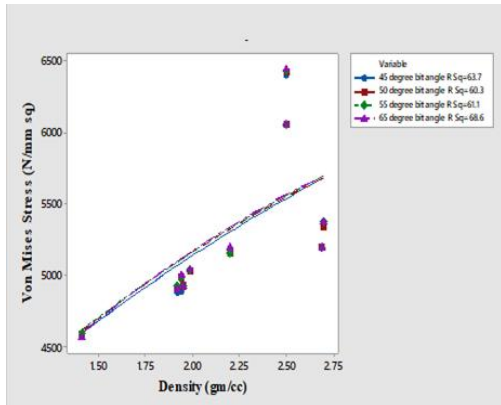


Figure 6.186 Influence of density on Von Mises Stress with FEM at 45° attack angle

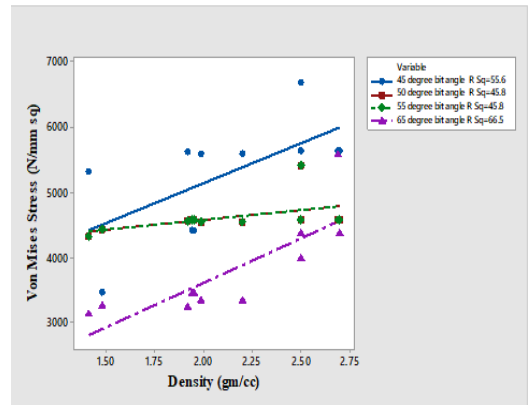


Figure 6.189 Influence of density on Von Mises Stress with FEM at 45° attack angle with 5 mm wear for all picks.

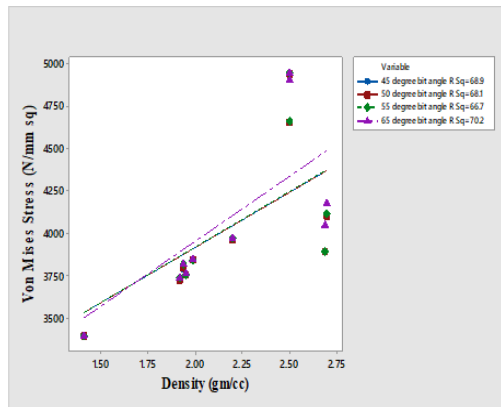


Figure 6.187 Influence of density on Von Mises Stress with FEM at 55° attack angle

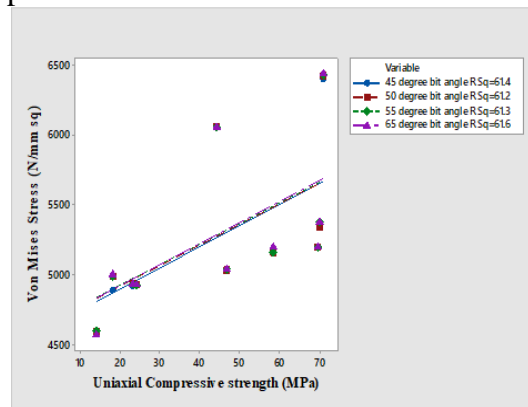


Figure 6.190 Influence of UCS on Von Mises Stress with FEM at 45° attack angle

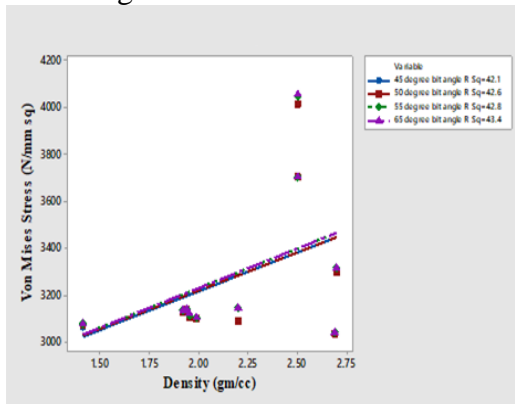


Figure 6.188 Influence of density on Von Mises Stress with FEM at 65° attack angle

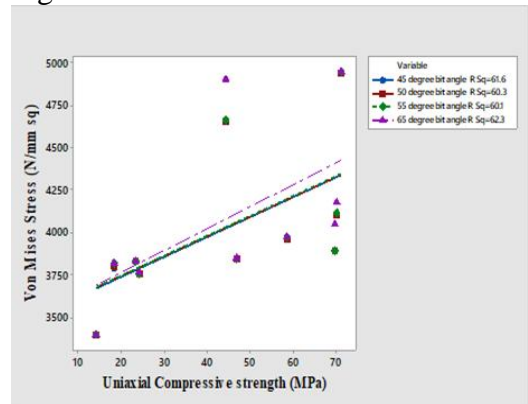


Figure 6.191 Influence of UCS on Von Mises Stress with FEM at 55° attack angle

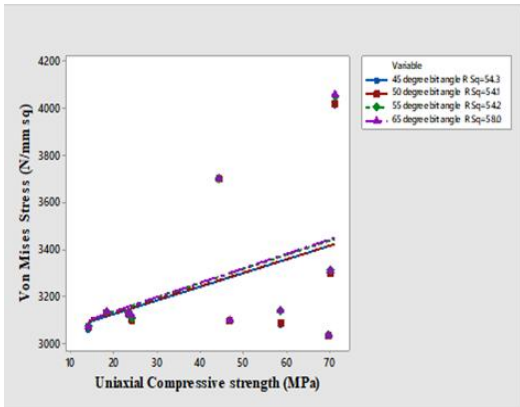


Figure 6.192 Influence of UCS on Von Mises Stress with FEM at 65° attack angle

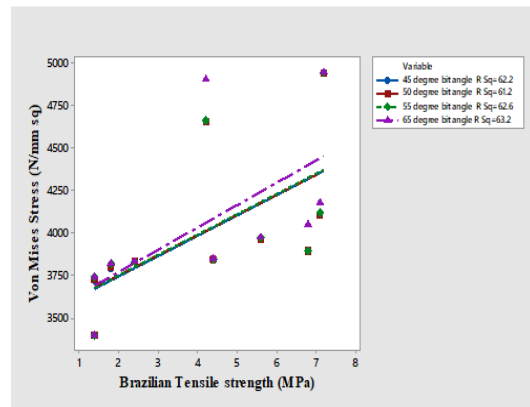


Figure 6.195 Influence of BTS on Von Mises Stress with FEM at 55° attack angle

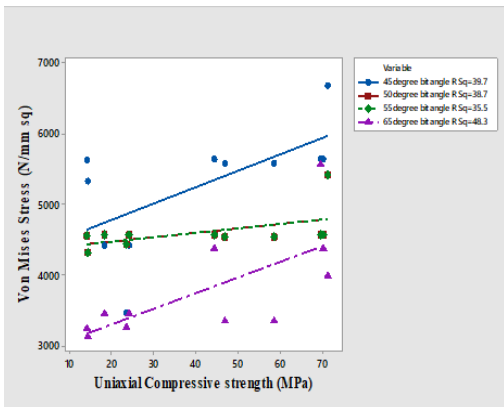


Figure 6.193 Influence of UCS on Von Mises Stress with FEM at 45° attack angle with 5 mm wear for all picks.

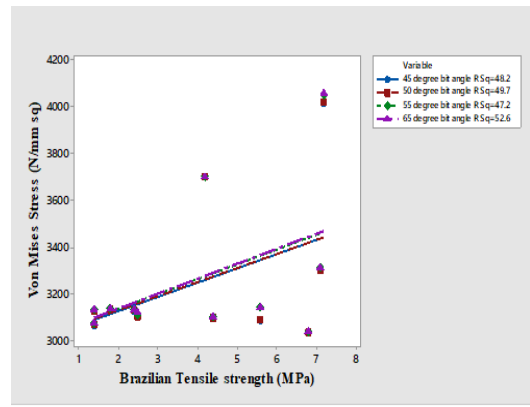


Figure 6.196 Influence of BTS on Von Mises Stress with FEM at 65° attack angle

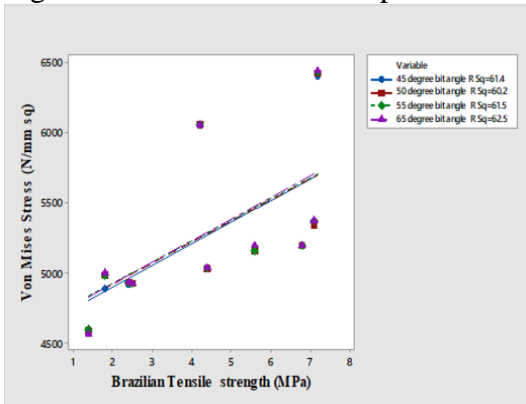


Figure 6.194 Influence of BTS on Von Mises Stress with FEM at 45° attack angle

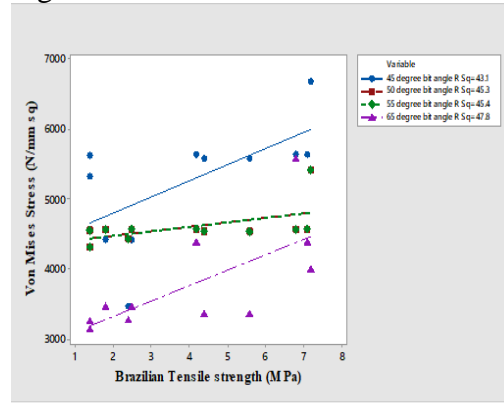


Figure 6.197 Influence of BTS on Von Mises Stress with FEM at 45° attack angle with 5 mm wear for all picks.

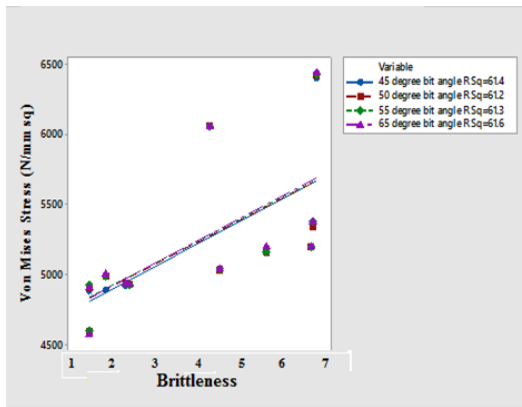


Figure 6.198 Influence of Brittleness on Von Mises Stress with FEM at 45° attack angle

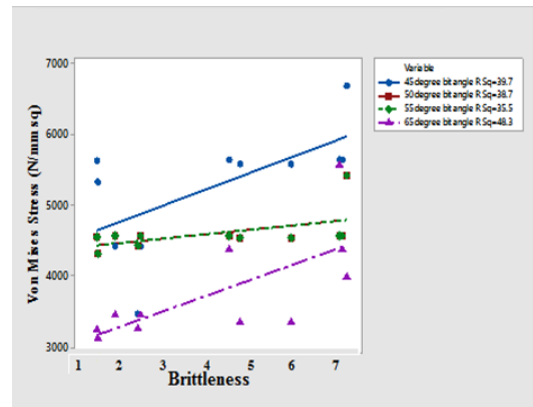


Figure 6.201 Influence of Brittleness on Von Mises Stress with FEM at 45° attack angle with 5 mm wear for all picks.

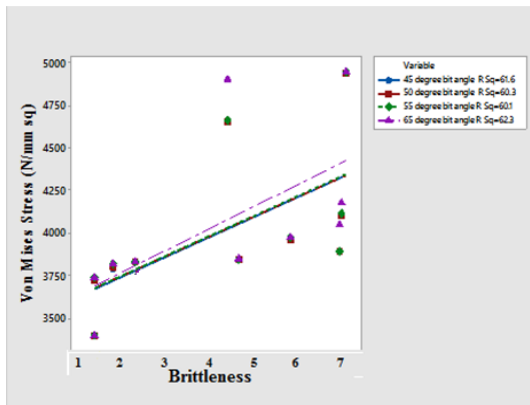


Figure 6.199 Influence of Brittleness on Von Mises Stress with FEM at 55° attack angle

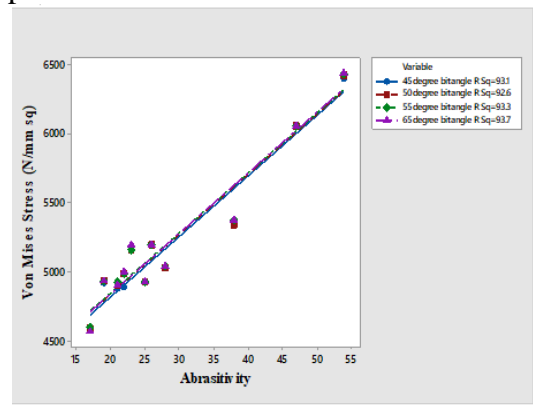


Figure 6.202 Influence of Abrasivity on Von Mises Stress with FEM at 45° attack angle

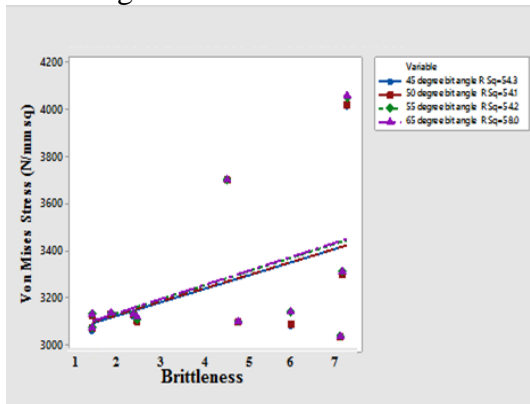


Figure 6.200 Influence of Brittleness on Von Mises Stress with FEM at 65° attack angle

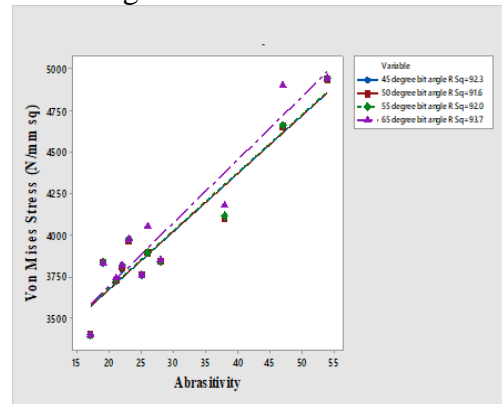


Figure 6.203 Influence of Abrasivity on Von Mises Stress with FEM at 55° attack angle

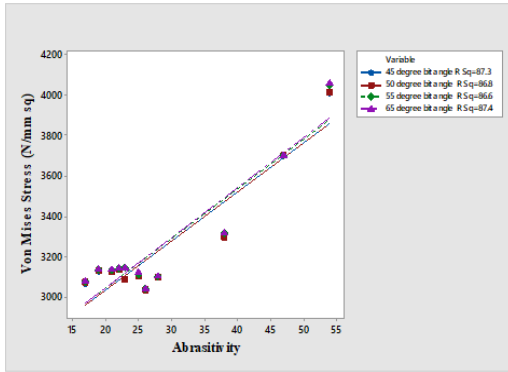


Figure 6.204 Influence of Abrasivity on Von Mises Stress with FEM at 65° attack angle

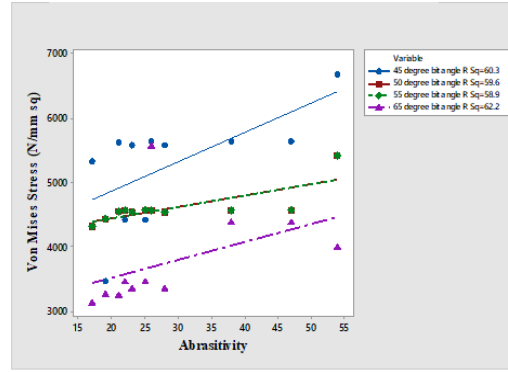


Figure 6.205 Influence of Abrasivity on Von Mises Stress with FEM at 45° attack angle

The magnitude of Von Mises stress developed along the X-axis, Y-axis and Z-axis for all rock types considered under the present study are given in Tables 6.7 to 6.10 (Appendix-II), and stress generated during the loading condition are shown in Figures 6.148 to 6.157 (Appendix-II). These represent the variation of the stresses in different rock types. It is observed that there is maximum Von Mises stress near the tip of the pick, and Figure 6.182 to 6.205 shows the stress generation graphically with rock properties considered under this study. The ANSYS analysis for the rock cutting tests, as shown in Tables 6.7 to 6.10 (Appendix-II).

6.7 Determination of Rock Cutting Resistance (RCR)

Rock Cutting Resistance is defined as the ratio of cutting force required to achieve a unit depth of cut. The RCR is calculated based on the depth of cut achieved from the experiment, and the cutting force is measured. The measured force from the experiment was resolved into $F \sin \alpha$ and considered an input parameter in numerical modelling to measure the depth of cut. The experimentally measured depth of cut and numerically computed depth of cut were compared to determine the Rock Cutting Resistance is determined as given in Eq. 6.5. The results are shown in Table.6.11 (Appendix-III), and the relationship between RCR and rock properties are shown in Figures 6.206 to 6.210.

$$RCR = \frac{\text{Cutting force (N)}}{\text{Depth of cut (mm)}} \quad \text{N/mm} \quad (6.5)$$

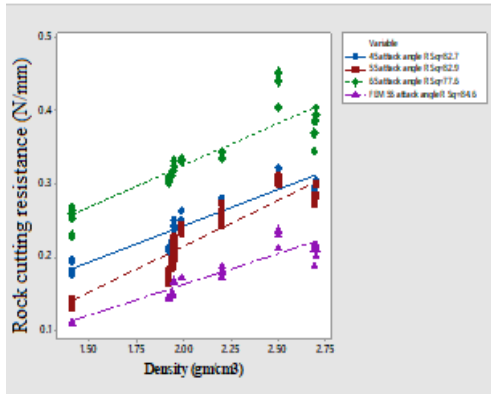


Figure 6.206 Influence of density on RCR with Experimental values and FEM values.

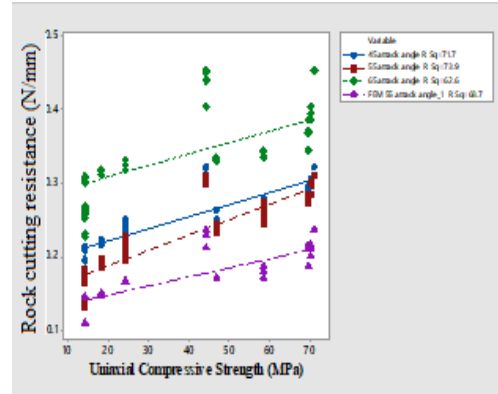


Figure 6.207 Influence of UCS on RCR with Experimental values and FEM values.

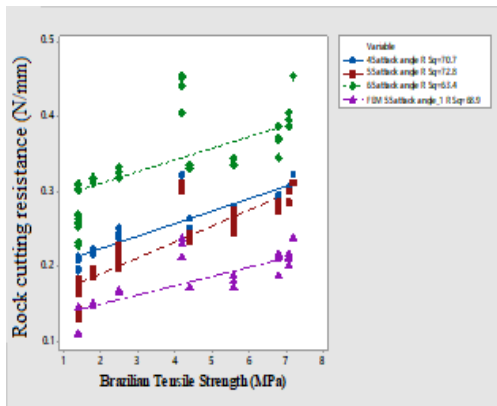


Figure 6.208 Influence of BTS on RCR with Experimental values and FEM values.

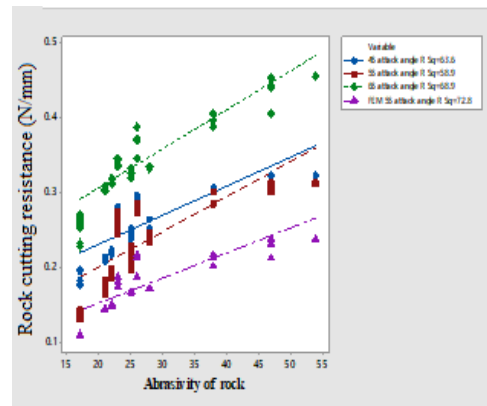


Figure 6.209 Influence of Abrasivity on RCR with Experimental values and FEM values.

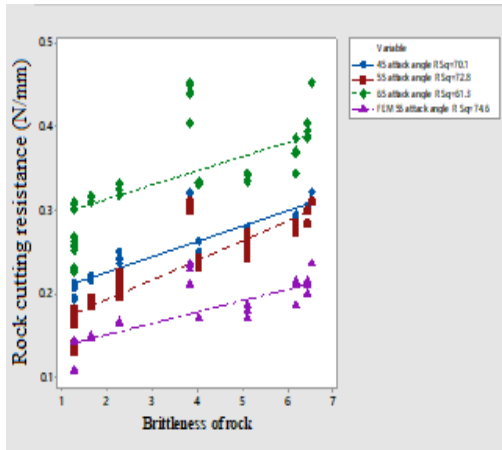


Figure 6.210 Influence of Brittleness on RCR with Experimental values and FEM values.

6.7.1 Analysis of Rock Cutting Resistance Results

RCR obtained from the FEM analysis is the least compared with experimental values. In the case of FEM analysis, the RCR values for the ideal conditions (Isotropic, uniform, homogeneous, linear elastic and devoid of any form of discontinuities) of rocks. Hence, the depth of cut achieved in FEM analysis was more significant than the cut's experimental depth.

It is found that maximum cutting rate was achieved with 65° pick angle and with 55° attack angle for all the rocks considered. Hence, the RCR was calculated only for this combination.

Similarly, in numerical modelling, when the resolving force (value of experimental investigation) is applied for a pick angle and attack angle combination considered, depth was noted down, and RCR was calculated using Eq 6.5.

It is observed that RCR increases linearly with the increase of the rock properties of all rocks considered. It is observed that RCR is more significant with 65° pick angle and 55° attack angle for all the pick-rock combinations considered and are given in Table 6.11 (Appendix-III) and shown in Figures 6.206 to 6.210 shows a graphical representation of RCR with rock properties considered under this study.

CHAPTER 7

CONCLUSIONS AND SCOPE FOR FUTURE WORK

7.1 Conclusion

In the present work, the cutting rate and specific energy (SE) required to remove one unit volume of rock by using point attack pick with different pick angles on various rocks at different attack angles have been studied. This study evaluates the influence of pick and attack angle on SE and cutting rate and specific energy performances of different picks. This study also evaluates the influence of mechanical properties on SE. The predictive models developed (regression and ANN) evaluate the estimation of SE in rock cutting and influencing parameters like operating variables and rock properties. The following conclusions are drawn from the current study.

1. The cutting parameters like pick angles, attack angles, rpm, torque and cutting force were used in identifying their impact on cutting rate and specific energy. The characteristic observations reveal that specific energy correlates indirectly as to cutting rate. Cutting rate increases linearly with an increase in pick angles. Alternatively, the specific energy decreases non-linearly with an increase in pick angle. The major influencer in both cutting rate and specific energy is the attack angle, whereas other cutting parameters show less significance in terms of percentage variations than attack angle. The attack angle 55° is an optimised attack angle for coal and sandstones. Whereas 45° attack angle is found optimised for limes stones and dolomite.

For cutting rate, the minimum and maximum variation irrespective of the rock type are found to be 0.3 to 4.8% for pick angles, 0.2 to 32% for attack angles, 0.05 to 4.08% for rpm, 0.05 to 3.2% for torque and 0.05 to 3.2% for cutting force.

With specific energy, the minimum and maximum variations irrespective of the rock type are found to be 0.023 to 4.41% for pick angles, 21.91 to 51.26% for attack angles, 0.03 to 4.41% for rpm, 0.03 to 7.8% for torque and 0.18 to

7.36% for cutting force. Hence, attack angle has more influence on cutting rate and specific energy.

With a tool wear rate of 5mm, a decrease in cutting rate is observed with a proportional decrease in specific energy. With a tool wear rate of 5mm, a decrease in cutting rate is observed with a proportional decrease in specific energy. The minimum and maximum variations irrespective of the rock type are 24.5 to 33.36% for pick angles, 24.5 to 30.36% for rpm, 21.56 to 35.16% for torque and 20.05 to 32.61% with cutting force for cutting rate. For specific energy, the minimum and maximum variations irrespective of the rock type are 21.86 to 35.81% for pick angles, 21.80 to 32.66% for rpm, 21.89 to 36.20% for rpm torque and 21.98 to 36.64% for cutting force.

2. The rock properties (density, uniaxial compressive strength (UCS), Brazilian tensile strength (BTS), abrasiveness and brittleness) influenced the SE. It was observed that SE increases with the increase in density, UCS, BTS, abrasivity and brittleness of the rock. This is because the resistance to rock cutting increases with the increase in strength of the rock.

3. The regression models shown in Equations 6.1, 6.2 and 6.3 were developed and can be used to estimate the SE during rock cutting as they can be used as guidance in practical applications. The developed regression model results showed that the SE's significant operating variables were attack angle, type of pick followed by other cutting parameters, such as the rock's mechanical properties. The results showed that input parameters were significant, and the model possesses an R-Square value of 99.55%. The respective variance account for (VAF), root mean square error RMSE, and mean absolute percentage error (MAPE) indices for predicting SE are 99.17, 12.08 and 0.032535, respectively, from the multiple regression model (testing). The result of the current study provides opportunities to evaluate the cuttability of rocks before involving complicated experimental procedures. Error graphs also resulted in the goodness of fits of a statistical model.

6. Artificial Neural Network (ANN), was developed to predict the SE. the input parameters include cutting force, pick angle, attack angle, depth of cut, volume

broken and rock properties like density, UCS, BTS, abrasivity and brittleness. The ANN results showed that the model's predictive performance for VAF, RMSE and MAPE indices are 99.98289, 9.47741, 0.0000158 for training and VAF, RMSE and MAPE for validation were 99.97602, 11.85352, 0.0000666. Error graphs also resulted in the goodness of fits of a statistical model.

7. A numerical model using Finite Element Method (FEM) analysis was constructed to determine the depth of cut for all pick-rock combinations considered using the cutting force values from experimental rock cutting tests (up to loading cycle only). Then the depth of penetration obtained in FEM analysis of all pick-rock combinations was compared with the respective depth of cut obtained in experimental results. The depth of penetration obtained during experiments is lesser than FEM analysis for all pick-rock combinations considered and ranges from 1 to 8% (except a few). Further, the results indicated that displacement decreases from the loading axes towards the boundary in all directions. The stress analysis was carried using Ansys workbench for all the pick-rocks combinations considered along X, Y and Z- directions. The results showed that the maximum compressive stress generated is at the tip of the cut zone.

8. Rock cutting resistance is a new concept developed in the present study, and the results of the RCR (Experimental and FEM) can be used to predict the depth of cut during rock cutting.

7.2 Scope for Future Work

In the present study only 10 rocks were considered. In future studies different types of rocks can be considered. It is suggested that more such investigations shall be conducted on different rocks for determining RCR for different pick-rock combination, which may help to improve the cutting performance. It is suggested to consider rock as an-isotropic instead of isotropic. Similar studies can be carried out using disc cutters.

Correlate RCR and SE which helps in improving the performance of the rock cutting

REFERENCES

- Aleman, V.P, (1982). "Characterisation of strata with particular reference to the performance of roadway drivage machines." (Doctoral dissertation, University of Nottingham).
- Altindag (2003). "Correlation of Specific energy from brittleness concept." *J S Afr Inst Min Metall*, pp 163-171.
- Altindag R. (2004). "Evaluation of drill cuttings in the prediction of penetration rate by using coarseness index and mean particle size in percussive drilling." *Geotech. Geolog Eng.*, 22,pp 417-425
- Altinoluk, S. (1981). "Investigations into the effects of tungsten carbide composition and geometry on the durability of rock excavation tools." (Doctoral dissertation, University of Newcastle upon Tyne).
- Alvarez. G.M, Babuska. R, (1999). "Fuzzy model for the prediction of unconfined compressive strength of rock samples." *Int.J. Rock Mech. Sci.*, 36, pp 339-349.
- Atici, U, Ersoy, A. (2009). "Correlation of Specific energy of Cutting Saws and Drilling Pick with Rock Brittleness and Destruction Energy." *Journal of Materials Processing Technology*, 209, pp 2602-2612.
- Australian T.S (2007). "Current & Emerging Rock Cutting Technology."
- Ayday, C. Göktan, R.M., (1992). "Correlations between L and N-type Schmidt hammer rebound values obtained during field testing." In J.A. Hudson ed., *Rock Characterization*, ISRM Symposium, Eurock'92, Chester, UK, 14–17 September, pp 47-50.
- Aydin, Gokhan, Izzet Karakurt, and Kerim Aydiner. (2013). "Development of Predictive Models for the Specific energy of Circular Diamond Saw blades in the Sawing of Granitic Rocks". *Rock mechanics and rock engineering* 46.4,pp 767-783.

Bailey, S.G. Perrott, C.M, (1974). "Wear processes exhibit by WC-Co rotary cutters in mining." *Wear*, 29(1), pp 117-128.

Benardos, A.G., Kaliampakos, D.C. (2004). "Modeling TBM performance with artificial neural networks." *Int. j. rock mech.min.sci.*,19, pp 597-605.

Bilgin, N., Yazici, S. and Eskikaya, S., (1996). "A model to predict the performance of roadheaders and impact hammers in tunnel drivages." In *ISRM International Symposium-EUROCK 96. International Society for Rock Mechanics*. January.

Bilgin, N., Kuzu, C., Eskikaya, S. and Özdemir, L., (1997). "Cutting performance of jack hammers and roadheaders in Istanbul metro drivages." *World Tunnel Congress*, Vol. 97, pp 455-460.

Bilgin, N., Tuncdemir, H., Balci, C., Copur, H. and Eskikaya, S. (2000). "A model to predict the performance of tunneling machines under stressed conditions." *Proceedings, AITES-ITA 2000 World Tunnel Congress*, May, pp 47-53.

Bilgin, N., Dincer, T. and Copur, H., (2002). "The performance prediction of impact hammers from Schmidt hammer rebound values in Istanbul metro tunnel drivages." *Tunnelling and Underground Space Technology*, 17(3), pp 237-247.

Bilgin N, Demircin M.A, Copur, H, Balci, C, Tuncdemir, H. and Akcin, N. (2006). "Dominant rock properties affecting the performance of conical picks and the comparison of some experimental and theoretical results." *Int J Rock Mech Min Sci.*,43(1), pp 139-156.

Blokhin V.S. (1982). "Improvement of Drilling Tool Efficiency." *TeKNika, Kiev*,

Brown ET. (1981). "Rock characterization testing and monitoring." *Oxford, Pergamon Press*; pp 211-220.

Carpinteri, A, Chiaia, B. and Invernizzi, S, (2004). "Numerical analysis of rock cutting fracture in quasi-brittle materials." *Engineering Fracture Mechanics*, 71(4), pp 567-577.

Colorado School of Mines, (1999), “Deep mine Access Technology Survey.” *Draft Copy*, March.

Copur H, Rostami J, Ozdemir L, Bilgin N, (1997). “Studies on performance prediction of roadheaders based on field data in mining and tunneling projects.” *In, Proceedings of the fourth international symposium on mine mechanization and automation*, Brisbane, Queensland, pp 41-47.

Copur H, Tuncdemir H, Bilgin N, Dincer T. (2001). “Specific energy as a criterion for the use of rapid excavation systems in Turkish mines.” *Trans Inst Min Metall, Sec A*; 110,A, pp 149–157.

Copur H, Bilgin N, Tuncdemir H, Balci C. (2003). “A set of indices based on rock cutting tests for assessment of rock cutting performance and rock properties.” *J S Afr Inst MinMetall*;103(9),pp589–600.

Dehghan,S, Sattari, Gh, Chehreh Chelgani, S, Aliabadi, M. A.(2010). “Prediction of Uniaxial Compressive Strength and Modulus of Elasticity for Travertine samples using Regression and Artificial Neural Networks.” *International journal of Mining Science and Technology*, 20, pp 41–46.

Deliac EP., (1985). “Recent developments in the design and optimization of drum type cutting machines in France.” *Proceedings of the rapid excavation tunnel congress*, NewYork. pp 264–83.

Deliac, EP. (1993). “Theoretical and practical rules for mechanical rock excavation.” *In, Hudson JA, editor. Comprehensive rock engineering*, vol. 4;. pp 177–227.

Dunn PG, Howarth DF, Schmidt SPJ, Bryan IJ. (1997). “A review of non explosive excavation projects for the Australian metalliferous mining industry.” *In, Proceedings of the fourth international symposium on mine mechanization and automation*, Brisbane, Queensland, A5–2/13.

Engin CI, Bayram F, Yasitli NE (2013).“Experimental and statistical evaluation of cutting methods in relation to Specific energy and rock properties.”*Rock Mech Rock Eng* 46, pp 755–766

Ersoy, A. Atici, U. (2007). “Correlation of P and S-waves with Cutting Specific energy and Dominant Properties of Volcanic and Carbonate Rocks.” *Rock Mechanics and Rock Engineering*, 40(5), pp 491-504.

Eskikaya S, Bilgin N, Ozdemir L, (2000). “Development of rapid excavation technologies for the Turkish mining and tunneling industries. NATO TU-Excavation SfS Programme.” *Project Report, Istanbul Technical University, Mining Engineering Department Preparation of Report*, September, pp 172-186.

Evans, I., (1958). “Theoretical aspects of coal ploughing.” *Mechanical Properties of Non-Metallic Brittle Materials*, pp 451-468.

Evans, I., (1962). “A theory of the basic mechanics of coal ploughing.” *In Proceedings of the international symposium on mining research*, 2, pp 761-768).

Evans, I. and Pomeroy, C.D., (1966). “The strength, fracture and workability of coal, a monograph on basic work on coal winning.” *the Mining Research Establishment, National Coal Board*. Elsevier.

Evans, I., (1982). “Optimum line spacing for cutting picks”. *Mining Engineer*, 141, pp 433-434.

Evans, I., (1984). “A theory of the cutting force for point-attack picks.” *Geotechnical and Geological Engineering*, 2(1), pp 63-71.

Evenden, M.P, Edwards, J.S., (1985). “Cutting theory and coal seam assessment techniques and their application to shearer design.” *Int J Rock Mech Min Sci*, ,2(4), pp 253-270.

Farmer, I.W. Garritty, PP, (1987), “Prediction of roadheader cutting performance from fracture toughness considerations.” *In Proceedings of the 6th International Congress on Rock Mechanics*. January. pp 621–624.

Fedorov, V.S, (1951). “Scientific Foundations of Drilling Regimes”. Moscow, Gostoptekhizdat.

Finnie, I., Streit, R. and Foote. L, (1977). “Relationship of coal properties and machine parameters to continuous mining machine cutting rates.” *Open file report (final) 15 Oct 76--15 Apr 77 (No. PB-297291). MB Associates, San Ramon, CA (USA).*

Finol. J., Guo. Y.K. and Jing. X.D. (2001). “A rule based fuzzy model for the prediction of petrophysical rock parameters.” *J. Pet. Sci. Eng.*, 29, pp 97-113.

Fowell RJ, McFeat-Smith I, (1976), “Factors influencing the cutting performance of a selective tunneling machine.” *In, Jones MJ, editor. Proceedings of the tunneling symposium, Tunneling '76, IMM, London. pp 301–309.*

Fowell RJ, Johson ST. (1982). “Rock classification and assessment of rapid excavation”. *Proceedings of the symposium on strata mechanics, Newcastle Upon Tyne;* pp 239–242.

Fowell, R.J., Johnson, S.T. and Speight, H.E., (1984). “36 Boom tunnelling machine studies for improved excavation performance.” *Proceeding of the Design and Performance of Underground Excavations, ISRM Symposium—Cambridge, UK, 3–6 Thomas Telford Publishing. September pp 305-312.*

Fowell, R.J., Hekimoglu, O.Z. and Altinoluk, S., (1987). “Drag tools employed on shearer drums and roadheaders.” *In Proceedings of 10th Turkish Mining Congress of Ankara,* pp 529-550.

Fowell RJ, Johson ST. (1991), “Cuttability assessment applied to drag tool tunneling machines”. *Proceedings of the Seventh International ISRM congress, Aachen,* pp 985–990.

Fowell RJ. (1993). “The mechanics of rock cutting.” *In, Hudson JA, editor. Comprehensive rock engineering,* 4. pp 155–175.

Fowell RJ, Richardson G, Gollick MJ (1994). "Prediction of boom tunneling machine excavation rates." *Proceedings of the symposium on rock mechanics models and measurements challenges from industry*. pp 243–51.

Gehring KH (1997). "Classification of drillability, cuttability, boreability and abrasivity in tunneling." *Felsbau*;15, pp 183–191.

Ghabousi, J., Garret Jr, J.H, Wu, X. (1991). "Knowledge based modeling of material behaviour with neural networks". *J. Eng. Mech. ASCE*, 117(1), pp 132–153.

Gokceoglu, C. (2002). "A fuzzy triangular chart to predict the uniaxial compressive strength of the Ankara Agglomerates from their petrographic composition." *Eng. Geol.*, 66, pp 39-51.

Goktan RM (1990). "Effect of cutter pick rake angle on the failure pattern of high-strength rocks." *International journal of Mining Science and Technology*; 11, pp 281–285.

Goktan RM. (1992), "A theoretical comparison of the performance of drag picks in relation to coal-strength parameters." *J S Afr Inst Min Metall*;92, pp 85–87.

Goktan RM, Ozdemir L, Hanna K (1995), "Prediction of drag pick cutting force in hard rocks." *Proceedings of the third international symposium on mine mechanization and automation*;pp 1031–1039.

Goktan R.M (1995). "Prediction of drag pick cutting force in hard rock's." *In Proc. of the 3rd Int.Symp on Mine Mechanization and Automation.. Golden, Colorado*.

Goktan R.M, Gunes N. (2005). "A semi-empirical approach to cutting force prediction for point-attack picks." *J South Afr Inst Min Metall.*,105, pp 257- 263.

Goktan R.M, Yilmaz.N.G., (2005). "A new methodology for the analysis of the relationship between rock brittleness index and drag pick cutting" *J South Afr Inst Min Metall*, 105, pp. 727-733

Gray K., Armstrong F., and Gatlin C. (1962). "Two-Dimensional Study of Rock Breakage in Drag-Pick Drilling at Atmospheric Pressure." *Journal of Petroleum Technology*,.14(1), pp 93-98.

Guo H., Aziz N., Schmidt L (1992). "Rock cutting study using linear elastic fracture mechanics." *Engineering Fracture Mechanics*,.41(5), pp 771-778.

Haykin, S. (1998). "Neural Networks, A Comprehensive Foundation." *Prentice-Hall, Englewood Cliffs*.

Hekimoglu OZ, Fowell RJ (1990). "From research into practice, in-situ studies for design of boom tunneling machine cutting heads." *In, Proceedings of the 31st US rock mechanic symposium on rock mechanics contribution and challenges*; pp 481–88.

Hekimoglu OZ, Fowell RJ (1990). "Practical aspects of rear pick arrangements on boom-type tunneling machine heads." *Int J Rock Mech Min Sci*; 10, pp 221–30.

Hekimoglu OZ, Fowell RJ. (1991), "Theoretical and practical aspects of circumferential pick spacing on boom tunneling machine cutting heads." *Int J Rock Mech Min Sci* ; 13, pp 257–270.

Hekimoglu OZ (1995). "The radial line concepts for cutting head pick lacing arrangements." *Int J Rock Mech Min Sci Geomech Abstr*;32, pp 301–11.

Hekimoglu OZ, Tiryaki B (1997). "Effects of drum vibration on the performance of coal shearers." *Trans Inst Min Metall, Sect A*; 106,A91–4.

Hoek E. Bieniawski Z. (1965). "Brittle fracture propagation in rock under compression." *International Journal of Fracture*,.1(3),pp 137-155.

Hood M. and Alehossein H (2000). "A development in rock cutting technology." *Int J Rock Mech Min Sci*,37(1-2),pp 297-305.

Howarth D. and Bridge E (1988). "Microfracture beneath blunt disc cutters in rock." *Int J Rock Mech Min Sci* 25, pp 35–38.

- Huang, H., Damjanac, B. Detournay, E. (1998). "Normal wedge rock cutting in rocks with lateral confinement." *Rock Mechanics and Rock Engineering*, 31(2), pp 81–94.
- Hucka VA. (1965). "A rapid method for determining the strength of rocks in-situ." *Int J Rock Mech Min Sci*; pp 127–34.
- Hughes H (1972). "Some aspects of rock machining." *Int J Rock Mech Min Sci*;9, pp 205–11.
- Hurt KG, Laidlaw DD (1979). "Laboratory comparison of three rock cutting tools." *Tunnels and Tunnelling*; 11, pp 13–16.
- Hurt KG, Evans I. (1980), "A laboratory study of the rock cutting using point attack tools." In, Summers D, editor. *Proceedings of the 21st US rock mechanics symposium, Missouri-Rolla*, pp 112–121.
- Hurt KG (1980). "Rock cutting experiments with point attack tools". *Colliery Guardian Coal Int*, April, pp 47–50.
- Hurt KG, MacAndrew KM (1981). "Designing roadheader cutting heads". *Min Eng*; Sepp, pp 167–70.
- Hurt KG, Evans I. (1981). "Point attack tools, an evaluation of function and use for rock cutting." *Min Eng*; March, pp 673–679.
- Hurt KG, Morris CJ, MacAndrew KM (1982). "The design and operation of boom tunneling machine cutting heads." In, Baumgartner P, editor. *Proceedings of the 14th Canadian rock mechanics symposium, CIM Special Volume.30*, pp 54–58.
- Hurt KG, MacAndrew KM. (1985). "Cutting efficiency and life of rock cutting picks." *Int J Rock Mech Min Sci*,2, pp 139–151.
- Hurt KG, Morris CJ (1985). "Computer designed cutter heads improve roadheader performance." *Tunnels Tunnell*;17, pp 37–48.

Hurt KG (1988). “Roadheader cutting head and picks”. Colliery Guard;Sepp, pp 332–3.

Hurt KG, MacAndrew KM, Morris CJ. (1988). “Boom roadheader cutting vibration, measurement and prediction.” In, *Tunncliffe J, editor. Conference on applied rock engineering, CARE’88, IMM;*pp 89–97.

Ibrahim Ocak, Sadi Evren Seker (2012).” Estimation of Elastic Modulus of Intact Rocks by Artificial Neural Network.” *Rock Mech Rock Eng*, 45, pp 1047–1054.

Inyang H.I. (2002), “Developments in Drag Pick Cutting of Rocks for Energy Infrastructure.” *International Journal of Surface Mining, Reclamation and Environment*,**16**(4),pp 248-260.

Irfan Celal Engin, Fatih Bayram., Nazmi Erhan Yasitli. (2013). “Experimental and Statistical Evaluation of Cutting Methods in Relation to Specific energy and Rock Properties.” *Rock Mechanics and Rock Eng.*, 46, pp 755-766.

Jacobs N, Hagan P., (2009). “The effect of stylus hardness and some test parameters on the Cerchar Abrasivity Index,” in *Proceedings 43 rd US Rock Mechanics Symposium , June, Asheville, NC, USA*

Jing, L.A. (2003). “A review of techniques, advances and outstanding issues in numerical modeling for rock mechanics and rock engineering.”, *Int J Rock Mech Min Sci*, 40, pp 283–353.

Joel Langham, Paul hagan (2014).“An assessment of correlation between rock strength and cuttability of rock.” *Coal operators conference*, Feb pp186-192.

Johson ST, Fowell RJ (1984). “A rational approach to practical performance assessment for rapid excavation using boom-type tunneling machines.” In, *Proceedings of the 25th US symposium on rock mechanics Illinois*.pp 759–66.

Johson ST, Fowell RJ (1986). “Compressive strength is not enough”. In, *Hartman HL, editor. Proceedings of the 27th US rock mechanics symposium;* pp 840–845.

Jumikis, A. R. (1979). "Rock mechanics". *Trans Tech Publications, Clausthal, Germany*. pp 356-372.

Kahraman S, Bilgin N, Feridunoglu C (2003). "Dominant rock properties affecting the penetration of percussive drills." *Int J Rock Mech Min Sci*, 40, pp 711–23.

Kahraman, S., Altun, H., Tezekici. B.S. Fener. M. (2006). "Sawability predication of carbonate rocks from shear strength parameters using artificial neural networks." *Int. j. rock mech.min.sci.* 43, pp 157-164.

Kleinert, H.W., (1982), "New Test-Bed Results for Cutting Heads on Selective-Cut Heading Machines." *Gluckauf H- Translation*, 118,

Korinets A., Chen L., Alehossein H., and Lim W, (1996). "DIANA Modeling of a rolling disc cutter and rock indentation." *Second NARMS, rock mechanics tools and techniques. Montreal, Balkema*,pp 647–54.

Krupa V, Krepelka F, Bejda J, Imrich P, (1993). "The cutting constant of the rock does not depend on scale effect of rock mass jointing." *In, Cunha APD, editor. Proceedings of the Second international workshop on scale effect on rock masses. New York, Wiley*;pp 63–66.

Krupa. V, Krepelka. F, Sekula. F, Kristova. Z, (1993). "Specific energy as information source about strength properties of rock mass using TBM." *In, Proceedings of the geotechnical engineering of hard soils–soft rocks, Balkema*,pp 1475–1477.

Krupa V, Krepelka F, Imrich P (1994). "Continuous evaluation of rock mechanics and geological information at drilling and boring." *In Proceedings of the seventh international congress, International Association of Engineering Geology*,pp 1027–1030.

Kou, S.Q. (1998). "Identification of governing factors related to the rock indentation depth by using similarity analysis." *Engineering geology*, 49, PP 261-269.

Kou S., Lindqvist PA., Tang C., and Xu X., (1999). "Numerical simulation of the cutting of inhomogeneous rocks." *Int J Rock Mech Min Sci.*, 36(5),pp 711-717.

Kou, S.Q. (1999). "Numerical simulation of the cutting of homogenous rocks" *Int. j. rock mech.min.sci.*, 36(5), pp711-717.

Lindqvist PA. (1982), "Rock fragmentation by indentation and disc cutting some theoretical and experimental studies." *Ph.D. thesis, Lulea University of Technology, Lulea, Sweden.*

Lindqvist PA. (1984), "Stress fields and subsurface crack propagation of single and multiple rock indentation and disc cutting." *Rock Mechanics and Rock Engineering*,.17(2),pp 97-112.

Liu H (2002). "Numerical modeling of the rock fracture process under mechanical loading." *Ph.D. thesis, Lulea University of Technology, Lulea, Sweden.*

Liu, H.Y., Kou, S.Q., Lindqvist, PPA. Tang, C.A. (2002). "Numerical simulation of the rock fragmentation process induced by indenters." *Int J Rock Mech Min Sci*, 39, pp491–505.

MacGregor I., Baker R., and Luyckx S, (1990). "A comparison between the wear of continuous miner button picks and the wear of pointed picks used in South African collieries." *Int J Rock Mech Min Sci*,.11(2),pp 213-222.

McFeat-Smith, I. (1977). "Rock property testing for the assessment of tunneling machine Performance." *Tunnels and Tunnelling*", March, pp 23–33.

McFeat-Smith I, Fowell RJ, (1977). "Correlation of rock properties and cutting performance of tunnelling machines." *In, Potts ELJ, Attewell PB, editors. Proceedings of the conference on rock engineering. University of Newcastle Upon Tyne;*pp 582–602.

McFeat-Smith I, (1978). "Effective and economic excavation by roadheaders." *Tunnels Tunnell*; 10,pp43–48.

McFeat-Smith I, Fowell RJ, (1979). "The selection and application of roadheaders for rock tunneling." In, *Maevis AC, Hustrulid WA, editors. Proceedings of the rapid excavation and tunneling congress, Atlanta*, pp 261–79.

Mellor M. (1972). "Normalization of Specific energy values." *Int J Rock Mech Min Sci*, 9, pp 661–673.

Meulenkampp F, Alvarez grima, M., (1999). "Application of neural networks for the prediction of the unconfined compressive strength (UCS) from equotip hardness." *Int. j. rock mech.min.sci.*, 36, pp 29-39.

Mishnaevsky Jr L. (1998), "Rock fragmentation and optimization of drilling tools." In, *Fracture of Rock, Computational Mechanics Publications*.pp 167-203.

Mishnaevsky L., (1993). "A brief review of Soviet theoretical approaches to dynamic rock failure." *Int J Rock Mech Min Sci Geomech*,30, (6), December, pp 663-668

Moscalev A.N. (1972), "Increase in Intensity of Rock Fragmentation". Moscow. Nedra,

Murat Yurdakul., Hurriyet Akdas.,(2012). "Prediction of Specific Cutting Energy for Large Diameter Circular Saws during Natural Stone Cutting." *Int J Rock Mech Min Sci*, 53, pp 38-44.

Neil, D.M., Rostami, J., Ozdemir, L. and Gertsch, R., (1994). "Production estimating techniques for underground mining using roadheaders." *Preprints-Society of Mining Engineers of AIME*.

Nikiforovsky V.S, Shemyakin Y.I. (1972), "Impact Fracture of Solids." *Nauka, Novosibirsk*.

Nishimatsu Y (1972). "The mechanics of rock cutting." *Int J Rock Mech Min Sci Geomech*, Volume 9, Issue 2, pp 161-323.

Paithankar, A. G, Misra.G. B, (1976). "Critical appraisal of the protodyakonov index." *Int J Rock Mech Min Sci Geomech*,Abstract. v 13, pp 249-251.

Poole RW, Farmer IW (1980). “Consistency and repeatability of Schmidt hammer rebound data during field testing.” *Int J Rock Mech Min Sci Geomech*, Abstr; 17, pp 167–71.

Pool D. (1987); “The effectiveness of tunneling machines.” *Tunnels and Tunneling* 19, pp 66–67.

Ranman K.E. (1985). “A model describing rock cutting with conical picks.” *Rock Mechanics and Rock Engineering*, **18**(2),pp 131-140.

Richard, Fabrice Dagrain, Edmond Poyol, Emmanuel Detournay (2012), “Rock strength determination from scratch tests” *Engineering Geology, Elsevier*, 147, pp91-100

Roepke WW, Voltz JI. (1983). “Coal-cutting forces and primary dust generation using radial gage cutters”. *USBM RI 8800*, pp 24-32.

Roepke WW, Hanson BD, (1984). “Coal cutting forces on primary dust control during cutting.” *Min Eng*; 36, pp 636–643.

Rogers, S, Roberts, B, (1991). “Wear mechanisms associated with rock excavation using point attack picks.” *Int J Rock Mech Min Sci*,12, pp 317–323

Rostami J, Ozdemir L, Neil D (1994). “Performance prediction, a key issue in mechanical hard rock mining.” *Min Eng*, (Nov),pp1264–1267.

Rostami J, Ozdemir L(1994). “Roadheader performance optimization for mining and civil construction.” *Proceedings of the 13th annual technical conference, Institute of Shaft Drilling Technology, Las Vegas; Nevada*,pp 12–15.

Roxborough F.F. (1973). “Cutting Rocks with Picks.” *The mining engineer*, pp 445-452.

Roxborough FF, Rispin A. (1973). “A laboratory investigation into the application of picks for mechanized tunnel boring in the lower chalk”. *Min Eng*; May, pp1–13.

Roxborough FF, Rispin A. (1973). "The mechanical cutting characteristics of the lower chalk". *Tunnels and Tunnelling*, 5, pp 45-67

Roxborough FF, Phillips HR. (1975), "Rock excavation by disc cutter". *Int J Rock Mech Min Sci*; 12, pp 361–366.

Roxborough FF, King P, Pedroncelli EJ (1981). "Tests on the cutting performance of a continuous miner." *J S Afr Inst Min Metall*; 81, pp 9–26.

Roxborough FF, Pedroncelli EJ. (1982). "A practical evaluation of some coal cutting theories using a continuous miner." *Min Eng;Sepp*, pp 145–156.

Roxborough FF, (1986). "Research in mechanical excavation, progress and prospects". In, Mann CD, Kelly MN, editors. *Proceedings of the rapid excavation tunn congress, Las Vegas*,pp 225–244.

Roxborough, F. F. (1987). "The role of some basic rock properties in assessing cuttability." In Seminar on Tunnels, Wholly Engineered Structures. April.

Roxborough F.F. Liu Z.C (1995). "Theoretical considerations on pick shape in rock and coal cutting."In *Proceedings of the sixth underground operator's conference.. Kalgoorlie, WA, Australia*. Pp 163-169.

Rumelhart, D., McClelland, J. (1986). "Parallel distributed processing, explorations in the microstructure of cognition." *Bradford*.

Saksala, T., Gomon, D., Hokka, M., and Kuokkala, V.T. (2013). "Numerical modeling and experimentation of dynamic rock cutting with single and triple indenters on Kuru granite.", *Rock Dynamics and Applications – State of the Art – Zhao & Li (eds) Taylor & Francis Group*,pp 415-421.

Saouma V.E. and Kleinosky M.J. (1984), "Finite element simulation of rock cutting, a fracture mechanics approach." *The 25th U.S. Symposium on Rock Mechanics (USRMS)*, pp 25-27

Sarkar, K., Tiwary, A. and Singh, T.N, (2010). “Estimation of strength parameters of rock using artificial neural networks.” *Bulletin of engineering geology and the environment*, 69(4), pp 599-606.

Schneider H (1988). "Criteria for selecting a boom type roadheader." *Min Mag Sepp*, pp 183–187.

Schneider H. (1988), “Estimating cutting capability for boom-type roadheaders.” *Eng Min J*; Jan,pp23–34.

Sekula F, Krupa V, Krepelka F. (1991). “Monitoring of the rock strength characteristics in the course of full of face driving process.” *In, Rakowski Z, editor. Proceedings of the international conference on geomechanics.* pp 299–303.

Simpson, PP K. (1990). “Artificial neural system-foundation, paradigm, application and implementation.” *Pergamon Press*, New York.

Singh, T. N., Kanchan, R., Verma, A. K., Singh, S. (2003). “An intelligent approach for prediction of triaxial properties using unconfined uniaxial strength.” *Min. Eng. J*, 5, pp 12–16.

Singh, V.K., Singh, D., Singh, T.N. (2001). “Prediction of strength properties of some schistose rocks.” *Int Rock Mech Min Sci.*, 38(2), pp 269–284.

Stolarski, Nakasone, Yosimoto, (2006). “Engineering analysis with Ansys software.” *Butterworth-Heinemann, Elsevier*, pp 480-510.

Sulem, Miguel Cerrolazab (2002).” Finite element analysis of the indentation test on rocks with microstructure.” *Computers and Geotechnics*, 29, pp 95–117.

Sonmez, H., Gokceoglu, C., Nefeslioglu, H.A., Kayabasi,, A. (2006). “Estimation of rock modulus, for intact rocks with an artificial neural network and for rock masses with a new empirical equation.” *Int J Rock Mech Min Sci.*, 43(2), pp 224–235.

Sundae LS, Myren TA. (1987). “In situ comparison of radial and point attackpicks.” *USBM RI 9127*.pp 15-27.

Tang C. (1997). "Numerical simulation of progressive rock failure and associated seismicity." *Int J Rock Mech Min Sci.* 34(2), pp 249-261.

Teale, R, (1965). "The concept of Specific energy in Rock drilling." *Int J Rock Mech Min Sci Geomech, Abstracts*, 2, pp 57-73.

Thuro K, Plinninger RJ. (1998). "Geological limits in roadheader excavation four case studies." *Proceedings of the 8th International IAEG congress, Vancouver*, 2, pp 3545–3552.

Thuro, K. Plinninger, R.J., (1999). "Predicting roadheader advance rates." *Tunnels and Tunnelling International*, 6/1999, pp36-39.

Thuro K, Plinninger RJ. (2003). "Hard rock tunnel boring, cutting, drilling and blasting, rock parameters for excavatability." In, Merwe JN, editor. *Proceedings of the 10th international ISRM congress on technology roadmap for rock mechanics, South African Institute of Mining and Metallurgy*. pp 1227–33.

Tiryaki B, Ayhan M, Hekimoglu OZ. (2001). "A new computer program for cutting head design of roadheaders and drum shearers." In, *Proceedings of the 17th international mining congress and exhibition of Turkey, Ankara*, pp 655–662.

Tiryaki, B. (2008a). "Application of artificial neural networks for predicting the cuttability of rocks by drag tools." *Tunnelling Underground Space Technology*, 23, pp 273-280.

Tiryaki, B. (2008b). "Predicting intact rock strength for mechanical excavation using multivariate statistics, artificial neural networks and regression trees." *Eng. Geol.*, 99, pp 51-60.

Tiryaki, B., Cagatay Dikmen, A.(2006). "Effects of Rock Properties on Specific Cutting Energy in Linear Cutting of Sandstones by Picks." *Rock Mechanics and Rock Engineering*, 39(2), pp 89-120.

- Uehigashi K, Tokairin Y, Ishikawa K, Kikuchi T. (1987). “Possibility of rock excavation by boom-type tunneling machines.” *Proceedings of the 6th Australian tunnelling conference, Melbourne*, pp 253–259.
- Wang, J.K., Lehnhoff, T.F. (1976). “Pick penetration into rock, a finite element study.” *Int J Rock Mech Min Sci*, 13, pp 11–16.
- Wang, S. Y., Sloan, S. W., Liu, H. Y. and Tang, C. A.(2011).”Numerical simulation of the rock fragmentation process induced by two drill picks subjected to static and dynamic (impact) loading.” *Rock Mech and Rock Eng.*, 44, pp 317–332.
- Wei X., Wang C.Y., Yuan H.L., and Xie Z. (2003). “Study of Fracture Mechanism of Rock Cutting. Key Engineering Materials”, 250, pp 200-208.
- West G. (1989). “Rock abrasiveness testing for tunneling”. *Int J Rock Mech Min Sci*; 26, pp 151–160.
- Yilmaz, I, Oguz Kaynar. (2011). “Multiple regressions, ANN (RBF, MLP) and ANFIS models for prediction of swell potential of clayey soils.” *Expert systems with Applications*, 38, pp 5958-5966.
- Yilmaz, I. and Sendir, H. (2002). “Correlation of Schmidt hardness with unconfined compressive strength and young’s modulus in gypsum from Sivas.” (Turkey), *Engineering Geology*, 66, pp 211-219.
- Yilmaz, I. and Yuksek, A. G. (2008). “Technical Note An Example of Artificial Neural Network (ANN) Application for Indirect Estimation of Rock Parameters”. *Rock Mechanics and Rock Engineering*, 41 (5), pp 781–795.
- Yilmaz, I. and Yuksek, A.G. (2009). “Prediction of the strength and elasticity modulus of gypsum using multiple regressions, ANN, ANFIS models and their comparison.” *Int. J. Rock Mech. Min. Sci.*, 46(4), pp 803-810.
- Zeuch D., Holcomb D., and Lauson H. (1985). “Analysis of consolidation of granulated rock salt using a plastic flow model of isostatic hot-pressing”, *Sandia National Labs., Albuquerque, NM (USA)*.

Zeuch D., Swenson D., and Finger J. (1983). "Subsurface Damage Development In Rock During Drag-Pick Cutting." *Observations Nd ModelpRedictions*.

Zhu, W.C., Tang, C.A. (2006). "Numerical simulation of Brazilian disk rock failure under static and dynamic loading." *Int J Rock Mech Min Sci*, 43, pp 236–252.

Zienkiewicz, O.C. (1968). "Continuum mechanics as an approach to rock mass problems." *Rock Mechanics in Engineering Practice, Wiley and Son*.pp 237-273,

Zienkiewicz, O.C. (1968). "The Finite Element Method." *Mcgraw hill, London*.

Zipf R. and Bieniawski Z., (1988). "Estimating the crush zone size under a cutting tool in coal". *Geotechnical and Geological Engineering*, 6(4),pp 279-295.

Zorlu.K, Gokceoglu C, Ocakoglu F.Nefeslioglu H.A.Acikalin.S. (2008). "Prediction of uniaxial compressive strength of sandstones using photography-based models." *Engineering Geology*, 96, pp 141-158.

APPENDIX-I

Table 3.4 Experimental Result for 45° attack angle with Different Pick Angles

SI No	Type of Rock	Pick Angle	rpm	Cutting Force,	Torque	Depth of cut	Volume	Cutting rate	Specific Energy
				N	N-m	(mm)	(m ³)	(m ³ /sec)	(J/m ³)
1	2	3	4	5	6	7	8	9	10
1	Coal	45°	225	1.499	14.91	8.31	0.00631	45.072	1974
			225	1.497	14.91	8.31	0.00631	45.072	1971
			225	1.494	14.92	8.32	0.00632	45.073	1967
			300	1.496	14.92	8.32	0.00632	45.073	1969
			300	1.497	14.93	8.33	0.00633	45.108	1970
			300	1.495	14.94	8.33	0.00633	45.108	1967
			325	1.496	14.91	8.33	0.00634	45.14	1966
			325	1.495	14.93	8.34	0.00634	45.18	1967
			325	1.496	14.92	8.34	0.00635	45.18	1965
			350	1.497	14.91	8.33	0.00636	45.19	1961
			350	1.495	14.93	8.34	0.00637	45.252	1957
			350	1.494	14.92	8.34	0.00638	45.26	1953
		50°	225	1.495	14.91	8.21	0.00611	44.532	2009
			225	1.497	14.91	8.21	0.00611	44.532	2012
			225	1.494	14.92	8.21	0.00612	44.542	2004
			300	1.494	14.92	8.22	0.00612	44.542	2007
			300	1.494	14.93	8.22	0.00613	44.552	2003
			300	1.494	14.94	8.22	0.00613	44.552	2003
			325	1.496	14.91	8.23	0.00614	44.562	2005
			325	1.495	14.93	8.24	0.00614	44.568	2006
			325	1.493	14.92	8.25	0.00615	44.568	2003
			350	1.492	14.91	8.23	0.00615	44.64	1997
			350	1.493	14.93	8.24	0.00616	44.64	1997
			350	1.491	14.92	8.25	0.00616	44.712	1997
		55°	225	1.49	14.91	8.41	0.00637	45.648	1967
			225	1.485	14.91	8.42	0.00637	45.648	1963
			225	1.486	14.92	8.43	0.00638	45.65	1963
			300	1.486	14.92	8.43	0.00639	45.725	1960
			300	1.485	14.93	8.43	0.00641	45.725	1953
			300	1.484	14.94	8.44	0.00641	45.73	1954
			325	1.485	14.91	8.44	0.00642	45.735	1952
			325	1.484	14.93	8.44	0.00642	45.77	1951
			325	1.483	14.92	8.45	0.00643	45.79	1949
			350	1.483	14.91	8.44	0.00644	45.828	1944
			350	1.482	14.93	8.44	0.00645	45.828	1939
			350	1.483	14.92	8.45	0.00645	45.9	1943
		65°	225	1.484	14.81	8.45	0.00641	45.648	1956
			225	1.484	14.91	8.43	0.00641	45.648	1952
			225	1.482	14.82	8.44	0.00642	45.65	1948
			300	1.482	14.82	8.45	0.00642	45.72	1951
			300	1.483	14.83	8.46	0.00643	45.72	1951
			300	1.482	14.84	8.45	0.00643	45.75	1948
			325	1.481	14.81	8.45	0.00644	45.78	1943
			325	1.48	14.83	8.46	0.00644	45.792	1944
			325	1.481	14.82	8.46	0.00645	45.792	1943
			350	1.482	14.81	8.45	0.00648	45.828	1933
			350	1.481	14.83	8.46	0.00651	45.828	1925
			350	1.48	14.82	8.46	0.00652	45.9	1920

2	Sand stone 1	45°	225	1.596	15.81	7.53	0.0053	41.472	2268
			225	1.597	15.91	7.53	0.00531	41.472	2265
			225	1.596	15.92	7.53	0.00531	41.48	2263
			300	1.595	15.92	7.54	0.00532	41.508	2261
			300	1.594	15.93	7.54	0.00532	41.508	2259
			300	1.594	15.94	7.55	0.00533	41.52	2258
			325	1.595	15.91	7.55	0.00533	41.52	2259
			325	1.594	15.93	7.55	0.00534	41.58	2254
			325	1.593	15.92	7.55	0.00534	41.58	2252
			350	1.592	15.91	7.56	0.00535	41.652	2250
			350	1.593	15.93	7.56	0.00535	41.652	2251
			350	1.591	15.92	7.56	0.00536	41.688	2244
		50°	225	1.59	15.91	7.56	0.00521	40.55	2307
			225	1.586	15.91	7.56	0.00522	40.6	2297
			225	1.587	15.92	7.56	0.00523	40.65	2294
			300	1.589	15.92	7.56	0.00524	40.7	2293
			300	1.588	15.93	7.56	0.00525	40.75	2287
			300	1.587	15.94	7.57	0.00531	41.8	2262
			325	1.587	15.91	7.57	0.00531	41.85	2262
			325	1.588	15.93	7.57	0.00532	41.9	2260
			325	1.587	15.92	7.57	0.00533	41.9	2254
			350	1.586	15.91	7.57	0.00534	41.92	2248
			350	1.585	15.93	7.57	0.00535	41.93	2243
			350	1.586	15.92	7.57	0.00536	41.95	2240
		55°	225	1.588	15.91	7.57	0.0052	40.84	2312
			225	1.587	15.91	7.62	0.00521	40.85	2321
			225	1.586	15.92	7.63	0.00521	40.86	2323
			300	1.585	15.92	7.63	0.00522	40.932	2317
			300	1.586	15.93	7.63	0.00522	40.932	2318
			300	1.585	15.94	7.63	0.00523	40.94	2312
			325	1.585	15.91	7.63	0.00523	40.948	2312
			325	1.583	15.93	7.63	0.00524	40.968	2305
			325	1.584	15.92	7.64	0.00524	40.968	2309
			350	1.586	15.91	7.64	0.00525	41.04	2308
			350	1.585	15.93	7.64	0.00525	41.04	2307
			350	1.584	15.92	7.64	0.00526	41.112	2301
		65°	225	1.584	15.91	7.64	0.00521	40.86	2323
			225	1.585	15.91	7.64	0.00521	40.86	2324
			225	1.584	15.92	7.65	0.00522	40.88	2321
			300	1.583	15.92	7.65	0.00522	40.932	2320
			300	1.582	15.93	7.65	0.00523	40.932	2314
			300	1.583	15.94	7.66	0.00523	40.942	2319
			325	1.585	15.91	7.66	0.00524	40.952	2317
			325	1.583	15.83	7.66	0.00524	40.968	2314
			325	1.582	15.82	7.67	0.00525	40.968	2311
			350	1.582	15.81	7.67	0.00525	41.04	2311
			350	1.582	15.83	7.67	0.00526	41.04	2307
			350	1.58	15.82	7.67	0.00527	41.112	2300

3	Sand stone 2	45°	225	1.632	16.21	7.56	0.00501	40.248	2463
			225	1.631	16.21	7.33	0.00501	40.248	2386
			225	1.632	16.22	7.33	0.00503	40.28	2378
			300	1.634	16.22	7.33	0.00504	40.32	2376
			300	1.633	16.23	7.34	0.00505	40.32	2374
			300	1.631	16.24	7.34	0.00521	40.932	2298
			325	1.631	16.21	7.34	0.00521	40.932	2298
			325	1.632	16.23	7.35	0.00521	40.968	2302
			325	1.631	16.22	7.35	0.00521	40.968	2301
			350	1.631	16.21	7.35	0.00523	41.04	2292
			350	1.63	16.23	7.35	0.00524	41.04	2286
			350	1.631	16.22	7.35	0.00524	41.112	2288
		50°	225	1.632	16.31	7.35	0.00501	40.248	2394
			225	1.628	16.31	7.36	0.00501	40.248	2392
			225	1.627	16.32	7.36	0.00502	40.249	2385
			300	1.627	16.32	7.36	0.00502	40.32	2385
			300	1.628	16.33	7.36	0.00503	40.32	2382
			300	1.626	16.34	7.37	0.00503	40.34	2382
			325	1.626	16.31	7.37	0.00504	40.36	2378
			325	1.625	16.33	7.38	0.00504	40.392	2379
			325	1.625	16.32	7.38	0.00505	40.392	2375
			350	1.627	16.31	7.38	0.00505	40.428	2378
			350	1.626	16.33	7.38	0.00506	40.428	2372
			350	1.625	16.32	7.39	0.00501	40.448	2397
		55°	225	1.625	16.31	7.39	0.00491	39.708	2446
			225	1.625	16.31	7.42	0.00491	39.708	2456
			225	1.624	16.32	7.42	0.00492	39.715	2449
			300	1.624	16.32	7.43	0.00492	39.715	2453
			300	1.623	16.33	7.43	0.00493	39.72	2446
			300	1.623	16.34	7.44	0.00494	39.72	2444
			325	1.626	16.31	7.44	0.00494	39.725	2449
			325	1.625	16.33	7.45	0.00495	39.728	2446
			325	1.624	16.32	7.45	0.00495	39.728	2444
			350	1.624	16.31	7.45	0.00496	39.78	2439
			350	1.624	16.33	7.45	0.00497	39.78	2434
			350	1.623	16.32	7.45	0.00498	39.79	2428
		65°	225	1.623	16.31	7.45	0.0049	39.672	2468
			225	1.621	16.31	7.47	0.00491	39.672	2466
			225	1.622	16.32	7.47	0.00491	39.673	2468
			300	1.624	16.32	7.48	0.00492	39.673	2469
			300	1.623	16.33	7.48	0.00492	39.674	2467
			300	1.622	16.34	7.57	0.00493	39.674	2491
			325	1.622	16.31	7.57	0.00493	39.675	2491
			325	1.623	16.33	7.57	0.00494	39.675	2487
			325	1.621	16.32	7.58	0.00495	39.676	2482
			350	1.621	16.31	7.58	0.00495	39.676	2482
			350	1.62	16.33	7.59	0.00496	39.677	2479
			350	1.621	16.32	7.59	0.00497	39.678	2476

4	Sand stone 3	45°	225	1.64	16.41	6.76	0.00471	39.06	2354
			225	1.639	16.41	6.76	0.00471	39.105	2352
			225	1.638	16.42	6.76	0.00472	39.12	2346
			300	1.637	16.42	6.76	0.00472	39.125	2345
			300	1.638	16.43	6.76	0.00473	39.132	2341
			300	1.637	16.44	6.76	0.00473	39.132	2340
			325	1.637	16.41	6.76	0.00474	39.145	2335
			325	1.636	16.43	6.86	0.00474	39.168	2368
			325	1.637	16.42	6.95	0.00475	39.168	2395
			350	1.639	16.41	6.95	0.00475	39.225	2398
			350	1.638	16.43	6.95	0.00476	39.852	2392
			350	1.637	16.42	6.96	0.00476	39.888	2394
		50°	225	1.637	16.41	6.96	0.00441	37.052	2584
			225	1.638	16.41	6.96	0.00441	37.088	2585
			225	1.637	16.42	6.96	0.00442	37.872	2578
			300	1.636	16.42	6.96	0.00442	37.908	2576
			300	1.635	16.43	6.96	0.00443	37.908	2569
			300	1.636	16.44	6.96	0.00443	37.92	2570
			325	1.638	16.41	6.96	0.00444	37.92	2568
			325	1.637	16.43	6.96	0.00444	37.98	2566
			325	1.636	16.42	6.97	0.00445	37.98	2562
			350	1.636	16.41	6.97	0.00445	38.99	2562
			350	1.637	16.43	6.97	0.00441	37.908	2587
			350	1.635	16.42	6.97	0.00441	37.87	2584
		55°	225	1.635	16.41	6.97	0.00442	37.872	2578
			225	1.634	16.41	6.97	0.00442	37.92	2577
			225	1.635	16.42	6.97	0.00443	37.93	2572
			300	1.637	16.42	6.97	0.00443	37.94	2576
			300	1.636	16.43	6.97	0.00444	37.95	2568
			300	1.635	16.44	6.97	0.00444	37.968	2567
			325	1.635	16.41	6.98	0.00445	37.988	2565
			325	1.636	16.43	6.98	0.00445	38.855	2566
			325	1.635	16.42	6.98	0.00446	38.89	2559
			350	1.635	16.41	6.98	0.00446	38.99	2559
			350	1.634	16.43	6.98	0.00447	38.995	2552
			350	1.635	16.42	6.98	0.00447	38.998	2553
		65°	225	1.637	16.41	6.98	0.00411	36.648	2780
			225	1.636	16.41	7.23	0.00412	36.648	2871
			225	1.634	16.42	7.23	0.00413	36.658	2860
			300	1.634	16.42	7.24	0.00421	36.72	2810
			300	1.635	16.43	7.24	0.00422	36.72	2805
			300	1.634	16.44	7.24	0.00424	36.82	2790
			325	1.634	16.41	7.25	0.00426	36.88	2781
			325	1.633	16.43	7.25	0.00431	37.368	2747
			325	1.633	16.42	7.25	0.00432	38.052	2741
			350	1.635	16.41	7.25	0.00433	38.088	2738
			350	1.634	16.43	7.32	0.00434	38.088	2756
			350	1.633	16.42	7.32	0.00411	38.124	2908

5	Lime stone 1	45°	225	1.686	16.81	6.74	0.00412	36.648	2758
			225	1.689	16.81	6.74	0.00413	36.648	2756
			225	1.688	16.82	6.74	0.00413	36.655	2755
			300	1.687	16.82	6.74	0.00414	36.72	2746
			300	1.686	16.83	6.74	0.00414	36.72	2745
			300	1.687	16.84	6.74	0.00415	36.75	2740
			325	1.689	16.81	6.74	0.00416	36.778	2737
			325	1.688	16.83	6.75	0.00416	36.792	2739
			325	1.686	16.82	6.75	0.00417	36.792	2729
			350	1.686	16.81	6.75	0.00417	36.828	2729
			350	1.687	16.83	6.75	0.00418	36.828	2724
			350	1.685	16.82	6.75	0.00418	36.9	2721
		50°	225	1.685	16.81	6.75	0.00411	36.648	2767
			225	1.684	16.81	6.75	0.00412	36.653	2759
			225	1.685	16.92	6.75	0.00414	36.666	2747
			300	1.687	16.92	6.75	0.00415	36.695	2744
			300	1.686	16.93	6.75	0.00416	36.756	2736
			300	1.685	16.94	6.75	0.00417	36.768	2728
			325	1.685	16.91	6.75	0.00418	36.773	2721
			325	1.686	16.93	6.75	0.00419	36.782	2716
			325	1.685	16.92	6.75	0.0042	36.794	2708
			350	1.684	16.91	6.76	0.00421	36.852	2704
			350	1.683	16.93	6.76	0.00422	36.861	2696
			350	1.684	16.92	6.76	0.00422	36.897	2698
		55°	225	1.686	16.91	6.76	0.00411	36.648	2773
			225	1.685	16.91	6.76	0.00412	36.648	2765
			225	1.684	16.92	6.76	0.00413	36.652	2756
			300	1.684	16.92	6.76	0.00414	36.72	2750
			300	1.685	16.93	6.76	0.00415	36.725	2745
			300	1.683	16.94	6.76	0.00416	36.732	2735
			325	1.683	16.91	6.76	0.00417	36.738	2728
			325	1.682	16.93	6.76	0.00418	36.792	2720
			325	1.683	16.92	6.76	0.00419	36.792	2715
			350	1.685	16.91	6.77	0.0042	36.828	2716
			350	1.684	16.93	6.77	0.00421	36.828	2708
			350	1.682	16.92	6.77	0.00422	36.9	2698
		65°	225	1.682	16.91	6.77	0.00412	36.645	2764
			225	1.683	16.91	6.77	0.00413	36.648	2759
			225	1.682	16.92	6.77	0.00414	36.648	2751
			300	1.682	16.92	6.77	0.00414	36.72	2751
			300	1.681	16.93	6.77	0.00416	36.72	2736
			300	1.682	16.94	6.77	0.00417	36.726	2731
			325	1.684	16.91	6.77	0.00417	36.728	2734
			325	1.683	16.93	6.77	0.00419	36.792	2719
			325	1.681	16.92	6.78	0.0042	36.792	2714
			350	1.681	16.91	6.78	0.00421	36.828	2707
			350	1.682	16.93	6.78	0.00422	36.828	2702
			350	1.681	16.92	6.78	0.00412	36.9	2766

6	Lime stone 2	45°	225	1.757	17.41	6.34	0.00371	34.812	3003
			225	1.757	17.41	6.34	0.00372	34.848	2994
			225	1.758	17.42	6.34	0.00373	34.848	2988
			300	1.76	17.42	6.34	0.00374	34.92	2984
			300	1.759	17.43	6.34	0.00375	34.92	2974
			300	1.757	17.44	6.34	0.00376	34.925	2963
			325	1.757	17.41	6.34	0.00377	34.928	2955
			325	1.758	17.43	6.34	0.00378	34.992	2949
			325	1.756	17.52	6.34	0.00379	34.992	2937
			350	1.756	17.41	6.35	0.00379	35.028	2942
			350	1.755	17.43	6.35	0.00381	35.028	2925
			350	1.756	17.52	6.35	0.00381	35.1	2927
		50°	225	1.758	17.51	6.35	0.00381	34.832	2930
			225	1.757	17.51	6.35	0.00381	34.848	2928
			225	1.756	17.52	6.36	0.00382	34.848	2924
			300	1.756	17.52	6.44	0.00382	34.915	2960
			300	1.757	17.53	6.44	0.00383	34.92	2954
			300	1.755	17.54	6.44	0.00383	34.92	2951
			325	1.755	17.51	6.44	0.00384	34.925	2943
			325	1.754	17.53	6.44	0.00384	34.992	2942
			325	1.755	17.52	6.44	0.00385	34.992	2936
			350	1.757	17.51	6.45	0.00385	35.028	2944
			350	1.756	17.53	6.45	0.00386	35.028	2934
			350	1.755	17.52	6.45	0.00386	35.1	2933
		55°	225	1.755	17.51	6.45	0.00361	34.256	3136
			225	1.756	17.51	6.45	0.00362	34.272	3129
			225	1.755	17.52	6.45	0.00363	34.272	3118
			300	1.754	17.52	6.45	0.00364	34.308	3108
			300	1.753	17.53	6.46	0.00365	34.308	3103
			300	1.754	17.54	6.46	0.00365	34.31	3104
			325	1.756	17.51	6.46	0.00366	34.315	3099
			325	1.755	17.53	6.46	0.00366	34.38	3098
			325	1.754	17.52	6.46	0.00367	34.38	3087
			350	1.754	17.51	6.46	0.00367	34.452	3087
			350	1.755	17.53	6.46	0.00368	34.452	3081
			350	1.753	17.52	6.46	0.00368	35.1	3077
		65°	225	1.753	17.51	6.46	0.00365	34.263	3103
			225	1.752	17.51	6.46	0.00373	34.272	3034
			225	1.753	17.52	6.46	0.00383	34.272	2957
			300	1.755	17.52	6.46	0.00383	34.362	2960
			300	1.754	17.53	6.46	0.00384	34.446	2951
			300	1.753	17.54	6.46	0.00384	34.586	2949
			325	1.753	17.51	6.46	0.00385	34.648	2941
			325	1.754	17.53	6.46	0.00385	34.992	2943
			325	1.753	17.52	6.46	0.00386	34.992	2934
			350	1.752	17.51	6.47	0.00387	35.028	2929
			350	1.74	17.53	6.47	0.00388	35.028	2901
			350	1.741	17.52	6.47	0.00389	35.1	2896

7	Lime stone 3	45°	225	1.753	17.51	6.46	0.00365	34.263	3103
			225	1.752	17.51	6.46	0.00373	34.272	3034
			225	1.753	17.52	6.46	0.00383	34.272	2957
			300	1.755	17.52	6.46	0.00383	34.362	2960
			300	1.754	17.53	6.46	0.00384	34.446	2951
			300	1.753	17.54	6.46	0.00384	34.586	2949
			325	1.753	17.51	6.46	0.00385	34.648	2941
			325	1.754	17.53	6.46	0.00385	34.992	2943
			325	1.753	17.52	6.46	0.00386	34.992	2934
			350	1.752	17.51	6.47	0.00387	35.028	2929
			350	1.74	17.53	6.47	0.00388	35.028	2901
			350	1.741	17.52	6.47	0.00389	35.1	2896
		50°	225	1.753	17.51	6.46	0.00365	34.263	3103
			225	1.752	17.51	6.46	0.00373	34.272	3034
			225	1.753	17.52	6.46	0.00383	34.272	2957
			300	1.755	17.52	6.46	0.00383	34.362	2960
			300	1.754	17.53	6.46	0.00384	34.446	2951
			300	1.753	17.54	6.46	0.00384	34.586	2949
			325	1.753	17.51	6.46	0.00385	34.648	2941
			325	1.754	17.53	6.46	0.00385	34.992	2943
			325	1.753	17.52	6.46	0.00386	34.992	2934
			350	1.752	17.51	6.47	0.00387	35.028	2929
			350	1.74	17.53	6.47	0.00388	35.028	2901
			350	1.741	17.52	6.47	0.00389	35.1	2896
		55°	225	1.753	17.51	6.46	0.00365	34.263	3103
			225	1.752	17.51	6.46	0.00373	34.272	3034
			225	1.753	17.52	6.46	0.00383	34.272	2957
			300	1.755	17.52	6.46	0.00383	34.362	2960
			300	1.754	17.53	6.46	0.00384	34.446	2951
			300	1.753	17.54	6.46	0.00384	34.586	2949
			325	1.753	17.51	6.46	0.00385	34.648	2941
			325	1.754	17.53	6.46	0.00385	34.992	2943
			325	1.753	17.52	6.46	0.00386	34.992	2934
			350	1.752	17.51	6.47	0.00387	35.028	2929
			350	1.74	17.53	6.47	0.00388	35.028	2901
			350	1.741	17.52	6.47	0.00389	35.1	2896
		65°	225	1.756	17.61	6.37	0.00361	34.256	3099
			225	1.754	17.61	6.37	0.00362	34.272	3086
			225	1.753	17.62	6.37	0.00363	34.272	3076
			300	1.753	17.62	6.37	0.00364	34.308	3068
			300	1.754	17.63	6.37	0.00365	34.308	3061
			300	1.753	17.64	6.37	0.00366	34.315	3051
			325	1.753	17.61	6.38	0.00367	34.318	3047
			325	1.752	17.63	6.38	0.00368	34.38	3037
			325	1.753	17.62	6.38	0.00369	34.38	3031
			350	1.755	17.61	6.38	0.0037	34.452	3026
			350	1.754	17.63	6.38	0.00371	34.452	3016
			350	1.752	17.62	6.38	0.00372	34.488	3005

8	Lime stone4	45°	225	1.837	18.41	6.34	0.00358	33.25	3253
			225	1.84	18.41	6.34	0.00359	34.272	3249
			225	1.839	18.42	6.34	0.00362	34.272	3221
			300	1.837	18.42	6.34	0.00363	34.282	3208
			300	1.836	18.43	6.34	0.00363	34.296	3207
			300	1.837	18.44	6.34	0.00365	34.308	3191
			325	1.839	18.41	6.35	0.00366	34.308	3191
			325	1.838	18.43	6.35	0.00367	34.38	3180
			325	1.836	18.42	6.35	0.00368	34.38	3168
			350	1.836	18.41	6.35	0.00369	34.452	3160
			350	1.837	18.43	6.35	0.0037	34.452	3153
			350	1.836	18.42	6.35	0.00371	34.488	3142
		50°	225	1.836	18.41	6.35	0.00359	34.215	3248
			225	1.834	18.41	6.35	0.00363	34.272	3208
			225	1.835	18.42	6.35	0.00364	34.272	3201
			300	1.837	18.42	6.35	0.00365	34.308	3196
			300	1.836	18.43	6.35	0.00366	34.308	3185
			300	1.835	18.44	6.35	0.00367	34.325	3175
			325	1.835	18.41	6.35	0.00368	34.336	3166
			325	1.836	18.43	6.35	0.00369	34.38	3160
			325	1.834	18.42	6.36	0.00371	34.38	3144
			350	1.834	18.41	6.36	0.00372	34.452	3136
			350	1.833	18.43	6.36	0.00373	34.452	3125
			350	1.833	18.42	6.36	0.00374	34.488	3117
		55°	225	1.835	18.41	6.36	0.00348	34.21	3354
			225	1.834	18.41	6.36	0.00356	34.272	3276
			225	1.833	18.42	6.36	0.00363	34.272	3212
			300	1.832	18.32	6.36	0.00363	34.308	3210
			300	1.833	18.33	6.36	0.00364	34.308	3203
			300	1.832	18.34	6.36	0.00365	34.315	3192
			325	1.832	18.31	6.36	0.00366	34.32	3183
			325	1.83	18.33	6.36	0.00367	34.38	3171
			325	1.831	18.32	6.37	0.00368	34.38	3169
			350	1.827	18.31	6.37	0.00369	34.452	3154
			350	1.826	18.33	6.37	0.0037	34.452	3144
			350	1.825	18.32	6.37	0.00371	34.488	3133
		65°	225	1.824	18.31	6.37	0.00361	34.222	3219
			225	1.825	18.31	6.37	0.00362	34.272	3211
			225	1.824	18.32	6.37	0.00363	34.273	3201
			300	1.824	18.32	6.37	0.00364	34.308	3192
			300	1.823	18.33	6.37	0.00365	34.308	3182
			300	1.823	18.34	6.37	0.00366	34.315	3173
			325	1.825	18.31	6.37	0.00367	34.326	3168
			325	1.824	18.33	6.37	0.00368	34.38	3157
			325	1.822	18.22	6.38	0.00369	34.38	3150
			350	1.822	18.21	6.38	0.0037	34.488	3142
			350	1.822	18.23	6.38	0.00371	34.524	3133
			350	1.821	18.22	6.38	0.00372	34.529	3123

9	Dolomite 1	45°	225	1.867	18.61	6.15	0.00349	33.559	3290
			225	1.867	18.61	6.15	0.0035	33.66	3281
			225	1.868	18.62	6.15	0.00351	33.66	3273
			300	1.869	18.62	6.16	0.00352	33.732	3271
			300	1.868	18.63	6.16	0.00353	33.732	3260
			300	1.867	18.64	6.17	0.00353	33.739	3263
			325	1.867	18.61	6.17	0.00354	33.759	3254
			325	1.868	18.63	6.18	0.00354	33.768	3261
			325	1.866	18.62	6.18	0.00355	33.768	3248
			350	1.866	18.61	6.18	0.00356	33.84	3239
			350	1.865	18.63	6.18	0.00357	33.84	3228
			350	1.866	18.62	6.19	0.00358	33.912	3226
		50°	225	1.868	18.71	6.19	0.00347	33.563	3332
			225	1.867	18.71	6.22	0.00348	33.66	3337
			225	1.866	18.72	6.23	0.00349	33.66	3331
			300	1.866	18.72	6.23	0.0035	33.732	3321
			300	1.867	18.73	6.23	0.00352	33.732	3304
			300	1.866	18.74	6.23	0.00353	33.756	3293
			325	1.866	18.71	6.24	0.00354	33.769	3289
			325	1.864	18.73	6.24	0.00355	33.771	3276
			325	1.865	18.72	6.24	0.00356	33.779	3269
			350	1.867	18.71	6.25	0.00362	33.84	3223
			350	1.866	18.73	6.25	0.00363	33.84	3213
			350	1.864	18.72	6.25	0.00364	33.912	3201
		55°	225	1.864	18.71	6.25	0.00351	33.012	3319
			225	1.865	18.71	6.25	0.00351	33.048	3321
			225	1.864	18.72	6.25	0.00352	33.048	3310
			300	1.864	18.72	6.25	0.00352	33.12	3310
			300	1.863	18.73	6.25	0.00353	33.129	3299
			300	1.864	18.74	6.25	0.00353	33.136	3300
			325	1.866	18.71	6.25	0.00354	33.139	3294
			325	1.865	18.73	6.25	0.00354	33.768	3293
			325	1.863	18.72	6.26	0.00355	33.768	3285
			350	1.863	18.71	6.26	0.00355	33.84	3285
			350	1.864	18.73	6.26	0.00356	33.84	3278
			350	1.863	18.72	6.26	0.00356	33.912	3276
		65°	225	1.863	18.71	6.26	0.00331	33.225	3523
			225	1.861	18.71	6.26	0.00332	33.226	3509
			225	1.862	18.72	6.26	0.00333	33.228	3500
			300	1.864	18.72	6.27	0.00334	33.229	3499
			300	1.863	18.73	6.27	0.00335	33.3	3487
			300	1.862	18.74	6.27	0.00338	33.36	3454
			325	1.862	18.71	6.27	0.00342	33.372	3414
			325	1.863	18.73	6.27	0.00343	33.372	3406
			325	1.861	19.92	6.27	0.00344	33.408	3392
			350	1.861	18.71	6.27	0.00345	33.495	3382
			350	1.86	18.73	6.27	0.00346	33.502	3371
			350	1.861	19.92	6.27	0.00346	33.52	3372

10	Dolomite 2	45°	225	1.968	19.61	6.12	0.00341	33.025	3532
			225	1.969	19.61	6.12	0.00342	33.048	3523
			225	1.968	19.62	6.13	0.00343	33.12	3517
			300	1.967	19.62	6.13	0.00344	33.128	3505
			300	1.968	19.63	6.13	0.00345	33.129	3497
			300	1.967	19.64	6.14	0.00346	33.192	3491
			325	1.967	19.61	6.14	0.00347	33.192	3481
			325	1.966	19.73	6.14	0.00348	33.228	3469
			325	1.967	19.72	6.14	0.00349	33.228	3461
			350	1.969	19.71	6.14	0.0035	33.256	3454
			350	1.967	19.73	6.14	0.00351	33.259	3441
			350	1.966	19.72	6.15	0.00352	33.286	3435
		50°	225	1.966	19.71	6.15	0.00336	33.192	3598
			225	1.967	19.71	6.15	0.00338	33.228	3579
			225	1.966	19.72	6.15	0.0034	33.228	3556
			300	1.966	19.72	6.15	0.00341	33.233	3546
			300	1.965	19.73	6.15	0.00341	33.356	3544
			300	1.966	19.74	6.15	0.00342	33.362	3535
			325	1.968	19.71	6.15	0.00343	33.375	3529
			325	1.966	19.73	6.16	0.00343	33.378	3531
			325	1.965	19.72	6.16	0.00344	33.379	3519
			350	1.965	19.71	6.16	0.00345	33.385	3509
			350	1.966	19.73	6.16	0.00346	33.389	3500
			350	1.965	19.72	6.16	0.00347	33.392	3488
		55°	225	1.965	19.71	6.16	0.00328	33.191	3690
			225	1.963	19.71	6.16	0.00332	33.192	3642
			225	1.964	19.72	6.16	0.00334	33.224	3622
			300	1.966	19.72	6.16	0.00336	33.226	3604
			300	1.965	19.73	6.17	0.00336	33.228	3608
			300	1.964	19.74	6.17	0.00337	33.232	3596
			325	1.964	19.71	6.17	0.00339	33.236	3575
			325	1.965	19.73	6.17	0.00341	33.338	3555
			325	1.963	19.72	6.17	0.00342	33.3339	3541
			350	1.963	19.71	6.17	0.00343	33.334	3531
			350	1.962	19.73	6.17	0.00344	33.3341	3519
			350	1.963	19.72	6.17	0.00345	33.3342	3511
		65°	225	1.965	19.71	6.17	0.00341	33.228	3555
			225	1.964	19.71	6.17	0.00341	33.229	3554
			225	1.963	19.72	6.17	0.00342	33.23	3541
			300	1.963	19.72	6.17	0.00342	33.231	3541
			300	1.964	19.73	6.18	0.00343	33.332	3539
			300	1.962	19.74	6.18	0.00343	33.333	3535
			325	1.962	19.71	6.18	0.00344	33.334	3525
			325	1.961	19.73	6.18	0.00344	33.354	3523
			325	1.962	19.72	6.18	0.00345	33.358	3515
			350	1.963	19.71	6.18	0.00346	33.368	3506
			350	1.962	19.73	6.18	0.00346	33.372	3504
			350	1.961	19.72	6.18	0.00347	33.372	3493

Table 3.5 Experimental Result for 55° attack angle with Different Pick Angles

SI No	Type of Rock	Pick Angle	rpm	Cutting Force	Torque	Depth of cut	Volume	Cutting rate	Specific Energy
				N	N-m	(mm)	(m ³)	(m ³ /sec)	(J/m ³)
1	2	3	4	5	6	7	8	9	10
1	Coal	45°	225	1.396	13.94	10.32	0.00941	54.72	1531
			225	1.397	13.93	10.32	0.00941	54.72	1532
			225	1.395	13.93	10.33	0.00942	54.73	1530
			300	1.393	13.93	10.33	0.00943	55.08	1526
			300	1.395	13.92	10.33	0.00944	55.08	1527
			300	1.393	13.92	10.33	0.00945	55.09	1523
			325	1.394	13.82	10.33	0.00946	55.44	1522
			325	1.391	13.82	10.34	0.00947	55.44	1519
			325	1.392	13.81	10.34	0.00948	55.45	1518
			350	1.395	13.81	10.34	0.00949	55.46	1520
			350	1.392	13.81	10.34	0.00951	55.8	1513
			350	1.391	13.81	10.34	0.00952	55.82	1511
		50°	225	1.39	13.81	10.34	0.00941	54.71	1527
			225	1.39	13.81	10.34	0.00942	54.72	1526
			225	1.389	13.82	10.35	0.00943	54.72	1525
			300	1.387	13.82	10.35	0.00944	54.73	1521
			300	1.386	13.83	10.35	0.00945	55.08	1518
			300	1.387	13.84	10.35	0.00946	55.08	1517
			325	1.389	13.81	10.35	0.00947	55.44	1518
			325	1.387	13.83	10.35	0.00948	55.44	1514
			325	1.386	13.82	10.35	0.00949	55.45	1512
			350	1.386	13.81	10.35	0.0095	55.46	1510
			350	1.387	13.83	10.35	0.00951	55.8	1510
			350	1.385	13.82	10.35	0.00952	55.8	1506
		55°	225	1.385	13.81	10.35	0.00941	54.71	1523
			225	1.384	13.81	10.36	0.00942	54.72	1522
			225	1.385	13.82	10.36	0.00943	54.72	1522
			300	1.387	13.82	10.36	0.00944	55.08	1522
			300	1.386	13.83	10.36	0.00945	55.08	1519
			300	1.384	13.84	10.36	0.00946	55.09	1516
			325	1.384	13.81	10.36	0.00947	55.44	1514
			325	1.385	13.83	10.36	0.00948	55.44	1514
			325	1.384	13.82	10.36	0.00949	55.45	1511
			350	1.384	13.81	10.36	0.0095	55.46	1509
			350	1.382	13.83	10.36	0.00951	55.8	1506
			350	1.383	13.82	10.36	0.00961	55.8	1491
		65°	225	1.385	13.81	10.36	0.00941	54.44	1525
			225	1.384	13.81	10.36	0.00942	54.72	1522
			225	1.383	13.82	10.37	0.00942	54.72	1522
			300	1.382	13.72	10.37	0.00943	55.08	1520
			300	1.383	13.73	10.37	0.00944	55.08	1519
			300	1.382	13.74	10.37	0.00945	55.44	1517
			325	1.382	13.71	10.37	0.00946	55.44	1515
			325	1.381	13.73	10.37	0.00947	55.45	1512
			325	1.382	13.72	10.37	0.00948	55.46	1512
350	1.383		13.71	10.37	0.00949	55.8	1511		
350	1.381		13.73	10.37	0.0095	55.8	1507		
350	1.38		13.72	10.37	0.00951	55.88	1505		

2	Sand stone 1	45°	225	1.483	14.81	8.11	0.00588	42.74	2045
			225	1.524	14.91	8.11	0.00589	42.75	2098
			225	1.493	14.92	8.12	0.0059	42.76	2055
			300	1.493	14.92	8.12	0.00591	42.77	2051
			300	1.492	14.93	8.13	0.00592	42.78	2049
			300	1.493	14.94	8.13	0.00592	42.79	2050
			325	1.494	14.91	8.13	0.00593	42.8	2048
			325	1.493	14.93	8.13	0.00594	42.81	2043
			325	1.492	14.92	8.14	0.00595	42.82	2041
			350	1.492	14.91	8.14	0.00595	42.83	2041
			350	1.492	14.93	8.14	0.00596	42.84	2038
			350	1.491	14.92	8.14	0.00596	42.86	2036
		50°	225	1.491	14.91	8.11	0.00585	42.22	2067
			225	1.49	14.91	8.14	0.00586	42.26	2070
			225	1.491	14.92	8.13	0.00587	42.28	2065
			300	1.493	14.92	8.15	0.00588	42.35	2069
			300	1.491	14.93	8.15	0.00589	43.39	2063
			300	1.49	14.94	8.15	0.0059	43.42	2058
			325	1.49	14.91	8.15	0.00591	43.48	2055
			325	1.491	14.93	8.16	0.00592	43.56	2055
			325	1.49	14.92	8.16	0.00593	43.56	2050
			350	1.49	14.91	8.17	0.00594	43.62	2049
			350	1.489	14.93	8.17	0.00595	43.88	2045
			350	1.489	14.92	8.16	0.00595	43.92	2042
			225	1.491	14.91	8.16	0.00591	42.22	2059
			225	1.489	14.91	8.16	0.00591	42.23	2056
			225	1.488	14.92	8.16	0.00592	43.24	2051
			300	1.488	14.92	8.16	0.00592	43.25	2051
			300	1.489	14.93	8.16	0.00593	43.29	2049
			300	1.488	14.94	8.17	0.00593	43.56	2050
			325	1.487	14.91	8.17	0.00594	43.56	2045
			325	1.486	14.93	8.17	0.00595	43.57	2040
			325	1.486	14.92	8.17	0.00595	43.58	2040
			350	1.488	14.91	8.17	0.00596	43.59	2040
			350	1.487	14.93	8.17	0.00601	43.92	2021
			350	1.486	14.92	8.17	0.00601	43.92	2020
		65°	225	1.485	14.91	8.17	0.0588	42.22	206.3
			225	1.486	14.91	8.17	0.00591	42.84	2054
			225	1.485	14.92	8.17	0.00591	42.84	2053
			300	1.485	14.92	8.18	0.00592	42.94	2052
			300	1.483	14.93	8.18	0.00593	43.21	2046
			300	1.484	14.94	8.18	0.00594	43.22	2044
			325	1.486	14.91	8.18	0.00594	43.56	2046
			325	1.485	14.83	8.18	0.00601	43.56	2021
			325	1.483	14.82	8.18	0.00601	43.58	2018
350	1.483		14.81	8.19	0.00602	43.62	2018		
350	1.484		14.83	8.19	0.00603	43.92	2016		
350	1.483		14.82	8.19	0.00604	43.92	2011		

3	Sand stone 2	45°	225	1.523	15.31	8.11	0.00584	42.56	2115
			225	1.522	15.31	8.12	0.00586	42.84	2109
			225	1.533	15.32	8.12	0.00589	42.84	2113
			300	1.535	15.32	8.13	0.00591	42.85	2112
			300	1.534	15.33	8.13	0.00591	43.2	2110
			300	1.533	15.34	8.14	0.00592	43.2	2108
			325	1.533	15.31	8.15	0.00592	43.21	2110
			325	1.534	15.33	8.16	0.00593	43.56	2111
			325	1.533	15.32	8.16	0.00594	43.56	2106
			350	1.533	15.31	8.15	0.00594	43.58	2103
			350	1.532	15.33	8.16	0.00596	43.92	2098
			350	1.533	15.32	8.16	0.00596	43.92	2099
		50°	225	1.535	15.31	8.13	0.0059	42.56	2115
			225	1.534	15.31	8.14	0.0059	42.84	2116
			225	1.533	15.32	8.14	0.0051	42.84	2447
			300	1.533	15.32	8.16	0.00591	43.2	2117
			300	1.534	15.33	8.14	0.00592	43.2	2109
			300	1.532	15.34	8.16	0.00592	43.21	2112
			325	1.532	15.31	8.17	0.00593	43.32	2111
			325	1.531	15.33	8.17	0.00593	43.56	2109
			325	1.532	15.32	8.18	0.00594	43.56	2110
			350	1.534	15.31	8.17	0.00594	43.65	2110
			350	1.533	15.33	8.19	0.00595	43.69	2110
			350	1.532	15.32	8.18	0.00595	43.92	2106
		55°	225	1.532	15.31	8.14	0.00591	42.84	2110
			225	1.533	15.31	8.15	0.00591	42.84	2114
			225	1.531	15.32	8.16	0.00592	43.2	2110
			300	1.531	15.42	8.15	0.00592	43.2	2108
			300	1.53	15.43	8.15	0.00593	43.25	2103
			300	1.53	15.44	8.16	0.00593	43.56	2105
			325	1.533	15.41	8.17	0.00594	43.56	2109
			325	1.532	15.43	8.16	0.00594	43.58	2105
			325	1.53	15.42	8.15	0.00595	43.75	2096
			350	1.53	15.41	8.17	0.00595	43.92	2101
			350	1.531	15.43	8.18	0.00596	43.92	2101
			350	1.529	15.42	8.18	0.00596	43.98	2099
		65°	225	1.528	15.31	8.17	0.0059	42.56	2116
			225	1.527	15.31	8.17	0.0059	42.84	2115
			225	1.527	15.32	8.18	0.00591	43.2	2114
			300	1.529	15.32	8.19	0.00591	43.2	2119
			300	1.527	15.33	8.18	0.00592	43.28	2110
			300	1.526	15.34	8.19	0.00593	43.56	2108
			325	1.525	15.41	8.18	0.00593	43.56	2104
			325	1.526	15.43	8.18	0.00601	43.58	2077
			325	1.524	15.42	8.19	0.00603	43.92	2070
			350	1.523	15.41	8.18	0.00603	43.92	2066
			350	1.522	15.43	8.18	0.00604	44.28	2061
			350	1.523	15.42	8.19	0.00604	44.28	2065

4	Sand stone 3	45°	225	1.541	15.41	7.8	0.0054	41.4	2226
			225	1.541	15.41	7.79	0.00541	41.4	2219
			225	1.54	15.42	7.79	0.00541	41.42	2217
			300	1.539	15.42	7.8	0.00542	41.42	2215
			300	1.54	15.43	7.81	0.00542	41.44	2219
			300	1.538	15.44	7.8	0.00543	41.46	2209
			325	1.538	15.41	7.82	0.00543	41.48	2215
			325	1.536	15.43	7.8	0.00544	41.76	2202
			325	1.537	15.42	7.82	0.00544	41.76	2209
			350	1.539	15.41	7.85	0.00551	41.77	2193
			350	1.537	15.43	7.82	0.00551	41.77	2181
			350	1.536	15.42	7.83	0.00553	42.12	2175
		50°	225	1.536	15.41	7.82	0.0055	41.02	2184
			225	1.537	15.41	7.83	0.00551	41.04	2184
			225	1.536	15.42	7.8	0.00551	41.04	2174
			300	1.536	15.42	7.84	0.00552	41.4	2182
			300	1.535	15.43	7.83	0.00552	41.4	2177
			300	1.535	15.44	7.85	0.00553	41.56	2179
			325	1.537	15.41	7.82	0.00553	41.76	2173
			325	1.536	15.43	7.83	0.00554	41.76	2171
			325	1.535	15.42	7.84	0.00554	41.83	2172
			350	1.535	15.41	7.85	0.00555	41.83	2171
			350	1.536	15.43	7.86	0.00555	42.12	2175
			350	1.535	15.42	7.87	0.00556	42.12	2173
		55°	225	1.535	15.41	7.83	0.00541	40.68	2222
			225	1.534	15.41	7.83	0.00541	40.68	2220
			225	1.535	15.42	7.84	0.00542	41.04	2220
			300	1.537	15.42	7.84	0.00542	41.4	2223
			300	1.536	15.43	7.84	0.00543	41.42	2218
			300	1.535	15.44	7.85	0.00543	41.52	2219
			325	1.534	15.41	7.85	0.00544	41.76	2214
			325	1.535	15.43	7.85	0.00545	41.76	2211
			325	1.534	15.42	7.85	0.00546	41.82	2205
			350	1.534	15.41	7.85	0.00557	41.88	2162
			350	1.533	15.43	7.86	0.00558	42.12	2159
			350	1.534	15.42	7.86	0.00558	42.12	2161
		65°	225	1.536	15.41	7.86	0.00551	41.12	2191
			225	1.535	15.41	7.86	0.00551	41.4	2190
			225	1.534	15.42	7.87	0.00552	41.4	2187
			300	1.534	15.42	7.87	0.00552	41.45	2187
			300	1.534	15.43	7.87	0.00553	41.45	2183
			300	1.533	15.44	7.87	0.00553	41.76	2182
			325	1.533	15.41	7.88	0.00554	42.12	2181
			325	1.532	15.43	7.88	0.00554	42.12	2179
			325	1.533	15.42	7.88	0.00555	42.38	2177
			350	1.535	15.41	7.88	0.00555	42.42	2179
			350	1.534	15.43	7.89	0.00556	42.48	2177
			350	1.533	15.42	7.89	0.00556	42.48	2175

5	Lime stone 1	45°	225	1.586	15.81	6.8	0.0041	35.64	2630
			225	1.588	15.81	6.8	0.00411	35.64	2627
			225	1.587	15.82	6.82	0.00411	35.65	2633
			300	1.587	15.82	6.82	0.00412	36	2627
			300	1.586	15.83	6.83	0.00412	36	2629
			300	1.586	15.84	6.82	0.00413	36.1	2619
			325	1.588	15.81	6.82	0.00414	36.36	2616
			325	1.587	15.83	6.82	0.00414	36.36	2614
			325	1.586	15.82	6.83	0.00422	36.46	2567
			350	1.586	15.81	6.82	0.00422	36.56	2563
			350	1.586	15.83	6.82	0.00423	36.62	2557
			350	1.585	15.82	6.83	0.00423	36.72	2559
		50°	225	1.585	15.71	6.8	0.0041	35.23	2629
			225	1.584	15.71	6.8	0.00411	35.64	2621
			225	1.585	15.82	6.82	0.00411	35.64	2630
			300	1.587	15.82	6.82	0.00412	36	2627
			300	1.586	15.83	6.83	0.00412	36	2629
			300	1.585	15.84	6.82	0.00413	36.36	2617
			325	1.585	15.81	6.82	0.00413	36.36	2617
			325	1.586	15.83	6.82	0.00414	36.38	2613
			325	1.585	15.82	6.83	0.00414	36.42	2615
			350	1.585	15.81	6.82	0.00422	36.44	2562
			350	1.584	15.83	6.82	0.00422	36.72	2560
			350	1.585	15.82	6.83	0.00425	36.72	2547
		55°	225	1.587	15.81	6.8	0.0041	35.64	2632
			225	1.585	15.81	6.82	0.00411	35.64	2630
			225	1.584	15.82	6.82	0.00411	35.65	2628
			300	1.584	15.82	6.82	0.00421	35.68	2566
			300	1.585	15.83	6.82	0.00421	36	2568
			300	1.584	15.84	6.83	0.00422	36	2564
			325	1.584	15.81	6.83	0.00422	36.36	2564
			325	1.583	15.83	6.83	0.00423	36.36	2556
			325	1.584	15.82	6.83	0.00423	36.45	2558
			350	1.586	15.81	6.83	0.00424	36.52	2555
			350	1.585	15.83	6.83	0.00425	36.72	2547
			350	1.584	15.82	6.83	0.00426	36.72	2540
		65°	225	1.583	15.81	6.86	0.0042	35.32	2586
			225	1.584	15.81	6.86	0.00421	35.64	2581
			225	1.583	15.82	6.87	0.00422	35.64	2577
			300	1.583	15.82	6.87	0.00422	36	2577
			300	1.582	15.83	6.88	0.00423	36	2573
			300	1.583	15.84	6.86	0.00423	36.36	2567
			325	1.585	15.81	6.87	0.00424	36.72	2568
			325	1.583	15.83	6.87	0.00424	36.72	2565
			325	1.582	15.82	6.88	0.00425	36.82	2561
			350	1.582	15.81	6.87	0.00426	36.82	2551
			350	1.582	15.83	6.87	0.00426	36.92	2551
			350	1.581	15.82	6.88	0.00427	37.08	2547

6	Lime stone 2	45°	225	1.653	16.41	6.52	0.00375	34.12	2874
			225	1.653	16.41	6.52	0.00379	34.2	2844
			225	1.654	16.42	6.53	0.0038	34.2	2842
			300	1.656	16.42	6.53	0.00381	34.56	2838
			300	1.655	16.43	6.54	0.00381	34.56	2841
			300	1.654	16.44	6.54	0.00382	34.62	2832
			325	1.654	16.41	6.55	0.00382	34.92	2836
			325	1.654	16.43	6.55	0.00383	34.92	2829
			325	1.653	16.42	6.55	0.00384	34.95	2820
			350	1.653	16.41	6.55	0.00385	34.98	2812
			350	1.652	16.43	6.55	0.00386	35.28	2803
			350	1.653	16.42	6.55	0.00387	35.28	2798
		50°	225	1.655	16.41	6.51	0.00345	34.35	3123
			225	1.654	16.41	6.52	0.00378	33.48	2853
			225	1.653	16.42	6.53	0.00379	33.84	2848
			300	1.653	16.42	6.53	0.0038	33.84	2841
			300	1.654	16.43	6.54	0.0038	34.2	2847
			300	1.653	16.44	6.55	0.00381	34.2	2842
			325	1.652	16.41	6.55	0.00381	34.22	2840
			325	1.651	16.53	6.55	0.00382	34.24	2831
			325	1.652	16.52	6.56	0.00382	34.26	2837
			350	1.654	16.41	6.55	0.00383	34.56	2829
			350	1.653	16.53	6.55	0.00385	34.56	2812
			350	1.652	16.52	6.56	0.00385	35.28	2815
		55°	225	1.652	16.41	6.42	0.00365	33.42	2906
			225	1.652	16.41	6.43	0.00367	33.48	2894
			225	1.651	16.42	6.42	0.00369	33.48	2872
			300	1.651	16.42	6.44	0.0037	33.84	2874
			300	1.65	16.43	6.43	0.00371	33.84	2860
			300	1.651	16.44	6.45	0.00371	34.2	2870
			325	1.653	16.51	6.44	0.00372	34.2	2862
			325	1.652	16.53	6.45	0.00372	34.23	2864
			325	1.651	16.52	6.46	0.00373	34.25	2859
			350	1.651	16.51	6.44	0.00373	34.25	2851
			350	1.652	16.53	6.45	0.00375	34.56	2841
			350	1.651	16.52	6.46	0.00375	34.56	2844
		65°	225	1.651	16.41	6.52	0.0038	34.12	2833
			225	1.65	16.41	6.52	0.00381	34.2	2824
			225	1.651	16.42	6.53	0.00381	34.2	2830
			300	1.652	16.42	6.53	0.00382	34.56	2824
			300	1.651	16.43	6.54	0.00382	34.56	2827
			300	1.65	16.54	6.54	0.00383	34.92	2817
			325	1.65	16.51	6.55	0.00383	34.92	2822
			325	1.651	16.53	6.54	0.00384	34.95	2812
			325	1.65	16.52	6.55	0.00385	34.95	2807
			350	1.65	16.51	6.55	0.00385	34.98	2807
			350	1.649	16.53	6.54	0.00386	35.28	2794
			350	1.649	16.52	6.55	0.00387	35.28	2791

7	Lime stone 3	45°	225	1.653	16.41	6.41	0.0037	33.12	2864
			225	1.658	16.41	6.42	0.00371	33.48	2869
			225	1.657	16.42	6.42	0.00371	33.84	2867
			300	1.657	16.42	6.42	0.00372	33.84	2860
			300	1.658	16.43	6.43	0.00372	34.2	2866
			300	1.657	16.54	6.43	0.00373	34.2	2856
			325	1.657	16.51	6.43	0.00375	34.22	2841
			325	1.656	16.53	6.43	0.00375	34.25	2839
			325	1.657	16.52	6.43	0.00376	34.56	2834
			350	1.658	16.51	6.44	0.00376	34.56	2840
			350	1.657	16.53	6.44	0.00377	34.92	2831
			350	1.656	16.52	6.44	0.00378	35.28	2821
		50°	225	1.656	16.41	6.44	0.0037	33.32	2882
			225	1.657	16.41	6.44	0.00371	33.48	2876
			225	1.656	16.52	6.44	0.00371	33.49	2875
			300	1.656	16.52	6.44	0.00373	33.84	2859
			300	1.655	16.53	6.45	0.00374	33.84	2854
			300	1.656	16.54	6.45	0.00375	34.2	2848
			325	1.658	16.51	6.45	0.00375	34.2	2852
			325	1.657	16.53	6.45	0.00376	34.25	2842
			325	1.655	16.52	6.45	0.00376	34.29	2839
			350	1.655	16.51	6.45	0.00377	34.56	2831
			350	1.656	16.53	6.45	0.00377	34.56	2833
			350	1.655	16.52	6.45	0.00379	35.64	2817
		55°	225	1.655	16.41	6.45	0.0038	34.2	2809
			225	1.654	16.41	6.46	0.00381	34.2	2804
			225	1.655	16.52	6.46	0.00381	34.25	2806
			300	1.657	16.52	6.46	0.00382	34.56	2802
			300	1.656	16.53	6.46	0.00382	34.56	2800
			300	1.654	16.54	6.46	0.00383	34.62	2790
			325	1.654	16.51	6.46	0.00384	34.92	2783
			325	1.655	16.53	6.46	0.00384	34.92	2784
			325	1.654	16.52	6.47	0.00385	34.98	2780
			350	1.654	16.51	6.47	0.00385	34.99	2780
			350	1.653	16.53	6.48	0.00386	35.28	2775
			350	1.653	16.52	6.48	0.00387	35.28	2768
		65°	225	1.655	16.51	6.52	0.00371	33.2	2909
			225	1.654	16.51	6.52	0.00371	33.48	2907
			225	1.653	16.52	6.53	0.00372	33.84	2902
			300	1.653	16.52	6.53	0.00372	33.84	2902
			300	1.653	16.53	6.54	0.00373	34.2	2898
			300	1.652	16.54	6.54	0.00373	34.2	2897
			325	1.652	16.51	6.54	0.00374	34.26	2889
			325	1.651	16.53	6.54	0.00374	34.56	2887
			325	1.652	16.52	6.55	0.00375	34.56	2885
			350	1.654	16.51	6.55	0.00376	34.62	2881
			350	1.652	16.53	6.55	0.00377	34.92	2870
			350	1.651	16.52	6.55	0.00378	35.28	2861

8	Lime stone 4	45°	225	1.726	17.31	6.41	0.00371	33.48	2982
			225	1.728	17.31	6.42	0.00371	33.49	2990
			225	1.727	17.32	6.43	0.00372	33.49	2985
			300	1.727	17.32	6.43	0.00372	33.84	2985
			300	1.726	17.33	6.44	0.00373	33.84	2980
			300	1.727	17.34	6.45	0.00373	33.95	2986
			325	1.729	17.31	6.45	0.00374	34.2	2982
			325	1.728	17.33	6.45	0.00374	34.2	2980
			325	1.727	17.32	6.46	0.00375	34.26	2975
			350	1.726	17.31	6.45	0.00375	34.29	2969
			350	1.727	17.33	6.45	0.00376	34.56	2963
			350	1.726	17.32	6.46	0.00376	34.56	2965
		50°	225	1.726	17.31	6.42	0.0037	33.28	2995
			225	1.725	17.31	6.43	0.00371	33.48	2990
			225	1.726	17.32	6.42	0.00371	33.48	2987
			300	1.728	17.32	6.44	0.00372	33.84	2991
			300	1.727	17.33	6.43	0.00372	33.84	2985
			300	1.726	17.34	6.45	0.00373	34.2	2985
			325	1.726	17.31	6.44	0.00373	34.2	2980
			325	1.727	17.33	6.45	0.00374	34.26	2978
			325	1.726	17.32	6.46	0.00374	34.29	2981
			350	1.726	17.31	6.44	0.00375	34.56	2964
			350	1.725	17.33	6.45	0.00376	34.56	2959
			350	1.726	17.32	6.46	0.00377	34.62	2958
		55°	225	1.728	17.31	6.42	0.0037	33.32	2998
			225	1.726	17.31	6.42	0.00371	33.48	2987
			225	1.725	17.32	6.43	0.00371	33.48	2990
			300	1.725	17.32	6.43	0.00372	33.52	2982
			300	1.726	17.33	6.44	0.00372	33.84	2988
			300	1.724	17.34	6.44	0.00373	33.84	2977
			325	1.724	17.31	6.45	0.00373	34.2	2981
			325	1.723	17.33	6.44	0.00374	34.2	2967
			325	1.724	17.32	6.45	0.00374	34.26	2973
			350	1.726	17.31	6.45	0.00375	34.29	2969
			350	1.725	17.33	6.44	0.00375	34.56	2962
			350	1.724	17.32	6.45	0.00376	34.56	2957
		65°	225	1.724	17.31	6.44	0.0029	33.42	3828
			225	1.725	17.31	6.43	0.003	33.84	3697
			225	1.724	17.32	6.44	0.00367	33.98	3025
			300	1.724	17.32	6.44	0.00369	34.2	3009
			300	1.723	17.33	6.45	0.0037	33.48	3004
			300	1.723	17.34	6.46	0.0037	33.84	3008
			325	1.725	17.31	6.46	0.00371	34.29	3004
			325	1.724	17.33	6.47	0.00371	34.2	3007
			325	1.723	17.32	6.48	0.00372	34.56	3001
			350	1.723	17.31	6.46	0.00373	33.48	2984
			350	1.724	17.33	6.47	0.00374	34.56	2982
			350	1.723	17.32	6.48	0.00378	34.67	2954

9	Dolomite 1	45°	225	1.763	17..51	6.22	0.0035	32.12	3133
			225	1.766	17..51	6.22	0.0035	32.42	3138
			225	1.767	17..52	6.23	0.00351	32.45	3136
			300	1.769	17..52	6.23	0.00351	32.76	3140
			300	1.768	17..53	6.24	0.00352	32.76	3134
			300	1.767	17..54	6.24	0.00353	33.12	3124
			325	1.767	17..51	6.25	0.00354	33.12	3120
			325	1.768	17..53	6.25	0.00354	33.16	3121
			325	1.767	17..52	6.25	0.00355	33.18	3111
			350	1.766	17..51	6.25	0.00355	33.48	3109
			350	1.765	17..51	6.25	0.00356	33.48	3099
		350	1.766	17..52	6.25	0.00358	33.58	3083	
		50°	225	1.768	17..52	6.23	0.00351	32.4	3138
			225	1.767	17..53	6.23	0.00351	32.4	3136
			225	1.766	17..54	6.24	0.00352	32.42	3131
			300	1.766	17..51	6.25	0.00352	32.76	3136
			300	1.767	17..53	6.25	0.00353	32.76	3129
			300	1.766	17..52	6.25	0.00353	33.12	3127
			325	1.766	17..51	6.26	0.00354	33.12	3123
			325	1.765	17..51	6.26	0.00355	33.26	3112
			325	1.766	17..52	6.27	0.00356	33.32	3110
			350	1.768	17..52	6.26	0.00357	33.48	3100
			350	1.766	17..53	6.26	0.00358	33.48	3088
		350	1.765	17..54	6.27	0.00359	33.62	3083	
		55°	225	1.765	17..51	6.25	0.00342	32.4	3226
			225	1.766	17..53	6.25	0.00346	32.4	3190
			225	1.765	17..52	6.26	0.00346	32.76	3193
			300	1.765	17.52	6.26	0.00348	33.12	3175
			300	1.764	17.53	6.26	0.00348	33.12	3173
			300	1.765	17.54	6.27	0.00349	33.16	3171
			325	1.766	17.51	6.27	0.00349	33.19	3173
			325	1.765	17.53	6.28	0.0035	33.23	3167
			325	1.764	17.52	6.28	0.0035	33.48	3165
			350	1.764	17.51	6.27	0.00351	33.48	3151
			350	1.765	17.53	6.28	0.00351	33.84	3158
		350	1.764	17.52	6.28	0.00352	33.84	3147	
		65°	225	1.764	17.51	6.25	0.00345	32.4	3196
			225	1.763	17.51	6.25	0.00346	32.4	3185
			225	1.764	17.52	6.26	0.00346	32.76	3192
			300	1.765	17.52	6.26	0.00348	33.12	3175
			300	1.764	17.53	6.26	0.00348	33.12	3173
			300	1.763	17.54	6.27	0.00349	33.16	3167
			325	1.763	17.51	6.28	0.00349	33.18	3172
			325	1.764	17.53	6.29	0.0035	33.29	3170
			325	1.763	17.52	6.29	0.00351	33.48	3159
350	1.763		17.51	6.28	0.00352	33.48	3145		
350	1.762		17.53	6.29	0.00354	33.84	3131		
350	1.763		17.52	6.29	0.00356	33.84	3115		

10	Dolomite 2	45°	225	1.875	18.61	6.22	0.00341	32.38	3420
			225	1.878	18.61	6.22	0.00342	32.4	3416
			225	1.877	18.62	6.23	0.00342	32.4	3419
			300	1.877	18.62	6.23	0.00343	32.42	3409
			300	1.878	18.63	6.24	0.00343	32.76	3417
			300	1.877	18.64	6.24	0.00344	32.76	3405
			325	1.877	18.61	6.25	0.00344	33.12	3410
			325	1.876	18.63	6.25	0.00345	33.12	3399
			325	1.877	18.62	6.25	0.00345	33.15	3400
			350	1.878	18.61	6.25	0.00346	33.19	3392
			350	1.877	18.63	6.25	0.00346	33.48	3391
			350	1.876	18.62	6.25	0.00348	33.48	3369
		50°	225	1.876	18.61	6.23	0.0034	32.4	3437
			225	1.877	18.61	6.23	0.00341	32.4	3429
			225	1.876	18.62	6.24	0.00342	32.42	3423
			300	1.876	18.62	6.25	0.00342	32.48	3428
			300	1.875	18.63	6.25	0.00343	32.76	3417
			300	1.876	18.64	6.25	0.00343	32.76	3418
			325	1.878	18.61	6.26	0.00344	33.12	3418
			325	1.877	18.63	6.26	0.00344	33.12	3416
			325	1.876	18.62	6.27	0.00345	33.16	3409
			350	1.876	18.61	6.26	0.00345	33.16	3404
			350	1.876	18.63	6.26	0.0035	33.48	3355
			350	1.875	18.62	6.27	0.00353	33.48	3330
		55°	225	1.875	18.61	6.25	0.00341	33.4	3437
			225	1.874	18.61	6.25	0.00341	32.4	3435
			225	1.875	18.62	6.26	0.00342	32.76	3432
			300	1.877	18.62	6.26	0.00342	32.76	3436
			300	1.876	18.63	6.26	0.00343	32.82	3424
			300	1.875	18.64	6.27	0.00343	33.12	3427
			325	1.874	18.61	6.27	0.00344	33.12	3416
			325	1.875	18.63	6.28	0.00344	33.48	3423
			325	1.874	18.62	6.28	0.00345	33.48	3411
			350	1.874	18.61	6.27	0.00345	33.56	3406
			350	1.873	18.63	6.28	0.0035	33.62	3361
			350	1.874	18.62	6.28	0.00356	33.84	3306
		65°	225	1.876	18.61	6.25	0.00351	32.76	3340
			225	1.875	18.61	6.25	0.00351	32.76	3339
			225	1.874	18.62	6.26	0.00352	32.85	3333
			300	1.873	18.62	6.26	0.00352	33.12	3331
			300	1.874	18.63	6.27	0.00353	33.12	3329
			300	1.873	18.64	6.27	0.00353	33.48	3327
			325	1.873	18.61	6.28	0.00354	33.48	3323
			325	1.872	18.63	6.28	0.00361	33.52	3257
			325	1.873	18.62	6.29	0.00362	33.56	3254
			350	1.875	18.61	6.28	0.00363	33.64	3244
			350	1.874	18.63	6.28	0.00365	33.84	3224
			350	1.873	18.62	6.29	0.00371	33.84	3176

Table3.6 Experimental Result for 65° attack angle with Different Pick Angles

SI No	Type of Rock	Pick Angle	rpm	Cutting Force	Torque	Depth of cut	Volume	Cutting rate	Specific Energy
				N	N-m	(mm)	Q(m ³)	(m ³ /sec)	(J/m ³)
1	2	3	4	5	6	7	8	9	10
1	Coal	45°	225	1.672	16.62	7.81	0.00548	40.068	2383
			225	1.671	16.63	7.81	0.00549	40.428	2377
			225	1.671	16.63	7.81	0.00551	40.428	2369
			300	1.669	16.63	7.81	0.00551	40.788	2366
			300	1.67	16.62	7.79	0.00552	40.788	2357
			300	1.669	16.62	7.8	0.00552	40.788	2358
			325	1.669	16.62	7.81	0.00553	41.292	2357
			325	1.667	16.62	7.82	0.00554	41.292	2353
			325	1.669	16.61	7.82	0.00555	41.328	2352
			350	1.668	16.61	7.81	0.00556	41.328	2343
			350	1.667	16.61	7.82	0.00557	41.76	2340
			350	1.666	16.61	7.82	0.00558	42.12	2335
		50°	225	1.667	16.61	7.83	0.0056	40.392	2331
			225	1.668	16.61	7.84	0.00561	40.752	2331
			225	1.667	16.62	7.84	0.00561	40.752	2330
			300	1.667	16.62	7.85	0.00562	41.112	2328
			300	1.666	16.63	7.85	0.00562	41.112	2327
			300	1.667	16.64	7.86	0.00563	41.112	2327
			325	1.668	16.61	7.86	0.00563	41.472	2329
			325	1.668	16.63	7.87	0.00564	41.508	2328
			325	1.667	16.62	7.88	0.00564	41.58	2329
			350	1.668	16.61	7.86	0.00565	41.58	2320
			350	1.666	16.63	7.87	0.00566	41.94	2317
			350	1.666	16.62	7.88	0.00567	42.3	2315
		55°	225	1.665	16.61	7.8	0.0055	40.14	2361
			225	1.667	16.61	7.82	0.00551	40.572	2366
			225	1.666	16.62	7.83	0.00551	40.572	2367
			300	1.666	16.62	7.82	0.00552	40.86	2360
			300	1.665	16.63	7.79	0.00552	40.932	2350
			300	1.666	16.64	7.8	0.00553	40.932	2350
			325	1.667	16.61	7.81	0.00553	41.292	2354
			325	1.666	16.63	7.82	0.00554	41.292	2352
			325	1.666	16.62	7.82	0.00555	41.4	2347
			350	1.665	16.61	7.81	0.00556	41.472	2339
			350	1.666	16.63	7.82	0.00558	41.868	2335
			350	1.666	16.62	7.82	0.00561	42.228	2322
		65°	225	1.666	16.61	7.83	0.0056	40.392	2329
			225	1.665	16.61	7.84	0.00561	40.752	2327
			225	1.666	16.62	7.87	0.00561	40.788	2337
			300	1.665	16.62	7.85	0.00562	41.112	2326
			300	1.664	16.63	7.88	0.00562	41.112	2333
			300	1.663	16.64	7.86	0.00563	41.148	2322
			325	1.665	16.61	7.87	0.00563	41.508	2327
			325	1.664	16.63	7.88	0.00564	41.508	2325
			325	1.664	16.62	7.89	0.00564	41.58	2328
			350	1.662	16.61	7.87	0.00565	41.58	2315
			350	1.662	16.63	7.88	0.00566	41.94	2314
			350	1.661	16.63	7.89	0.00567	42.3	2311

2	Sand stone 1	45°	225	1.699	16.91	6.42	0.0037	32.58	2948
			225	1.699	16.91	6.42	0.00371	32.94	2940
			225	1.698	17.92	6.43	0.00371	33.012	2943
			300	1.698	16.92	6.43	0.00372	33.3	2935
			300	1.699	17.93	6.43	0.00373	33.3	2929
			300	1.698	16.94	6.44	0.00373	33.372	2932
			325	1.697	16.91	6.44	0.00375	33.732	2914
			325	1.698	16.93	6.44	0.00381	33.84	2870
			325	1.697	16.92	6.45	0.00381	33.912	2873
			350	1.697	16.91	6.44	0.00382	33.912	2861
			350	1.695	16.93	6.44	0.00382	34.272	2858
			350	1.697	16.92	6.45	0.00383	34.668	2858
		50°	225	1.696	16.91	6.45	0.00381	32.76	2871
			225	1.696	16.91	6.45	0.00381	33.192	2871
			225	1.695	16.92	6.45	0.00382	33.192	2862
			300	1.696	16.92	6.45	0.00382	33.48	2864
			300	1.697	16.93	6.46	0.00383	33.552	2862
			300	1.696	16.94	6.46	0.00383	33.552	2861
			325	1.696	16.91	6.51	0.00384	33.948	2875
			325	1.695	16.93	6.52	0.00384	33.948	2878
			325	1.695	16.92	6.52	0.00385	34.02	2870
			350	1.696	16.91	6.51	0.00386	34.02	2860
			350	1.696	16.93	6.52	0.00387	34.452	2857
			350	1.695	16.92	6.52	0.00388	34.848	2848
		55°	225	1.696	16.91	6.52	0.00386	33.552	2865
			225	1.695	16.91	6.52	0.00391	33.84	2826
			225	1.694	16.92	6.52	0.00391	33.84	2825
			300	1.693	16.92	6.53	0.00392	34.2	2820
			300	1.695	16.93	6.53	0.00392	34.2	2824
			300	1.694	16.94	6.53	0.00393	34.272	2815
			325	1.694	16.91	6.53	0.00393	34.452	2815
			325	1.693	16.93	6.53	0.00394	34.452	2806
			325	1.694	16.92	6.54	0.00394	34.488	2812
			350	1.695	16.91	6.53	0.00395	34.488	2802
			350	1.694	16.93	6.53	0.00396	34.848	2793
			350	1.694	16.92	6.54	0.00397	35.208	2791
		65°	225	1.692	16.91	6.54	0.0039	33.3	2837
			225	1.693	16.91	6.54	0.00391	33.66	2832
			225	1.694	16.92	6.54	0.00391	33.732	2833
			300	1.694	16.92	6.54	0.00392	34.02	2826
			300	1.693	16.93	6.54	0.00392	34.02	2825
			300	1.694	16.94	6.55	0.00393	34.092	2823
			325	1.693	16.91	6.55	0.00393	34.452	2822
			325	1.692	16.83	6.58	0.00394	34.452	2826
			325	1.691	16.82	6.55	0.00394	34.488	2811
350	1.693		16.81	6.5	0.00395	34.488	2786		
350	1.691		16.83	6.55	0.00395	34.92	2804		
350	1.691	16.82	6.58	0.00396	35.28	2810			

3	Sand stone 2	45°	225	1.71	17.11	6.42	0.0037	32.688	2967
			225	1.718	17.21	6.42	0.00371	33.048	2973
			225	1.719	17.22	6.43	0.00371	33.048	2979
			300	1.717	17.22	6.43	0.00372	33.408	2968
			300	1.717	17.23	6.43	0.00372	33.408	2968
			300	1.715	17.24	6.44	0.00373	33.408	2961
			325	1.716	17.21	6.44	0.00373	33.84	2963
			325	1.717	17.23	6.44	0.00374	33.84	2957
			325	1.717	17.22	6.44	0.00374	33.912	2957
			350	1.716	17.21	6.44	0.00381	33.912	2901
			350	1.716	17.23	6.44	0.00381	34.272	2901
			350	1.715	17.22	6.44	0.00384	34.668	2876
		50°	225	1.715	17.21	6.45	0.0038	32.76	2911
			225	1.714	17.21	6.45	0.00381	33.192	2902
			225	1.716	17.22	6.45	0.00381	33.192	2905
			300	1.715	17.22	6.45	0.00382	33.48	2896
			300	1.715	17.23	6.45	0.00383	33.552	2888
			300	1.714	17.24	6.45	0.00383	33.552	2887
			325	1.715	17.21	6.46	0.00384	33.948	2885
			325	1.716	17.23	6.46	0.00384	33.948	2887
			325	1.714	17.22	6.46	0.00385	34.02	2876
			350	1.714	17.21	6.46	0.00385	34.02	2876
			350	1.713	17.23	6.46	0.00386	34.452	2867
			350	1.714	17.22	6.46	0.00388	34.848	2854
		55°	225	1.715	17.21	6.46	0.0038	32.832	2916
			225	1.715	17.21	6.47	0.00381	33.228	2912
			225	1.714	17.22	6.48	0.00381	33.228	2915
			300	1.715	17.22	6.51	0.00382	33.552	2923
			300	1.714	17.23	6.52	0.00382	33.588	2925
			300	1.714	17.24	6.52	0.00383	33.588	2918
			325	1.713	17.21	6.52	0.00383	34.02	2916
			325	1.715	17.23	6.53	0.00384	34.02	2916
			325	1.713	17.22	6.53	0.00384	34.092	2913
			350	1.713	17.21	6.52	0.00385	34.092	2901
			350	1.712	17.23	6.53	0.00385	34.488	2904
			350	1.713	17.22	6.53	0.00386	34.848	2898
		65°	225	1.714	17.21	6.53	0.0039	33.3	2870
			225	1.713	17.21	6.53	0.00391	33.732	2861
			225	1.713	17.22	6.54	0.00391	33.732	2865
			300	1.712	17.22	6.54	0.00392	34.02	2856
			300	1.713	17.23	6.54	0.00392	34.092	2858
			300	1.714	17.24	6.54	0.00393	34.092	2852
			325	1.713	17.11	6.54	0.00393	34.452	2851
			325	1.712	17.13	6.55	0.00394	34.452	2846
			325	1.713	17.12	6.55	0.00394	34.488	2848
350	1.712		17.21	6.56	0.00395	34.488	2843		
350	1.712		17.23	6.55	0.00396	34.848	2832		
350	1.71	17.12	6.57	0.00397	35.28	2830			

4	Sand stone 2	45°	225	1.734	17..31	5.8	0.003	29.232	3352
			225	1.733	17..31	5.81	0.00301	29.628	3345
			225	1.733	17.42	5.81	0.00301	29.628	3345
			300	1.731	17..32	5.82	0.00302	29.952	3336
			300	1.732	17..33	5.79	0.00302	29.988	3321
			300	1.733	17..34	5.8	0.00303	29.988	3317
			325	1.732	17..31	5.81	0.00303	30.42	3321
			325	1.732	17..31	5.82	0.00304	30.42	3316
			325	1.73	17.42	5.82	0.00304	30.528	3312
			350	1.731	17..32	5.81	0.00309	30.528	3255
			350	1.732	17..33	5.82	0.00313	30.96	3221
			350	1.731	17..34	5.82	0.00313	31.32	3219
		50°	225	1.73	17..31	5.83	0.0031	29.448	3254
			225	1.731	17..31	5.84	0.00311	29.808	3250
			225	1.73	17.42	5.84	0.00311	29.88	3249
			300	1.727	17.32	5.85	0.00312	30.168	3238
			300	1.726	17.33	5.85	0.00312	30.168	3236
			300	1.728	17.34	5.86	0.00313	30.24	3235
			325	1.727	17.31	5.86	0.00314	30.672	3223
			325	1.727	17.33	5.87	0.00315	30.672	3218
			325	1.725	17.32	5.88	0.00316	30.708	3210
			350	1.726	17.31	5.86	0.00318	30.78	3181
			350	1.726	17.33	5.87	0.00319	31.14	3176
			350	1.725	17.32	5.88	0.0032	31.5	3170
		55°	225	1.725	17.31	5.8	0.0031	29.232	3227
			225	1.722	17.21	5.82	0.00301	29.628	3330
			225	1.723	17.22	5.83	0.00301	29.628	3337
			300	1.724	17.32	5.82	0.00302	29.952	3322
			300	1.724	17.33	5.79	0.00302	29.988	3305
			300	1.723	17.34	5.8	0.00303	29.988	3298
			325	1.724	17.31	5.81	0.00303	30.42	3306
			325	1.723	17.33	5.82	0.00304	30.42	3299
			325	1.723	17.21	5.82	0.00305	30.528	3288
			350	1.721	17.21	5.81	0.00311	30.528	3215
			350	1.723	17.23	5.82	0.00311	30.96	3224
			350	1.722	17.22	5.82	0.00312	31.32	3212
		65°	225	1.722	17.21	5.86	0.0031	29.448	3255
			225	1.721	17.21	5.86	0.00311	29.88	3243
			225	1.722	17.22	5.85	0.00311	29.88	3239
			300	1.723	17.22	5.87	0.00312	30.168	3242
			300	1.722	17..21	5.85	0.00312	30.24	3229
			300	1.721	17.24	5.86	0.00313	30.24	3222
			325	1.72	17.21	5.87	0.00313	30.672	3226
			325	1.721	17.23	5.88	0.00314	30.672	3223
			325	1.722	17.22	5.89	0.00314	30.708	3230
			350	1.721	17.21	5.87	0.00315	30.708	3207
			350	1.72	17.23	5.88	0.00315	31.14	3211
			350	1.721	17.22	5.89	0.00316	31.5	3208

5	Lime stone1	45°	225	1.741	17.41	5.2	0.00241	26.028	3757
			225	1.741	17.41	5.21	0.00242	26.388	3748
			225	1.74	17.42	5.21	0.00242	26.46	3746
			300	1.741	17.42	5.22	0.00251	26.748	3621
			300	1.74	17.43	5.19	0.00251	26.748	3598
			300	1.739	17.44	5.2	0.00252	26.82	3588
			325	1.738	17.41	5.21	0.00252	27.18	3593
			325	1.739	17.43	5.22	0.00253	27.18	3588
			325	1.74	17.42	5.22	0.00254	27.288	3576
			350	1.739	17.41	5.21	0.00255	27.288	3553
			350	1.739	17.43	5.22	0.00256	27.72	3546
			350	1.738	17.42	5.22	0.00257	28.08	3530
		50°	225	1.738	17.41	5.23	0.0025	26.28	3636
			225	1.739	17.41	5.24	0.00251	26.64	3630
			225	1.739	17.42	5.24	0.00251	26.712	3630
			300	1.738	17.42	5.25	0.00252	27	3621
			300	1.739	17.43	5.25	0.00252	27	3623
			300	1.738	17.44	5.26	0.00253	27.072	3613
			325	1.737	17.41	5.26	0.00254	27.432	3597
			325	1.736	17.43	5.27	0.00254	27.468	3602
			325	1.738	17.42	5.28	0.00255	27.468	3599
			350	1.737	17.41	5.26	0.00256	27.468	3569
			350	1.737	17.43	5.27	0.00257	27.9	3562
			350	1.736	17.42	5.28	0.00258	28.26	3553
		55°	225	1.737	17.41	5.2	0.00251	26.1	3599
			225	1.738	17.41	5.22	0.00251	26.46	3614
			225	1.737	17.42	5.23	0.00252	26.532	3605
			300	1.736	17.42	5.22	0.00252	26.82	3596
			300	1.735	17.43	5.19	0.00253	26.82	3559
			300	1.736	17.44	5.2	0.00254	26.892	3554
			325	1.737	17.41	5.21	0.00255	27.252	3549
			325	1.736	17.43	5.22	0.00255	27.288	3554
			325	1.735	17.42	5.22	0.00256	27.36	3538
			350	1.736	17.41	5.21	0.00257	27.432	3519
			350	1.735	17.43	5.22	0.00258	27.792	3510
			350	1.734	17.42	5.22	0.00259	28.08	3495
		65°	225	1.732	17.41	5.23	0.0025	26.28	3623
			225	1.734	17.41	5.24	0.0025	26.712	3634
			225	1.733	17.42	5.25	0.00251	26.712	3625
			300	1.732	17.32	5.25	0.00251	27	3623
			300	1.731	17.33	5.25	0.00251	27.072	3621
			300	1.732	17.34	5.26	0.00252	27.072	3615
			325	1.733	17.31	5.27	0.00252	27.468	3624
			325	1.732	17.33	5.28	0.00253	27.468	3615
			325	1.731	17.32	5.29	0.00254	27.468	3605
			350	1.73	17.31	5.27	0.00254	27.54	3589
			350	1.731	17.33	5.28	0.00255	27.9	3584
			350	1.731	17.32	5.29	0.00256	28.26	3577

6	Lime stone 2	45°	225	1.753	17.51	5.2	0.0024	26.1	3798
			225	1.752	17.51	5.21	0.00241	26.46	3788
			225	1.753	17.52	5.21	0.00251	26.532	3639
			300	1.751	17.52	5.22	0.00252	26.82	3627
			300	1.751	17.53	5.19	0.00253	26.82	3592
			300	1.75	17.54	5.2	0.00254	26.892	3583
			325	1.752	17.51	5.21	0.00255	27.252	3580
			325	1.751	17.53	5.22	0.00256	27.252	3570
			325	1.751	17.52	5.22	0.00257	27.288	3557
			350	1.75	17.51	5.21	0.00257	27.288	3548
			350	1.75	17.53	5.22	0.00258	27.72	3541
			350	1.751	17.52	5.22	0.00259	28.08	3529
		50°	225	1.75	17.51	5.23	0.00251	26.352	3646
			225	1.749	17.51	5.24	0.00251	26.712	3651
			225	1.748	17.52	5.24	0.00252	26.712	3635
			300	1.749	17.52	5.25	0.00252	27.072	3644
			300	1.75	17.53	5.25	0.00253	27.072	3631
			300	1.75	17.54	5.26	0.00253	27.072	3638
			325	1.749	17.51	5.26	0.00254	27.432	3622
			325	1.75	17.53	5.27	0.00254	27.468	3631
			325	1.748	17.52	5.28	0.00255	27.468	3619
			350	1.747	17.51	5.26	0.00255	27.468	3604
			350	1.746	17.53	5.27	0.00256	27.9	3594
			350	1.748	17.52	5.28	0.00257	28.26	3591
		55°	225	1.747	17.51	5.2	0.00242	26.1	3754
			225	1.747	17.51	5.22	0.00245	26.46	3722
			225	1.746	17.52	5.23	0.0025	26.46	3653
			300	1.747	17.52	5.22	0.00251	26.82	3633
			300	1.748	17.53	5.19	0.00251	26.82	3614
			300	1.746	17.54	5.2	0.00252	26.82	3603
			325	1.746	17.51	5.21	0.00253	27.252	3596
			325	1.745	17.53	5.22	0.00253	27.252	3600
			325	1.745	17.52	5.22	0.00254	27.288	3586
			350	1.746	17.51	5.21	0.00255	27.288	3567
			350	1.746	17.53	5.22	0.00255	27.72	3574
			350	1.744	17.52	5.22	0.00256	28.08	3556
		65°	225	1.745	17.51	5.23	0.00251	26.28	3636
			225	1.743	17.51	5.24	0.00251	26.64	3639
			225	1.743	17.52	5.25	0.00252	26.712	3631
			300	1.742	17.52	5.25	0.00252	27	3629
			300	1.744	17.53	5.25	0.00253	27	3619
			300	1.743	17.54	5.26	0.00255	27.072	3595
			325	1.743	17.51	5.27	0.00255	27.432	3602
			325	1.741	17.43	5.28	0.00256	27.468	3591
			325	1.742	17.42	5.29	0.00256	27.468	3600
			350	1.742	17.41	5.27	0.00257	27.468	3572
			350	1.74	17.43	5.28	0.00258	27.9	3561
			350	1.74	17.42	5.29	0.00259	28.26	3554

7	Lime stone 3	45°	225	1.76	17.61	5.1	0.0024	25.56	3740
			225	1.761	17.61	5.11	0.00241	25.92	3734
			225	1.762	17.62	5.11	0.00241	25.92	3736
			300	1.76	17.62	5.12	0.00242	26.28	3724
			300	1.759	17.63	5.09	0.00242	26.28	3700
			300	1.76	17.64	5.1	0.00243	26.28	3694
			325	1.759	17.61	5.11	0.00244	26.712	3684
			325	1.759	17.63	5.12	0.00245	26.712	3676
			325	1.757	17.62	5.12	0.00245	26.748	3672
			350	1.759	17.61	5.11	0.00246	26.748	3654
			350	1.758	17.63	5.12	0.00247	27.18	3644
			350	1.757	17.62	5.12	0.00248	27.54	3627
		50°	225	1.756	17.61	5.13	0.0024	25.56	3753
			225	1.757	17.61	5.14	0.00241	25.992	3747
			225	1.758	17.62	5.14	0.00241	25.992	3749
			300	1.757	17.62	5.15	0.00243	26.28	3724
			300	1.757	17.63	5.15	0.00245	26.352	3693
			300	1.756	17.64	5.16	0.00245	26.352	3698
			325	1.757	17.61	5.16	0.00246	26.748	3685
			325	1.758	17.63	5.17	0.00246	26.82	3695
			325	1.757	17.62	5.18	0.00247	26.82	3685
			350	1.756	17.61	5.16	0.00248	26.928	3654
			350	1.757	17.63	5.17	0.00249	27.36	3648
			350	1.756	17.62	5.18	0.00249	27.72	3653
		55°	225	1.756	17.61	5.1	0.0024	25.56	3732
			225	1.755	17.61	5.12	0.00241	25.992	3728
			225	1.757	17.62	5.13	0.00241	25.992	3740
			300	1.756	17.62	5.12	0.00242	26.28	3715
			300	1.756	17.63	5.09	0.00242	26.352	3693
			300	1.755	17.64	5.1	0.00243	26.352	3683
			325	1.756	17.61	5.11	0.00243	26.748	3693
			325	1.757	17.63	5.12	0.00244	26.748	3687
			325	1.755	17.62	5.12	0.00244	26.82	3683
			350	1.755	17.61	5.11	0.00245	26.82	3660
			350	1.754	17.63	5.12	0.00246	27.252	3651
			350	1.755	17.62	5.12	0.00247	27.612	3638
		65°	225	1.756	17.61	5.13	0.00241	25.74	3738
			225	1.756	17.61	5.14	0.00241	26.1	3745
			225	1.755	17.62	5.15	0.00243	26.1	3719
			300	1.756	17.62	5.15	0.00243	26.46	3722
			300	1.754	17.63	5.15	0.00244	26.46	3702
			300	1.754	17.64	5.16	0.00244	26.46	3709
			325	1.753	17.61	5.17	0.00245	26.82	3699
			325	1.755	17.63	5.18	0.00245	26.928	3711
			325	1.754	17.62	5.18	0.00246	26.928	3693
			350	1.754	17.61	5.17	0.00247	26.928	3671
			350	1.753	17.63	5.18	0.00248	27.36	3662
			350	1.753	17.62	5.19	0.00249	27.72	3654

8	Lime stone 4	45°	225	1.898	18.91	5.1	0.00241	25.56	4017
			225	1.897	18.91	5.11	0.00241	25.92	4022
			225	1.897	18.92	5.11	0.00242	25.92	4006
			300	1.896	18.92	5.12	0.00242	26.28	4011
			300	1.897	18.93	5.09	0.00243	26.28	3974
			300	1.897	18.84	5.1	0.00243	26.28	3981
			325	1.897	18.81	5.11	0.00244	26.712	3973
			325	1.896	18.93	5.12	0.00244	26.712	3978
			325	1.897	18.92	5.12	0.00245	26.748	3964
			350	1.896	18.91	5.11	0.00246	26.748	3938
			350	1.896	18.93	5.12	0.00247	27.18	3930
			350	1.895	18.92	5.12	0.00248	27.54	3912
		50°	225	1.897	18.91	5.13	0.0024	25.668	4055
			225	1.896	18.91	5.14	0.00241	26.028	4044
			225	1.896	18.92	5.13	0.00241	26.1	4036
			300	1.895	18.92	5.14	0.00242	26.388	4025
			300	1.896	18.93	5.14	0.00242	26.388	4027
			300	1.896	18.84	5.15	0.00242	26.46	4035
			325	1.895	18.81	5.15	0.00243	26.82	4016
			325	1.895	18.93	5.16	0.00243	26.892	4024
			325	1.894	18.92	5.16	0.00244	26.892	4005
			350	1.895	18.91	5.17	0.00244	26.892	4015
			350	1.896	18.93	5.18	0.00245	27.288	4009
			350	1.896	18.92	5.16	0.00245	27.648	3993
		55°	225	1.895	18.91	5.1	0.0024	25.632	4027
			225	1.895	18.81	5.12	0.00241	26.028	4026
			225	1.894	18.82	5.13	0.00241	26.028	4032
			300	1.894	18.82	5.12	0.00242	26.352	4007
			300	1.893	18.93	5.09	0.00242	26.388	3982
			300	1.895	18.94	5.1	0.00243	26.388	3977
			325	1.893	18.81	5.11	0.00243	26.82	3981
			325	1.893	18.93	5.12	0.00244	26.82	3972
			325	1.892	18.92	5.12	0.00244	26.892	3970
			350	1.892	18.81	5.11	0.00245	26.892	3946
			350	1.893	18.83	5.12	0.00246	27.288	3940
			350	1.89	18.82	5.12	0.00247	27.648	3918
		65°	225	1.89	18.81	5.17	0.0024	25.668	4071
			225	1.887	18.81	5.18	0.00241	26.1	4056
			225	1.888	18.82	5.15	0.00241	26.1	4035
			300	1.888	18.82	5.15	0.00242	26.388	4018
			300	1.888	18.83	5.15	0.00242	26.46	4018
			300	1.886	18.84	5.16	0.00243	26.46	4005
			325	1.887	18.81	5.17	0.00243	26.892	4015
			325	1.886	18.83	5.18	0.00244	26.892	4004
			325	1.884	18.82	5.19	0.00244	26.928	4007
			350	1.882	18.81	5.17	0.00245	26.928	3971
			350	1.884	18.83	5.18	0.00245	27.36	3983
			350	1.881	18.72	5.19	0.00246	27.72	3968

9	Dolomite 1	45°	225	1.897	18.91	4.8	0.00211	23.94	4315
			225	1.896	18.91	4.81	0.00211	24.3	4322
			225	1.897	18.92	4.81	0.00212	24.372	4304
			300	1.898	18.92	4.82	0.00212	24.66	4315
			300	1.897	18.93	4.79	0.00213	24.66	4266
			300	1.896	18.84	4.8	0.00213	24.732	4273
			325	1.895	18.81	4.81	0.00214	25.092	4259
			325	1.896	18.93	4.82	0.00215	25.092	4251
			325	1.897	18.92	4.82	0.00216	25.128	4233
			350	1.897	18.91	4.81	0.00217	25.128	4205
			350	1.896	18.93	4.82	0.00217	25.56	4211
			350	1.897	18.92	4.82	0.00218	25.92	4194
		50°	225	1.896	18.91	4.83	0.00211	24.3	4340
			225	1.896	18.91	4.84	0.00211	24.66	4349
			225	1.895	18.92	4.84	0.00212	24.732	4326
			300	1.897	18.92	4.85	0.00212	25.02	4340
			300	1.896	18.93	4.85	0.00213	25.02	4317
			300	1.895	18.84	4.86	0.00213	25.092	4324
			325	1.894	18.81	4.86	0.00214	25.452	4301
			325	1.895	18.93	4.87	0.00214	25.452	4312
			325	1.896	18.92	4.88	0.00215	25.488	4303
			350	1.895	18.91	4.86	0.00216	25.488	4264
			350	1.895	18.93	4.87	0.00217	25.92	4253
			350	1.894	18.92	4.88	0.00221	26.28	4182
		55°	225	1.895	18.91	4.8	0.00211	23.94	4311
			225	1.895	18.81	4.82	0.00211	24.372	4329
			225	1.895	18.82	4.83	0.00212	24.372	4317
			300	1.894	18.82	4.82	0.00212	24.66	4306
			300	1.907	19.13	4.79	0.00213	24.732	4289
			300	1.906	19.14	4.8	0.00214	24.732	4275
			325	1.906	19.11	4.81	0.00215	25.128	4264
			325	1.902	19.13	4.82	0.00216	25.128	4244
			325	1.904	19.12	4.82	0.00217	25.2	4229
			350	1.902	18.91	4.81	0.00218	25.2	4197
			350	1.902	18.93	4.82	0.00219	25.632	4186
			350	1.901	19.12	4.82	0.00219	25.992	4184
		65°	225	1.9	18.91	4.83	0.00211	24.372	4349
			225	1.901	18.91	4.84	0.00212	24.732	4340
			225	1.9	18.92	4.85	0.00213	24.768	4326
			300	1.9	18.92	4.85	0.00214	25.092	4306
			300	1.898	18.93	4.85	0.00215	25.092	4282
			300	1.899	18.94	4.86	0.00216	25.128	4273
			325	1.9	18.91	4.87	0.00217	25.488	4264
			325	1.9	18.93	4.88	0.00218	25.488	4253
			325	1.899	18.92	4.89	0.00219	25.56	4240
			350	1.9	18.91	4.87	0.0022	25.56	4206
			350	1.898	18.93	4.88	0.00221	25.992	4191
			350	1.898	18.92	4.89	0.00221	26.352	4200

10	Dolomite 2	45°	225	2.089	20.21	4.6	0.0019	22.968	5058
			225	2.091	20.21	4.61	0.00191	23.4	5047
			225	2.09	20.22	4.61	0.00191	23.4	5044
			300	2.086	20.22	4.62	0.00192	23.688	5019
			300	2.085	20.23	4.59	0.00192	23.76	4984
			300	2.084	20.24	4.6	0.00193	23.76	4967
			325	2.085	20.21	4.61	0.00193	24.192	4980
			325	2.082	20.13	4.62	0.00194	24.228	4958
			325	2.078	20.12	4.62	0.00194	24.3	4949
			350	2.077	20.11	4.61	0.00195	24.3	4910
			350	2.078	20.13	4.62	0.00201	24.768	4776
			350	2.079	20.12	4.62	0.00201	25.128	4779
		50°	225	2.079	20.11	4.63	0.00201	23.04	4789
			225	2.077	20.11	4.64	0.00201	23.472	4795
			225	2.077	20.12	4.64	0.00202	23.472	4771
			300	2.076	20.12	4.65	0.00202	23.76	4779
			300	2.076	20.13	4.65	0.00203	23.832	4755
			300	2.075	20.14	4.66	0.00203	23.832	4763
			325	2.077	20.11	4.66	0.00204	24.192	4745
			325	2.075	20.13	4.67	0.00205	24.228	4727
			325	2.074	20.12	4.68	0.00206	24.228	4712
			350	2.071	20.11	4.66	0.00207	24.228	4662
			350	2.07	20.13	4.67	0.00208	24.66	4648
			350	2.071	20.12	4.68	0.00209	25.02	4637
		55°	225	2.07	20.11	4.6	0.00191	22.968	4985
			225	2.069	20.11	4.62	0.00191	23.328	5005
			225	2.068	20.12	4.63	0.00192	23.4	4987
			300	2.069	20.12	4.62	0.00192	23.688	4979
			300	2.07	20.13	4.59	0.00193	23.688	4923
			300	2.07	20.14	4.6	0.00194	23.76	4908
			325	2.068	20.11	4.61	0.00195	24.192	4889
			325	2.069	20.13	4.62	0.00195	24.192	4902
			325	2.068	20.12	4.62	0.00196	24.228	4875
			350	2.068	20.11	4.61	0.00198	24.228	4815
			350	2.066	20.13	4.62	0.00199	24.66	4796
			350	2.068	20.12	4.62	0.00201	25.02	4753
		65°	225	2.067	20.11	4.63	0.00201	22.968	4761
			225	2.066	20.11	4.64	0.00201	23.4	4769
			225	2.065	20.12	4.65	0.00202	23.4	4754
			300	2.066	20.12	4.65	0.00202	23.688	4756
			300	2.067	20.13	4.65	0.00203	23.76	4735
			300	2.066	20.14	4.66	0.00204	23.76	4719
			325	2.066	20.11	4.67	0.00204	24.192	4730
			325	2.064	20.13	4.68	0.00205	24.192	4712
			325	2.065	20.12	4.69	0.00206	24.228	4701
			350	2.065	20.11	4.67	0.00207	24.228	4659
			350	2.063	20.13	4.68	0.00208	24.66	4642
			350	2.064	20.12	4.69	0.00209	25.02	4632

Table3.7 Experimental Result for 45° attack angle with 5mm wear for all Pick angles

SI No	Type of Rock	Pick Angle	rpm	Cutting Force	Torque	Depth of cut	Volume	Cutting rate	Specific Energy
				N	N-m	(mm)	Q(m ³)	(m ³ /sec)	(J/m ³)
1	2	3	4	5	6	7	8	9	10
1	Coal	45°	225	1.729	17.34	6.52	0.00375	34.02	3006
			225	1.728	17.33	6.52	0.00389	34.092	2896
			225	1.728	17.33	6.53	0.00391	34.38	2886
			300	1.727	17.33	6.53	0.00391	34.452	2884
			300	1.728	17.32	6.54	0.00392	34.452	2883
			300	1.726	17.32	6.54	0.00392	34.74	2880
			325	1.727	17.32	6.51	0.00393	34.812	2861
			325	1.725	17.32	6.54	0.00393	34.812	2871
			325	1.727	17.31	6.55	0.00394	34.814	2871
			350	1.726	17.31	6.55	0.00394	34.816	2869
			350	1.726	17.31	6.54	0.00395	35.1	2858
			350	1.725	17.31	6.55	0.00396	35.172	2853
		50°	225	1.726	17.31	6.51	0.0039	33.948	2881
			225	1.727	17.31	6.52	0.00391	34.02	2880
			225	1.726	17.32	6.53	0.00391	34.092	2883
			300	1.725	17.32	6.53	0.00392	34.308	2874
			300	1.724	17.33	6.53	0.00392	34.452	2872
			300	1.725	17.34	6.54	0.00393	34.74	2871
			325	1.726	17.31	6.54	0.00393	34.74	2872
			325	1.726	17.33	6.55	0.00394	34.812	2869
			325	1.725	17.32	6.55	0.00394	34.812	2868
			350	1.726	17.31	6.54	0.00395	35.1	2858
			350	1.725	17.33	6.55	0.00396	35.172	2853
			350	1.725	17.32	6.55	0.00397	35.172	2846
		55°	225	1.724	17.31	6.42	0.00371	33.48	2983
			225	1.726	17.31	6.43	0.00371	33.552	2991
			225	1.725	17.32	6.42	0.00372	33.84	2977
			300	1.725	17.32	6.44	0.00372	33.84	2986
			300	1.724	17.33	6.43	0.00373	33.948	2972
			300	1.725	17.34	6.45	0.00381	34.2	2920
			325	1.726	17.31	6.44	0.00381	34.2	2917
			325	1.725	17.33	6.45	0.00382	34.272	2913
			325	1.725	17.32	6.46	0.00382	34.272	2917
			350	1.723	17.31	6.44	0.00383	34.308	2897
			350	1.724	17.33	6.45	0.00383	34.56	2903
			350	1.725	17.32	6.46	0.00384	34.632	2902
		65°	225	1.725	17.31	6.52	0.00387	34.02	2906
			225	1.724	17.31	6.54	0.00387	34.128	2913
			225	1.725	17.32	6.53	0.00388	34.128	2903
			300	1.724	17.32	6.55	0.00388	34.452	2910
			300	1.724	17.33	6.54	0.00389	34.452	2898
			300	1.723	17.34	6.54	0.00391	34.74	2882
			325	1.725	17.31	6.55	0.00391	34.74	2890
			325	1.723	17.33	6.54	0.00392	34.812	2875
			325	1.723	17.32	6.55	0.00392	34.848	2879
			350	1.722	17.31	6.55	0.00393	35.172	2870
			350	1.723	17.33	6.54	0.00393	35.28	2867
			350	1.724	17.32	6.55	0.00394	38.751	2866

2	Sand stone 1	45°	225	1.827	18.31	5.79	0.003	29.952	3526
			225	1.827	18.31	5.79	0.00301	29.988	3514
			225	1.826	18.42	5.8	0.00301	29.988	3519
			300	1.827	18.32	5.8	0.00302	30.312	3509
			300	1.828	18.33	5.8	0.00302	30.42	3511
			300	1.827	18.34	5.8	0.00303	30.6	3497
			325	1.826	18.31	5.81	0.00303	30.6	3501
			325	1.827	18.33	5.81	0.00304	30.672	3492
			325	1.826	18.32	5.81	0.00308	30.78	3445
			350	1.826	18.31	5.81	0.00309	30.852	3433
			350	1.825	18.33	5.81	0.00397	31.032	2671
			350	1.826	18.32	5.81	0.00398	31.14	2666
		50°	225	1.825	18.31	5.81	0.00306	30.06	3465
			225	1.825	18.31	5.82	0.00308	30.168	3449
			225	1.824	18.32	5.82	0.00309	30.168	3435
			300	1.825	18.32	5.82	0.00311	30.42	3415
			300	1.826	18.33	5.82	0.00311	30.492	3417
			300	1.825	18.34	5.82	0.00312	30.708	3404
			325	1.825	18.31	5.82	0.00312	30.708	3404
			325	1.823	18.33	5.82	0.00313	30.78	3390
			325	1.824	18.32	5.83	0.00313	30.852	3397
			350	1.824	18.31	5.82	0.00314	30.96	3381
			350	1.824	18.33	5.82	0.00314	31.14	3381
			350	1.823	18.32	5.83	0.00316	31.248	3363
		55°	225	1.824	18.31	5.83	0.00305	30.06	3487
			225	1.823	18.31	5.83	0.00307	30.24	3462
			225	1.823	18.32	5.84	0.00308	30.42	3457
			300	1.822	18.32	5.84	0.00309	30.492	3444
			300	1.824	18.33	5.84	0.00309	30.708	3447
			300	1.823	18.34	5.85	0.00311	30.78	3429
			325	1.823	18.31	5.85	0.00311	30.852	3429
			325	1.822	18.33	5.85	0.00312	30.852	3416
			325	1.823	18.32	5.85	0.00312	30.888	3418
			350	1.823	18.21	5.85	0.00313	31.068	3407
			350	1.822	18.23	5.85	0.00313	31.14	3405
			350	1.822	18.22	5.85	0.00314	31.32	3394
		65°	225	1.821	18.21	5.85	0.00305	30.24	3493
			225	1.822	18.21	5.86	0.00307	30.312	3478
			225	1.823	18.22	5.86	0.00308	30.492	3468
			300	1.823	18.22	5.86	0.00309	30.6	3457
			300	1.822	18.23	5.87	0.00309	30.78	3461
			300	1.822	18.24	5.87	0.0031	31.032	3450
			325	1.821	18.21	5.88	0.00311	31.032	3443
			325	1.821	18.23	5.88	0.00312	31.068	3432
			325	1.82	18.22	5.89	0.00313	31.14	3425
			350	1.821	18.21	5.88	0.00314	31.392	3410
			350	1.82	18.23	5.88	0.00316	31.428	3387
			350	1.82	18.22	5.89	0.00318	31.572	3371

3	Sand stone 2	45°	225	1.844	18.41	5.19	0.00241	26.82	3971
			225	1.845	18.41	5.19	0.00241	26.82	3973
			225	1.846	18.42	5.2	0.00244	27.108	3934
			300	1.844	18.52	5.2	0.00244	27.18	3930
			300	1.844	18.53	5.2	0.00245	27.252	3914
			300	1.843	18.44	5.2	0.00245	27.54	3912
			325	1.844	18.41	5.21	0.00251	27.54	3828
			325	1.844	18.53	5.21	0.00251	27.59	3828
			325	1.842	18.52	5.21	0.00252	27.612	3808
			350	1.843	18.51	5.21	0.00253	27.612	3795
			350	1.844	18.53	5.21	0.00253	27.828	3797
			350	1.843	18.52	5.21	0.00254	27.972	3780
		50°	225	1.843	18.51	5.21	0.00239	26.892	4018
			225	1.842	18.41	5.22	0.00239	27	4023
			225	1.844	18.42	5.22	0.0024	27.252	4011
			300	1.842	18.42	5.22	0.00241	27.252	3990
			300	1.842	18.43	5.22	0.00241	27.288	3990
			300	1.841	18.44	5.22	0.00243	27.612	3955
			325	1.842	18.41	5.22	0.00243	27.612	3957
			325	1.843	18.43	5.22	0.00244	27.648	3943
			325	1.842	18.42	5.23	0.00244	27.72	3948
			350	1.842	18.41	5.22	0.00246	27.972	3909
			350	1.841	18.43	5.22	0.00247	27.972	3891
			350	1.842	18.42	5.23	0.00249	28.152	3869
		55°	225	1.843	18.41	5.23	0.00239	27.072	4033
			225	1.842	18.41	5.23	0.00239	27.072	4031
			225	1.841	18.42	5.24	0.0024	27.36	4020
			300	1.842	18.42	5.24	0.0024	27.36	4022
			300	1.841	18.43	5.24	0.00241	27.468	4003
			300	1.841	18.44	5.25	0.00241	27.642	4010
			325	1.84	18.41	5.25	0.00243	27.72	3975
			325	1.841	18.43	5.25	0.00243	27.72	3977
			325	1.84	18.42	5.25	0.00244	27.792	3959
			350	1.84	18.41	5.25	0.00244	27.792	3959
			350	1.839	18.43	5.25	0.00245	28.152	3941
			350	1.84	18.42	5.25	0.00245	28.288	3943
		65°	225	1.841	18.41	5.25	0.00241	27.072	4010
			225	1.839	18.41	5.26	0.00241	27.18	4014
			225	1.839	18.42	5.26	0.00242	27.18	3997
			300	1.837	18.42	5.26	0.00242	27.468	3993
			300	1.838	18.43	5.27	0.00243	27.468	3986
			300	1.838	18.44	5.27	0.00243	27.792	3986
			325	1.838	18.41	5.28	0.00244	27.828	3977
			325	1.837	18.43	5.28	0.00244	27.828	3975
			325	1.838	18.42	5.29	0.00245	27.9	3969
			350	1.836	18.41	5.28	0.00249	27.972	3893
			350	1.836	18.43	5.28	0.0025	28.188	3878
			350	1.834	18.42	5.29	0.00252	28.26	3850

4	Sand stone 2	45°	225	1.852	18.51	5.19	0.00241	26.712	3988
			225	1.851	18.51	5.19	0.00242	26.892	3970
			225	1.851	18.52	5.2	0.00242	26.892	3977
			300	1.85	18.52	5.2	0.00243	27.068	3959
			300	1.851	18.53	5.2	0.00243	27.072	3961
			300	1.851	18.54	5.2	0.00244	27.18	3945
			325	1.85	18.51	5.21	0.00244	27.36	3950
			325	1.85	18.53	5.21	0.00245	27.432	3934
			325	1.849	18.52	5.21	0.00245	27.432	3932
			350	1.849	18.51	5.21	0.00246	27.468	3916
			350	1.85	18.53	5.21	0.00246	27.54	3918
			350	1.848	18.52	5.21	0.00248	27.828	3882
		50°	225	1.847	18.51	5.21	0.00251	26.892	3834
			225	1.848	18.51	5.22	0.00251	26.928	3843
			225	1.847	18.52	5.22	0.00252	27.072	3826
			300	1.847	18.52	5.22	0.00252	27.252	3826
			300	1.846	18.53	5.22	0.00253	27.36	3809
			300	1.848	18.54	5.22	0.00254	27.612	3798
			325	1.847	18.51	5.23	0.00255	27.648	3788
			325	1.846	18.53	5.23	0.00255	27.648	3786
			325	1.845	18.52	5.23	0.00256	27.72	3769
			350	1.846	18.51	5.23	0.00256	27.972	3771
			350	1.847	18.53	5.23	0.00257	28.008	3759
			350	1.846	18.52	5.23	0.00258	28.152	3742
		55°	225	1.846	18.51	5.23	0.00251	27	3846
			225	1.845	18.51	5.23	0.00251	27.072	3844
			225	1.846	18.52	5.24	0.00252	27.288	3839
			300	1.846	18.52	5.24	0.00252	27.36	3839
			300	1.846	18.53	5.24	0.00253	27.468	3823
			300	1.845	18.54	5.25	0.00254	27.648	3813
			325	1.846	18.51	5.25	0.00255	27.648	3801
			325	1.845	18.53	5.25	0.00256	27.72	3784
			325	1.845	18.52	5.25	0.00257	27.828	3769
			350	1.843	18.51	5.25	0.00258	27.828	3750
			350	1.845	18.53	5.25	0.00259	28.008	3740
			350	1.844	18.52	5.25	0.00259	28.152	3738
		65°	225	1.844	18.51	5.25	0.00251	27.072	3857
			225	1.842	18.51	5.26	0.00251	27.18	3860
			225	1.843	18.52	5.26	0.00252	27.468	3847
			300	1.844	18.52	5.26	0.00252	27.54	3849
			300	1.843	18.53	5.27	0.00253	27.792	3839
			300	1.842	18.44	5.27	0.00255	27.792	3807
			325	1.841	18.41	5.28	0.00255	27.828	3812
			325	1.842	18.53	5.28	0.00256	27.9	3799
			325	1.843	18.52	5.29	0.00256	27.972	3808
			350	1.843	18.41	5.28	0.00257	28.152	3786
			350	1.841	18.43	5.28	0.00258	28.188	3768
			350	1.842	18.52	5.29	0.00259	28.332	3762

5	Lime stone1	45°	225	1.878	18.71	5.09	0.00241	26.28	3966
			225	1.878	18.71	5.09	0.00241	26.352	3966
			225	1.877	18.72	5.1	0.00242	26.46	3956
			300	1.879	18.72	5.1	0.00242	26.64	3960
			300	1.878	18.83	5.1	0.00243	26.748	3941
			300	1.877	18.74	5.1	0.00243	26.928	3939
			325	1.876	18.71	5.11	0.00244	26.928	3929
			325	1.877	18.73	5.11	0.00244	27	3931
			325	1.878	18.72	5.11	0.00245	27.108	3917
			350	1.877	18.71	5.11	0.00245	27.18	3915
			350	1.877	18.73	5.11	0.00246	27.36	3899
			350	1.876	18.72	5.11	0.00247	27.432	3881
		50°	225	1.877	18.71	5.11	0.00241	26.352	3980
			225	1.878	18.71	5.12	0.00241	26.46	3990
			225	1.878	18.72	5.12	0.00242	26.748	3973
			300	1.877	18.72	5.12	0.00242	26.748	3971
			300	1.878	18.73	5.12	0.00243	26.892	3957
			300	1.877	18.74	5.12	0.00243	27.072	3955
			325	1.877	18.71	5.13	0.00244	27.108	3946
			325	1.875	18.73	5.13	0.00244	27.108	3942
			325	1.877	18.72	5.13	0.00245	27.125	3930
			350	1.876	18.71	5.13	0.00246	27.252	3912
			350	1.876	18.73	5.13	0.00247	27.468	3896
			350	1.875	18.72	5.13	0.00248	27.54	3879
		55°	225	1.876	18.71	5.13	0.00241	26.46	3993
			225	1.877	18.71	5.13	0.00241	26.532	3995
			225	1.876	18.72	5.14	0.00242	26.568	3985
			300	1.876	18.72	5.14	0.00243	26.82	3968
			300	1.875	18.73	5.14	0.00244	26.892	3950
			300	1.876	18.74	5.15	0.00244	27.252	3960
			325	1.877	18.71	5.15	0.00245	27.252	3946
			325	1.877	18.73	5.15	0.00246	27.269	3929
			325	1.875	18.72	5.15	0.00247	27.288	3909
			350	1.876	18.71	5.15	0.00248	27.612	3896
			350	1.875	18.73	5.15	0.00248	27.612	3894
			350	1.875	18.72	5.15	0.00249	27.648	3878
		65°	225	1.874	18.71	5.15	0.00241	26.568	4005
			225	1.876	18.71	5.16	0.00242	26.64	4000
			225	1.875	18.72	5.16	0.00242	26.892	3998
			300	1.874	18.72	5.16	0.00243	26.928	3979
			300	1.873	18.73	5.17	0.00244	27.072	3969
			300	1.874	18.74	5.17	0.00245	27.288	3955
			325	1.875	18.71	5.18	0.00246	27.288	3948
			325	1.874	18.73	5.18	0.00247	27.298	3930
			325	1.874	18.72	5.19	0.00248	27.36	3922
			350	1.872	18.71	5.18	0.00248	27.432	3910
			350	1.873	18.73	5.18	0.00249	27.612	3896
			350	1.871	18.72	5.19	0.00249	27.72	3900

6	Lime stone 2	45°	225	1.882	18.71	5.09	0.00241	26.28	3975
			225	1.881	18.71	5.09	0.00241	26.28	3973
			225	1.882	18.72	5.1	0.00242	26.568	3966
			300	1.881	18.72	5.1	0.00242	26.64	3964
			300	1.881	18.73	5.1	0.00243	26.712	3948
			300	1.879	18.74	5.1	0.00243	27	3944
			325	1.881	18.71	5.11	0.00244	27	3939
			325	1.88	18.73	5.11	0.00244	27.056	3937
			325	1.88	18.72	5.11	0.00245	27.072	3921
			350	1.879	18.71	5.11	0.00245	27.072	3919
			350	1.88	18.73	5.11	0.00246	27.288	3905
		350	1.881	18.72	5.11	0.00247	27.432	3891	
		50°	225	1.879	18.71	5.11	0.00241	26.388	3984
			225	1.879	18.71	5.12	0.00241	26.46	3992
			225	1.878	18.72	5.12	0.00242	26.748	3973
			300	1.879	18.72	5.12	0.00243	26.748	3959
			300	1.88	18.73	5.12	0.00243	27.072	3961
			300	1.88	18.74	5.12	0.00244	27.108	3945
			325	1.879	18.71	5.13	0.00245	27.108	3934
			325	1.88	18.73	5.13	0.00246	27.18	3920
			325	1.879	18.72	5.13	0.00246	27.252	3918
			350	1.878	18.71	5.13	0.00247	27.432	3900
			350	1.877	18.73	5.13	0.00248	27.468	3883
		55°	350	1.879	18.72	5.13	0.00249	27.612	3871
			225	1.878	18.71	5.13	0.00241	26.46	3998
			225	1.878	18.71	5.13	0.00241	26.532	3998
			225	1.877	18.72	5.14	0.00242	26.568	3987
			300	1.878	18.72	5.14	0.00242	26.82	3989
			300	1.879	18.73	5.14	0.00243	26.928	3975
			300	1.878	18.74	5.15	0.00244	27.18	3964
			325	1.878	18.71	5.15	0.00244	27.18	3964
			325	1.877	18.73	5.15	0.00245	27.252	3946
			325	1.878	18.72	5.15	0.00246	27.288	3932
			350	1.878	18.71	5.15	0.00247	27.288	3916
		65°	350	1.878	18.73	5.15	0.00248	27.612	3900
			350	1.877	18.72	5.15	0.00249	27.612	3882
			225	1.878	18.71	5.15	0.00241	26.532	4013
			225	1.877	18.71	5.16	0.00241	26.64	4019
			225	1.877	18.72	5.16	0.00242	26.64	4002
			300	1.876	18.72	5.16	0.00243	26.928	3984
			300	1.877	18.73	5.17	0.00244	27	3977
			300	1.876	18.74	5.17	0.00244	27.252	3975
			325	1.876	18.71	5.18	0.00245	27.288	3966
			325	1.875	18.73	5.18	0.00246	27.288	3948
			325	1.876	18.72	5.19	0.00247	27.36	3942
		350	1.877	18.71	5.18	0.00247	27.432	3936	
		350	1.875	18.73	5.18	0.00248	27.648	3916	
		350	1.875	18.72	5.19	0.00249	27.72	3908	

7	Lime stone 3	45°	225	1.953	19.61	4.79	0.00211	24.588	4434
			225	1.954	19.61	4.79	0.00211	24.66	4436
			225	1.955	19.62	4.8	0.00212	24.732	4426
			300	1.955	19.62	4.8	0.00212	24.948	4426
			300	1.954	19.63	4.8	0.00213	25.092	4403
			300	1.955	19.64	4.8	0.00214	25.38	4385
			325	1.954	19.61	4.81	0.00214	25.38	4392
			325	1.954	19.63	4.81	0.00215	25.425	4372
			325	1.953	19.62	4.81	0.00215	25.452	4369
			350	1.954	19.61	4.81	0.00216	25.74	4351
			350	1.953	19.63	4.81	0.00217	25.74	4329
			350	1.953	19.62	4.81	0.00218	25.848	4309
		50°	225	1.952	19.51	4.81	0.00211	24.768	4450
			225	1.953	19.61	4.82	0.00211	24.768	4461
			225	1.954	19.62	4.82	0.00213	25.092	4422
			300	1.953	19.62	4.82	0.00213	25.128	4419
			300	1.953	19.63	4.82	0.00215	25.2	4378
			300	1.951	19.54	4.83	0.00215	25.488	4383
			325	1.952	19.51	4.83	0.00216	25.488	4365
			325	1.953	19.53	4.83	0.00216	25.498	4367
			325	1.953	19.52	4.83	0.00217	25.56	4347
			350	1.952	19.51	4.83	0.00218	25.56	4325
			350	1.953	19.53	4.83	0.00218	25.812	4327
			350	1.952	19.52	4.83	0.00219	25.92	4305
		55°	225	1.952	19.51	4.83	0.00211	24.912	4468
			225	1.951	19.51	4.83	0.00211	24.948	4466
			225	1.953	19.52	4.84	0.00212	25.272	4459
			300	1.951	19.52	4.84	0.00212	25.272	4454
			300	1.951	19.53	4.84	0.00213	25.56	4433
			300	1.95	19.54	4.85	0.00213	25.632	4440
			325	1.951	19.51	4.85	0.00214	25.632	4422
			325	1.952	19.53	4.85	0.00215	25.668	4403
			325	1.951	19.52	4.85	0.00215	25.74	4401
			350	1.951	19.51	4.85	0.00216	25.92	4381
			350	1.95	19.53	4.85	0.00217	25.92	4358
			350	1.951	19.52	4.85	0.00218	25.992	4341
		65°	225	1.952	19.51	4.85	0.00211	24.912	4487
			225	1.951	19.51	4.86	0.00211	25.092	4494
			225	1.95	19.52	4.86	0.00212	25.308	4470
			300	1.951	19.52	4.86	0.00213	25.38	4452
			300	1.95	19.53	4.87	0.00214	25.38	4438
			300	1.95	19.54	4.87	0.00215	25.632	4417
			325	1.949	19.51	4.88	0.00216	25.632	4403
			325	1.95	19.53	4.88	0.00216	25.668	4406
			325	1.949	19.52	4.89	0.00217	25.74	4392
			350	1.949	19.51	4.88	0.00218	25.812	4363
			350	1.948	19.53	4.88	0.00218	25.992	4361
			350	1.949	19.52	4.89	0.02101	26.028	453.6

8	Lime stone 4	45°	225	1.959	19.61	4.59	0.00191	23.652	4708
			225	1.958	19.61	4.59	0.00191	23.58	4705
			225	1.958	19.62	4.6	0.00192	23.58	4691
			300	1.956	19.62	4.6	0.00192	23.94	4686
			300	1.957	19.63	4.6	0.00193	24.012	4664
			300	1.958	19.64	4.6	0.00193	24.228	4667
			325	1.958	19.61	4.61	0.00194	24.228	4653
			325	1.956	19.63	4.61	0.00195	24.3	4624
			325	1.957	19.62	4.61	0.00195	24.372	4627
			350	1.956	19.61	4.61	0.00196	24.372	4601
			350	1.956	19.63	4.61	0.00197	24.66	4577
			350	1.955	19.62	4.61	0.00198	24.66	4552
		50°	225	1.957	19.61	4.61	0.00191	23.652	4723
			225	1.956	19.61	4.62	0.00191	23.76	4731
			225	1.956	19.62	4.62	0.00192	24.048	4707
			300	1.955	19.62	4.62	0.00193	24.048	4680
			300	1.956	19.63	4.62	0.00193	24.192	4682
			300	1.957	19.64	4.63	0.00194	24.372	4671
			325	1.956	19.61	4.63	0.00194	24.408	4668
			325	1.956	19.63	4.63	0.00195	24.408	4644
			325	1.955	19.62	4.63	0.00195	24.42	4642
			350	1.955	19.61	4.63	0.00196	24.552	4618
			350	1.956	19.63	4.63	0.00197	24.768	4597
			350	1.956	19.62	4.63	0.00199	24.84	4551
		55°	225	1.955	19.61	4.63	0.00201	23.76	4503
			225	1.956	19.61	4.63	0.00201	23.76	4506
			225	1.955	19.62	4.64	0.00202	23.868	4491
			300	1.955	19.62	4.64	0.00202	24.12	4491
			300	1.954	19.63	4.64	0.00203	24.192	4466
			300	1.956	19.64	4.65	0.00203	24.48	4480
			325	1.955	19.61	4.65	0.00204	24.48	4456
			325	1.955	19.63	4.65	0.00205	24.552	4435
			325	1.954	19.62	4.65	0.00206	24.588	4411
			350	1.955	19.61	4.65	0.00207	24.84	4392
			350	1.955	19.63	4.65	0.00208	24.912	4371
			350	1.954	19.62	4.65	0.00209	24.948	4347
		65°	225	1.954	19.61	4.65	0.00201	23.94	4520
			225	1.953	19.61	4.66	0.00201	23.94	4528
			225	1.954	19.62	4.66	0.00202	24.228	4508
			300	1.954	19.62	4.66	0.00202	24.3	4508
			300	1.954	19.63	4.67	0.00203	24.372	4495
			300	1.953	19.64	4.67	0.00203	24.588	4493
			325	1.954	19.61	4.68	0.00204	24.588	4483
			325	1.953	19.63	4.68	0.00205	24.66	4459
			325	1.952	19.52	4.69	0.00206	24.66	4444
			350	1.951	19.51	4.68	0.00207	24.732	4411
			350	1.953	19.53	4.68	0.00208	24.948	4394
			350	1.951	19.52	4.69	0.00209	25.02	4378

9	Dolomite 1	45°	225	1.962	19.61	4.79	0.00211	24.66	4454
			225	1.961	19.61	4.79	0.00211	24.732	4452
			225	1.962	19.62	4.8	0.00212	25.02	4442
			300	1.962	19.62	4.8	0.00213	25.02	4421
			300	1.961	19.63	4.8	0.00214	25.308	4399
			300	1.963	19.64	4.8	0.00214	25.38	4403
			325	1.96	19.61	4.81	0.00215	25.38	4385
			325	1.961	19.63	4.81	0.00216	25.452	4367
			325	1.962	19.62	4.81	0.00217	25.488	4349
			350	1.961	19.61	4.81	0.00217	25.668	4347
			350	1.96	19.63	4.81	0.00218	25.74	4325
			350	1.959	19.62	4.81	0.00219	25.848	4303
		50°	225	1.96	19.61	4.81	0.00211	24.768	4468
			225	1.96	19.61	4.82	0.00211	24.768	4477
			225	1.959	19.62	4.82	0.00212	24.912	4454
			300	1.961	19.62	4.82	0.00212	25.128	4459
			300	1.96	19.63	4.82	0.00213	25.2	4435
			300	1.96	19.64	4.83	0.00214	25.452	4424
			325	1.958	19.61	4.83	0.00215	25.452	4399
			325	1.959	19.63	4.83	0.00215	25.488	4401
			325	1.96	19.62	4.83	0.00216	25.56	4383
			350	1.959	19.61	4.83	0.00217	25.632	4360
			350	1.959	19.63	4.83	0.00218	25.848	4340
			350	1.958	19.62	4.83	0.00219	25.848	4318
		55°	225	1.959	19.61	4.83	0.00211	24.912	4484
			225	1.96	19.61	4.83	0.00211	24.912	4487
			225	1.96	19.62	4.84	0.00212	25.272	4475
			300	1.959	19.62	4.84	0.00213	25.308	4451
			300	1.96	19.63	4.84	0.00214	25.308	4433
			300	1.958	19.64	4.85	0.00215	25.56	4417
			325	1.958	19.61	4.85	0.00216	25.56	4396
			325	1.957	19.63	4.85	0.00217	25.632	4374
			325	1.959	19.62	4.85	0.00217	25.632	4378
			350	1.958	19.61	4.85	0.00218	25.668	4356
			350	1.958	19.63	4.85	0.00218	25.992	4356
			350	1.957	19.62	4.85	0.00219	26.028	4334
		65°	225	1.958	19.61	4.85	0.00211	24.84	4501
			225	1.959	19.61	4.86	0.00211	25.02	4512
			225	1.957	19.62	4.86	0.00212	25.2	4486
			300	1.957	19.62	4.86	0.00212	25.38	4486
			300	1.956	19.63	4.87	0.00213	25.452	4472
			300	1.957	19.64	4.87	0.00214	25.56	4454
			325	1.958	19.61	4.88	0.00215	25.632	4444
			325	1.958	19.63	4.88	0.00215	25.632	4444
			325	1.957	19.62	4.89	0.00216	25.74	4430
			350	1.957	19.61	4.88	0.00217	25.812	4401
			350	1.956	19.63	4.88	0.00218	25.92	4379
			350	1.955	19.62	4.89	0.00219	26.1	4365

10	Dolomite 2	45°	225	2.049	20.11	4.79	0.00211	24.588	4652
			225	2.051	20.11	4.79	0.00211	24.66	4656
			225	2.05	20.12	4.8	0.00213	24.732	4620
			300	2.05	20.12	4.8	0.00214	24.948	4598
			300	2.049	20.13	4.8	0.00215	25.02	4575
			300	2.049	20.14	4.8	0.00215	25.308	4575
			325	2.05	20.11	4.81	0.00216	25.38	4565
			325	2.049	20.13	4.81	0.00216	25.38	4563
			325	2.049	20.12	4.81	0.00217	25.452	4542
			350	2.047	20.11	4.81	0.00217	25.668	4537
			350	2.048	20.13	4.81	0.00218	25.74	4519
			350	2.049	20.12	4.81	0.00219	25.812	4500
		50°	225	2.049	20.11	4.81	0.00211	24.768	4671
			225	2.047	20.11	4.81	0.00211	24.768	4666
			225	2.048	20.12	4.82	0.00212	25.092	4656
			300	2.047	20.12	4.82	0.00212	25.128	4654
			300	2.047	20.13	4.82	0.00213	25.2	4632
			300	2.046	20.14	4.83	0.00214	25.452	4618
			325	2.048	20.11	4.83	0.00215	25.452	4601
			325	2.047	20.13	4.83	0.00216	25.455	4577
			325	2.047	20.12	4.83	0.00217	25.56	4556
			350	2.046	20.11	4.83	0.00218	25.56	4533
			350	2.047	20.13	4.83	0.00218	25.812	4535
			350	2.047	20.12	4.83	0.00219	25.848	4515
		55°	225	2.046	20.11	4.83	0.00211	24.768	4683
			225	2.046	20.11	4.83	0.00211	24.948	4683
			225	2.045	20.12	4.84	0.00212	25.2	4669
			300	2.046	20.12	4.84	0.00212	25.272	4671
			300	2.047	20.13	4.84	0.00213	25.488	4651
			300	2.047	20.14	4.85	0.00214	25.488	4639
			325	2.046	20.11	4.85	0.00215	25.56	4615
			325	2.047	20.13	4.85	0.00215	25.632	4618
			325	2.046	20.12	4.85	0.00216	25.668	4594
			350	2.046	20.11	4.85	0.00217	25.848	4573
			350	2.045	20.13	4.85	0.00218	25.92	4550
			350	2.047	20.12	4.85	0.00219	26.028	4533
		65°	225	2.045	20.11	4.85	0.00211	24.948	4701
			225	2.045	20.11	4.86	0.00211	25.02	4710
			225	2.044	20.12	4.86	0.00212	25.092	4686
			300	2.045	20.12	4.86	0.00212	25.308	4688
			300	2.046	20.13	4.87	0.00213	25.38	4678
			300	2.045	20.14	4.87	0.00214	25.668	4654
			325	2.045	20.11	4.88	0.00215	25.668	4642
			325	2.043	20.13	4.88	0.00215	25.689	4637
			325	2.044	20.12	4.89	0.00216	25.74	4627
			350	2.044	20.11	4.88	0.00217	25.812	4597
			350	2.043	20.13	4.88	0.00218	26.028	4573
			350	2.043	20.12	4.89	0.00221	26.1	4520

APPENDIX-II

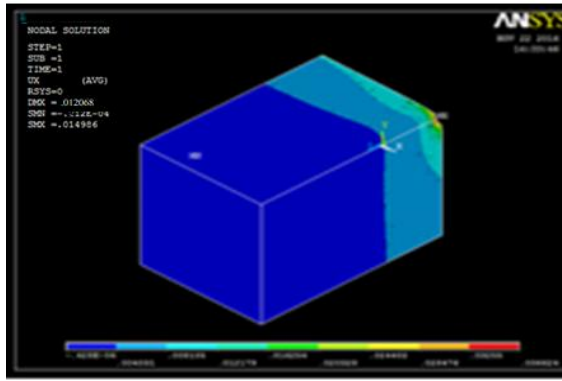


Figure 6.138 Displacement along XYZ with 45° pick angle at 45° attack angle for coal 1.

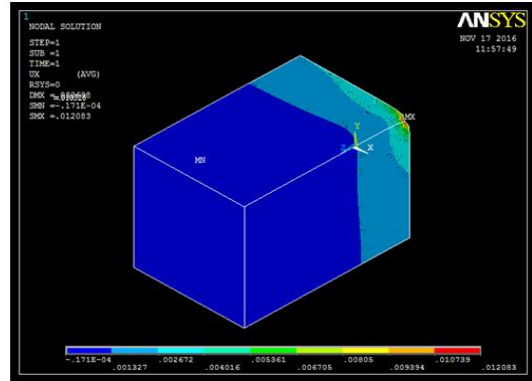


Figure 6.141 Displacement along XYZ with 45° pick angle at 45° attack angle for Sandstone 3.

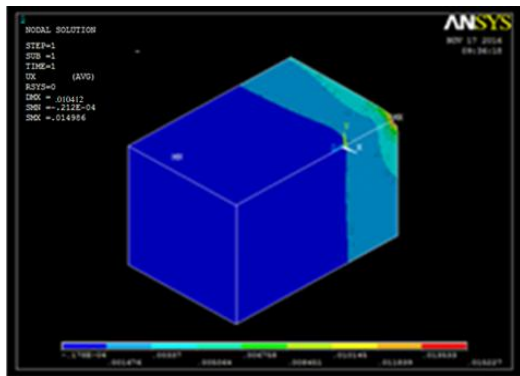


Figure 6.139 Displacement along XYZ with 45° pick angle at 45° attack angle for Sandstone 1.

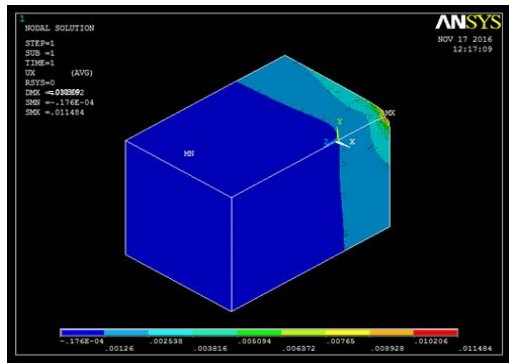


Figure 6.142 Displacement along XYZ with 45° pick angle at 45° attack angle for Limestone 1.

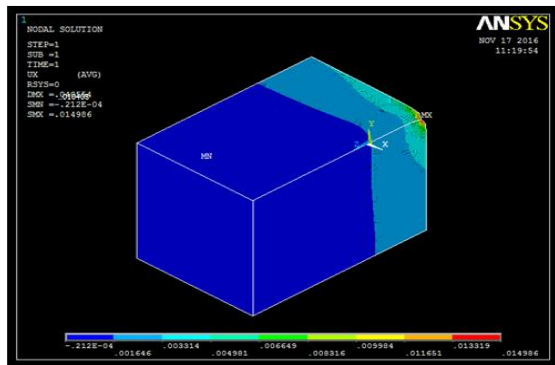


Figure 6.140 Displacement along XYZ with 45° pick angle at 45° attack angle for Sandstone 2.

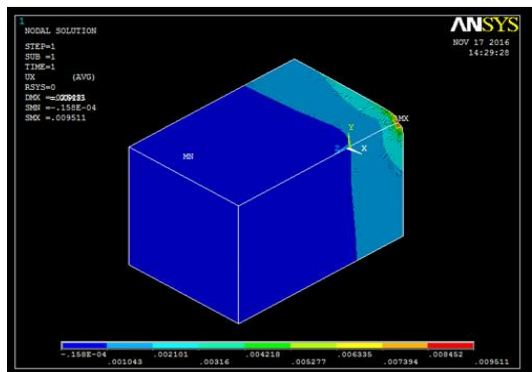


Figure 6.143 Displacement along XYZ with 45° pick angle at 45° attack angle for Limestone 2.

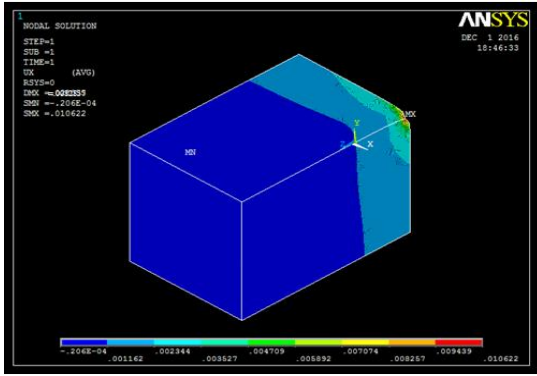


Figure 6.144 Displacement along XYZ with 45° pick angle at 45° attack angle for Limestone 3.

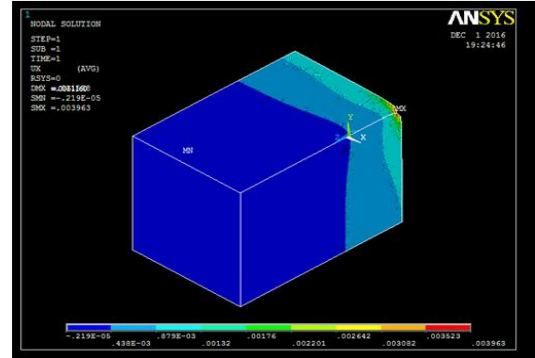


Figure 6.147 Displacement along XYZ with 45° pick angle at 45° attack angle for Dolomite 2.

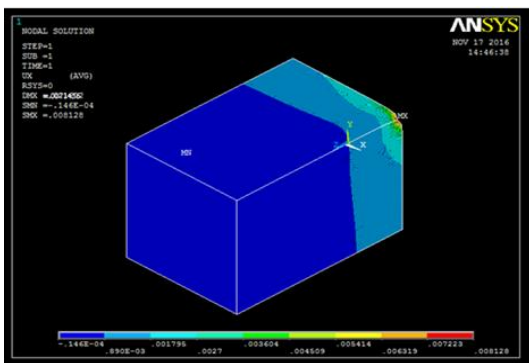


Figure 6.145 Displacement along XYZ with 45° pick angle at 45° attack angle for Limestone 4.

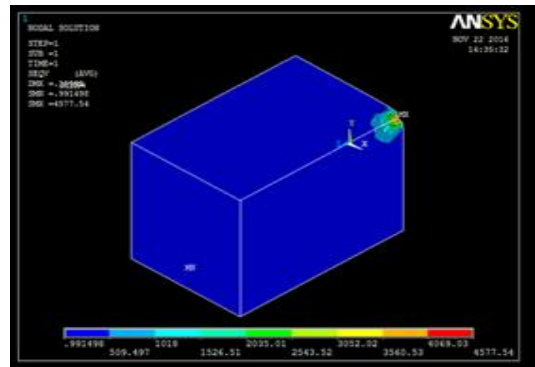


Figure 6.148 Von Mises stresses with 45° pick angle at 45° attack angle for Coal 1.

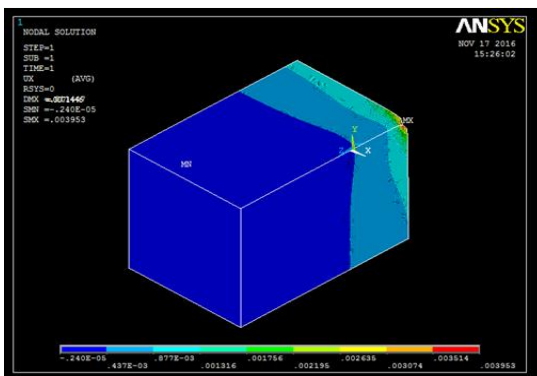


Figure 6.146 Displacement along XYZ with 45° pick angle at 45° attack angle for Dolomite 1.

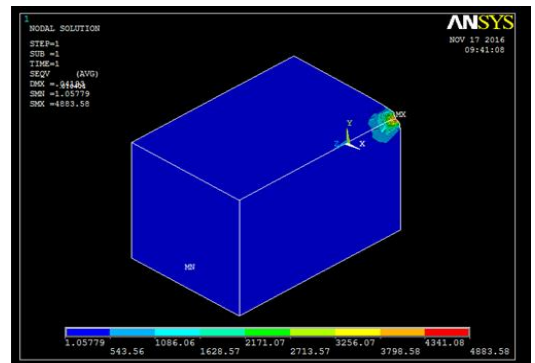


Figure 6.149 Von Mises stresses with 45° pick angle at 45° attack angle for Sandstone 1.

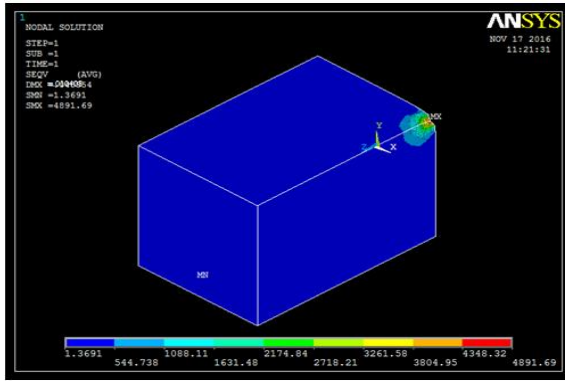


Figure 6.150 Von Misses stresses with 45° pick angle at 45° attack angle for Sandstone 2.

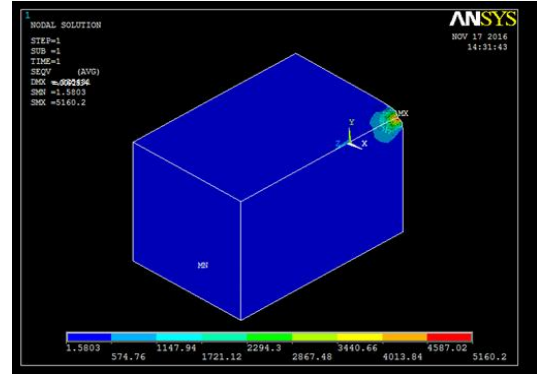


Figure 6.153 Von Misses stresses with 45° pick angle at 45° attack angle for Lime stone 2.

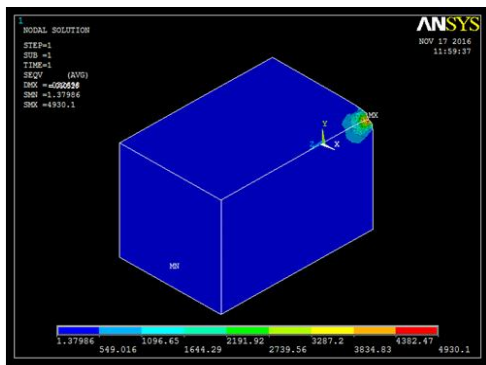


Figure 6.151 Von Misses stresses with 45° pick angle at 45° attack angle for Sandstone 3.

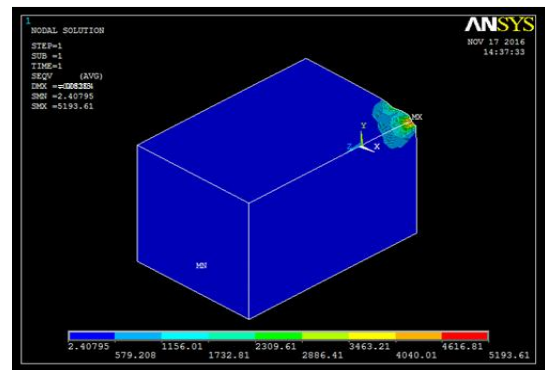


Figure 6.154 Von Misses stresses with 45° pick angle at 45° attack angle for Limestone 3.

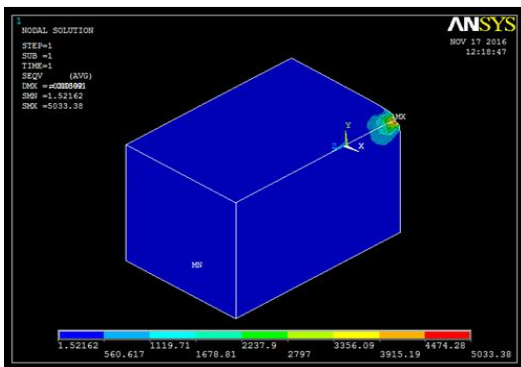


Figure 6.152 Von Misses stresses with 45° pick angle at 45° attack angle for Limestone 1.

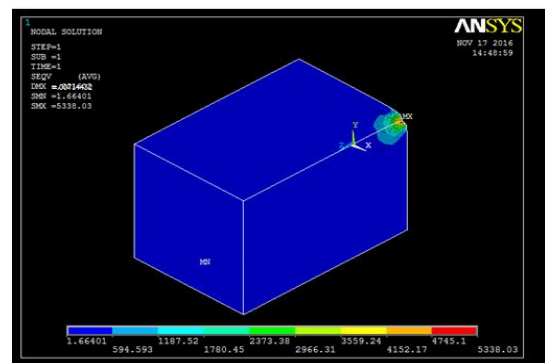


Figure 6.156 Von Misses stresses with 45° pick angle at 45° attack angle for Dolomite 1..

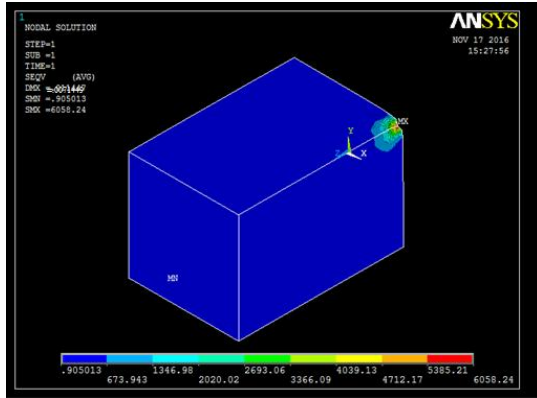


Figure 6.155 Von Mises stresses with 45° pick angle at 45° attack angle for Limestone 4.

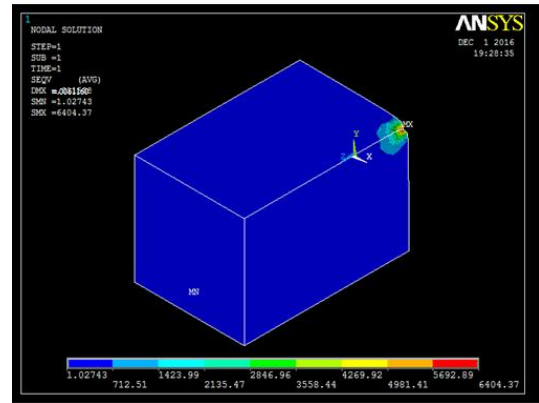


Figure 6.157 Von Mises stresses with 45° pick angle at 45° attack angle for Dolomite 2.

Table 6.7 Displacement and Von Misses Stress distribution for 45° attack angle with Different Pick Angles

No	Type of Rock	Pick Angle	Fsin α	DISPLACEMENT									Von Misses Stresses N/mm ²
				Depth of cut (mm)			X Direction			Y Direction			
				FEM	Experiment	Error	D _{MAX}	S _{MIN}	S _{MAX}	D _{MAX}	S _{MIN}	S _{MAX}	
1	Coal	45°	1.06	12.06	8.31	3.75	12.06	0.04258	0.036624	12.06	0.004301	0.004386	4577.54
		50°	1.145	12.09	8.25	3.84	12.09	-0.04284	0.036656	12.09	-4.30489	0.004393	4587.44
		55°	1.22	12.16	8.44	3.72	12.16	-0.040243	0.036688	12.16	-4.21342	0.004553	4597.44
		65°	1.344	12.18	8.46	3.72	12.18	-0.040351	0.036786	12.18	-4.22472	0.004565	4567.44
2	Sand stone 1	45°	1.129	10.41	7.56	2.85	10.41	-0.040178	0.015227	10.41	-0.001788	0.001825	4883.58
		50°	1.218	10.42	7.57	2.85	10.42	-0.040179	0.015281	10.42	-0.001795	0.001831	4901.07
		55°	1.3	10.42	7.64	2.78	10.42	-0.040180	0.015363	10.42	-0.001804	0.001841	4927.3
		65°	1.435	10.43	7.67	2.76	10.43	-0.040180	0.015281	10.43	-0.001795	0.001831	4901.07
3	Sand stone 2	45°	1.153	10.4	7.35	3.05	10.4	-0.040180	0.014986	10.4	-0.001875	0.001607	4891.69
		50°	1.25	10.4	7.38	3.02	10.4	-0.040185	0.014875	10.4	-0.001785	0.00172	4986.03
		55°	1.331	10.4	7.45	2.95	10.4	-0.040185	0.014875	10.4	-0.001785	0.00172	4986.03
		65°	1.47	10.42	7.58	2.84	10.42	-0.040185	0.014927	10.42	-0.001791	0.001726	5003.39
4	Sand stone 3	45°	1.159	10.32	6.95	3.37	10.32	-0.040171	0.012083	10.32	-0.001512	0.001295	4930.1
		50°	1.254	10.32	6.96	3.36	10.32	-0.040171	0.012083	10.32	-0.001512	0.001295	4930.1
		55°	1.339	10.32	6.98	3.34	10.32	-0.040171	0.012083	10.32	-0.001512	0.001295	4930.1
		65°	1.483	10.33	7.25	3.08	10.33	-0.040171	0.012083	10.33	-0.001512	0.001295	4930.1
5	Lime stone 1	45°	1.192	10.3	6.74	3.56	10.3	-0.040176	0.011484	10.3	-0.001466	0.001183	5033.38
		50°	1.29	10.3	6.75	3.55	10.3	-0.040176	0.011484	10.3	-0.001466	0.001183	5033.38
		55°	1.381	10.3	6.76	3.54	10.3	-0.017651	0.011503	10.3	-1046828	0.001185	5041.84
		65°	1.524	10.33	6.77	3.56	10.33	-0.017651	0.011503	10.33	-1046828	0.118548	5041.84
6	Lime stone 2	45°	1.242	9.25	6.34	2.91	9.25	-0.040158	0.009511	9.25	-0.001238	0.941E-03	5160.2
		50°	1.346	9.25	6.45	2.8	9.25	-0.040158	0.009511	9.25	-0.001238	0.941E-03	5160.2
		55°	1.437	9.25	6.46	2.79	9.25	-0.040158	0.009511	9.25	-0.001238	0.941E-03	5160.2
		65°	1.588	9.28	6.47	2.81	9.28	-0.040158	0.01129	9.28	-0.001242	0.001199	5193.61
7	Lime stone 3	45°	1.243	8.28	6.34	1.94	8.28	-0.040283	0.01129	8.28	-0.001242	0.001199	5193.61
		50°	1.345	8.28	6.35	1.93	8.28	-0.040283	0.01129	8.28	-0.001242	0.001199	5193.61
		55°	1.437	8.28	6.37	1.91	8.28	-0.040283	0.01129	8.28	-0.001242	0.001199	5193.61
		65°	1.591	8.29	6.38	1.91	8.29	-0.040283	0.01129	8.29	-0.001242	0.001199	5193.61

8	Lime stone 4	45°	1.3	7.21	6.35	0.86	7.21	-0.040146	0.008128	7.21	-0.001078	0.00771	5338.03
		50°	1.406	7.21	6.36	0.85	7.21	-0.040146	0.008128	7.21	-0.001078	0.00771	5338.03
		55°	1.503	7.21	6.37	0.84	7.21	-0.040147	0.008185	7.21	-0.001085	0.00776	5375.33
		65°	1.654	7.24	6.38	0.86	7.24	-0.040147	0.008185	7.24	-0.001085	0.00776	5375.33
9	Dolomite 1	45°	1.32	7.11	6.18	0.93	7.11	-0.050240	0.003953	7.11	-0.00370	0.00629	6058.24
		50°	1.43	7.11	6.24	0.87	7.11	-0.050240	0.003953	7.11	-0.00370	0.00629	6058.23
		55°	1.527	7.11	6.26	0.85	7.11	-0.050240	0.003953	7.11	-0.00370	0.00629	6058.22
		65°	1.688	7.12	6.27	0.85	7.12	-0.050240	0.003953	7.12	-0.00370	0.00629	6058.24
10	Dolomite 2	45°	1.392	6.11	6.14	-0.03	6.11	-0.050219	0.003963	6.11	-0.00360	0.00649	6404.37
		50°	1.506	6.11	6.16	-0.05	6.11	-0.050219	0.003963	6.11	-0.00362	0.00651	6427.49
		55°	1.609	6.11	6.17	-0.06	6.11	-0.050220	0.003961	6.11	-0.00362	0.00652	6432.11
		65°	1.78	6.13	6.18	-0.05	6.13	-0.050220	0.003986	6.13	-0.00363	0.00652	6441.36

Table 6.8 Displacement and Von Misses Stress distribution for 55° attack angle with Different Pick Angles

Sl No	Type of Rock	Pick Angle	F sin α	DISPLACEMENT									Von Misses Stresses N/mm ²
				Depth of cut (mm)			X Direction			Y Direction			
				FEM	Experiment	Error	D _{MAX}	S _{MIN}	S _{MAX}	D _{MAX}	S _{MIN}	S _{MAX}	
1	Coal	45°	0.987	12.63	10.34	2.29	0.01263	-0.03238	0.27707	0.01263	-3.25394	-3.32072	3400.100
		50°	1.064	12.77	10.35	2.42	0.01277	-0.03250	0.27805	0.01277	-3.26545	-3.33246	3400.220
		55°	1.135	12.77	10.36	2.41	0.01277	-0.03255	0.27847	0.01277	-3.27038	-3.33749	3400.180
		65°	1.255	12.79	10.37	2.42	0.01279	-0.03268	0.27966	0.01277	-3.28434	-3.35175	3400.050
2	Sandstone 1	45°	1.077	10.32	8.13	2.19	0.01032	-0.00001	0.01160	0.01032	-0.00136	0.00139	3720.620
		50°	1.142	10.3	8.17	2.13	0.01030	-0.00001	0.01163	0.01032	-0.00137	0.00139	3729.360
		55°	1.221	10.31	8.17	2.14	0.01031	-0.00001	0.01166	0.01032	-0.00137	0.00140	3738.100
		65°	1.345	10.34	8.19	2.15	0.01034	-0.00001	0.01167	0.01032	-0.00137	0.00140	3742.480
3	Sandstone 2	45°	1.084	10.32	8.16	2.16	0.01032	-0.00001	0.01132	0.01032	-0.00136	0.00131	3792.680
		50°	1.175	10.29	8.14	2.15	0.01029	-0.00002	0.01019	0.01020	-0.00018	0.00020	3803.500
		55°	1.921	10.28	8.17	2.11	0.01028	-0.00001	0.01139	0.01020	-0.00137	0.00132	3818.720
		65°	1.385	10.33	8.19	2.14	0.01033	-0.00001	0.01139	0.01020	-0.00137	0.00132	3818.720
4	Sandstone 3	45°	1.089	9.24	7.8	1.44	0.00924	-0.00001	0.00922	0.00924	-0.00115	0.00099	3760.540
		50°	1.177	9.23	7.83	1.4	0.00923	-0.00001	0.00922	0.00924	-0.00115	0.00099	3760.540
		55°	1.258	9.22	7.85	1.37	0.00922	-0.00001	0.00922	0.00924	-0.00115	0.00099	3760.540
		65°	1.39	9.25	7.88	1.37	0.00925	-0.00001	0.00923	0.00924	-0.00116	0.00099	3764.810
5	Limestone 1	45°	1.77	9.23	6.83	2.4	0.00923	-0.00001	0.00877	0.00923	-0.00112	0.00090	3844.820
		50°	1.215	9.24	6.82	2.42	0.00924	-0.00001	0.00877	0.00923	-0.00112	0.00090	3844.820
		55°	1.298	9.24	6.83	2.41	0.00924	-0.00001	0.00877	0.00923	-0.00112	0.00090	3844.820
		65°	1.435	9.26	6.87	2.39	0.00926	-0.00001	0.00878	0.00923	-0.00112	0.00091	3849.050
6	Limestone 2	45°	1.17	9.19	6.55	2.64	0.00919	-0.00001	0.00731	0.00919	-0.00095	0.00072	3966.480
		50°	1.267	9.17	6.55	2.62	0.00917	-0.00001	0.00731	0.00919	-0.00095	0.00072	3966.480
		55°	1.354	9.18	6.45	2.73	0.00918	-0.00001	0.00733	0.00919	-0.00095	0.00073	3974.860
		65°	1.495	9.2	6.55	2.65	0.00920	-0.00001	0.00733	0.00919	-0.00095	0.00073	3974.860
7	Limestone 3	45°	1.172	9.19	6.43	2.76	0.00919	-0.00001	0.00733	0.00919	-0.00099	679.00000	3896.520
		50°	1.268	9.17	6.45	2.72	0.00917	-0.00001	0.00733	0.00919	-0.00099	679.00000	3896.520

		55°	1.357	9.18	6.46	2.72	0.00918	-0.00001	0.00733	0.00919	-0.00099	679.00000	3896.520
		65°	1.499	9.2	6.55	2.65	0.00920	-0.00001	0.00762	0.00920	-0.00103	0.00071	4052.220
8	Limestone 4	45°	1.22	8.16	6.45	1.71	0.00816	-0.00001	0.00625	0.00816	-0.00083	0.00059	4102.990
		50°	1.323	8.17	6.44	1.73	0.00817	-0.00001	0.00625	0.00816	-0.00083	0.00059	4102.990
		55°	1.415	8.18	6.45	1.73	0.00818	-0.00001	0.00627	0.00816	-0.00083	0.00060	4119.870
		65°	1.563	8.2	6.47	1.73	0.00820	-0.00001	0.00637	0.00816	-0.00084	0.00060	4181.730
		45°	1.25	8.8	6.23	2.57	0.00880	-0.00001	0.00304	0.00880	-0.00029	0.00048	4658.770
9	Dolomite 1	50°	1.354	8.6	6.25	2.35	0.00860	-0.00001	0.00304	0.00880	-0.00029	0.00048	4658.770
		55°	1.446	8.7	6.27	2.43	0.00870	-0.00001	0.00304	0.00880	-0.00029	0.00049	4663.380
		65°	1.598	8.9	6.29	2.61	0.00890	-0.00001	0.00320	0.00880	-0.00030	0.00057	4907.360
		45°	1.327	7.9	6.24	1.66	0.00790	-0.00001	0.00306	0.00790	-0.00028	0.00050	4943.160
10	Dolomite 2	50°	1.436	7.6	6.26	1.34	0.00760	-0.00001	0.00306	0.00790	-0.00028	0.00050	4943.160
		55°	1.535	7.8	6.26	1.54	0.00780	-0.00001	0.00306	0.00790	-0.00028	0.00050	4947.780
		65°	1.696	8.1	6.29	1.81	0.00810	-0.00001	0.00306	0.00790	-0.00028	0.00050	4947.780

Table 6.9 Displacement and Von Misses Stress distribution for 65° attack angle with Different Pick Angles

Sl No	Type of Rock	Pick Ang	F sin α	DISPLACEMENT									Von Misses Stresses N/mm ²
				Depth of cut (mm)			Y Direction			Z Direction			
				FEM	Experiment	Error	D _{MAX}	S _{MIN}	S _{MAX}	D _{MAX}	S _{MIN}	S _{MAX}	
1	Coal	45°	1.182	11.74	7.81	3.93	11.74	-0.00003	0.02452	11.74	-0.00288	0.00294	3064.810
		50°	1.277	11.74	7.86	3.88	11.74	-0.00003	0.02459	11.74	-0.00289	0.00295	3073.550
		55°	1.365	11.74	7.82	3.92	11.74	-0.00003	0.02463	11.74	-0.00289	0.00295	3077.920
		65°	1.508	11.85	7.89	3.96	11.85	-0.00003	0.02463	11.85	-0.00289	0.00295	3077.920
2	Sandstone 1	45°	1.2	9.28	6.44	2.84	9.28	-0.00001	0.00975	9.28	-0.00115	0.00117	3126.020
		50°	1.298	9.6	6.51	3.09	9.6	-0.00001	0.00975	9.6	-0.00115	0.00117	3126.020
		55°	1.388	9.37	6.54	2.83	9.37	-0.00001	0.00977	9.37	-0.00115	0.00117	3134.760
		65°	1.535	9.28	6.55	2.73	9.28	-0.00001	0.00977	9.28	-0.00115	0.00117	3134.760
3	Sandstone 2	45°	1.215	9.36	6.44	2.92	9.36	-0.00001	0.00936	9.36	-0.00112	0.00108	3137.420
		50°	1.314	9.47	6.46	3.01	9.47	-0.00001	0.00936	9.47	-0.00112	0.00108	3137.420
		55°	1.404	9.48	6.53	2.95	9.48	-0.00001	0.00937	9.48	-0.00113	0.00108	3141.760
		65°	1.553	9.34	6.54	2.8	9.34	-0.00001	0.00937	9.34	-0.00113	0.00108	3141.760
4	Sandstone 3	45°	1.226	8.28	5.8	2.48	8.28	-0.00001	0.00761	8.28	-0.00095	0.00082	3103.190
		50°	1.325	8.21	5.87	2.34	8.21	-0.00001	0.00761	8.21	-0.00095	0.00082	3103.190
		55°	1.412	8.34	5.79	2.55	8.34	-0.00001	0.00763	8.34	-0.00095	0.00082	3111.730
		65°	1.561	8.38	5.89	2.49	8.38	-0.00001	0.00765	8.38	-0.00096	0.00082	3120.260
5	Limestone 1	45°	1.231	7.21	5.22	1.99	7.21	-0.00001	0.00707	7.21	-0.00090	0.00073	3100.390
		50°	1.332	7.28	5.25	2.03	7.28	-0.00001	0.00707	7.28	-0.00090	0.00073	3100.390
		55°	1.422	7.23	5.23	2	7.23	-0.00001	0.00708	7.23	-0.00090	0.00073	3104.620
		65°	1.588	7.23	5.27	1.96	7.23	-0.00001	0.00708	7.23	-0.00090	0.00073	3104.620
6	Limestone 2	45°	1.236	6.28	5.22	1.06	6.28	-0.00001	0.00569	6.28	-0.00074	0.00056	3086.900
		50°	1.238	6.23	5.28	0.95	6.23	-0.00001	0.00570	6.23	-0.00007	0.00056	3091.090
		55°	1.429	6.17	5.19	0.98	6.17	-0.00001	0.00508	6.17	-0.00009	0.00015	3144.760
		65°	1.596	6.28	5.29	0.99	6.28	-0.00001	0.00508	6.28	-0.00009	0.00015	3144.760
7	Limestone 3	45°	1.243	6.23	5.12	1.11	6.23	-0.00001	0.00571	6.23	-0.00077	0.00053	3036.090
		50°	1.345	6.17	5.14	1.03	6.17	-0.00001	0.00571	6.17	-0.00077	0.00053	3036.090
		55°	1.438	6.12	5.12	1	6.12	-0.00001	0.00572	6.12	-0.00077	0.00053	3040.190
		65°	1.719	6.12	5.15	0.97	6.12	-0.00001	0.00572	6.12	-0.00077	0.00053	3040.190
		45°	1.341	5.2	5.12	0.08	5.2	-0.00001	0.00502	5.2	-0.00067	0.00048	3298.970
		50°	1.45	5.16	5.15	0.01	5.16	-0.00001	0.00502	5.16	-0.00067	0.00048	3298.970

8	Limestone 4	55°	1.548	5.16	5.12	0.04	5.16	-0.00001	0.00505	5.16	-0.00067	0.00048	3315.550
		65°	1.72	5.16	5.17	-0.01	5.16	-0.00001	0.00505	5.16	-0.00067	0.00048	3315.550
9	Dolomite 1	45°	1.341	5.88	4.79	1.09	5.88	-0.00001	0.00239	5.88	-0.00022	0.00039	3703.900
		50°	1.451	5.88	4.85	1.03	5.88	-0.00001	0.00239	5.88	-0.00022	0.00039	3703.900
		55°	1.556	5.88	4.79	1.09	5.88	-0.00001	0.00239	5.88	-0.00022	0.00039	3703.900
		65°	1.893	5.88	4.85	1.03	5.88	-0.00001	0.00239	5.88	-0.00022	0.00039	3703.900
10	Dolomite 2	45°	1.468	4.74	4.6	0.14	4.74	-0.00001	0.00252	4.74	-0.00024	0.00040	4014.280
		50°	1.592	4.72	4.65	0.07	4.72	-0.00001	0.00252	4.72	-0.00024	0.00040	4018.880
		55°	1.694	4.76	4.62	0.14	4.76	-0.00001	0.00251	4.76	-0.00023	0.00041	4050.710
		65°	1.872	4.82	4.69	0.13	4.82	-0.00001	0.00251	4.82	-0.00023	0.00041	4059.950

Table 6.10 Displacement and Von Misses Stress distribution for 45° attack angle with 5mm wear for all picks for different rocks.

Sl No	Type of Rock	Pick Angle	F sin α	DISPLACEMENT									Von Misses Stresses N/mm ²
				Depth of cut (mm)			X Direction			Y Direction			
				FEM	Experiment	Error	D _{MAX}	S _{MIN}	S _{MAX}	D _{MX}	S _{MIN}	S _{MAX}	
1	Coal	45°	1.222	14.74	6.52	8.22	14.74	0.00003	0.04264	14.74	0.00501	0.00511	5329.530
		50°	1.322	14.95	6.52	8.43	14.95	0.00004	0.03460	14.95	0.00407	0.00414	4323.960
		55°	1.413	14.95	6.43	8.52	14.95	0.00004	0.03460	14.95	0.00407	0.00414	4323.960
		65°	1.563	14.7	6.55	8.15	14.7	0.00005	0.02550	14.7	0.00300	0.00306	3137.230
2	Sandstone 1	45°	1.291	13.48	5.8	7.68	13.48	0.00002	0.01754	13.48	0.00206	0.00210	5626.830
		50°	1.398	13.92	5.82	8.1	13.92	0.00002	0.01423	13.92	0.00167	0.00171	4564.420
		55°	1.494	13.92	5.85	8.07	13.92	0.00002	0.01423	13.92	0.00167	0.00171	4564.420
		65°	1.652	12.79	5.89	6.9	12.79	0.00001	0.01013	12.79	0.00117	0.00121	3248.430
3	Sandstone 2	45°	1.303	12.6	5.2	7.4	12.6	0.00002	0.01679	12.6	0.00202	0.00194	4424.810
		50°	1.412	12.74	5.22	7.52	12.74	0.00002	0.01366	12.74	0.00164	0.00158	4578.120
		55°	1.508	12.74	5.24	7.5	12.74	0.00002	0.01366	12.74	0.00164	0.00158	4578.120
		65°	1.666	12.76	5.29	7.47	12.76	0.00001	0.00987	12.76	0.00110	0.00126	3457.160
4	Sandstone 3	45°	1.309	11.6	5.21	6.39	11.6	0.00002	0.01679	11.6	0.00202	0.00194	4424.810
		50°	1.415	11.74	5.22	6.52	11.74	0.00002	0.01366	11.74	0.00164	0.00158	4578.120
		55°	1.512	11.74	5.24	6.5	11.74	0.00002	0.01366	11.74	0.00164	0.00158	4578.120
		65°	1.67	11.74	5.27	6.47	11.74	0.00001	0.00987	11.74	0.00110	0.00126	3457.160
5	Limestone 1	45°	1.328	11.32	5.1	6.22	11.32	0.00002	0.01276	11.32	0.00168	0.00132	5591.700
		50°	1.438	10.79	5.12	5.67	10.79	0.00002	0.01037	10.79	0.00132	0.00107	4546.960
		55°	1.537	10.79	5.15	5.64	10.79	0.00002	0.01037	10.79	0.00132	0.00107	4546.960
		65°	1.699	10.79	5.18	5.61	10.79	0.00001	0.00764	10.79	0.00098	0.00079	3349.960
6	Limestone 2	45°	1.33	10.43	5.11	5.32	10.43	0.00002	0.01276	10.43	0.00163	0.00132	5591.700
		50°	1.439	10.28	5.13	5.15	10.28	0.00002	0.01037	10.28	0.00132	0.00107	4546.960
		55°	1.537	10.28	5.15	5.13	10.28	0.00002	0.01037	10.28	0.00132	0.00107	4546.960
		65°	1.701	10.28	5.15	5.13	10.28	0.00001	0.00764	10.28	0.00098	0.00077	3349.950
7	Limestone 3	45°	1.382	9.28	4.8	4.48	9.28	0.00002	0.01062	9.28	0.00143	0.00098	5646.060
		50°	1.496	9.23	4.82	4.41	9.23	0.00002	0.00869	9.23	0.00117	0.00080	4580.770
		55°	1.599	9.23	4.85	4.38	9.23	0.00002	0.00869	9.23	0.00117	0.00080	4580.770
		65°	1.767	9.17	4.88	4.29	9.17	0.00001	0.00640	9.17	0.00086	0.593-03	5576.160
		45°	1.384	8.28	4.61	3.67	8.28	0.00002	0.01062	8.28	0.00143	0.00098	5646.060
		50°	1.499	8.23	4.63	3.6	8.23	0.00002	0.00869	8.23	0.00117	0.00080	4580.770

8	Limestone 4	55°	1.602	8.23	4.65	3.58	8.23	0.00002	0.00869	8.23	0.00117	0.00080	4580.770
		65°	1.77	8.17	4.68	3.49	8.17	0.00001	0.00640	8.17	0.00087	0.00059	4376.160
9	Dolomite 1	45°	1.387	8.28	4.8	3.48	8.28	0.00002	0.01062	8.28	0.00143	0.00098	5646.060
		50°	1.501	8.23	4.83	3.4	8.23	0.00002	0.00869	8.23	0.00117	0.00080	4580.770
		55°	1.604	8.23	4.85	3.38	8.23	0.00002	0.00869	8.23	0.00117	0.00080	4580.770
		65°	1.774	8.17	4.88	3.29	8.17	0.00001	0.00640	8.17	0.00087	0.00059	4376.160
10	Dolomite 2	45°	1.448	8.12	4.81	3.31	8.12	0.00001	0.00414	8.12	0.00058	0.00068	6686.440
		50°	1.568	8.12	4.83	3.29	8.12	0.00001	0.00335	8.12	0.00031	0.00055	5419.440
		55°	1.676	8.12	4.85	3.27	8.12	0.00001	0.00335	8.12	0.00031	0.00055	5419.440
		65°	1.854	7.2	4.88	2.32	7.2	0.00001	0.00247	7.2	0.00023	0.00041	3996.220

APPENDIX-III

Table 6.11 Comparison of Rock Cutting Resistance with Laboratory Experiment and Finite Element Method.

Type of Rock	Pick angle	RCR from Experiment values (N/mm)				FEM Predicted RCR (N/mm)			
		45° attack angle	55° attack angle	65° attack angle	45° attack angle With 5mm wear for all picks	45° attack angle	55° attack angle	65° attack angle	45° attack angle With 5mm wear for all picks
Coal	45°	0.1763	0.1315	0.2275	0.2537	0.1228	0.1093	0.1415	0.1170
		0.1764	0.1316	0.2275	0.2537	0.1228	0.1094	0.1415	0.1170
		0.1787	0.1316	0.2277	0.2537	0.1229	0.1094	0.1416	0.1170
		0.1788	0.1317	0.2310	0.2537	0.1230	0.1095	0.1416	0.1170
		0.1788	0.1331	0.2311	0.2537	0.1230	0.1096	0.1417	0.1170
		0.1789	0.1331	0.2311	0.2537	0.1231	0.1096	0.1417	0.1170
		0.1790	0.1331	0.2523	0.2537	0.1232	0.1096	0.1418	0.1170
		0.1790	0.1331	0.2523	0.2537	0.1232	0.1096	0.1418	0.1170
		0.1815	0.1345	0.2523	0.2537	0.1233	0.1097	0.1418	0.1170
		0.1807	0.1345	0.2523	0.2537	0.1225	0.1085	0.1418	0.1154
		0.1807	0.1345	0.2523	0.2537	0.1225	0.1085	0.1418	0.1154
		0.1809	0.1345	0.2523	0.2538	0.1226	0.1085	0.1418	0.1154

	50°	0.1809	0.1359	0.2523	0.2538	0.1226	0.1086	0.1418	0.1154
		0.1810	0.1359	0.2523	0.2538	0.1227	0.1086	0.1418	0.1154
		0.1810	0.1359	0.2523	0.2540	0.1227	0.1086	0.1418	0.1155
		0.1811	0.1359	0.2523	0.2540	0.1228	0.1086	0.1418	0.1155
		0.1833	0.1360	0.2523	0.2540	0.1228	0.1087	0.1418	0.1155
		0.1833	0.1360	0.2523	0.2540	0.1228	0.1087	0.1418	0.1155
	55°	0.1938	0.1360	0.2523	0.2537	0.1227	0.1086	0.1418	0.1173
		0.1939	0.1360	0.2562	0.2537	0.1228	0.1086	0.1418	0.1173
		0.1940	0.1361	0.2603	0.2538	0.1229	0.1087	0.1419	0.1174
		0.1940	0.1361	0.2603	0.2538	0.1229	0.1087	0.1419	0.1174
		0.1942	0.1361	0.2603	0.2538	0.1229	0.1087	0.1419	0.1174
		0.1943	0.1361	0.2644	0.2540	0.1230	0.1087	0.1419	0.1175
		0.1943	0.1375	0.2644	0.2540	0.1230	0.1088	0.1419	0.1175
		0.1944	0.1375	0.2644	0.2540	0.1231	0.1088	0.1419	0.1175
		0.1946	0.1377	0.2687	0.2540	0.1232	0.1090	0.1419	0.1175
	65°	0.1943	0.1378	0.2687	0.2578	0.1228	0.1090	0.1406	0.1163
		0.1943	0.1379	0.2689	0.2578	0.1228	0.1091	0.1407	0.1163
		0.1943	0.1393	0.2689	0.2578	0.1228	0.1091	0.1407	0.1163
		0.1944	0.1394	0.2689	0.2578	0.1228	0.1092	0.1407	0.1163
		0.1944	0.1394	0.2689	0.2578	0.1228	0.1092	0.1407	0.1163
		0.1970	0.1408	0.2689	0.2579	0.1228	0.1092	0.1407	0.1164

		0.1971	0.1409	0.2690	0.2579	0.1229	0.1092	0.1408	0.1164
		0.1971	0.1424	0.2690	0.2581	0.1229	0.1092	0.1408	0.1165
		0.1972	0.1427	0.2690	0.2581	0.1230	0.1095	0.1408	0.1165
Sandstone 1	45°	0.2080	0.1650	0.3021	0.2802	0.1517	0.1439	0.1824	0.1424
		0.2082	0.1650	0.3023	0.2802	0.1518	0.1439	0.1825	0.1424
		0.2083	0.1650	0.3023	0.2802	0.1519	0.1439	0.1825	0.1424
		0.2084	0.1650	0.3025	0.2802	0.1520	0.1439	0.1826	0.1424
		0.2084	0.1669	0.3025	0.2802	0.1520	0.1439	0.1826	0.1424
		0.2084	0.1669	0.3025	0.2802	0.1520	0.1439	0.1826	0.1424
		0.2086	0.1670	0.3027	0.2802	0.1521	0.1440	0.1827	0.1424
		0.2086	0.1670	0.3027	0.2802	0.1521	0.1440	0.1827	0.1424
		0.2087	0.1709	0.3027	0.2802	0.1522	0.1441	0.1827	0.1424
	50°	0.2087	0.1709	0.3027	0.2845	0.1522	0.1441	0.1766	0.1446
		0.2087	0.1709	0.3027	0.2847	0.1522	0.1441	0.1766	0.1446
		0.2088	0.1710	0.3027	0.2847	0.1523	0.1442	0.1766	0.1446
		0.2090	0.1730	0.3029	0.2847	0.1524	0.1442	0.1767	0.1446
		0.2088	0.1730	0.3029	0.2847	0.1523	0.1442	0.1767	0.1446
		0.2090	0.1730	0.3029	0.2847	0.1524	0.1442	0.1767	0.1446
		0.2117	0.1752	0.3029	0.2847	0.1524	0.1443	0.1767	0.1446
		0.2119	0.1753	0.3029	0.2848	0.1525	0.1444	0.1767	0.1447
		0.2119	0.1753	0.3029	0.2848	0.1525	0.1444	0.1767	0.1447

	55°	0.2123	0.1774	0.3029	0.2845	0.1527	0.1444	0.1809	0.1429
		0.2124	0.1775	0.3030	0.2847	0.1528	0.1445	0.1811	0.1430
		0.2125	0.1775	0.3030	0.2847	0.1529	0.1445	0.1811	0.1430
		0.2125	0.1776	0.3030	0.2847	0.1529	0.1446	0.1811	0.1430
		0.2127	0.1798	0.3030	0.2847	0.1530	0.1446	0.1811	0.1430
		0.2128	0.1798	0.3032	0.2847	0.1531	0.1446	0.1812	0.1430
		0.2129	0.1798	0.3032	0.2847	0.1532	0.1446	0.1812	0.1430
		0.2131	0.1798	0.3032	0.2848	0.1533	0.1446	0.1812	0.1431
		0.2127	0.1799	0.3032	0.2848	0.1530	0.1447	0.1812	0.1431
	65°	0.2115	0.1799	0.3032	0.2852	0.1522	0.1447	0.1831	0.1431
		0.2116	0.1799	0.3032	0.2852	0.1523	0.1447	0.1831	0.1431
		0.2115	0.1799	0.3032	0.2852	0.1522	0.1447	0.1831	0.1431
		0.2115	0.1799	0.3034	0.2852	0.1522	0.1447	0.1832	0.1431
		0.2116	0.1800	0.3089	0.2852	0.1523	0.1448	0.1832	0.1431
		0.2115	0.1822	0.3089	0.2867	0.1522	0.1448	0.1832	0.1439
		0.2117	0.1822	0.3089	0.2867	0.1524	0.1448	0.1832	0.1439
		0.2119	0.1823	0.3091	0.2867	0.1525	0.1449	0.1833	0.1439
		0.2119	0.1823	0.3093	0.2867	0.1525	0.1449	0.1834	0.1439
Sandstone 2	45°	0.2163	0.1860	0.3113	0.2867	0.1559	0.1478	0.1829	0.1582
		0.2164	0.1860	0.3113	0.2869	0.1560	0.1478	0.1829	0.1583
		0.2164	0.1860	0.3113	0.2869	0.1560	0.1478	0.1829	0.1583
		0.2164	0.1860	0.3113	0.2869	0.1560	0.1478	0.1829	0.1583
		0.2164	0.1860	0.3113	0.2869	0.1560	0.1478	0.1829	0.1583

		0.2165	0.1861	0.3113	0.2869	0.1561	0.1479	0.1829	0.1583
		0.2165	0.1862	0.3113	0.2869	0.1561	0.1480	0.1829	0.1583
		0.2195	0.1863	0.3113	0.2869	0.1561	0.1481	0.1829	0.1583
		0.2195	0.1865	0.3113	0.2873	0.1561	0.1482	0.1829	0.1586
	50°	0.2196	0.1866	0.3172	0.3018	0.1561	0.1500	0.1808	0.1568
	50°	0.2196	0.1866	0.3172	0.3018	0.1561	0.1500	0.1808	0.1568
	50°	0.2196	0.1867	0.3172	0.3018	0.1561	0.1501	0.1808	0.1568
	50°	0.2197	0.1868	0.3172	0.3018	0.1562	0.1502	0.1808	0.1568
	50°	0.2197	0.1893	0.3172	0.3018	0.1562	0.1503	0.1808	0.1568
	50°	0.2197	0.1893	0.3172	0.3018	0.1562	0.1503	0.1808	0.1568
	50°	0.2197	0.1893	0.3172	0.3018	0.1562	0.1503	0.1808	0.1568
	50°	0.2197	0.1894	0.3172	0.3018	0.1562	0.1504	0.1808	0.1568
	50°	0.2197	0.1894	0.3174	0.3018	0.1562	0.1504	0.1809	0.1568
	55°	0.2199	0.1894	0.3174	0.3018	0.1563	0.1504	0.1809	0.1568
	55°	0.2199	0.1894	0.3174	0.3018	0.1563	0.1504	0.1809	0.1568
	55°	0.2199	0.1894	0.3174	0.3018	0.1563	0.1504	0.1809	0.1568
	55°	0.2229	0.1895	0.3174	0.3018	0.1563	0.1505	0.1809	0.1568
	55°	0.2229	0.1919	0.3174	0.3018	0.1563	0.1505	0.1809	0.1568
	55°	0.2230	0.1919	0.3174	0.3018	0.1564	0.1505	0.1809	0.1568
	55°	0.2230	0.1919	0.3174	0.3018	0.1564	0.1505	0.1809	0.1568
	55°	0.2232	0.1919	0.3174	0.3018	0.1565	0.1505	0.1809	0.1568
	55°	0.2232	0.1943	0.3174	0.3018	0.1565	0.1505	0.1809	0.1568
	65°	0.2236	0.1943	0.3176	0.3018	0.1568	0.1505	0.1836	0.1626

		0.2237	0.1943	0.3176	0.3018	0.1569	0.1505	0.0500	0.1626
		0.2237	0.1943	0.3176	0.3018	0.1569	0.1505	0.1836	0.1626
		0.2237	0.1943	0.3176	0.3018	0.1569	0.1505	0.1836	0.1626
		0.2237	0.1943	0.3176	0.3018	0.1569	0.1505	0.1836	0.1626
		0.2237	0.1968	0.3176	0.3018	0.1569	0.1505	0.1836	0.1626
		0.2237	0.1968	0.3176	0.3018	0.1569	0.1505	0.1836	0.1626
		0.2238	0.1968	0.3178	0.3018	0.1570	0.1505	0.1837	0.1626
		0.2238	0.1968	0.3178	0.3020	0.1570	0.1505	0.1837	0.1627
Sandstone 3	45°	0.2238	0.1968	0.3187	0.3176	0.1582	0.1661	0.2079	0.1707
		0.2238	0.1968	0.3187	0.3176	0.1582	0.1661	0.2079	0.1707
		0.2238	0.1962	0.3187	0.3176	0.1582	0.1662	0.2079	0.1707
		0.2269	0.1969	0.3187	0.3176	0.1582	0.1662	0.2079	0.1707
		0.2269	0.1995	0.3187	0.3176	0.1582	0.1662	0.2079	0.1707
		0.2271	0.1995	0.3187	0.3176	0.1583	0.1662	0.2079	0.1707
		0.2271	0.1995	0.3247	0.3176	0.1583	0.1662	0.2079	0.1707
		0.2271	0.1995	0.3247	0.3176	0.1583	0.1662	0.2079	0.1707
		0.2370	0.1995	0.3247	0.3178	0.1583	0.1662	0.2079	0.1708

	50°	0.2370	0.2049	0.3247	0.3178	0.1583	0.1663	0.2098	0.1708
		0.2370	0.2049	0.3247	0.3178	0.1583	0.1663	0.2098	0.1708
		0.2370	0.2049	0.3247	0.3293	0.1583	0.1663	0.2098	0.1709
		0.2370	0.2049	0.3249	0.3295	0.1583	0.1663	0.2099	0.1710
		0.2371	0.2049	0.3249	0.3295	0.1584	0.1663	0.2099	0.1710
		0.2371	0.2077	0.3249	0.3295	0.1584	0.1663	0.2099	0.1710
		0.2371	0.2077	0.3249	0.3295	0.1584	0.1663	0.2099	0.1710
		0.2371	0.2077	0.3249	0.3295	0.1584	0.1663	0.2099	0.1710
		0.2371	0.2077	0.3251	0.3295	0.1584	0.1663	0.2100	0.1710
	55°	0.2371	0.2106	0.3251	0.3178	0.1584	0.1663	0.2065	0.1767
		0.2373	0.2106	0.3253	0.3178	0.1585	0.1663	0.2066	0.1767
		0.2373	0.2106	0.3255	0.3293	0.1585	0.1663	0.2068	0.1768
		0.2373	0.2106	0.3257	0.3295	0.1585	0.1663	0.2069	0.1769
		0.2373	0.2135	0.3319	0.3295	0.1585	0.1663	0.2069	0.1769
		0.2373	0.2135	0.3319	0.3295	0.1585	0.1663	0.2069	0.1769
		0.2373	0.2135	0.3319	0.3295	0.1585	0.1663	0.2069	0.1769
		0.2373	0.2136	0.3319	0.3295	0.1585	0.1665	0.2069	0.1769
		0.2373	0.2197	0.3323	0.3295	0.1585	0.1665	0.2071	0.1769
	65°	0.2374	0.2197	0.3329	0.3296	0.1586	0.1665	0.2091	0.1796
		0.2374	0.2197	0.3329	0.3358	0.1586	0.1665	0.2091	0.1797
		0.2374	0.2229	0.3329	0.3362	0.1586	0.1665	0.2091	0.1799

		0.2374	0.2230	0.3329	0.3424	0.1586	0.1666	0.2091	0.1799
		0.2375	0.2230	0.3329	0.3424	0.1587	0.1666	0.2091	0.1799
		0.2410	0.2230	0.3329	0.3424	0.1587	0.1666	0.2091	0.1799
		0.2446	0.2265	0.3329	0.3424	0.1587	0.1667	0.2091	0.1799
		0.2446	0.2266	0.3329	0.3424	0.1587	0.1668	0.2091	0.1799
		0.2510	0.2268	0.3329	0.3424	0.1629	0.1669	0.2091	0.1799
Limestone 1	45°	0.2512	0.2328	0.3310	0.3530	0.1633	0.1715	0.2389	0.2032
		0.2512	0.2329	0.3310	0.3530	0.1633	0.1716	0.2389	0.2032
		0.2512	0.2331	0.3310	0.3534	0.1633	0.1717	0.2389	0.2035
		0.2512	0.2331	0.3310	0.3534	0.1633	0.1717	0.2389	0.2035
		0.2512	0.2366	0.3310	0.3536	0.1633	0.1717	0.2389	0.2036
		0.2513	0.2366	0.3310	0.3538	0.1634	0.1717	0.2389	0.2037
		0.2513	0.2366	0.3310	0.3538	0.1634	0.1717	0.2389	0.2037
		0.2513	0.2366	0.3310	0.3538	0.1634	0.1717	0.2389	0.2037
	50°	0.2513	0.2366	0.3337	0.3538	0.1634	0.1717	0.2383	0.2020
		0.2513	0.2366	0.3337	0.3538	0.1634	0.1717	0.2383	0.2020
		0.2515	0.2366	0.3337	0.3538	0.1635	0.1717	0.2383	0.2020
		0.2515	0.2366	0.3337	0.3538	0.1635	0.1717	0.2383	0.2020
		0.2515	0.2366	0.3337	0.3538	0.1635	0.1717	0.2383	0.2020
		0.2515	0.2366	0.3337	0.3538	0.1635	0.1717	0.2383	0.2020

		0.2515	0.2366	0.3339	0.3538	0.1635	0.1717	0.2384	0.2020
		0.2516	0.2366	0.3339	0.3538	0.1635	0.1717	0.2384	0.2020
		0.2516	0.2366	0.3339	0.3538	0.1635	0.1717	0.2384	0.2020
	55°	0.2516	0.2366	0.3339	0.3538	0.1635	0.1717	0.2401	0.2032
	55°	0.2516	0.2366	0.3340	0.3538	0.1635	0.1717	0.2403	0.2032
	55°	0.2516	0.2366	0.3340	0.3538	0.1635	0.1717	0.2403	0.2032
	55°	0.2516	0.2366	0.3340	0.3538	0.1635	0.1717	0.2403	0.2032
	55°	0.2518	0.2366	0.3340	0.3538	0.1636	0.1717	0.2403	0.2032
	55°	0.2518	0.2402	0.3340	0.3538	0.1636	0.1717	0.2403	0.2032
	55°	0.2518	0.2403	0.3340	0.3538	0.1636	0.1718	0.2403	0.2032
	55°	0.2518	0.2403	0.3340	0.3538	0.1636	0.1718	0.2403	0.2032
	55°	0.2518	0.2403	0.3340	0.3538	0.1636	0.1718	0.2403	0.2032
	65°	0.2636	0.2403	0.3340	0.3538	0.1636	0.1718	0.2423	0.2045
	65°	0.2636	0.2403	0.3340	0.3538	0.1636	0.1718	0.2423	0.2045
	65°	0.2638	0.2403	0.3340	0.3606	0.1637	0.1718	0.2423	0.2045
	65°	0.2638	0.2405	0.3340	0.3606	0.1637	0.1719	0.2423	0.2045
	65°	0.2638	0.2405	0.3342	0.3606	0.1637	0.1719	0.2424	0.2045
	65°	0.2639	0.2406	0.3342	0.3606	0.1638	0.1720	0.2424	0.2045
	65°	0.2639	0.2406	0.3342	0.3606	0.1638	0.1720	0.2424	0.2045
	65°	0.2639	0.2443	0.3344	0.3606	0.1638	0.1720	0.2426	0.2045
	65°	0.2722	0.2445	0.3344	0.3608	0.1690	0.1722	0.2426	0.2046
	45°	0.2723	0.2539	0.3348	0.3608	0.1883	0.1795	0.2772	0.2266
	45°	0.2723	0.2540	0.3350	0.3608	0.1883	0.1797	0.2774	0.2266

Limestone 2		0.2723	0.2542	0.3350	0.3608	0.1883	0.1798	0.2774	0.2266	
		0.2725	0.2542	0.3352	0.3610	0.1885	0.1798	0.2775	0.2267	
		0.2725	0.2542	0.3354	0.3610	0.1885	0.1798	0.2777	0.2267	
		0.2725	0.2542	0.3354	0.3610	0.1885	0.1798	0.2777	0.2267	
		0.2725	0.2543	0.3356	0.3610	0.1885	0.1799	0.2778	0.2267	
		0.2725	0.2543	0.3356	0.3610	0.1885	0.1799	0.2778	0.2267	
		0.2727	0.2543	0.3356	0.3610	0.1886	0.1799	0.2778	0.2267	
	50°	0.2727	0.2543	0.3358	0.3610	0.1886	0.1799	0.2803	0.2281	
		0.2728	0.2543	0.3358	0.3610	0.1887	0.1799	0.2803	0.2281	
		0.2728	0.2543	0.3360	0.3610	0.1887	0.1799	0.2804	0.2281	
		0.2728	0.2583	0.3360	0.3610	0.1887	0.1799	0.2804	0.2281	
		0.2728	0.2583	0.3360	0.3610	0.1887	0.1799	0.2804	0.2281	
		0.2730	0.2583	0.3362	0.3610	0.1888	0.1799	0.2806	0.2281	
		0.2730	0.2583	0.3362	0.3610	0.1888	0.1799	0.2806	0.2281	
		0.2730	0.2583	0.3364	0.3610	0.1888	0.1799	0.2808	0.2281	
	55°	0.2730	0.2584	0.3364	0.3610	0.1888	0.1800	0.2808	0.2281	
		0.2730	0.2584	0.3429	0.3610	0.1888	0.1800	0.2835	0.2298	
		0.2730	0.2584	0.3429	0.3610	0.1888	0.1800	0.2835	0.2298	
			0.2775	0.2584	0.3429	0.3610	0.1889	0.1800	0.2835	0.2298

		0.2776	0.2584	0.3429	0.3610	0.1890	0.1800	0.2835	0.2298
		0.2776	0.2586	0.3431	0.3610	0.1890	0.1801	0.2837	0.2298
		0.2776	0.2586	0.3433	0.3610	0.1890	0.1801	0.2838	0.2298
		0.2781	0.2586	0.3433	0.3610	0.1893	0.1801	0.2838	0.2298
		0.2783	0.2586	0.3433	0.3610	0.1894	0.1801	0.2838	0.2298
		0.2783	0.2586	0.3433	0.3610	0.1894	0.1801	0.2838	0.2298
	65°	0.2783	0.2586	0.3435	0.3610	0.1888	0.1801	0.2790	0.2267
		0.2783	0.2586	0.3435	0.3610	0.1888	0.1801	0.2790	0.2267
		0.2783	0.2586	0.3435	0.3610	0.1888	0.1801	0.2790	0.2267
		0.2783	0.2586	0.3437	0.3610	0.1888	0.1801	0.2791	0.2267
		0.2784	0.2588	0.3437	0.3612	0.1889	0.1802	0.2791	0.2268
		0.2784	0.2588	0.3437	0.3614	0.1889	0.1802	0.2791	0.2269
		0.2784	0.2588	0.3437	0.3614	0.1889	0.1802	0.2791	0.2269
		0.2784	0.2588	0.3437	0.3614	0.1889	0.1802	0.2791	0.2269
	45°	0.2784	0.2588	0.3439	0.3750	0.2118	0.1802	0.2816	0.2370
		0.2784	0.2589	0.3439	0.3750	0.2118	0.1803	0.2816	0.2370
		0.2786	0.2589	0.3439	0.3750	0.2119	0.1803	0.2816	0.2370
		0.2786	0.2589	0.3439	0.3750	0.2119	0.1803	0.2816	0.2370
0.2786		0.2589	0.3439	0.3750	0.2119	0.1803	0.2816	0.2370	
0.2786		0.2630	0.3439	0.3750	0.2119	0.1803	0.2816	0.2370	
Limestone 3									

		0.2786	0.2630	0.3439	0.3750	0.2119	0.1803	0.2816	0.2370
		0.2786	0.2630	0.3439	0.3750	0.2119	0.1803	0.2816	0.2370
		0.2786	0.2630	0.3439	0.3750	0.2119	0.1803	0.2816	0.2370
	50°	0.2787	0.2632	0.3441	0.3750	0.2120	0.1804	0.2845	0.2387
	50°	0.2787	0.2632	0.3441	0.3750	0.2120	0.1804	0.2845	0.2387
	50°	0.2787	0.2632	0.3441	0.3750	0.2120	0.1804	0.2845	0.2387
	50°	0.2787	0.2632	0.3441	0.3750	0.2120	0.1804	0.2845	0.2387
	50°	0.2787	0.2633	0.3441	0.3750	0.2120	0.1805	0.2845	0.2387
	50°	0.2787	0.2633	0.3441	0.3750	0.2120	0.1805	0.2845	0.2387
	50°	0.2787	0.2633	0.3441	0.3754	0.2120	0.1805	0.2845	0.2389
	50°	0.2789	0.2633	0.3441	0.3754	0.2121	0.1805	0.2845	0.2389
	50°	0.2789	0.2633	0.3441	0.3754	0.2121	0.1805	0.2845	0.2389
	55°	0.2789	0.2633	0.3441	0.3750	0.2121	0.1805	0.2867	0.2401
	55°	0.2789	0.2633	0.3441	0.3750	0.2121	0.1805	0.2867	0.2401
	55°	0.2789	0.2633	0.3443	0.3750	0.2121	0.1805	0.2869	0.2401
	55°	0.2789	0.2633	0.3443	0.3750	0.2121	0.1805	0.2869	0.2401
	55°	0.2789	0.2633	0.3443	0.3750	0.2121	0.1805	0.2869	0.2401
	55°	0.2789	0.2633	0.3443	0.3750	0.2121	0.1805	0.2869	0.2401
	55°	0.2791	0.2633	0.3443	0.3754	0.2122	0.1805	0.2869	0.2404
	55°	0.2791	0.2633	0.3443	0.3754	0.2122	0.1805	0.2869	0.2404
	55°	0.2791	0.2633	0.3443	0.3754	0.2122	0.1805	0.2869	0.2404

	65°	0.2791	0.2633	0.3445	0.3754	0.2122	0.1803	0.2871	0.2175
		0.2792	0.2633	0.3445	0.3754	0.2124	0.1803	0.2871	0.2175
		0.2792	0.2633	0.3445	0.3754	0.2124	0.1803	0.2871	0.2175
		0.2792	0.2633	0.3445	0.3754	0.2124	0.1803	0.2871	0.2175
		0.2805	0.2738	0.3447	0.3754	0.2133	0.1875	0.2873	0.2175
		0.2806	0.2738	0.3447	0.3754	0.2134	0.1875	0.2873	0.2175
		0.2808	0.2738	0.3447	0.3754	0.2136	0.1875	0.2873	0.2175
		0.2808	0.2738	0.3447	0.3754	0.2136	0.1875	0.2873	0.2175
		0.2891	0.2738	0.3449	0.3754	0.2198	0.1875	0.2874	0.2175
Limestone 4	45°	0.2892	0.2738	0.3688	0.3754	0.2525	0.2114	0.3619	0.2712
		0.2894	0.2738	0.3690	0.3754	0.2526	0.2114	0.3621	0.2712
		0.2894	0.2738	0.3692	0.3754	0.2526	0.2114	0.3623	0.2712
		0.2895	0.2741	0.3692	0.3754	0.2528	0.2116	0.3623	0.2712
		0.2895	0.2741	0.3694	0.3758	0.2528	0.2116	0.3624	0.2715
		0.2897	0.2741	0.3696	0.3758	0.2529	0.2116	0.3626	0.2715
		0.2897	0.2741	0.3696	0.3758	0.2529	0.2116	0.3626	0.2715
		0.2898	0.2741	0.3698	0.3758	0.2530	0.2116	0.3628	0.2715
		0.2898	0.2741	0.3700	0.3758	0.2530	0.2116	0.3630	0.2715
	50°	0.2898	0.2741	0.3706	0.3758	0.2530	0.2116	0.3663	0.2729
		0.2900	0.2741	0.3708	0.3758	0.2532	0.2116	0.3665	0.2729
		0.2900	0.2741	0.3710	0.3758	0.2532	0.2116	0.3667	0.2729

		0.2900	0.2741	0.3710	0.3758	0.2532	0.2116	0.3667	0.2729
		0.2910	0.2741	0.3712	0.3758	0.2540	0.2116	0.3669	0.2729
		0.2910	0.2741	0.3712	0.3758	0.2540	0.2116	0.3669	0.2729
		0.2911	0.2744	0.3712	0.3758	0.2542	0.2119	0.3669	0.2729
		0.2911	0.2744	0.3714	0.3831	0.2542	0.2119	0.3671	0.2729
		0.2913	0.2746	0.3714	0.3831	0.2543	0.2120	0.3671	0.2729
	55°	0.2913	0.2748	0.3714	0.3758	0.2542	0.2121	0.3671	0.2729
	55°	0.2913	0.2751	0.3714	0.3758	0.2542	0.2124	0.3671	0.2729
	55°	0.2914	0.2751	0.3867	0.3758	0.2544	0.2124	0.3672	0.2729
	55°	0.2914	0.2752	0.3867	0.3758	0.2544	0.2125	0.3672	0.2729
	55°	0.2914	0.2752	0.3867	0.3758	0.2544	0.2125	0.3672	0.2729
	55°	0.2916	0.2752	0.3867	0.3758	0.2545	0.2125	0.3672	0.2729
	55°	0.2916	0.2752	0.3867	0.3758	0.2545	0.2125	0.3625	0.2729
	55°	0.2916	0.2752	0.3867	0.3831	0.2545	0.2125	0.3672	0.2729
	55°	0.2916	0.2752	0.3867	0.3831	0.2545	0.2125	0.3672	0.2729
	65°	0.2918	0.2752	0.3867	0.3831	0.2547	0.2125	0.3672	0.2729
	65°	0.2918	0.2756	0.3867	0.3831	0.2547	0.2127	0.3672	0.2729
	65°	0.2918	0.2756	0.3867	0.3831	0.2547	0.2127	0.3672	0.2729
	65°	0.2918	0.2759	0.3867	0.3833	0.2547	0.2130	0.3672	0.2730
	65°	0.2918	0.2794	0.3867	0.3833	0.2547	0.2157	0.3672	0.2730
	65°	0.2966	0.2840	0.3867	0.3833	0.2548	0.2158	0.3672	0.2730

		0.2966	0.2844	0.3867	0.3833	0.2548	0.2161	0.3672	0.2730
		0.2966	0.2844	0.3867	0.3833	0.2548	0.2161	0.3672	0.2730
		0.3002	0.2845	0.3867	0.3835	0.2578	0.2162	0.3672	0.2732
Dolomite 1	45°	0.3003	0.2847	0.3867	0.3835	0.2617	0.2006	0.3223	0.2843
		0.3005	0.2847	0.3869	0.3835	0.2619	0.2006	0.3224	0.2843
		0.3005	0.2847	0.3869	0.3835	0.2619	0.2006	0.3224	0.2843
		0.3005	0.2847	0.3869	0.3835	0.2618	0.2006	0.3224	0.2843
		0.3005	0.2847	0.3869	0.3835	0.2619	0.2006	0.3224	0.2843
		0.3007	0.2847	0.3869	0.3837	0.2620	0.2006	0.3224	0.2844
		0.3007	0.2847	0.3871	0.3837	0.2620	0.2006	0.3226	0.2844
		0.3007	0.2847	0.3871	0.3837	0.2620	0.2006	0.3226	0.2844
		0.3007	0.2847	0.3871	0.3837	0.2620	0.2006	0.3226	0.2844
	50°	0.3008	0.2847	0.3871	0.3839	0.2621	0.2006	0.3226	0.2846
		0.3008	0.2847	0.3871	0.3839	0.2621	0.2006	0.3226	0.2846
		0.3008	0.2847	0.3871	0.3839	0.2621	0.2006	0.3226	0.2846
		0.3008	0.2847	0.3871	0.3839	0.2621	0.2006	0.3226	0.2846
		0.3008	0.2848	0.3871	0.3839	0.2621	0.2007	0.3226	0.2846
		0.3010	0.2848	0.3871	0.3839	0.2623	0.2007	0.3226	0.2846
		0.3010	0.2850	0.3871	0.3839	0.2623	0.2008	0.3226	0.2846
		0.3010	0.2850	0.3871	0.3839	0.2623	0.2008	0.3226	0.2846
		0.3010	0.2850	0.3871	0.3839	0.2623	0.2008	0.3226	0.2846

	55°	0.3010	0.2850	0.3871	0.3839	0.2623	0.2008	0.3226	0.2846
		0.3010	0.2850	0.3871	0.3839	0.2623	0.2008	0.3226	0.2846
		0.3011	0.2850	0.3871	0.3839	0.2624	0.2008	0.3226	0.2846
		0.3011	0.2850	0.3871	0.3839	0.2624	0.2008	0.3226	0.2846
		0.3011	0.2850	0.3954	0.3839	0.2624	0.2008	0.3228	0.2846
		0.3011	0.2850	0.3954	0.3839	0.2624	0.2008	0.3228	0.2846
		0.3061	0.2850	0.3954	0.3839	0.2624	0.2008	0.3228	0.2846
		0.3061	0.2850	0.3954	0.3839	0.2624	0.2008	0.3228	0.2846
		0.3061	0.2850	0.3954	0.3839	0.2624	0.2008	0.3228	0.2846
	65°	0.3062	0.2850	0.3956	0.3839	0.2626	0.2008	0.3230	0.2846
		0.3062	0.2852	0.3956	0.3996	0.2626	0.2009	0.3230	0.2846
		0.3062	0.2853	0.3956	0.3996	0.2626	0.2010	0.3230	0.2846
		0.3062	0.2853	0.3958	0.3996	0.2626	0.2010	0.3231	0.2846
		0.3062	0.3000	0.4043	0.3996	0.2626	0.2114	0.3231	0.2846
		0.3064	0.3002	0.4045	0.3998	0.2627	0.2115	0.3233	0.2847
		0.3064	0.3005	0.4045	0.3998	0.2627	0.2117	0.3233	0.2847
		0.3064	0.3005	0.4047	0.3998	0.2627	0.2117	0.3235	0.2847
		0.3215	0.3005	0.4051	0.3998	0.2756	0.2118	0.3238	0.2847
	Dolomite 2	45°	0.3216	0.3008	0.4394	0.4174	0.3208	0.2361	0.4311
0.3218			0.3008	0.4394	0.4174	0.3210	0.2361	0.4311	0.3012
0.3218			0.3081	0.4394	0.4174	0.3210	0.2361	0.4311	0.3012
0.3218			0.3008	0.4394	0.4174	0.3210	0.2361	0.4311	0.3012
0.3220			0.3008	0.4394	0.4174	0.3212	0.2361	0.4311	0.3012

		0.3220	0.3057	0.4394	0.4174	0.3212	0.2361	0.4311	0.3012
		0.3220	0.3057	0.4394	0.4174	0.3212	0.2308	0.4311	0.3012
		0.3221	0.3057	0.4394	0.4174	0.3213	0.2361	0.4311	0.3012
		0.3221	0.3057	0.4394	0.4174	0.3213	0.2361	0.4311	0.3012
	50°	0.3221	0.3057	0.4394	0.4174	0.3213	0.2361	0.4311	0.3012
		0.3221	0.3057	0.4394	0.4174	0.3213	0.2361	0.4311	0.3012
		0.3221	0.3057	0.4400	0.4174	0.3213	0.2361	0.4373	0.3012
		0.3221	0.3057	0.4400	0.4174	0.3213	0.2361	0.4373	0.3012
		0.3221	0.3057	0.4400	0.4174	0.3213	0.2361	0.4373	0.3012
		0.3223	0.3059	0.4400	0.4351	0.3215	0.2362	0.4317	0.3012
		0.3223	0.3059	0.4400	0.4351	0.3215	0.2362	0.4317	0.3012
		0.3223	0.3061	0.4400	0.4351	0.3215	0.2363	0.4317	0.3012
	55°	0.3223	0.3061	0.4400	0.4351	0.3215	0.2363	0.4317	0.3012
		0.3225	0.3061	0.4400	0.4174	0.3216	0.2363	0.4317	0.3012
		0.3225	0.3061	0.4400	0.4174	0.3216	0.2363	0.4317	0.3012
		0.3225	0.3061	0.4404	0.4174	0.3216	0.2363	0.4322	0.3012
0.3225		0.3061	0.4409	0.4174	0.3216	0.2363	0.4326	0.3012	
0.3225		0.3061	0.4413	0.4174	0.3216	0.2363	0.4330	0.3012	
65°	0.3225	0.3061	0.4415	0.4351	0.3216	0.2363	0.4332	0.3012	
	0.3226	0.3061	0.4415	0.4351	0.3218	0.2363	0.4332	0.3012	
	0.3226	0.3061	0.4417	0.4351	0.3218	0.2363	0.4334	0.3012	
	0.3226	0.3061	0.4513	0.4357	0.3218	0.2363	0.4334	0.3016	

		0.3226	0.3061	0.4517	0.4357	0.3218	0.2363	0.4338	0.3016
		0.3226	0.3112	0.4517	0.4357	0.3218	0.2363	0.4338	0.3016
		0.3228	0.3113	0.4517	0.4357	0.3219	0.2365	0.4338	0.3016
		0.3228	0.3113	0.4517	0.4357	0.3219	0.2365	0.4338	0.3016
		0.3228	0.3115	0.4524	0.4357	0.3219	0.2366	0.4344	0.3016
		0.3228	0.3115	0.4528	0.4357	0.3219	0.2366	0.4349	0.3016
		0.3228	0.3115	0.4533	0.4357	0.3219	0.2366	0.4353	0.3016
		0.3230	0.3115	0.4539	0.4357	0.3221	0.2366	0.4359	0.3016

List of Publications based on PhD Research Work

Sl. No	Title of the Paper	Authors (in the order as in the paper. Underline the Research Scholar's name)	Name of the Journal/Conference/Symposium, Vol., No, Pages	Month & Year of Publication	Category*
1.	Prediction of Cuttability with Rock Cutting Resistance	Vijaya Raghavan ¹ , Dr. Ch.S.N.Murthy ² ,	The journal of The South African Institute of Mining & Metallurgy (SAIMM)	March 2018, Vol 118, Page 321-329	1
2	Study on Assessment and Prediction of Specific Energy in rock cutting with Artificial Neural Network (ANN)	Vijaya Raghavan ¹ , Dr. Ch.S.N.Murthy ² ,	Indian Journal of Engineering,	July-September 2017 14(37), pp167-190	1
3.	Prediction of Specific Energy in rock cutting with Artificial Neural Network	Vijaya Raghavan ¹ , Dr. Ch.S.N.Murthy ² ,	Journal of Advance Research in Dynamical and Control Systems	Dec 2017, pp1955-1965	2
4.	Prediction of Specific Energy in rock cutting with Artificial Neural Network	Vijaya Raghavan ¹ , Dr. Ch.S.N.Murthy ² ,	Future Trends in Engineering and Business (Future Trends2017)	26 & 27 May 2017 pp 221-227	3
5	Assessment and Prediction of Specific Energy using Rock Brittleness in Rock Cutting.	Raghavan V., Murthy Ch.S.N	International Conference on Emerging Trends in Engineering (ICETE) Springer International Publication	vol 2. March (2020) pp 374-382	3

*Category, 1. Journal paper, full paper reviewed 2. Journal paper, Abstract reviewed

3. Conference/Symposium paper, full paper reviewed 4. Conference/Symposium paper, Abstract reviewed

5. Others (including papers in Workshops, NITK Research Bulletins, Short notes etc.)

(If the paper has been accepted for publication, but not yet published, the supporting documents must be attached).

Bio-Data

- 1. Name** : Vijaya Raghavan
2. Father's Name : Shri. B.Perumal
3. Date of Birth : 06-02-1979
4. Nationality : Indian
5. Marital Status : Married
6. Present Position : Associate Professor
7. Address for Communication : Department of Mining Engineering,
Dr.T.Thimmaiah Institute of Technology
(Formerly Golden Valley Institute of Technology),
Oorgaum, Kolar Gold Fields,
Kolar District, Karnataka,
India.
8. Mobile : +91-9480244255
9. E-mail : raghavan_pp@rediffmail.com

10. Academic Qualifications

School/ Degree	University/Board	Specialisation	Year of Passing	Marks/ CGPA	Class Obtained
ME	Sathyabama University, Chennai	Environmental Engg.	2010	8.375	FCD
BE	VTU,Belgaum	Mining Engg.	2006	65.65	First
Diploma	DTE,B.lore	Mining Engg.	2002	64.62	First

11. Work Experience

Employer	Present Designation	Period Experience		Year of Experience
		From	To	
GVIT, K.G.F	Associate Professor, Department of Mining, DrTTIT, K.G.F.	23.03.2007	Till Date	10.8 Years

12. Membership of professional Bodies: Member of the Institution of Engineers (India).

13. Publications, Total No.

International Conferences : 02
International Journals Published : 03